Royal Norwegian Council
for Scientific and Industrial Research
(NTNF)

NORSAR

NORSAR Scientific Report No. 1-90/91

Semiannual Technical Summary

1 April — 30 September 1990

Kjeller, November 1990

UNCLASSIFIED
ECURITY CLASSIFICATION OF THIS PAGE

REPORT DOCUMENTATION PAGE

Form Approved
OMB No. 0704-0188

1a. REPORT SECURITY CLASSIFICATION UNCLASSIFIED	1b. RESTRICTIVE MARKINGS NOT APPLICABLE
2a. SECURITY CLASSIFICATION AUTHORITY NOT APPLICABLE	3. DISTRIBUTION/AVAILABILITY OF REPORT APPROVED FOR PUBLIC RELEASE DISTRIBUTION UNLIMITED
2b. DECLASSIFICATION/DOWNGRADING SCHEDULE NOT APPLICABLE	
4. PERFORMING ORGANIZATION REPORT NUMBER(S) Scientific Rep. 1-90/91	5. MONITORING ORGANIZATION REPORT NUMBER(S) Scientific Rep. 1-90/91
6a. NAME OF PERFORMING ORGANIZATION NTNF/NORSAR	6b. OFFICE SYMBOL (If applicable)
7a. NAME OF MONITORING ORGANIZATION HQ/AFTAC/TTS	
6c. ADDRESS (City, State, and ZIP Code) Post Box 51 N-2007 Kjeller, Norway	7b. ADDRESS (City, State, and ZIP Code) Patrick AFB, FL 32925-6001
8a. NAME OF FUNDING/SPONSORING ORGANIZATION Defense Advanced Research Projects Agency	8b. OFFICE SYMBOL (If applicable) NMRO
9. PROCUREMENT INSTRUMENT IDENTIFICATION NUMBER Contract No. F08606-89-C-0005	
8c. ADDRESS (City, State, and ZIP Code) 1400 Wilson Blvd. Arlington, VA 22209-2308	10. SOURCE OF FUNDING NUMBERS PROGRAM ELEMENT NO.: R&D PROJECT NO.: NORSAR PHASE 3 TASK NO.: SOW TASK 5.0 WORK UNIT ACCESSION NO.: SEQUENCE No.003A2

11. TITLE (Include Security Classification)

SEMIANNUAL TECHNICAL SUMMARY, 1 APRIL - 30 SEPTEMBER 1990 (UNCLASSIFIED)

12. PERSONAL AUTHOR(S)
L.B. Loughran (ed.)

13a. TYPE OF REPORT	13b. TIME COVERED	14. DATE OF REPORT (Year, Month, Day)	15. PAGE COUNT
SCIENTIFIC SUMMARY	FROM 1 Apr TO 30 Sep 90	Nov 1990	134

16. SUPPLEMENTARY NOTATION

NOT APPLICABLE

17. COSATI CODES			18. SUBJECT TERMS (Continue on reverse if necessary and identify by block number)
FIELD	GROUP	SUB-GROUP	
8	11		NORSAR, NORWEGIAN SEISMIC ARRAY

19. ABSTRACT (Continue on reverse if necessary and identify by block number)

(Please see reverse side)

20. DISTRIBUTION/AVAILABILITY OF ABSTRACT ☐ UNCLASSIFIED/UNLIMITED ☐ SAME AS RPT. ☐ DTIC USERS	21. ABSTRACT SECURITY CLASSIFICATION UNCLASSIFIED
22a. NAME OF RESPONSIBLE INDIVIDUAL MR. LEE BRIDGES	22b. TELEPHONE (Include Area Code) (407) 494-7765
	22c. OFFICE SYMBOL AFTAC/TTS

Form 1473, JUN 86 *Previous editions are obsolete.* SECURITY CLASSIFICATION OF THIS PAGE

Abstract

This Semiannual Technical Summary describes the operation, maintenance and research activities at the Norwegian Seismic Array (NORSAR), the Norwegian Regional Seismic Array (NORESS) and the Arctic Regional Seismic Array (ARCESS) for the period 1 April – 30 September 1990. Statistics are also presented for additional seismic stations, which through cooperative agreements with institutions in the host countries provide continuous data to the NORSAR Data Processing Center (NPDC). These stations comprise the Finnish Experimental Seismic Array (FINESA), the German Experimental Seismic Array (GERESS), and from the fall of 1990, two 3-component station in Poland: Ksiaz and Stary Folwark. This Semiannual Report also presents statistics from operation of the Intelligent Monitoring System (IMS). The IMS has been operated in an experimental mode using NORESS and ARCESS data, and the performance has been very satisfactory.

The NORSAR Detection Processing system has been operated throughout the period with an average uptime of 98.0% as compared to 91.8% for the previous reporting period. A total of 2359 seismic events have been reported in the NORSAR monthly seismic bulletin. The performance of the continuous alarm system and the automatic bulletin transfer by telex to AFTAC has been satisfactory. A system for direct retrieval of NORSAR waveform data through an X.25 connection has been implemented, and has been tested successfully for acquiring such data by AFTAC. Processing of requests for full NORSAR/NORESS data on magnetic tapes has progressed according to established schedules.

On-line detection processing and data recording at the NORSAR Data Processing Center (NDPC) of NORESS, ARCESS and FINESA data have been conducted throughout the period, with an average uptime of 92.9% for NORESS and 95.6% for ARCESS. The field computer at the FINESA array was damaged by a thunderstorm in May, and FINESA was out of operation until the end of August. The Intelligent Monitoring System was installed at NORSAR in December 1989 and has been operated experimentally since 1 January 1990. Results of the IMS analysis for the reporting period are given.

There have been no modifications made to the NORSAR data acquisition system. The process of evaluating technical options for upgrading the array is continuing. A test of a full subarray acquisition system will be performed during the next reporting period.

The routine detection processing of NORESS, ARCESS and FINESA is running satisfactorily on each of the arrays' SUN-3/280 data acquisition systems. The routine processing of FINESA data at NORSAR is similar to what is done in Helsinki. GERESS data acquisition and detection processing has commenced during the period.

Maintenance activities in the period comprise preventive/corrective maintenance in connection with all the NORSAR subarrays, NORESS and ARCESS. In addition, the maintenance center has been involved with modification of equipment for FINESA and preparatory work in connection with NORESS HF instrumentation. Other activities involved testing of the NORSAR communications systems.

We have continued our work aimed at evaluating the stability of RMS Lg for yield estimation purposes. Using yield data which have recently become available in a Soviet publication, we have found that NORSAR RMS Lg correlates significantly better with yield than does world-wide m_b. These same yield data have been used to evaluate the NORESS detection threshold for Semipalatinsk explosions, and the 90 per cent threshold in terms of yield is found to be as low as 0.1 kt. This low threshold assumes that the explosion is fully coupled and that the background noise is at a normal level.

An initial assessment of results from real-time processing of GERESS array data has been conducted. We have found that a "generic" beam deployment, identical to that in use at NORESS and ARCESS, also works well for the GERESS array. As more experience is gained, we expect, however, that some of the special signal and noise characteristics at the GERESS site will make it desirable to modify some parameters in order to optimize detection performance. So far, GERESS detects a number of earthquake and man-made explosions within 500 km which are not detected by other regional array stations. It also provides additional information which will improve the location accuracy for events detected by multiple stations in the regional network.

The generalized beamforming technique developed by Ringdal and Kværna is now being applied to the network of 4 regional arrays (NORESS, ARCESS, FINESA, GERESS). Initial experience has confirmed the effectiveness of this method in automatically and rapidly providing initial phase associations and epicenter estimates for regional events. For a five-day test period, several hundred regional events were associated, most of which were detected by one array only (P and Lg phases). A total of 37 events had 4 or more phase detections by the regional network. Analyst inspection revealed that 36 of these were properly associated and located, whereas one represented a coincidental match of unrelated phase detections. Further work is now being conducted to fine tune the parameters used by this method, and also to consider incorporating a dynamic consistency check using the thresholds computed by the threshold monitoring technique to assess the likelihood of phase associations.

The concept of threshold monitoring, introduced by Ringdal and Kværna, is a method of monitoring the seismic amplitude levels for the purpose of using this information to assess the largest size of events that might go undetected by a given network. In an effort to demonstrate the capabilities of this threshold

monitoring concept, a preliminary version has been implemented into the Intelligent Monitoring System (IMS). Using recordings by the NORESS, ARCESS and FINESA arrays, the method has been applied for monitoring continuously the Novaya Zemlya test site for a full one-week period. It is demonstrated that the implementation of the threshold monitoring method in the IMS system enables real-time operation. The displays provided by the threshold monitor are particularly valuable in pointing out time intervals of special interest, thus aiding the analyst in his work. The interesting intervals can then be examined by different processing techniques to locate and identify the events. In the actual one-week monitoring experiment, we have found that the combined three-array threshold for Novaya Zemlya is $m_b = 2.2$ or lower 50 % of the time, and $m_b = 2.5$ or lower 99 % of the time. All instances where the threshold exceeds $m_b = 2.5$ correspond to actual interfering seismic events, either regional or teleseismic. Methods are currently being studied on how to further analyze the data during such interference, with the aim to establish operationally reliable monitoring at the lowest possible threshold.

The concept of a very small "hybrid" array/3-component station has been studied. We have used the NORESS A-ring subarray as a test station for a one-week on-line detection processing experiment. We have found that this small array, which has a diameter of only 300 m (i.e., 1/10 of that of NORESS) has a remarkably good performance in distinguishing P and S phases (based on phase velocity estimates) and in obtaining useful azimuth estimates for all phase types. Thus it would appear that supplementing 3-component stations with small triangular arrays of the A-ring type would to a large extent alleviate the problems now encountered in 3-component analysis of secondary phases.

Work is proceeding toward establishing two modern 3-component stations in Poland (Ksiaz and Stary Folwark) with continuous data transmission by satellite to NDPC for integration into the IMS processing. An initial report on the system design, including site descriptions, communication arrangements and the NDPC data acquisition system is presented. An example of data recorded at Ksiaz indicates that data from this station are of high quality and will give a valuable contribution to the regional station network.

Further work on statistically optimal array detection, using a generalization of Capon's maximum likelihood technique, is reported. Examples are presented both for array detection and onset time estimation of regional and teleseismic phases. It is shown in particular that the very strong, low frequent microseismic noise observed at NORESS and ARCESS can be effectively suppressed, due to the high noise coherency. Thus it is possible to regenerate signal waveforms for which the signal is represented in an undistorted way, whereas the microseismic noise is suppressed by as much as 12–18 dB.

AFTAC Project Authorization	:	T/9141/B/PKP
ARPA Order No.	:	4138 AMD # 16
Program Code No.	:	0F10
Name of Contractor	:	Royal Norwegian Council for Scientific and Industrial Research
Effective Date of Contract	:	1 Oct 1988
Contract Expiration Date	:	30 Sep 1991
Project Manager	:	Frode Ringdal (06) 81 71 21
Title of Work	:	The Norwegian Seismic Array (NORSAR) Phase 3
Amount of Contract	:	$ 6,401,883
Contract Period Covered by Report	:	1 Apr – 30 Sep 1990

This research was supported by the Advanced Research Projects Agency of the Department of Defense and was monitored by AFTAC, Patrick AFB, FL 32925, under contract no. F08606-89-C-0005.

NORSAR Contribution No. 434

Table of Contents

Page

1. **Summary** 1

2. **NORSAR Operation** 3

2.1 Detection processor (DP) operation 3
2.2 Array communications 8
2.3 Event detection operation 13

3. **Operation of Regional Arrays** 14

3.1 Recording of NORESS data at NDPC, Kjeller 14
3.2 Recording of ARCESS data at NDPC, Kjeller 18
3.3 Recording of FINESA data at NDPC, Kjeller 23
3.4 Event detection operation 27
3.5 IMS operation 41

4. **Improvements and Modifications** 44

4.1 NORSAR 44
4.2 NORESS/ARCESS/FINESA/GERESS 44

5. **Maintenance Activities** 50

5.1 Activities in the field and at the Maintenance Center 50
5.2 Array status 54

6. **Documentation Developed** 55

Page

7. Summmary of Technical Reports / Papers Published 56

7.1 Detection and yield estimation studies 56
7.2 Initial results from real-time processing of GERESS array data 67
7.3 Generalized beamforming using a network of four regional arrays 75
7.4 Continuous threshold monitoring of the Novaya Zemlya test site 82
7.5 Real-time processing using a hybrid 3-component/small array station 96
7.6 Development of two three-component stations in Poland 110
7.7 Optimal group filtering and noise attenuation for the NORESS and 115
ARCESS arrays

1 Summary

This Semiannual Technical Summary describes the operation, maintenance and research activities at the Norwegian Seismic Array (NORSAR), the Norwegian Regional Seismic Array (NORESS) and the Arctic Regional Seismic Array (ARCESS) for the period 1 April – 30 September 1990. Statistics are also presented for additional seismic stations, which through cooperative agreements with institutions in the host countries provide continuous data to the NORSAR Data Processing Center (NPDC). These stations comprise the Finnish Experimental Seismic Array (FINESA), the German Experimental Seismic Array (GERESS), and from the fall of 1990, two 3-component station in Poland: Ksiaz and Stary Folwark. This Semiannual Report also presents statistics from operation of the Intelligent Monitoring System (IMS). The IMS has been operated in an experimental mode using NORESS and ARCESS data, and the performance has been very satisfactory.

The NORSAR Detection Processing system has been operated throughout the period with an average uptime of 98.0% as compared to 91.8% for the previous reporting period. A total of 2359 seismic events have been reported in the NORSAR monthly seismic bulletin. The performance of the continuous alarm system and the automatic bulletin transfer by telex to AFTAC has been satisfactory. A system for direct retrieval of NORSAR waveform data through an X.25 connection has been implemented, and has been tested successfully for acquiring such data by AFTAC. Processing of requests for full NORSAR/NORESS data on magnetic tapes has progressed according to established schedules.

On-line detection processing and data recording at the NORSAR Data Processing Center (NDPC) of NORESS, ARCESS and FINESA data have been conducted throughout the period, with an average uptime of 92.9% for NORESS and 95.6% for ARCESS. The field computer at the FINESA array was damaged during a thunderstorm in May, and FINESA was out of operation until the end of August. The Intelligent Monitoring System was installed at NORSAR in December 1989 and has been operated experimentally since 1 January 1990. Results of the IMS analysis for the reporting period are given.

There have been no modifications made to the NORSAR data acquisition system. The process of evaluating technical options for upgrading the array is continuing. A test of a full subarray acquisition system will be performed during the next reporting period.

The routine detection processing of NORESS, ARCESS and FINESA is running satisfactorily on each of the arrays' SUN-3/280 data acquisition systems. The routine processing of FINESA data at NORSAR is similar to what is done in Helsinki. GERESS data acquisition and detection processing has

commenced during the period.

Maintenance activities in the period comprise preventive/corrective maintenance in connection with all the NORSAR subarrays, NORESS and ARCESS. In addition, the maintenance center has been involved with modification of equipment for FINESA and preparatory work in connection with NORESS HF instrumentation. Other activities involved testing of the NORSAR communications systems.

The research activity is summarized in Section 7. Section 7.1 presents a continuation of the evaluation of the stability of RMS Lg for yield estimation purposes. Initial results from real-time processing of GERESS array data are given in Section 7.2. In Section 7.3 a study of generalized beamforming using a network of regional arrays is presented. The continuous threshold monitoring technique as applied to the Novaya Zemlya test site is discussed in Section 7.4. Section 7.5 discusses real-time processing using data from a hybrid 3-component/small array station. In Section 7.6 development work, including system design, site descriptions, communication arrangements and the NDPC data acquisition system, in connection with two new three-component stations in Poland is presented. Optimal group filtering and noise attenuation for the NORESS and ARCESS arrays is discussed in Section 7.7.

2 NORSAR Operation

2.1 Detection Processor (DP) operation

There have been 55 breaks in the otherwise continuous operation of the NORSAR online system within the current 6-month reporting interval. The uptime percentage for the period is 98.0 as compared to 91.8 for the previous period.

Fig. 2.1.1 and the accompanying Table 2.1.1 both show the daily DP downtime for the days between 1 April and 30 September 1990. The monthly recording times and percentages are given in Table 2.1.2.

The breaks can be grouped as follows:

a)	Hardware failure	12
b)	Stops related to program work or error	4
c)	Hardware maintenance stops	2
d)	Power jumps and breaks	3
e)	TOD error correction	10
f)	Communication lines	24

The total downtime for the period was 87 hours and 11 minutes. The mean-time-between-failures (MTBF) was 3.2 days, as compared to 1.6 for the previous period.

J. Torstveit

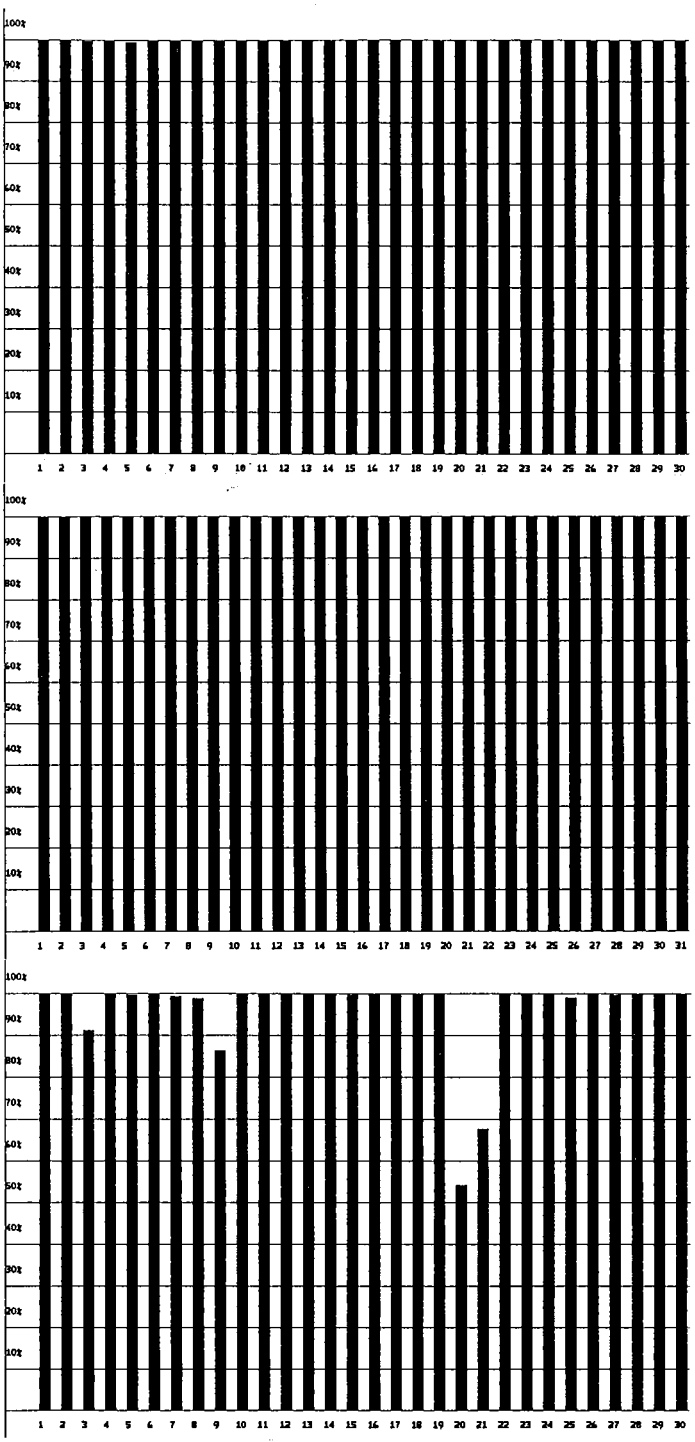

Fig. 2.1.1 Detection Processor downtime for April (top), May (middle) and June (bottom) 1990.

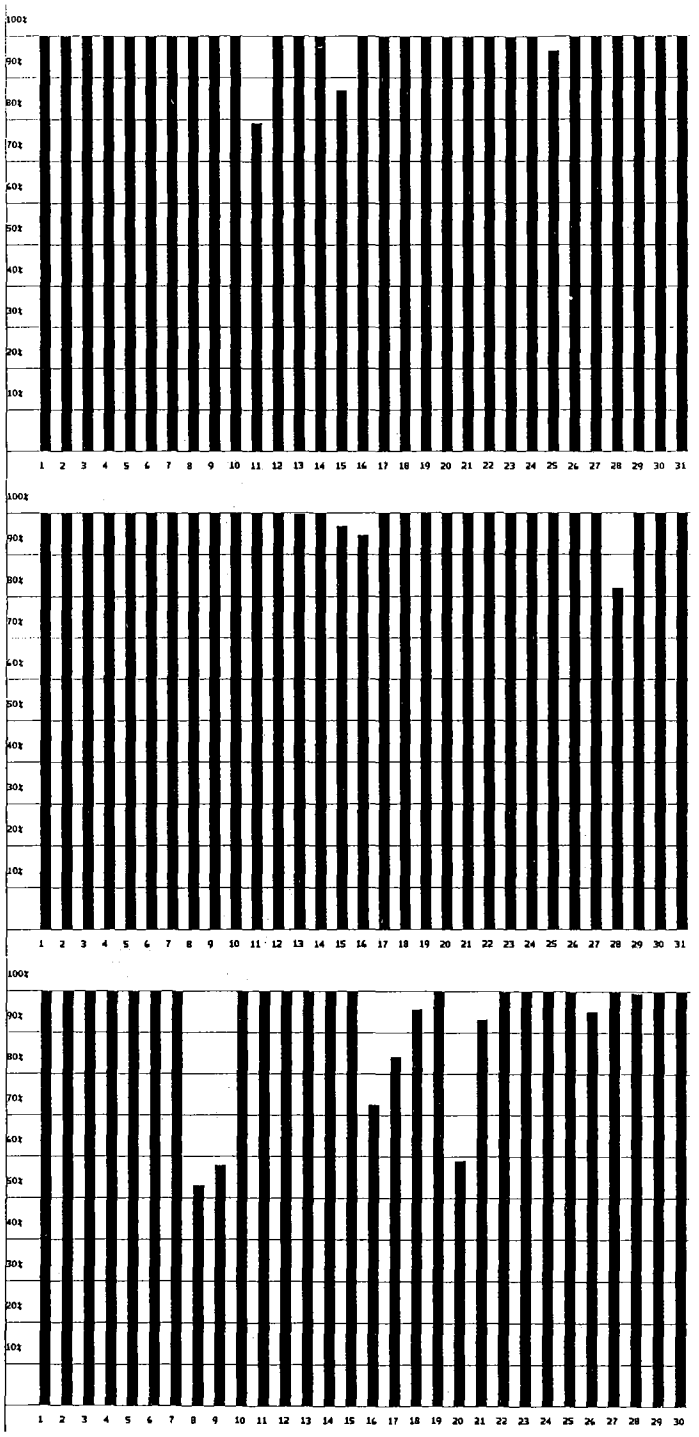

Fig. 2.1.1 Detection Processor downtime for July (top), August (middle) and September (bottom) 1990.

LIST OF BREAKS IN DP PROCESSING THE LAST HALF-YEAR

DAY	START		STOP		COMMENTS.....
92	5	40	5	42	TOD RETARED 14MS
93	4	57	5	0	TOD RETARED 7MS
95	7	59	8	6	TOD ADJUSTMENT
107	6	0	6	2	TOD RETARED 27MS
113	6	14	6	16	TOD RETARED 13MS
116	12	35	12	37	TOD RETARED 40MS
122	12	0	12	2	TOD RETARED 12 S
154	6	14	8	19	CPU FAILURE
156	6	54	6	57	TOD RETARED 7MS
158	6	10	6	14	LINE FAILURE
158	11	24	11	28	LINE FAILURE
159	8	45	8	48	LINE FAILURE
159	9	2	9	7	LINE FAILURE
159	9	37	9	40	LINE FAILURE
159	9	58	10	0	LINE FAILURE
159	12	12	12	14	LINE FAILURE
160	18	21	21	36	AIRCOND. FAILURE
166	9	16	9	19	LINE FAILURE
171	13	0	24	0	LINE FAILURE
172	0	0	7	44	LINE FAILURE
176	12	8	12	22	CE MAINTENANC
178	6	31	6	34	TOD RETARED 31MS
184	5	42	5	43	LINE FAILURE
184	10	53	10	54	LINE FAILURE
185	10	28	10	29	LINE FAILURE
185	10	34	10	35	LINE FAILURE
187	11	29	11	30	LINE FAILURE
192	6	28	11	27	MODCOMP FAILURE
196	16	35	19	42	AIRCOND. FAILURE
199	11	48	11	50	LINE FAILURE
200	12	25	12	27	LINE FAILURE
201	10	18	10	20	LINE FAILURE
206	8	30	9	19	POWER FAILURE
225	6	48	6	50	LINE FAILURE
225	11	55	11	57	LINE FAILURE
227	11	2	12	47	DP-ONLINE TEST
228	10	7	11	20	DP-ONLINE TEST
228	11	32	11	34	LINE FAILURE
232	6	23	6	25	LINE FAILURE
239	10	45	10	47	LINE FAILURE
240	1	30	4	40	POWER BREAKE
240	6	27	6	30	LINE FAILURE
240	6	34	7	38	POWER BREAKE
249	6	0	6	2	TOD RETARED 8MS
251	12	43	24	0	SOFTWARE PROBLEM
252	0	0	10	6	SOFTWARE PROBLEM
259	5	49	12	25	HARDWARE FAILURE
260	2	49	6	36	HARDWARE FAILURE
261	2	45	3	45	HARDWARE FAILURE
261	5	38	5	40	LINE FAILURE
263	0	18	5	20	SOFTWARE PROBLEM
263	13	43	18	0	MAINTENANCE POWER
263	19	15	19	45	HARDWARE FAILURE
264	12	1	12	15	HARDWARE FAILURE
264	21	59	23	22	HARDWARE FAILURE
269	19	25	20	33	HARDWARE FAILURE
271	13	18	13	25	HARDWARE FAILURE

Table 2.1.1 Daily DP downtime in the period 1 April – 30 September 1990.

Month	DP Uptime Hours	DP Uptime %	No. of DP Breaks	No. of Days with Breaks	DP MTBF* (days)
APR 90	719.72	99.96	6	6	4.3
MAY 90	743.97	100.00	1	1	
JUN 90	695.17	96.55	14	10	1.9
JUL 90	743.92	98.88	11	9	2.6
AUG 90	736.58	99.00	10	6	2.8
SEP 90	674.50	93.68	13	10	2.0
		98.03	55	42	3.2

*Mean-time-between-failures = total uptime/no. of up intervals.

Table 2.1.2 Online system performance, 1 April – 30 September 1990.

2.2 Array communications

General

Table 2.2.1 reflects the performance of the communications system throughout the reporting period.

April and May were good months regarding the communications systems. 02C failed due to loss of power, and 06C had problems due to an irregularity related to the CTV equipment.

June was characterized by unstable line conditions affecting all the subarrays, but also subarray electronics failed (02B) and a communication cable between Berger central and the CTV (04C) failed.

In July 02B lost power (week 28), 03C lost synchronization frequently (week 28), and 06C was down approximately 8 hours (week 27) in connection with loss of synchronization after TOD adjustment.

In August 4 subarrays were affected: 02B (weeks 33,34) caused by lightning and loss of power; 02C (week 33) due to an unknown cause; 04C also in connection with lightning and loss of power; 06C was interrupted 11 August, also due to an unknown reason and resumed operation 13 August after a Modcomp restart.

September was also a good period with regard to the communications systems. Only 02B was affected, experiencing spikes on SP channel 04. As previously stated in our reports, the TOD (Time of Day Generator) is less reliable than before, and will probably soon be replaced with by a new system.

Detailed summary

April (weeks 14–17), 2–29.4.90

02C was down from 28 April due to loss of power.

May (weeks 18–22), 30.4–3.6.90

As stated above 02C was affected by loss of power (week 22) and 06C was affected by an irregularity related to the CTV equipment (weeks 20, 21 and 22).

June (weeks 23–26), 4.6–1.7.90

In June all the subarray communications systems were affected by the NTA transmission system (20–21 June). In addition, individual subarrays were also affected: 02B by power outage and SLEM failure (weeks 23, 24 and 25) and 02C (weeks 23, 24) by power failure. Also 04C continued to fail in connection

with a bad cable section between Berger central and the CTV.

July (weeks 27–30), 2–29.7.90

02B, which is in an exposed position with respect to wind, lightning and snow conditions, again failed (9–16 July) due to loss of power. Afterwards NMC Hamar had to reset the SLEM. 03C was affected 4, 10–11 July by excessive resynchronization attempts.

The 04C communications problems, where NTA, NMC and NDPC were involved, were brought to an end 10 July. The next two weeks of the period the communications system operated well. 06C was affected 4 July for approximately 8 hours as a cable between Løten and the subarray was cut by an excavator.

August (weeks 31–35), 30.7–2.9.90

02B was affected 15 and 17 August by lightning and loss of power. In both cases visits to the subarray were necessary to restore the SLEM operation.

18 and 20 August 02C went down, reason not found. After Modcomp restart, the system resumed operation.

Also 04C was affected by lightning and power loss 9 and 16 August.

06C was interrupted 11 August due to an unknown cause. After a Modcomp restart 13 August, the system resumed operation.

September (weeks 36–39), 3–30.9.90

In September all communications systems functioned satisfactorily. 02B was affected between 22 and 24 September probably under the influence of spikes on SP channel 4.

O.A. Hansen

Sub-arrays	Apr 90 (4) 2-29.4	May 90 (5) 30.4-3.6	Jun 90 (4) 4.6-1.7	Jul 90 (4) 2-29.7	Aug 90 (5) 30.7-2.9	Sep 90 (4) 3-30.9	Average 1/2 year
01A	0.0020	0.0030	2)*0.002	0.002	0.012	0.003	0.004
01B	0.0060	0.0050	3)*0.004	0.009	0.003	0.012	0.006
02B	0.0020	0.0040	4)*N/A	9)*0.003	13)*0.002	17)*0.014	18)0.005
02C	0.0009	0.0020	5)*N/A	0.006	13)*0.007	0.003	19)0.004
03C	0.0010	0.0020	6)*0.600	10)*0.011	0.004	0.022	0.107
04C	0.0010	0.0010	7)*0.890	11)*0.008	15))*0.006	0.001	0.150
06C	0.0010	1)*0.0310	8)*0.890	12)*0.0007	16)*0.001	0.006	*0.103
AVER	0.0020	0.0070	0.470	0.005	0.005	0.009	0.054
LESS			02B 02C				

*See Section 2.2 regarding figures preceded by an asterisk.
Figures representing error rate (in per cent) preceded by a number 1), 2), etc., are related to legend below.

1),6),11),13)	Average 2 weeks (18,19 / 24,26 / 29,30 / 31,32)
4),5),7),8)	Average 1 week (26,24)
2),3),9),10),12)	Average 3 weeks (23,24,26 / 27,29,30 / 28-30)
14),15),16)	Average 3 weeks (31,32,35 / 31,34,35)
17)	Average 2 weeks (38,39)
18),19)	Average 5 months

Table 2.2.1 Communications performance. The numbers represent error rates in per cent based on total transmitted frames/week (1 April – 30 September 1990).

2.3 Event detection operation

In Table 2.3.1 some monthly statistics of the Detection and Event Processor operation are given. The table lists the total number of detections (DPX) triggered by the on-line detector, the total number of detections processed by the automatic event processor (EPX) and the total number of events accepted after analyst review (teleseismic phases, core phases and total).

	Total	Total	Accepted events			
	DPX	EPX	P-phases	Core phases	Sum	Daily
Apr 90	10350	1282	300	70	370	12.3
May 90	7100	1209	348	87	435	14.0
Jun 90	7700	1326	284	70	354	11.8
Jul 90	8100	1401	482	69	551	17.8
Aug 90	8025	1203	287	79	366	11.8
Sep 90	8475	1007	233	50	283	9.4
			1934	425	2359	12.9

Table 2.3.1. Detection and Event Processor statistics, 1 April – 30 September 1990.

B. Paulsen

3 Operation of Regional Arrays

3.1 Recording of NORESS data at NDPC, Kjeller

Table 3.1.1 lists the main outage times and reasons, and as can be seen the main reasons for the outages are hardware failure at the HUB and line failure.

The average recording time was 92.9% as compared to 96.9% for the previous period.

Date	Time	Cause
3 Apr	0216-0401	Power failure HUB
3 Apr	0640-0808	Power failure HUB
3 Apr	0829-1210	Power failure HUB
3 Apr	2041-2155	Power failure HUB
3 Apr	2159-	Power failure HUB
4 Apr	-1107	Power failure HUB
6 Apr	2338-	Software failure
7 Apr	-1415	Software failure
7 Apr	1742-1752	Transmission line failure
10 Apr	0511-0609	Transmission line failure
10 Apr	1200-2008	Hardware failure HUB
21 Apr	0014-0029	Transmission line failure
26 Apr	1937-1959	Transmission line maintenance
2 May	1931-	Hardware failure HUB
8 May	-1014	Hardware failure HUB
14 May	0734-	Hardware failure HUB
15 May	-0921	Hardware failure HUB
29 May	0039-0537	Transmission line failure
29 May	0555-0604	Transmission line failure
31 May	1423-1918	Power failure HUB
5 Jun	0523-1510	Software work
6 Jun	1256-1336	Transmission line failure
11 Jun	0600-0643	Transmission line failure
11 Jun	1106-1339	Transmission line failure
12 Jun	2207-2304	Power failure HUB
14 Jun	1050-1107	Hardware failure NDPC
19 Jun	2207-2319	Power break HUB
28 Jun	0859-1506	Power break HUB
28 Jun	1728-1753	Power break HUB

4	Jul	0727-	Hardware failure NDPC
5	Jul	-1718	Hardware failure NDPC
7	Jul	1102-1108	Transmission line failure
25	Jul	0830-0943	Power break NDPC
27	Jul	0004-0057	Hardware failure NDPC
27	Jul	0949-1158	Hardware failure NDPC
1	Aug	1150-1223	Hardware maintenance HUB
8	Aug	1542-1608	Hardware failure NDPC
17	Aug	1211-1235	Transmission line test
17	Aug	1259-1334	Transmission line test
21	Aug	0829-0902	Transmission line test
28	Aug	0156-0302	Power break NDPC
28	Aug	0823-1031	Power break NDPC
3	Sep	0844-0915	Power break NDPC
3	Sep	0952-1010	Power break NDPC
3	Sep	1023-1027	Power break NDPC
13	Sep	1101-1204	Transmission line test
17	Sep	1213-1234	Transmission line test
26	Sep	1239-1340	Hardware work HUB
30	Sep	0100-0200	Software failure

Table 3.1.1. Interruptions in recording of NORESS data at NDPC, 1 April – 30 September 1990.

Monthly uptimes for the NORESS on-line data recording task, taking into account all factors (field installations, transmissions line, data center operation) affecting this task were as follows:

April	:	93.6%
May	:	76.5%
June	:	96.3%
July	:	93.6%
August	:	98.5%
September	:	98.9%

Fig. 3.1.1 shows the uptime for the data recording task, or equivalently, the availability of NORESS data in our tape archive, on a day-by-day basis, for the reporting period.

J. Torstveit

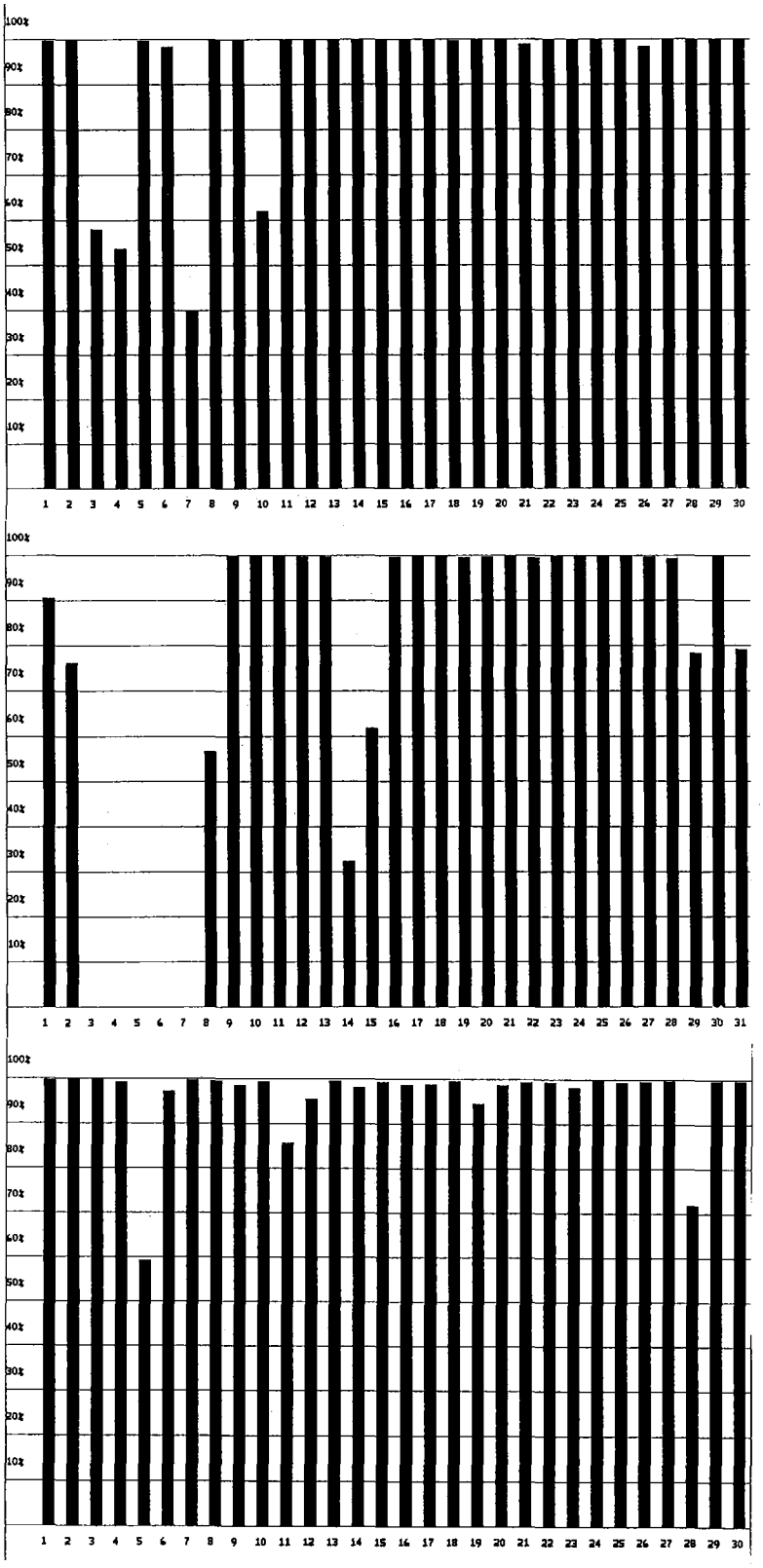

Fig. 3.1.1. NORESS data recording uptime for April (top), May (middle) and June (bottom) 1990.

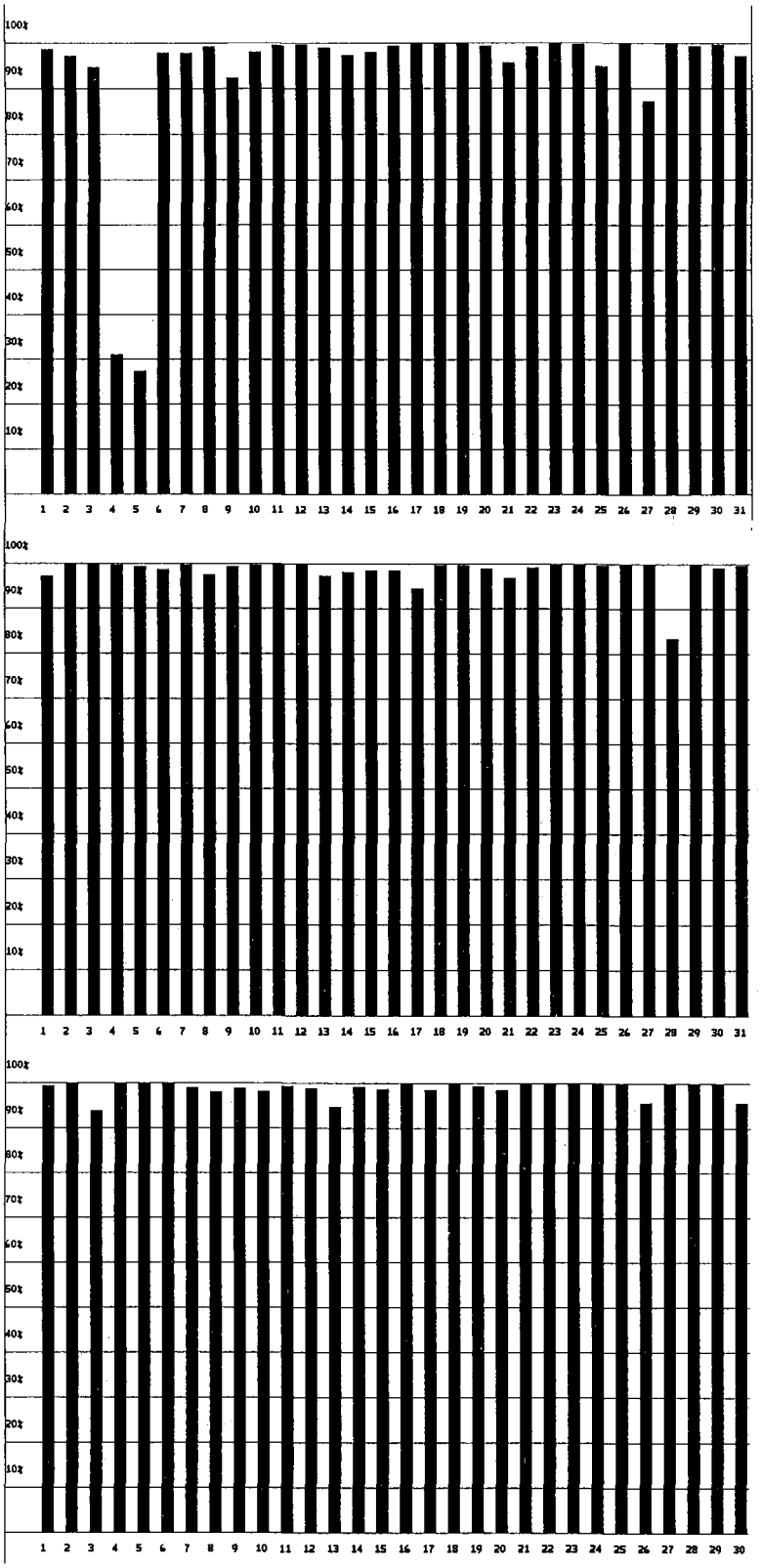

Fig. 3.1.1. (cont.) NORESS data recording uptime for July (top), August (middle) and September (bottom) 1990.

3.2 Recording of ARCESS data at NDPC, Kjeller

The main reasons causing most of the ARCESS outage in the period are: Hardware failure at NDPC or HUB, power failure at HUB and work by the power company to reinforce the line from which power is supplied for ARCESS. Outage intervals are listed in Table 3.2.1.

The average recording time was 95.6% as compared to 95.3% for the previous period.

Date	Time	Cause
24 Apr	2058-	Power break HUB
25 Apr	-0355	Power break HUB
25 Apr	1322-1336	Power break HUB
25 Apr	2100-	Power break HUB
26 Apr	-0408	Power break HUB
26 Apr	2110-0648	Power break HUB
9 May	1124-1348	Software maintenance
10 May	1426-	Hardware failure NDPC
11 May	-0451	Hardware failure NDPC
11 May	0641-0819	Hardware failure NDPC
13 May	2102-	Work on powerline HUB
14 May	-0605	Work on powerline HUB
14 May	2101-	Work on powerline HUB
15 May	-0527	Work on powerline HUB
15 May	2100-	Work on powerline HUB
16 May	-0535	Work on powerline HUB
20 May	2102-	Work on powerline HUB
21 May	-0324	Work on powerline HUB
21 May	2102-	Work on powerline HUB
22 May	-0608	Work on powerline HUB
22 May	2058-	Work on powerline HUB
23 May	-0451	Work on powerline HUB
25 May	2219-2319	Hardware failure NDPC
26 May	1315-1348	Hardware failure NDPC
6 Jun	1747-1916	Transmission line failure
7 Jun	1540-1724	Transmission line failure
8 Jun	1019-1052	Hardware failure NDPC
10 Jun	1149-1210	Hardware failure NDPC
1 Jul	0828-0912	Software failure
3 Jul	1437-	Transmission line failure

4 Jul	-1011	Transmission line failure
5 Jul	1058-1115	Software failure
5 Jul	1502-1553	Software failure
7 Jul	0850-0913	Software failure
7 Jul	1434-1447	Hardware failure NDPC
8 Jul	0902-0925	Hardware failure NDPC
9 Jul	2112-2125	Software failure
14 Jul	0504-0620	Software failure
14 Jul	1730-1738	Software failure
21 Jul	2134-	Software failure
22 Jul	-0809	Software failure
23 Jul	1156-	Hardware failure HUB
24 Jul	-1854	Hardware failure HUB
25 Jul	0757-0839	Power break NDPC
3 Aug	0705-0814	Software failure
4 Aug	0942-0952	Software failure
22 Aug	0437-0522	Software failure
23 Aug	0531-0556	Software failure
23 Aug	1832-1849	Software failure
28 Aug	0114-0305	Power break NDPC
28 Aug	0548-0715	Power break NDPC
28 Aug	0823-1031	Power break NDPC
3 Sep	0844-0915	Power break NDPC
3 Sep	0952-1010	Power break NDPC
3 Sep	1023-1027	Power break NDPC
13 Sep	2238-	Hardware failure NDPC
14 Sep	-0529	Hardware failure NDPC
20 Sep	1329-1339	Work on power NDPC
20 Sep	1632-1749	Power break HUB
25 Sep	1529-	Hardware failure NDPC
26 Sep	-0539	Hardware failure NDPC

Table 3.2.1. The main interruptions in recording of ARCESS data at NDPC, 1 April – 30 September 1990.

Monthly uptimes for the ARCESS on-line data recording task, taking into account all factors (field installations, transmissions line, data center operation) affecting this task were as follows:

April	:	96.7%
May	:	90.7%
June	:	99.4%
July	:	91.1%
August	:	98.9%
September	:	96.7%

Fig. 3.2.1 shows the uptime for the data recording task, or equivalently, the availability of ARCESS data in our tape archive, on a day-by-day basis, for the reporting period.

J. Torstveit

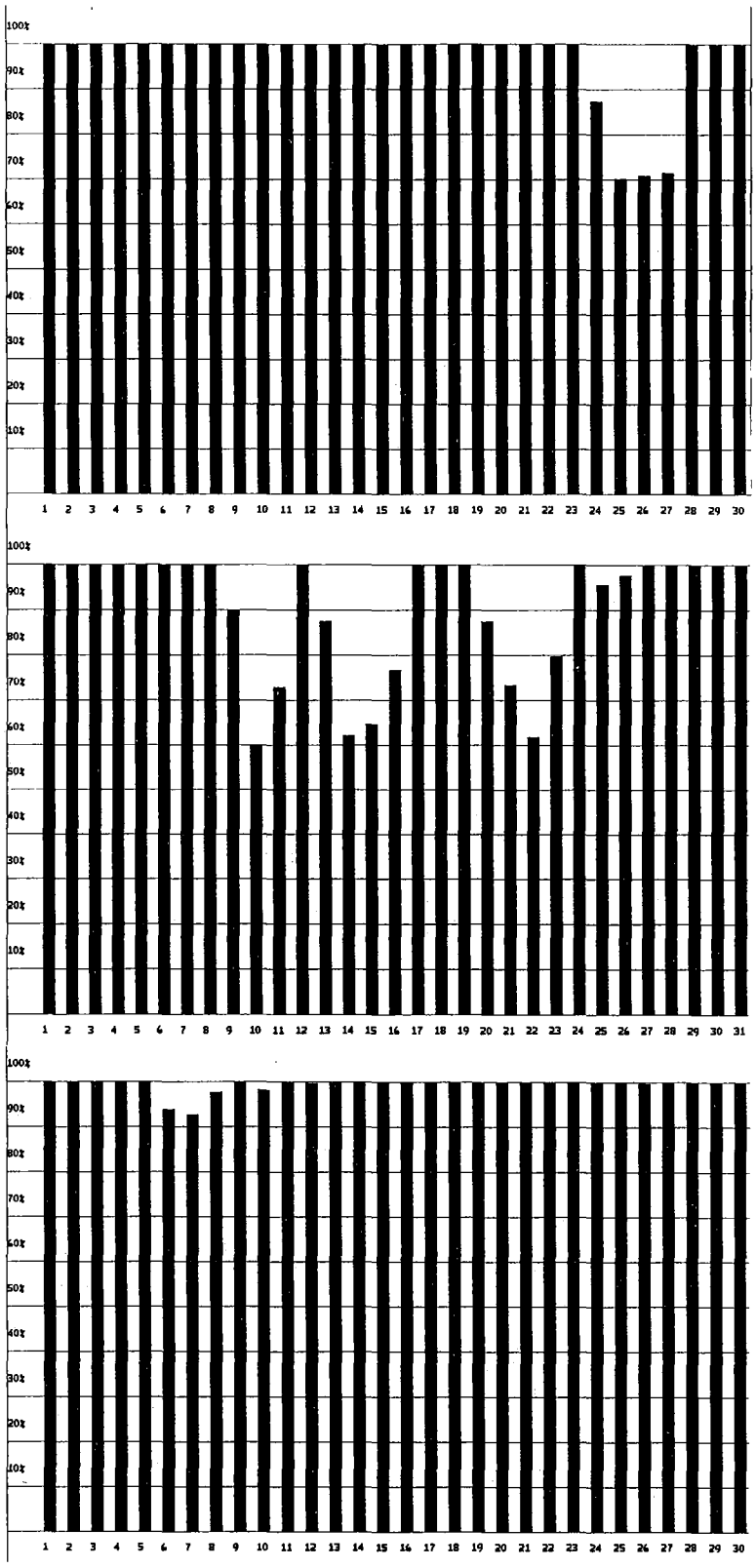

Fig. 3.2.1. ARCESS data recording uptime for April (top), May (middle) and June (bottom) 1990.

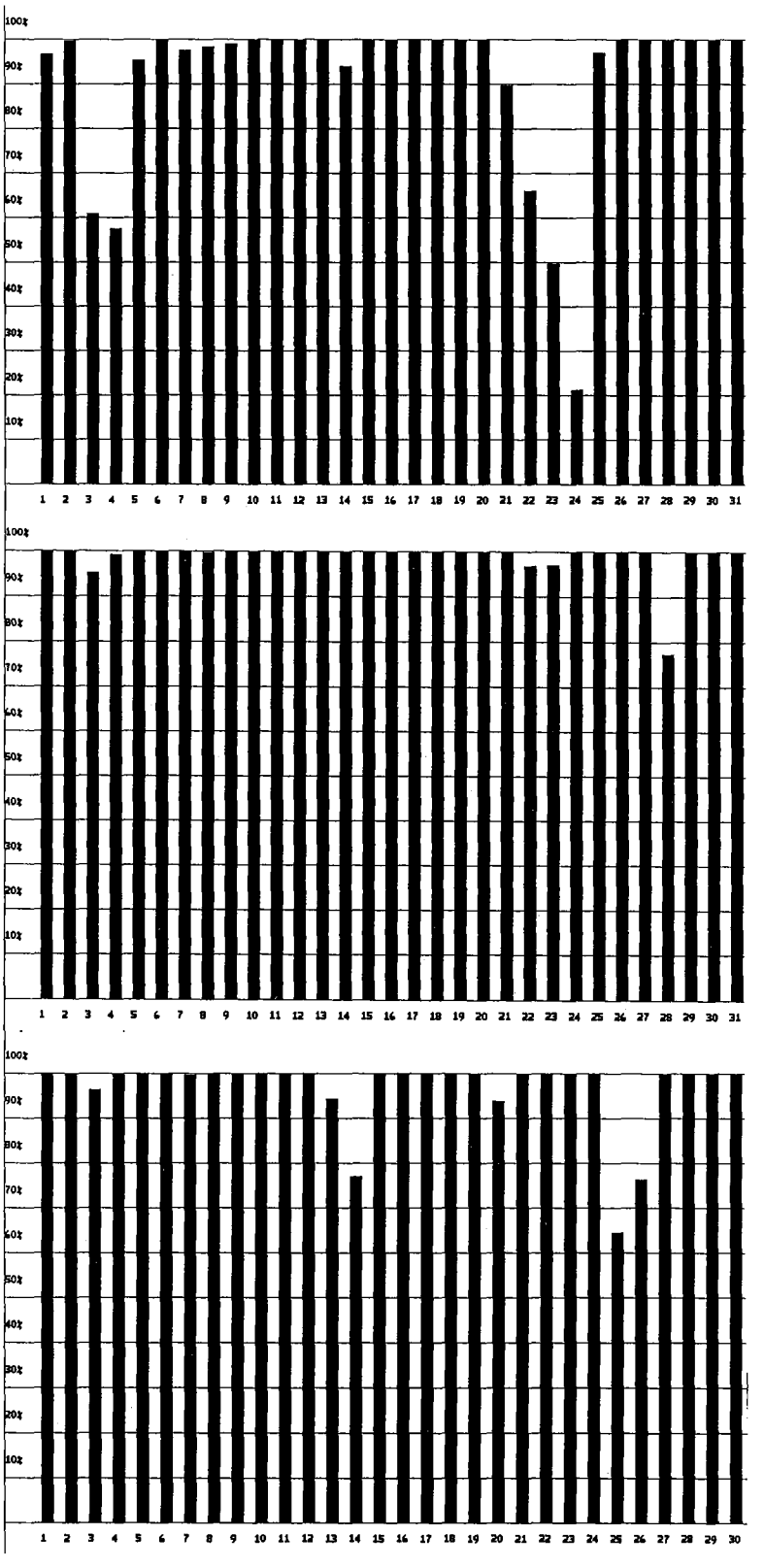

Fig. 3.2.1. (cont.) ARCESS data recording uptime for July (top), August (middle) and September (bottom) 1990.

3.3 Recording of FINESA data at NDPC, Kjeller

The average recording time was 39.0% as compared to 98.5% for the previous period. The main reason for the low uptime of the FINESA array was a thunderstorm on May 22 that put the field computer out of operation until August 26 except for a few hours on June 19.

Date	Time	Cause
2 May	0625-	Hardware/software problems NDPC
8 May	-1925	Hardware/software problems NDPC
15 May	0044-0119	Transmission line failure
15 May	1653-	Transmission line failure
16 May	-1103	Transmission line failure
22 May	0926-	Hardware failure HUB
19 Jun	-0752	Hardware failure HUB
19 Jun	1231-	Hardware failure HUB
26 Aug	-0830	Hardware failure HUB
26 Aug	2328-	Hardware failure HUB
29 Aug	-0955	Hardware failure HUB
29 Aug	1002-1009	Hardware failure HUB
31 Aug	1132-1956	Hardware failure HUB
6 Sep	0940-	Transmission line failure
12 Sep	-0805	Transmission line failure
13 Sep	2314-2332	Transmission line failure
14 Sep	0030-0054	Transmission line failure
18 Sep	0515-0520	Transmission line failure
20 Sep	1328-1400	Maintenance NDPC
20 Sep	1718-1737	Maintenance NDPC
26 Sep	0958-1019	Transmission line failure
26 Sep	1037-1154	Transmission line failure
27 Sep	0743-1302	Transmission line failure

Table 3.3.1 The main interruptions in recording of FINESA data at NDPC, 1 April – 30 September 1990.

Monthly uptimes for the FINESA on-line data recording task, taking into account all factors (field installations, transmissions line, data center operation) affecting this task were as follows:

April	:	100.0%
May	:	45.0%
June	:	0.6%
July	:	0.0%
August	:	9.2%
September	:	79.0%

Fig. 3.3.1 shows the uptime for the data recording task, or equivalently, the availability of FINESA data in our tape archive, on a day-by-day basis, for the reporting period.

J. Torstveit

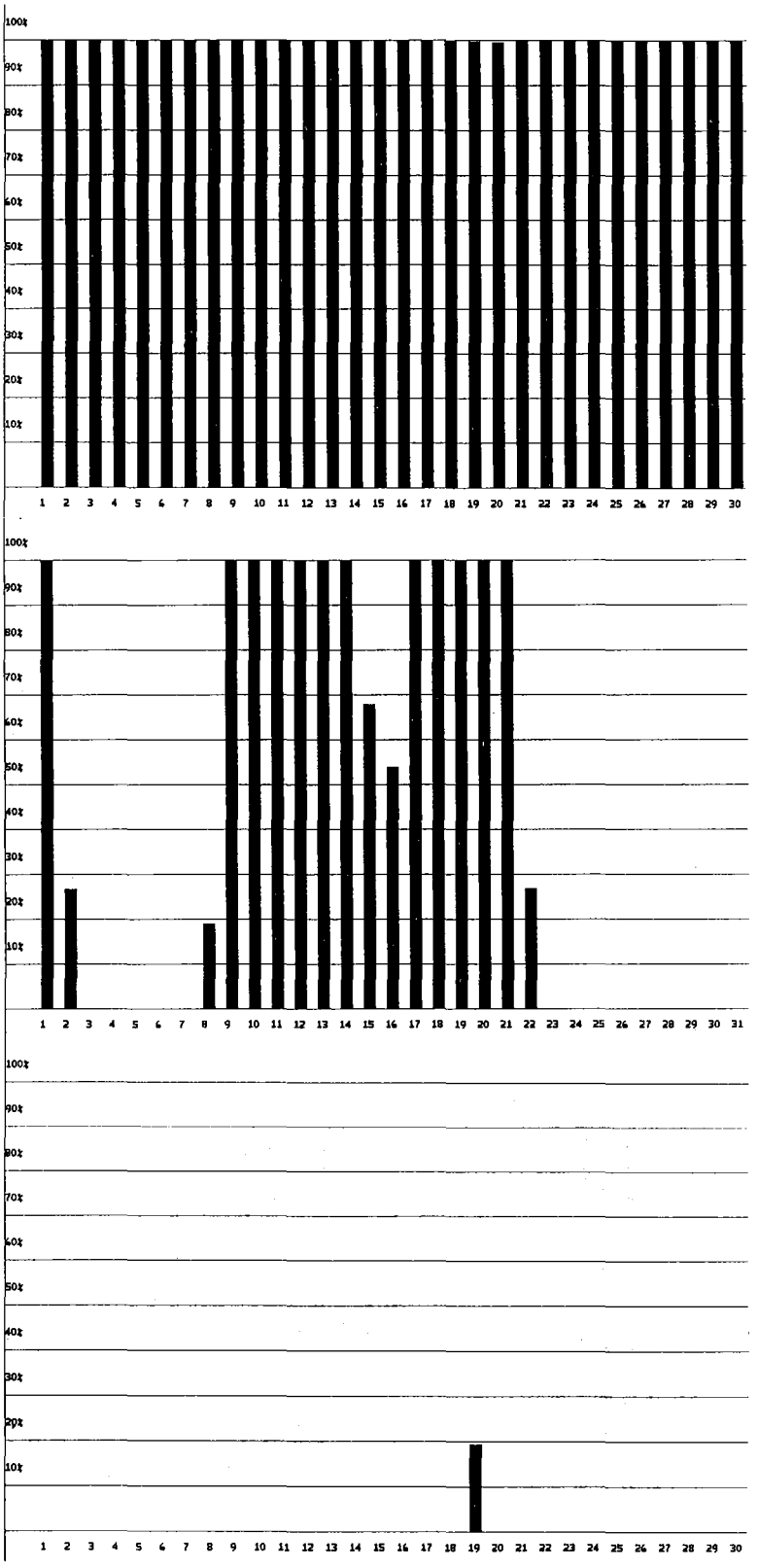

Fig. 3.3.1. FINESA data recording uptime for April (top), May (middle) and June (bottom) 1990.

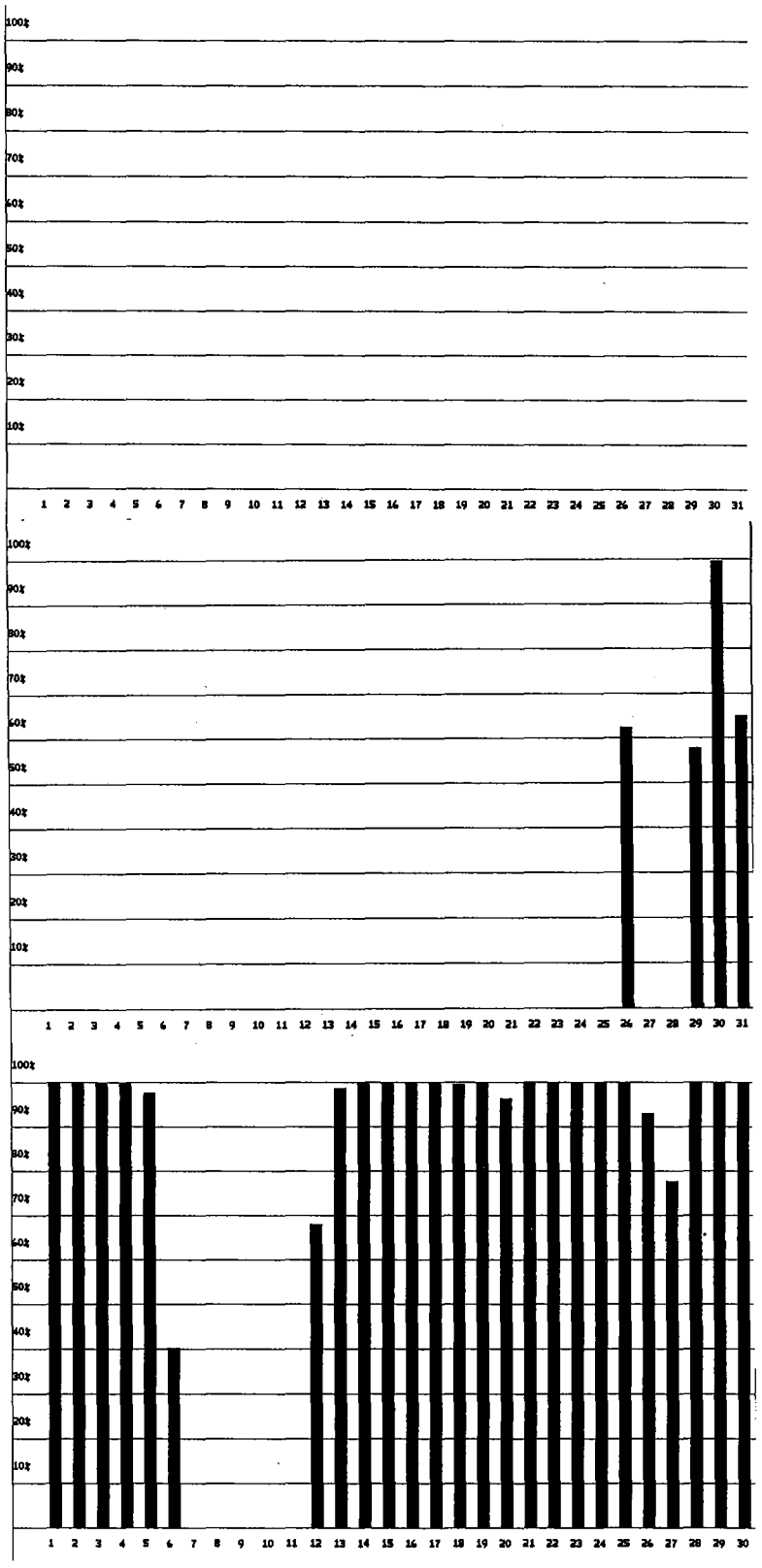

Fig. 3.3.1. (cont.) FINESA data recording uptime for July (top), August (middle) and September (bottom) 1990.

3.4 Event detection operation

NORESS detections

The number of detections (phases) reported during day 091, 1990, through day 273, 1990, was 43734, giving an average of 239 detections per processed day (183 days processed).

Table 3.4.1 shows daily and hourly distribution of detections for NORESS.

Events automatically located by NORESS

During days 091, 1990, through 273, 1990, 2275 local and regional events were located by NORESS, based on automatic association of P- and S-type arrivals. This gives an average 12.4 events per processed day (183 days processed). 60 % of these events are within 300 km, and 86 % of these events are within 1000 km.

ARCESS detections

The number of detections (phases) reported during day 091, 1990, through day 273, 1990, was 84203, giving an average of 460 detections per processed day (183 days processed).

Table 3.4.2 shows daily and hourly distribution of detections for ARCESS.

Events automatically located by ARCESS

During days 091, 1990, through 273, 1990, 4307 local and regional events were located by ARCESS, based on automatic association of P- and S-type arrivals. This gives an average 23.5 events per processed day (178 days processed). 49 % of these events are within 300 km, and 84 % of these events are within 1000 km.

FINESA detections

The number of detections (phases) reported during day 091, 1990, through day 273, 1990, was 28235, giving an average of 392 detections per processed day (72 days processed).

Table 3.4.3 shows daily and hourly distribution of detections for FINESA.

Events automatically located by FINESA

During days 091, 1990, through 273, 1990, 1385 local and regional events were located by FINESA, based on automatic association of P- and S-type arrivals. This gives an average 19.2 events per processed day (72 days processed). 68 % of these events are within 300 km, and 87 % of these events are within 1000 km.

J. Fyen

Day	00	01	02	03	04	05	06	07	08	09	10	11	12	13	14	15	16	17	18	19	20	21	22	23	Sum	Date
91	0	0	0	0	0	0	0	0	1	4	1	3	4	4	1	8	5	7	1	3	5	1	5	7	60	Apr 01 Sunday
92	8	3	11	5	3	4	9	4	3	5	11	4	15	24	22	10	11	12	26	7	19	1	4	10	231	Apr 02 Monday
93	6	10	9	0	2	4	0	0	8	0	0	0	13	6	24	5	7	19	21	8	19	1	1	0	163	Apr 03 Tuesday
94	0	0	0	0	0	0	0	0	0	0	0	15	20	13	8	10	18	12	10	7	12	3	1	12	141	Apr 04 Wednesday
95	1	10	6	0	3	4	3	1	8	7	13	36	11	17	9	5	14	4	11	0	0	0	0	0	163	Apr 05 Thursday
96	0	0	0	0	0	0	0	0	0	0	0	10	9	7	10	12	17	12	16	2	23	7	7	12	144	Apr 06 Friday
97	0	0	0	0	0	0	0	0	0	0	0	0	0	0	4	8	3	1	12	7	17	20	34	27	133	Apr 07 Saturday
98	29	29	38	38	34	11	7	16	12	11	12	14	9	4	4	13	3	7	1	5	9	5	5	5	321	Apr 08 Sunday
99	12	8	14	6	3	7	6	7	17	8	12	11	10	17	6	3	14	5	12	1	17	2	8	8	214	Apr 09 Monday
100	6	3	11	6	5	0	11	0	0	0	0	0	0	0	0	0	0	0	0	0	4	1	1	14	62	Apr 10 Tuesday
101	7	6	7	1	2	8	2	1	9	17	16	18	11	21	4	4	9	13	2	11	1	14	4	18	206	Apr 11 Wednesday
102	0	5	11	7	5	6	4	4	4	17	13	16	16	4	6	4	11	5	6	12	3	5	8	4	176	Apr 12 Thursday
103	9	0	2	7	7	1	9	4	15	13	28	30	16	18	8	4	6	6	3	9	2	4	3	3	207	Apr 13 Friday
104	3	4	3	2	4	11	8	5	10	5	10	4	7	2	4	6	4	3	14	3	4	2	4	2	124	Apr 14 Saturday
105	5	3	3	4	3	2	1	4	1	1	2	5	3	7	0	3	5	1	2	2	1	1	6	3	68	Apr 15 Sunday
106	0	7	10	1	1	1	1	0	1	7	4	8	2	2	2	5	1	8	1	4	4	2	6	5	83	Apr 16 Monday
107	0	11	20	3	3	6	9	1	5	7	5	8	25	7	9	4	10	6	21	9	9	1	3	3	185	Apr 17 Tuesday
108	14	10	11	8	0	10	1	8	11	11	7	22	16	23	28	9	11	8	20	18	23	2	0	10	281	Apr 18 Wednesday
109	6	7	21	5	2	4	7	2	6	14	10	16	12	16	5	8	17	11	9	2	19	1	8	11	219	Apr 19 Thursday
110	5	10	10	1	4	5	7	6	20	9	18	24	13	12	10	8	11	8	11	16	12	1	1	21	243	Apr 20 Friday
111	3	5	13	4	1	5	7	8	6	8	7	1	7	6	11	6	8	23	7	8	6	3	5	12	170	Apr 21 Saturday
112	17	8	5	3	4	4	12	4	4	6	2	30	0	4	6	20	9	27	5	6	6	4	5	19	210	Apr 22 Sunday
113	3	23	12	3	6	2	5	12	12	11	5	16	8	15	5	14	9	11	28	5	22	3	4	13	247	Apr 23 Monday
114	0	18	13	1	1	3	6	0	14	31	5	12	20	5	7	6	15	14	24	7	23	7	3	6	241	Apr 24 Tuesday
115	7	0	24	4	7	5	2	5	5	16	2	10	23	20	15	5	14	11	11	6	17	0	4	15	228	Apr 25 Wednesday
116	4	11	14	8	4	6	7	5	7	22	18	12	7	20	7	12	13	10	5	5	17	4	5	8	231	Apr 26 Thursday
117	4	8	8	4	0	7	4	12	26	14	28	25	13	16	7	12	6	12	23	17	26	11	9	8	300	Apr 27 Friday
118	10	11	11	11	16	14	11	6	7	10	8	8	7	8	13	1	3	4	2	6	9	9	7	13	205	Apr 28 Saturday
119	6	8	14	4	3	3	7	1	4	3	7	19	14	6	5	12	1	10	6	3	5	2	2	14	159	Apr 29 Sunday
120	6	8	12	1	7	4	5	3	2	20	5	4	8	7	3	5	17	7	19	4	15	5	4	6	177	Apr 30 Monday
121	12	11	12	3	9	8	11	0	3	2	1	8	2	5	2	11	8	5	8	2	3	6	5	13	150	May 01 Tuesday
122	1	12	10	3	6	3	4	7	5	1	18	32	18	38	21	3	6	6	7	6	16	5	5	8	241	May 02 Wednesday
123	4	4	7	2	0	3	6	7	5	4	12	2	11	3	4	6	3	12	9	2	5	2	1	4	118	May 03 Thursday
124	1	9	2	2	2	0	3	4	5	5	0	0	5	4	2	0	0	2	0	5	2	0	1	0	54	May 04 Friday
125	4	4	1	4	4	6	4	3	0	2	0	0	2	0	1	0	0	0	0	0	0	2	0	0	37	May 05 Saturday
126	0	0	2	1	0	0	2	0	0	0	3	1	0	0	0	0	8	0	0	0	0	0	0	0	17	May 06 Sunday
127	0	0	3	0	0	1	0	0	0	0	0	0	0	0	0	0	0	0	0	0	0	0	0	0	4	May 07 Monday
128	0	0	0	0	0	0	0	0	0	0	8	7	12	17	9	8	14	3	9	1	4	1	3	3	99	May 08 Tuesday
129	0	4	7	0	6	5	13	13	17	8	18	17	23	8	9	8	35	8	7	17	13	8	1	6	251	May 09 Wednesday
130	4	7	8	1	0	2	2	1	8	5	4	30	19	11	2	3	2	2	17	5	9	6	0	4	152	May 10 Thursday
131	5	3	6	3	2	11	6	5	2	21	9	8	10	14	13	4	3	2	4	14	6	1	3	11	166	May 11 Friday
132	2	4	3	0	4	11	5	2	3	2	4	4	1	1	2	3	5	12	8	1	5	4	2	0	88	May 12 Saturday
133	4	3	3	2	10	0	3	2	8	2	5	11	12	10	26	11	9	13	10	10	3	7	9	10	183	May 13 Sunday
134	9	7	18	7	3	5	4	4	0	0	0	0	0	0	0	0	0	0	0	0	0	0	0	0	57	May 14 Monday
135	0	0	0	0	0	0	0	0	0	7	22	5	22	21	21	9	14	9	19	7	15	10	7	11	199	May 15 Tuesday
136	12	14	14	10	9	7	6	2	8	14	13	16	30	35	9	13	17	16	12	11	16	18	8	17	327	May 16 Wednesday
137	10	26	19	23	21	9	15	15	15	14	40	29	9	17	14	11	18	14	10	11	6	6	2	19	373	May 17 Thursday
138	10	24	9	12	7	5	6	6	19	10	12	11	16	12	11	4	9	9	26	5	18	4	2	11	258	May 18 Friday
139	10	1	11	3	4	8	10	3	3	6	6	10	1	21	13	11	15	2	4	15	13	22	21	20	233	May 19 Saturday
140	36	20	10	5	6	5	12	11	13	5	27	8	13	15	3	18	3	10	10	4	15	1	4	11	265	May 20 Sunday
141	9	4	17	2	2	1	13	7	15	7	15	44	19	25	1	9	7	6	17	3	24	9	2	9	267	May 21 Monday
142	5	5	17	3	0	4	1	13	9	17	7	32	17	24	7	10	10	17	18	14	17	5	1	14	267	May 22 Tuesday
143	4	11	11	4	0	4	0	8	17	13	12	23	27	20	5	10	19	10	56	42	22	10	15	28	371	May 23 Wednesday
144	24	19	27	18	17	21	19	23	14	27	12	27	23	4	10	17	17	21	7	27	43	11	11	13	452	May 24 Thursday
145	26	17	24	14	8	8	6	3	19	20	14	17	10	10	13	9	17	14	20	28	12	19	18	13	359	May 25 Friday
146	8	15	20	14	20	8	13	2	3	12	2	14	7	4	10	4	15	38	16	28	7	4	7	3	274	May 26 Saturday

Table 3.4.1. (Page 1 of 4)

NRS .FKX Hourly distribution of detections

Day	00	01	02	03	04	05	06	07	08	09	10	11	12	13	14	15	16	17	18	19	20	21	22	23	Sum	Date
147	3	3	0	13	11	9	3	2	16	3	15	6	7	15	16	10	29	11	16	24	6	11	9	11	249	May 27 Sunday
148	6	5	5	12	4	10	0	10	14	17	13	19	10	16	13	17	16	17	18	19	6	4	2	12	265	May 28 Monday
149	3	0	0	0	0	0	2	10	11	9	9	19	22	15	9	2	6	20	13	6	14	2	2	5	179	May 29 Tuesday
150	3	12	21	16	2	9	15	19	15	14	20	24	35	15	10	12	10	12	6	8	16	9	1	5	309	May 30 Wednesday
151	11	4	9	9	10	11	9	21	12	8	10	21	15	12	7	0	0	0	0	16	14	4	2	8	213	May 31 Thursday
152	2	11	13	1	0	19	15	15	9	43	10	12	15	7	16	4	13	29	11	8	14	9	10	12	298	Jun 01 Friday
153	19	16	19	27	23	33	17	23	29	20	24	7	10	14	12	7	12	11	6	3	13	4	6	6	361	Jun 02 Saturday
154	0	2	6	3	5	1	12	7	13	3	8	14	6	5	27	15	14	4	5	1	3	12	7	1	174	Jun 03 Sunday
155	6	4	5	4	1	7	0	4	6	20	7	2	5	10	14	17	23	23	12	4	10	8	7	12	211	Jun 04 Monday
156	7	1	10	6	0	1	0	0	0	0	0	0	0	0	0	19	18	22	16	26	20	32	19	27	224	Jun 05 Tuesday
157	22	22	26	29	25	7	13	20	19	17	15	27	16	11	31	31	15	20	32	18	20	24	20	34	514	Jun 06 Wednesday
158	30	33	31	33	24	14	12	13	20	24	31	22	25	24	25	21	16	13	15	14	26	16	30	29	541	Jun 07 Thursday
159	29	15	16	13	9	11	7	6	22	16	15	15	8	19	7	21	19	21	14	19	24	13	19	24	382	Jun 08 Friday
160	20	20	26	27	33	21	23	21	17	45	61	50	20	24	14	45	20	35	36	31	37	38	24	23	711	Jun 09 Saturday
161	29	38	32	28	19	22	17	8	11	6	7	12	13	11	14	13	21	18	14	18	13	6	7	12	389	Jun 10 Sunday
162	15	12	12	7	3	6	0	6	6	11	8	1	0	4	14	6	17	8	13	7	19	3	2	17	197	Jun 11 Monday
163	8	17	14	19	1	11	6	11	1	13	17	22	11	15	16	10	22	31	28	8	26	5	1	19	332	Jun 12 Tuesday
164	9	10	18	8	3	11	8	9	9	8	11	14	14	11	12	15	18	11	13	11	12	5	11	13	264	Jun 13 Wednesday
165	8	2	16	10	3	3	5	22	10	9	14	18	19	21	14	13	4	7	14	22	15	2	12	14	277	Jun 14 Thursday
166	5	0	13	4	1	11	5	11	7	15	14	15	19	19	13	6	9	9	6	16	12	2	3	8	223	Jun 15 Friday
167	0	6	15	9	3	10	26	4	3	15	5	5	14	6	15	2	0	11	4	4	1	5	1	3	167	Jun 16 Saturday
168	1	4	2	1	3	12	4	3	0	15	4	5	3	4	13	8	11	13	12	1	13	20	2	13	167	Jun 17 Sunday
169	3	3	16	2	11	9	6	8	12	5	5	17	8	10	10	13	19	15	9	8	25	1	2	30	247	Jun 18 Monday
170	0	7	11	3	0	5	9	11	8	4	38	13	24	12	8	18	11	10	2	22	15	8	1	7	247	Jun 19 Tuesday
171	8	6	11	0	3	7	2	6	11	13	4	29	16	18	6	14	17	18	18	14	23	17	8	25	294	Jun 20 Wednesday
172	10	13	10	15	4	3	6	12	0	8	17	20	20	21	18	26	15	24	30	18	17	20	13	9	349	Jun 21 Thursday
173	5	3	8	5	2	6	14	10	15	13	18	15	20	12	10	7	18	16	2	1	15	2	4	8	229	Jun 22 Friday
174	2	4	4	2	0	8	7	5	6	10	13	6	14	4	23	16	14	4	9	17	13	10	9	15	215	Jun 23 Saturday
175	14	13	12	20	19	22	11	1	16	15	3	4	14	1	2	10	13	5	6	3	7	1	2	8	222	Jun 24 Sunday
176	4	2	9	0	0	3	4	9	15	7	14	5	9	18	10	5	15	16	14	9	10	3	4	8	193	Jun 25 Monday
177	14	8	7	6	10	10	9	15	28	13	14	9	22	10	18	5	14	32	28	10	16	12	11	9	330	Jun 26 Tuesday
178	13	13	13	5	8	16	7	6	6	8	11	17	26	20	8	16	22	12	6	8	24	6	10	8	289	Jun 27 Wednesday
179	12	11	19	7	1	5	6	16	7	0	0	0	0	0	0	4	11	11	16	9	21	5	2	13	176	Jun 28 Thursday
180	0	2	11	2	6	8	11	22	26	9	13	15	24	15	10	6	9	16	5	9	13	7	1	9	249	Jun 29 Friday
181	4	2	13	2	0	1	5	2	31	8	11	17	10	12	13	28	20	13	15	23	25	10	4	0	269	Jun 30 Saturday
182	8	9	8	14	14	12	11	7	3	17	8	7	20	17	6	10	8	15	6	19	16	14	12	7	268	Jul 01 Sunday
183	4	2	10	6	2	6	5	8	17	7	5	12	10	15	4	13	9	10	20	1	16	6	4	14	206	Jul 02 Monday
184	3	9	5	6	2	5	5	11	7	12	17	5	19	19	16	8	18	16	15	19	21	21	20	29	308	Jul 03 Tuesday
185	27	21	27	26	20	15	7	2	0	0	0	0	0	0	0	0	0	0	0	0	0	0	0	0	145	Jul 04 Wednesday
186	0	0	0	0	0	0	0	0	0	0	0	0	0	0	0	0	0	9	20	13	15	4	6	10	77	Jul 05 Thursday
187	4	4	16	8	1	11	1	18	8	11	5	6	14	14	10	4	18	15	10	10	10	4	4	10	216	Jul 06 Friday
188	2	5	17	1	4	3	8	6	0	14	4	5	0	14	15	20	19	36	22	18	26	28	26	29	322	Jul 07 Saturday
189	32	27	19	34	27	32	23	26	25	13	22	19	14	13	15	17	15	11	21	3	6	8	9	8	439	Jul 08 Sunday
190	1	3	9	5	5	12	1	14	13	7	12	19	10	19	13	23	11	12	9	2	4	0	1	2	207	Jul 09 Monday
191	2	1	7	6	0	7	13	16	24	13	12	7	10	15	4	5	11	14	13	10	3	3	3	9	208	Jul 10 Tuesday
192	4	0	7	0	2	8	2	13	15	8	10	14	10	20	8	10	11	11	12	4	11	5	0	7	192	Jul 11 Wednesday
193	1	2	5	1	4	10	84	20	14	47	34	20	11	33	17	5	9	7	9	23	14	1	1	8	380	Jul 12 Thursday
194	7	0	7	5	8	12	5	13	17	14	12	17	6	12	16	7	13	10	15	12	1	8	2	12	231	Jul 13 Friday
195	6	7	10	3	12	9	19	44	17	46	34	12	17	28	14	11	10	4	6	13	9	6	3	0	340	Jul 14 Saturday
196	8	2	0	1	1	8	2	2	2	9	7	3	0	4	5	9	17	24	13	2	14	11	7	11	162	Jul 15 Sunday
197	3	6	13	4	3	8	3	47	65	36	41	21	28	54	22	18	15	25	20	18	18	14	13	16	511	Jul 16 Monday
198	8	6	27	1	8	5	16	10	19	19	12	11	25	28	6	0	0	0	0	0	0	0	0	0	201	Jul 17 Tuesday
199	0	0	0	0	0	0	2	11	40	36	64	25	23	33	79	30	21	14	22	12	51	4	2	17	486	Jul 18 Wednesday
200	6	22	30	2	14	17	10	5	8	36	15	15	26	20	10	11	17	7	6	16	2	1	3	10	309	Jul 19 Thursday
201	2	4	24	4	12	38	6	8	7	17	13	12	10	6	10	10	32	31	30	13	7	5	3	25	329	Jul 20 Friday
202	2	3	20	8	14	7	12	12	6	10	12	6	4	13	11	7	8	6	14	9	14	0	2	4	204	Jul 21 Saturday

Table 3.4.1. (Page 2 of 4)

NRS .FKX Hourly distribution of detections

Day	00	01	02	03	04	05	06	07	08	09	10	11	12	13	14	15	16	17	18	19	20	21	22	23	Sum	Date		
203	0	29	14	9	3	9	26	4	3	9	11	8	6	3	6	4	29	29	18	13	5	4	6	11	259	Jul	22	Sunday
204	3	8	8	1	0	4	10	16	6	6	7	13	11	23	20	3	47	16	24	23	17	9	8	8	291	Jul	23	Monday
205	1	0	17	2	2	9	5	15	12	17	14	16	11	8	14	9	29	12	29	28	4	8	1	4	267	Jul	24	Tuesday
206	2	2	16	4	9	12	9	19	4	2	8	18	10	26	9	10	12	18	23	15	9	4	6	20	267	Jul	25	Wednesday
207	5	0	20	7	7	14	15	21	11	5	15	14	6	14	7	16	18	15	26	4	5	11	15	21	292	Jul	26	Thursday
208	2	8	18	16	19	28	23	9	6	11	0	0	17	30	19	11	20	20	27	9	6	6	8	17	330	Jul	27	Friday
209	1	4	6	2	11	12	10	5	3	13	10	6	13	16	4	10	10	9	9	14	2	4	4	5	183	Jul	28	Saturday
210	3	6	9	6	3	8	2	3	3	22	10	6	6	6	4	5	15	13	2	8	2	9	5	22	178	Jul	29	Sunday
211	0	3	19	2	10	9	5	3	8	8	10	10	18	19	8	25	41	65	79	66	92	76	82	144	802	Jul	30	Monday
212	88	113	116	88	81	69	65	99	84	99	62	91	0	0	0	0	0	0	0	0	0	0	0	0	1055	Jul	31	Tuesday
213	0	0	0	0	0	0	0	0	0	0	0	0	7	21	10	8	11	23	26	7	4	2	5	14	138	Aug	01	Wednesday
214	4	4	15	0	10	10	8	4	6	13	9	13	26	13	12	27	13	26	28	23	30	21	27	26	368	Aug	02	Thursday
215	24	13	21	8	3	8	4	5	14	15	10	27	19	9	7	19	22	12	8	20	1	7	3	10	289	Aug	03	Friday
216	2	6	13	5	4	9	7	8	7	0	4	4	5	2	3	5	4	3	2	0	1	0	2	1	97	Aug	04	Saturday
217	2	17	3	9	4	1	21	7	7	5	4	1	5	11	8	8	20	16	19	5	0	4	5	12	194	Aug	05	Sunday
218	1	1	13	9	0	9	1	8	3	13	9	12	16	11	15	11	14	13	4	4	17	6	1	7	198	Aug	06	Monday
219	1	0	13	5	3	9	8	9	9	27	9	20	19	20	12	6	18	13	9	13	12	3	2	7	247	Aug	07	Tuesday
220	5	4	18	0	9	8	18	13	4	15	10	15	13	7	10	7	15	7	19	20	10	1	2	12	242	Aug	08	Wednesday
221	3	8	14	9	3	4	9	9	8	18	6	10	23	16	13	6	12	14	7	15	9	2	3	9	230	Aug	09	Thursday
222	6	0	17	5	0	18	7	9	4	16	10	11	31	11	7	19	20	17	9	14	17	6	4	17	275	Aug	10	Friday
223	9	2	23	5	3	6	14	11	21	39	24	14	23	39	17	11	6	20	12	2	13	20	8	3	345	Aug	11	Saturday
224	6	5	15	4	5	17	9	7	13	31	27	8	3	11	6	8	25	26	9	5	4	7	3	15	269	Aug	12	Sunday
225	1	0	7	1	0	2	9	3	12	9	11	12	13	25	16	9	21	2	4	2	14	0	1	14	188	Aug	13	Monday
226	8	3	12	1	5	4	4	7	20	4	11	20	19	15	10	12	17	20	3	13	14	3	3	6	234	Aug	14	Tuesday
227	0	1	9	1	1	3	4	10	9	5	5	19	25	29	10	13	21	22	9	9	41	13	2	20	281	Aug	15	Wednesday
228	11	9	20	12	17	6	6	9	11	10	10	20	25	7	7	8	18	6	13	11	7	4	6	6	259	Aug	16	Thursday
229	4	5	21	4	9	5	3	8	7	10	10	20	6	10	4	5	18	11	8	26	9	6	5	8	222	Aug	17	Friday
230	0	7	14	1	5	9	5	2	5	7	11	10	5	5	16	21	6	16	11	13	2	6	3	0	180	Aug	18	Saturday
231	4	2	2	26	3	5	10	3	25	8	27	5	10	13	16	17	26	17	11	4	7	4	1	8	254	Aug	19	Sunday
232	6	8	11	4	3	6	10	17	6	14	4	10	19	11	12	5	13	15	18	14	4	12	3	10	235	Aug	20	Monday
233	5	15	8	10	4	5	8	5	4	9	3	17	19	18	13	5	17	20	19	10	24	4	1	19	262	Aug	21	Tuesday
234	4	3	7	6	21	10	9	14	8	3	11	11	14	16	7	6	21	29	3	0	14	6	1	18	242	Aug	22	Wednesday
235	1	20	29	1	0	8	9	8	16	10	8	22	13	10	19	6	13	11	10	6	21	0	1	11	253	Aug	23	Thursday
236	3	2	12	4	3	10	9	10	19	15	9	13	30	29	2	10	15	11	16	9	10	0	0	12	253	Aug	24	Friday
237	0	3	13	2	1	5	10	1	5	5	9	10	8	19	7	10	11	4	5	5	4	2	1	1	141	Aug	25	Saturday
238	2	1	3	3	8	0	0	0	0	0	0	0	0	5	8	12	13	12	7	3	6	14	9	15	121	Aug	26	Sunday
239	4	2	23	1	5	0	0	4	0	8	6	12	10	25	11	25	11	11	5	6	11	7	1	13	201	Aug	27	Monday
240	6	24	0	10	13	14	8	3	1	0	3	13	33	18	15	4	8	36	10	8	14	3	6	7	257	Aug	28	Tuesday
241	11	4	14	0	14	12	14	8	7	21	23	13	30	42	19	9	26	8	7	3	20	19	8	15	347	Aug	29	Wednesday
242	3	1	17	3	14	27	10	9	14	9	11	15	39	12	33	19	17	10	6	12	12	12	3	4	312	Aug	30	Thursday
243	0	1	8	3	8	16	5	13	13	30	11	29	13	9	15	10	6	10	11	8	0	2	3	10	234	Aug	31	Friday
244	0	1	14	9	5	8	16	2	9	5	13	5	3	5	2	1	2	4	6	3	6	6	6	2	133	Sep	01	Saturday
245	4	1	2	6	5	3	13	7	0	3	6	6	8	4	4	3	16	11	8	5	3	0	2	16	136	Sep	02	Sunday
246	3	3	23	2	13	11	17	22	4	4	19	8	12	10	12	14	7	5	8	10	13	2	5	12	239	Sep	03	Monday
247	87	18	55	4	21	14	15	9	42	21	20	18	28	8	5	9	11	6	4	11	17	7	3	12	445	Sep	04	Tuesday
248	2	2	9	4	16	33	9	14	34	25	13	8	22	19	7	10	9	10	14	3	24	3	2	10	302	Sep	05	Wednesday
249	3	1	10	5	16	21	8	2	8	7	8	11	15	24	13	11	14	9	3	7	15	1	7	6	225	Sep	06	Thursday
250	6	0	15	1	3	5	13	0	10	22	11	15	9	13	10	7	3	16	7	1	23	1	2	9	202	Sep	07	Friday
251	7	2	17	2	3	4	11	4	1	4	8	8	7	11	8	2	1	3	3	16	5	7	4	5	143	Sep	08	Saturday
252	5	2	6	17	3	15	12	8	5	6	20	3	6	2	3	1	7	12	11	11	3	5	7	9	179	Sep	09	Sunday
253	3	7	9	6	18	7	6	19	14	10	8	11	27	19	16	5	10	8	6	20	6	2	2	12	251	Sep	10	Monday
254	4	3	4	3	1	9	10	5	9	9	22	10	29	16	16	14	16	23	1	8	13	3	4	8	240	Sep	11	Tuesday
255	8	4	13	1	9	13	3	12	13	22	13	26	23	21	12	7	8	8	9	14	5	4	5	11	264	Sep	12	Wednesday
256	1	6	5	7	6	9	7	13	22	6	5	0	19	16	7	.5	13	18	8	7	14	2	5	5	206	Sep	13	Thursday
257	8	7	28	1	2	31	27	21	4	23	3	4	14	12	4	5	8	11	8	12	5	3	0	3	244	Sep	14	Friday
258	0	0	6	7	1	6	15	10	2	6	8	3	5	14	19	16	18	19	10	9	1	4	5	9	193	Sep	15	Saturday

Table 3.4.1. (Page 3 of 4)

NRS .FKX Hourly distribution of detections

Day	00	01	02	03	04	05	06	07	08	09	10	11	12	13	14	15	16	17	18	19	20	21	22	23	Sum	Date
259	3	5	4	7	5	3	9	13	4	5	11	6	4	4	10	11	19	15	8	9	1	4	1	9	170	Sep 16 Sunday
260	20	1	17	4	7	6	8	4	7	15	8	7	17	14	7	7	13	12	0	3	13	4	1	6	201	Sep 17 Monday
261	1	0	5	9	2	5	8	4	12	9	9	9	14	13	10	1	14	11	6	1	11	2	1	7	164	Sep 18 Tuesday
262	2	11	11	1	3	2	5	1	8	10	6	11	6	13	6	2	5	8	2	1	16	4	12	15	161	Sep 19 Wednesday
263	17	9	10	13	8	5	3	4	6	11	5	1	13	5	11	10	14	6	6	9	3	2	2	7	180	Sep 20 Thursday
264	5	1	9	6	4	1	4	4	7	9	12	16	6	13	6	2	10	3	16	0	3	0	3	7	147	Sep 21 Friday
265	2	3	13	1	1	2	10	7	3	8	1	7	2	4	6	10	2	3	4	1	7	3	4	7	111	Sep 22 Saturday
266	12	2	2	5	4	5	11	5	6	4	3	3	2	3	3	7	11	8	15	1	2	12	15	18	159	Sep 23 Sunday
267	2	7	18	2	5	7	2	3	3	9	5	6	11	14	9	3	13	4	7	3	3	4	1	9	150	Sep 24 Monday
268	7	0	18	1	2	4	4	10	17	2	13	10	24	8	7	4	17	18	12	0	2	1	2	13	196	Sep 25 Tuesday
269	1	1	17	2	6	5	8	7	6	12	6	17	5	6	7	9	14	4	13	0	8	0	1	13	168	Sep 26 Wednesday
270	2	6	7	2	4	10	1	3	9	9	6	12	12	17	3	6	16	9	13	3	1	11	1	5	168	Sep 27 Thursday
271	0	2	3	4	5	7	3	5	17	6	12	12	29	7	8	5	10	16	20	6	11	0	1	7	196	Sep 28 Friday
272	4	6	4	4	2	5	10	9	5	5	8	13	4	4	3	1	6	2	7	3	7	5	2	0	119	Sep 29 Saturday
273	3	0	3	4	1	4	14	13	8	19	24	5	11	1	3	4	2	15	24	12	5	16	4	4	199	Sep 30 Sunday
NRS	00	01	02	03	04	05	06	07	08	09	10	11	12	13	14	15	16	17	18	19	20	21	22	23		
Sum	1362	1289	1185	2283	1519	1174	1579	1537	2164	1860	2329	2089	2392	2385	1710	1868	2278	2307	1762	2194	1207	2179	2040	1042	43734	Total sum
183	7	7	12	6	6	8	8	9	10	12	11	13	13	13	10	9	13	12	12	10	12	7	6	11	239	Total average
123	7	7	14	6	6	8	8	9	11	12	11	14	16	15	11	9	13	13	13	10	14	6	5	12	253	Average workdays
60	7	8	10	8	7	8	10	7	8	11	11	9	8	9	9	10	11	12	9	8	8	7	6	9	210	Average weekends

Table 3.4.1. Daily and hourly distribution of NORESS detections. For each day is shown number of detections within each hour of the day, and number of detections for that day. The end statistics give total number of detections distributed for each hour and the total sum of detections during the period. The averages show number of processed days, hourly distribution and average per processed day. (Page 4 of 4)

FRS .FKX Hourly distribution of detections

Day	00	01	02	03	04	05	06	07	08	09	10	11	12	13	14	15	16	17	18	19	20	21	22	23	Sum	Date
91	21	35	53	40	49	47	15	19	9	7	10	16	6	17	9	6	12	7	18	9	17	40	61	73	596	Apr 01 Sunday
92	77	97	71	59	55	40	43	28	27	29	42	21	40	24	30	9	13	6	9	16	3	15	22	14	790	Apr 02 Monday
93	28	51	38	42	29	30	28	42	17	14	25	28	19	20	20	19	6	14	13	27	36	74	66	86	772	Apr 03 Tuesday
94	88	88	78	86	83	64	63	34	41	42	55	70	61	51	33	49	43	18	5	13	8	10	10	11	1104	Apr 04 Wednesday
95	6	4	6	9	10	8	12	14	13	16	20	28	19	28	20	13	10	13	5	7	8	54	55	59	437	Apr 05 Thursday
96	57	41	42	56	50	46	42	38	29	34	42	69	52	32	17	21	28	22	27	14	6	19	24	17	825	Apr 06 Friday
97	15	21	26	31	35	45	41	28	17	26	30	44	23	18	15	7	9	8	13	7	9	15	29	31	543	Apr 07 Saturday
98	32	33	49	78	91	59	48	36	17	19	32	24	30	23	20	24	10	16	13	12	11	13	20	7	717	Apr 08 Sunday
99	8	7	8	8	3	6	16	10	23	18	16	18	29	19	12	12	8	5	21	16	19	7	18	2	309	Apr 09 Monday
100	19	5	14	15	8	11	29	12	18	15	18	30	17	12	14	27	14	20	14	18	10	12	22	13	387	Apr 10 Tuesday
101	18	16	40	33	25	27	27	24	13	26	33	29	48	32	32	22	9	16	16	9	12	25	16	3	551	Apr 11 Wednesday
102	7	6	7	4	19	8	9	18	13	11	16	13	18	3	5	4	7	4	2	4	6	4	16	2	206	Apr 12 Thursday
103	6	3	8	8	10	4	11	6	13	9	25	33	19	11	6	4	15	9	11	8	14	8	13	5	259	Apr 13 Friday
104	4	12	9	14	16	19	20	13	24	12	22	29	12	1	6	19	18	21	11	9	15	7	10	5	328	Apr 14 Saturday
105	3	4	1	2	4	4	5	4	6	3	14	11	7	11	5	7	19	13	2	5	2	5	2	2	141	Apr 15 Sunday
106	4	14	11	6	2	4	9	7	15	10	8	13	8	22	10	6	13	1	7	15	10	10	17	6	228	Apr 16 Monday
107	3	8	16	9	9	12	7	14	33	13	20	22	30	16	13	6	11	24	24	21	9	19	12	1	352	Apr 17 Tuesday
108	4	4	15	8	6	16	22	10	11	15	18	29	25	19	50	29	15	24	26	45	23	22	17	20	473	Apr 18 Wednesday
109	10	8	7	10	9	7	15	8	20	23	14	34	15	24	19	25	10	15	17	9	6	15	34	9	363	Apr 19 Thursday
110	12	6	6	6	8	9	13	13	20	34	23	46	34	26	24	12	13	12	15	6	11	20	25	16	410	Apr 20 Friday
111	20	29	14	15	14	14	14	13	10	23	24	14	16	11	25	16	14	7	25	9	7	8	11	26	379	Apr 21 Saturday
112	15	21	19	12	14	9	15	6	6	17	9	14	5	14	24	24	24	30	22	13	9	13	13	7	355	Apr 22 Sunday
113	11	1	11	5	14	26	7	12	18	25	11	9	20	7	13	4	13	14	13	11	9	2	13	16	285	Apr 23 Monday
114	3	13	8	12	6	18	11	10	23	14	31	30	28	14	17	11	32	24	18	18	12	0	0	0	353	Apr 24 Tuesday
115	0	0	0	0	0	14	16	11	16	26	23	24	9	10	24	3	9	11	11	9	20	0	0	0	236	Apr 25 Wednesday
116	0	0	0	0	0	4	7	16	31	29	14	15	15	14	12	28	17	11	16	12	9	0	0	0	250	Apr 26 Thursday
117	0	0	0	0	0	0	2	27	26	18	16	52	33	17	9	12	9	9	22	10	11	14	20	14	321	Apr 27 Friday
118	8	10	17	11	23	13	11	7	11	13	11	16	19	18	26	6	8	4	24	7	32	6	22	1	324	Apr 28 Saturday
119	7	8	6	2	11	4	2	0	13	3	5	15	17	5	6	9	2	7	23	11	2	6	16	9	189	Apr 29 Sunday
120	8	7	7	3	8	16	21	8	8	13	19	18	23	8	30	11	12	13	14	12	19	10	12	8	308	Apr 30 Monday
121	4	4	2	6	3	9	8	2	6	9	7	11	9	6	5	5	13	1	4	9	6	3	23	2	157	May 01 Tuesday
122	1	3	5	4	7	8	7	17	5	13	12	26	22	9	18	9	9	8	8	15	7	14	9	25	261	May 02 Wednesday
123	5	6	9	3	15	27	14	14	17	22	23	18	17	19	11	13	10	9	16	15	7	13	25	7	335	May 03 Thursday
124	3	9	12	18	13	12	13	6	11	11	4	22	13	10	15	7	11	3	10	9	5	6	19	6	248	May 04 Friday
125	4	3	3	4	2	5	8	20	14	28	6	23	3	20	29	19	13	9	13	9	5	5	10	3	258	May 05 Saturday
126	5	4	5	13	1	11	3	5	6	12	12	12	2	7	9	8	3	2	11	21	14	4	15	6	191	May 06 Sunday
127	8	9	7	4	11	12	22	2	15	18	21	25	17	11	15	9	7	14	4	11	16	13	25	12	308	May 07 Monday
128	10	6	13	5	6	15	11	9	20	26	17	22	15	25	26	14	10	14	13	47	7	26	15	9	381	May 08 Tuesday
129	8	14	20	2	16	19	21	6	12	12	26	7	0	1	5	16	19	17	11	5	6	18	18	1	280	May 09 Wednesday
130	11	10	8	5	8	17	8	12	7	17	22	31	19	18	5	0	0	0	0	0	0	0	0	0	198	May 10 Thursday
131	0	0	0	0	1	20	14	0	11	17	20	25	32	33	10	6	13	19	32	23	15	32	29	26	378	May 11 Friday
132	13	6	10	20	13	29	16	29	5	24	47	66	54	50	10	5	2	20	10	11	11	18	19	8	496	May 12 Saturday
133	10	7	8	19	29	17	12	15	4	7	9	27	6	19	10	7	12	13	20	34	43	3	0	0	331	May 13 Sunday
134	0	0	0	0	0	0	14	13	5	22	13	29	19	15	15	24	14	8	13	25	20	0	0	0	249	May 14 Monday
135	0	0	0	0	0	4	6	9	15	18	30	46	32	28	27	15	10	15	8	10	19	0	0	0	292	May 15 Tuesday
136	0	0	0	0	0	12	20	22	15	17	25	38	29	29	24	5	4	16	18	7	12	19	23	6	341	May 16 Wednesday
137	5	9	3	7	9	12	8	2	13	4	12	17	9	18	13	5	15	20	9	5	9	23	18	11	256	May 17 Thursday
138	3	5	7	9	6	12	6	14	19	14	24	28	35	16	9	20	26	5	22	26	7	7	13	5	338	May 18 Friday
139	1	11	16	8	8	9	7	9	10	11	18	27	16	23	14	7	18	16	6	4	19	16	11	6	291	May 19 Saturday
140	15	10	11	7	3	13	12	7	5	7	25	6	16	16	7	18	15	10	16	13	8	2	0	0	242	May 20 Sunday
141	0	0	0	0	11	18	9	34	25	18	19	24	23	24	23	12	6	10	18	1	13	1	0	0	289	May 21 Monday
142	0	0	0	0	0	0	7	18	12	11	28	36	21	13	6	16	7	20	17	11	11	0	0	0	234	May 22 Tuesday
143	0	0	0	0	2	21	37	23	21	18	33	37	27	36	29	28	24	27	33	26	16	25	20	0	483	May 23 Wednesday
144	7	10	11	11	19	4	37	12	18	29	8	30	25	25	17	18	14	20	6	23	48	9	22	10	433	May 24 Thursday
145	6	23	18	11	9	13	17	25	25	22	41	49	31	23	17	7	12	19	10	8	22	14	3	4	429	May 25 Friday
146	0	5	4	10	2	12	5	11	22	19	18	30	15	9	15	4	16	15	26	10	6	1	18	9	282	May 26 Saturday

Table 3.4.2. (Page 1 of 4)

FRS .FKX Hourly distribution of detections

Day	00	01	02	03	04	05	06	07	08	09	10	11	12	13	14	15	16	17	18	19	20	21	22	23	Sum	Date
147	2	3	2	21	18	11	8	16	12	3	9	8	15	22	20	4	22	22	31	31	33	16	42	9	380	May 27 Sunday
148	29	14	14	10	21	21	9	19	33	36	28	27	25	35	14	15	14	7	22	19	6	22	14	8	462	May 28 Monday
149	5	14	11	10	11	13	5	14	27	28	25	20	17	23	25	12	13	22	35	28	22	13	23	4	420	May 29 Tuesday
150	6	13	13	11	13	12	19	5	13	12	28	36	15	14	4	22	20	14	20	14	12	14	18	9	357	May 30 Wednesday
151	25	5	13	18	14	10	18	23	25	32	14	35	32	22	22	25	13	13	24	16	6	25	14	7	451	May 31 Thursday
152	20	18	9	5	0	24	14	14	23	28	28	45	24	49	21	27	19	22	43	28	16	17	17	7	518	Jun 01 Friday
153	14	1	13	20	2	8	8	20	22	32	33	35	32	33	12	11	14	10	7	22	8	0	16	4	377	Jun 02 Saturday
154	4	3	5	8	7	13	14	17	13	16	17	20	19	19	16	5	8	11	9	4	3	1	9	0	241	Jun 03 Sunday
155	3	2	5	4	4	6	9	18	1	22	9	8	14	17	3	17	3	16	10	3	21	16	36	6	253	Jun 04 Monday
156	4	6	4	3	5	12	6	22	24	12	28	23	27	19	16	13	22	5	3	3	19	21	14	6	317	Jun 05 Tuesday
157	7	5	8	9	11	8	18	17	13	20	30	46	18	22	15	23	6	14	0	0	10	17	15	7	339	Jun 06 Wednesday
158	9	18	22	41	46	15	42	30	29	42	39	57	43	29	33	16	0	7	11	12	19	7	17	12	596	Jun 07 Thursday
159	10	1	9	4	7	18	31	23	22	21	13	0	50	29	13	23	19	12	25	15	7	23	7	8	390	Jun 08 Friday
160	8	10	0	7	7	14	41	3	51	59	50	92	65	23	51	37	14	52	41	0	8	6	14	6	659	Jun 09 Saturday
161	4	2	4	12	11	17	16	10	30	16	32	30	8	34	20	13	20	16	7	18	21	1	9	16	367	Jun 10 Sunday
162	12	2	4	8	14	18	72	67	25	27	37	54	63	27	16	12	28	15	5	5	7	13	20	2	553	Jun 11 Monday
163	3	0	5	5	4	14	8	27	13	15	39	65	40	25	57	54	25	17	10	14	12	19	16	20	507	Jun 12 Tuesday
164	20	2	13	11	4	16	37	10	40	17	32	48	23	25	27	15	29	13	9	22	6	38	14	7	478	Jun 13 Wednesday
165	6	9	8	12	16	10	23	35	45	36	39	33	64	37	44	47	37	32	10	12	13	24	31	7	630	Jun 14 Thursday
166	5	17	0	0	4	5	28	43	49	33	18	46	40	37	29	38	22	13	17	4	22	21	23	6	520	Jun 15 Friday
167	6	11	15	2	5	15	24	11	21	33	33	28	30	20	9	17	7	16	13	6	5	16	12	6	361	Jun 16 Saturday
168	2	7	4	15	13	19	11	11	4	18	12	24	19	18	10	13	19	8	21	8	6	17	12	6	297	Jun 17 Sunday
169	12	14	8	2	7	20	26	33	17	29	23	22	22	13	19	26	18	7	8	16	3	15	18	6	384	Jun 18 Monday
170	5	12	5	3	11	16	20	39	21	25	25	20	42	24	31	18	10	9	6	11	4	18	14	27	416	Jun 19 Tuesday
171	14	8	0	7	6	8	16	15	28	41	26	36	40	32	17	47	29	11	26	9	9	41	27	32	525	Jun 20 Wednesday
172	13	16	27	10	15	24	44	40	35	38	24	34	49	49	17	45	39	38	38	31	45	39	36	33	779	Jun 21 Thursday
173	15	26	15	27	12	17	33	29	44	37	22	53	66	44	58	25	32	29	45	15	46	57	51	50	848	Jun 22 Friday
174	39	14	17	26	8	34	30	30	55	41	91	71	67	92	61	121	144	116	154	150	154	188	162	209	2074	Jun 23 Saturday
175	125	140	118	108	194	125	136	111	104	67	132	135	87	0	0	0	0	0	0	0	0	0	0	0	1582	Jun 24 Sunday
176	0	0	0	0	0	0	0	0	0	0	0	0	0	0	0	0	0	0	0	0	0	18	15	6	39	Jun 25 Monday
177	6	20	12	12	8	23	32	55	30	171	181	64	59	44	37	18	16	18	27	19	6	11	18	5	892	Jun 26 Tuesday
178	8	12	21	6	9	20	24	19	27	34	54	37	40	33	23	19	19	10	17	5	4	9	31	13	494	Jun 27 Wednesday
179	15	10	12	16	10	14	12	30	15	26	23	20	33	29	16	9	24	12	15	7	12	31	20	6	417	Jun 28 Thursday
180	11	8	15	19	34	21	13	26	47	22	31	51	40	33	9	22	27	14	16	15	5	19	18	8	524	Jun 29 Friday
181	18	5	5	7	13	9	18	15	30	24	27	20	6	9	16	11	14	10	9	6	2	7	3	5	289	Jun 30 Saturday
182	4	2	11	2	10	12	35	8	3	39	26	37	29	19	7	11	17	13	14	8	19	22	6	9	363	Jul 01 Sunday
183	11	12	8	13	6	19	15	24	16	30	43	32	30	25	18	17	21	23	13	11	16	3	22	6	434	Jul 02 Monday
184	17	18	9	6	15	10	12	19	20	43	43	59	41	33	12	0	0	0	0	0	0	0	0	0	357	Jul 03 Tuesday
185	0	0	0	0	0	0	0	0	0	0	30	44	39	34	27	34	29	10	26	17	10	2	24	8	334	Jul 04 Wednesday
186	12	16	18	27	10	18	24	32	27	38	50	0	17	27	30	0	9	41	20	23	60	54	43	15	611	Jul 05 Thursday
187	18	15	14	8	15	15	15	25	30	29	34	38	38	15	25	11	39	10	36	29	18	7	18	6	508	Jul 06 Friday
188	2	1	2	4	5	18	17	24	20	21	35	23	30	25	14	7	32	18	11	3	21	9	7	9	358	Jul 07 Saturday
189	1	17	6	9	24	20	18	18	24	16	29	16	19	23	29	18	37	27	15	28	26	8	18	14	460	Jul 08 Sunday
190	5	10	7	9	18	20	25	30	41	51	35	45	43	47	53	58	36	45	38	48	44	25	46	30	809	Jul 09 Monday
191	52	42	31	35	43	31	29	43	15	33	37	49	43	32	27	20	26	13	31	7	10	16	13	14	692	Jul 10 Tuesday
192	4	11	7	36	54	31	31	52	65	43	38	63	58	29	23	29	19	24	26	24	17	20	12	8	724	Jul 11 Wednesday
193	16	21	14	19	14	20	19	25	27	47	24	37	44	34	45	25	29	32	8	10	20	5	22	17	574	Jul 12 Thursday
194	18	25	13	13	6	14	27	29	38	41	69	75	55	50	31	12	18	16	19	16	21	12	18	17	653	Jul 13 Friday
195	19	14	23	26	23	1	13	18	22	32	53	31	13	31	8	18	26	12	13	21	24	17	35	10	503	Jul 14 Saturday
196	8	12	10	18	26	20	25	17	32	19	16	47	14	31	3	19	21	25	17	10	11	9	13	9	432	Jul 15 Sunday
197	6	6	21	33	11	8	14	40	63	68	45	48	43	52	18	34	25	16	14	12	30	29	21	12	669	Jul 16 Monday
198	23	26	27	30	38	28	35	25	26	29	35	39	34	37	28	39	26	32	31	31	33	45	42	16	755	Jul 17 Tuesday
199	10	17	22	32	43	47	46	35	42	35	48	45	46	31	17	37	45	22	35	17	7	24	14	5	722	Jul 18 Wednesday
200	10	15	22	24	37	19	25	17	22	42	27	43	24	41	27	15	34	24	24	5	15	26	35	22	595	Jul 19 Thursday
201	3	26	9	16	15	22	28	45	40	52	50	74	79	71	45	52	56	40	31	36	20	25	28	15	878	Jul 20 Friday
202	8	28	9	34	32	24	12	34	26	25	35	33	16	31	20	19	24	22	10	15	23	3	0	0	483	Jul 21 Saturday

Table 3.4.2. (Page 2 of 4)

FRS .FKX Hourly distribution of detections

Day	00	01	02	03	04	05	06	07	08	09	10	11	12	13	14	15	16	17	18	19	20	21	22	23	Sum	Date
203	0	0	0	0	0	0	0	0	27	67	43	41	20	49	27	22	35	14	29	11	8	9	13	6	421	Jul 22 Sunday
204	7	20	12	12	17	18	33	16	24	26	25	15	0	0	0	0	0	0	0	0	0	0	0	0	225	Jul 23 Monday
205	0	0	0	0	0	0	0	0	0	0	0	0	0	0	0	0	0	0	0	15	17	24	11	15	82	Jul 24 Tuesday
206	13	7	17	17	11	14	24	15	19	55	24	47	42	28	19	13	21	15	33	13	18	15	12	6	498	Jul 25 Wednesday
207	5	7	3	5	16	31	21	73	52	19	16	27	40	29	20	12	36	12	20	13	11	15	24	5	512	Jul 26 Thursday
208	9	7	3	4	14	23	24	24	25	27	27	57	36	31	40	11	20	12	14	4	20	17	13	17	479	Jul 27 Friday
209	5	7	5	7	16	17	9	10	42	27	30	23	17	14	23	2	18	4	7	15	5	5	9	5	322	Jul 28 Saturday
210	3	4	4	7	9	28	19	17	18	34	42	25	35	18	23	11	12	4	10	6	5	20	9	21	384	Jul 29 Sunday
211	3	4	3	1	7	19	18	20	16	38	34	33	20	37	33	19	25	14	17	21	15	16	17	5	435	Jul 30 Monday
212	6	14	5	7	11	23	25	45	31	28	35	44	24	31	37	19	17	36	9	10	6	18	29	17	527	Jul 31 Tuesday
213	4	8	3	15	20	16	33	31	27	46	45	37	33	35	14	25	17	19	15	7	10	17	17	20	514	Aug 01 Wednesday
214	19	6	8	7	18	35	36	27	49	40	40	40	32	44	18	25	24	14	22	18	12	18	31	3	586	Aug 02 Thursday
215	11	6	5	13	9	24	11	0	36	37	47	76	38	33	14	28	39	28	33	16	19	12	13	1	549	Aug 03 Friday
216	4	10	14	11	9	15	10	10	19	28	34	37	20	31	9	15	13	16	17	14	18	3	13	3	373	Aug 04 Saturday
217	5	11	13	11	18	8	18	16	31	25	42	29	34	26	21	33	29	26	34	12	24	8	7	5	486	Aug 05 Sunday
218	8	8	19	11	13	15	26	11	24	26	25	23	29	25	35	13	49	10	10	11	8	10	15	17	441	Aug 06 Monday
219	11	12	5	13	11	22	15	39	9	25	52	51	39	37	25	13	14	3	24	16	15	23	16	14	504	Aug 07 Tuesday
220	13	10	7	13	14	16	18	21	23	37	44	44	39	42	26	30	34	8	21	15	13	22	13	22	545	Aug 08 Wednesday
221	14	6	4	2	23	7	13	29	27	27	33	35	48	62	40	27	15	23	21	13	8	11	17	4	509	Aug 09 Thursday
222	18	4	20	11	20	16	25	47	14	39	48	37	42	28	11	25	27	45	31	17	24	23	17	5	594	Aug 10 Friday
223	8	7	8	6	17	14	12	27	28	44	44	33	29	43	31	25	24	13	18	15	16	7	8	9	486	Aug 11 Saturday
224	7	4	14	12	9	16	21	18	28	15	29	14	9	24	17	4	35	37	24	19	8	20	11	15	410	Aug 12 Sunday
225	4	3	5	18	25	7	34	31	34	34	45	60	41	37	17	18	32	17	42	13	12	37	27	14	607	Aug 13 Monday
226	10	10	10	9	24	20	26	43	15	46	38	26	39	40	36	29	26	6	14	12	18	30	15	17	559	Aug 14 Tuesday
227	24	27	9	29	22	16	24	25	29	21	35	51	25	42	38	28	36	18	18	20	13	23	19	17	609	Aug 15 Wednesday
228	10	11	8	7	30	37	34	22	42	46	20	36	50	39	53	40	31	47	15	19	13	24	13	3	650	Aug 16 Thursday
229	9	10	27	24	14	15	22	25	23	28	39	34	33	55	41	11	30	4	10	19	6	22	16	4	521	Aug 17 Friday
230	3	9	5	23	30	12	20	20	25	32	47	35	5	35	9	17	101	17	19	13	9	8	13	8	515	Aug 18 Saturday
231	12	9	34	200	32	59	45	17	44	30	17	17	22	24	21	22	21	8	20	19	23	7	14	12	729	Aug 19 Sunday
232	38	5	7	3	21	38	11	22	33	21	26	41	24	35	25	34	36	23	25	11	11	10	10	4	514	Aug 20 Monday
233	5	12	6	12	11	14	36	43	48	26	28	61	37	40	49	21	20	21	25	12	12	12	32	8	591	Aug 21 Tuesday
234	12	3	5	7	12	9	33	25	32	24	43	25	37	34	47	16	16	27	13	26	11	18	10	8	493	Aug 22 Wednesday
235	4	12	13	9	7	9	0	22	19	16	46	35	34	31	27	27	14	38	15	34	55	21	23	6	517	Aug 23 Thursday
236	19	3	11	10	7	17	44	57	58	51	40	67	91	41	39	22	19	25	10	9	16	14	13	10	693	Aug 24 Friday
237	10	9	9	9	4	8	18	13	7	25	22	29	28	25	22	11	17	3	11	12	4	0	13	4	313	Aug 25 Saturday
238	10	5	0	7	16	15	8	12	21	23	44	7	24	23	21	23	17	5	35	11	4	14	22	9	376	Aug 26 Sunday
239	10	3	9	20	24	16	11	50	10	40	10	38	36	23	9	23	14	5	17	10	18	13	7	18	434	Aug 27 Monday
240	6	1	0	20	15	14	0	24	5	0	13	36	25	22	61	23	22	41	9	20	15	23	20	22	437	Aug 28 Tuesday
241	10	9	7	6	4	8	27	23	29	12	25	43	24	16	22	15	26	24	17	15	15	17	15	13	422	Aug 29 Wednesday
242	12	8	7	9	9	22	13	16	17	30	34	32	32	28	35	22	28	33	18	20	22	18	18	11	494	Aug 30 Thursday
243	13	1	8	16	10	16	11	22	28	40	16	35	25	26	13	8	16	23	15	20	2	23	15	9	411	Aug 31 Friday
244	8	16	2	6	8	10	13	6	11	19	21	26	10	26	20	7	10	8	11	2	7	3	13	13	276	Sep 01 Saturday
245	6	5	4	10	10	7	29	10	12	14	12	6	17	26	7	22	23	29	25	16	14	7	12	4	327	Sep 02 Sunday
246	3	7	16	6	13	20	15	20	25	6	20	17	12	20	31	23	8	17	11	14	32	16	15	10	377	Sep 03 Monday
247	1	5	3	5	16	14	17	31	16	10	37	30	16	46	25	23	30	27	43	16	15	25	19	11	481	Sep 04 Tuesday
248	4	4	2	15	4	23	41	47	38	44	27	42	38	29	19	26	12	10	20	18	7	6	8	8	492	Sep 05 Wednesday
249	13	6	2	12	14	33	6	34	29	27	8	32	51	39	37	23	32	30	35	21	17	23	28	18	570	Sep 06 Thursday
250	5	18	18	3	4	19	17	17	42	16	50	48	43	33	24	31	23	12	22	19	12	12	9	18	515	Sep 07 Friday
251	8	4	5	5	4	16	8	22	9	33	22	44	13	23	16	10	29	11	14	20	14	14	15	8	367	Sep 08 Saturday
252	10	11	9	8	5	18	9	21	11	5	17	9	33	11	41	5	24	6	20	16	2	11	22	6	330	Sep 09 Sunday
253	11	11	7	14	14	16	25	40	26	39	27	15	31	20	18	7	15	11	28	5	23	16	10	10	439	Sep 10 Monday
254	10	13	16	15	19	18	29	29	34	14	27	33	33	30	27	26	18	17	24	4	10	38	28	14	526	Sep 11 Tuesday
255	23	7	29	3	15	24	18	35	32	27	31	38	28	32	23	21	10	14	19	5	6	21	21	8	490	Sep 12 Wednesday
256	4	6	11	13	12	23	28	19	12	17	18	37	29	35	34	14	19	10	28	21	4	23	19	0	436	Sep 13 Thursday
257	0	0	0	0	0	15	26	42	37	39	31	51	27	16	24	18	26	35	28	17	15	20	24	5	496	Sep 14 Friday
258	4	8	6	14	11	26	15	12	10	12	38	30	21	34	15	27	21	16	16	13	6	5	14	20	394	Sep 15 Saturday

Table 3.4.2. (Page 3 of 4)

FRS .FKX Hourly distribution of detections

Day	00	01	02	03	04	05	06	07	08	09	10	11	12	13	14	15	16	17	18	19	20	21	22	23	Sum	Date
259	11	5	4	14	9	1	2	6	3	6	17	8	1	19	11	11	14	11	12	7	13	20	17	9	231	Sep 16 Sunday
260	10	7	11	13	10	20	33	11	21	27	18	18	28	32	20	13	18	6	21	23	12	15	20	23	430	Sep 17 Monday
261	7	5	11	28	8	19	30	40	25	40	33	37	38	15	37	73	30	26	22	23	19	15	29	5	615	Sep 18 Tuesday
262	20	20	11	5	19	21	15	20	24	39	29	53	25	17	22	23	15	13	23	6	10	14	22	22	488	Sep 19 Wednesday
263	6	2	5	18	10	24	6	15	32	36	34	31	38	38	41	40	8	4	20	27	30	24	23	24	536	Sep 20 Thursday
264	17	30	3	19	8	16	22	37	66	42	22	35	42	31	8	33	17	31	34	20	20	21	21	7	602	Sep 21 Friday
265	14	12	8	9	2	20	20	3	15	18	14	41	11	28	4	16	7	13	31	23	11	8	12	5	345	Sep 22 Saturday
266	9	7	4	6	3	1	13	12	19	2	23	9	12	16	14	5	5	19	55	7	8	14	39	14	316	Sep 23 Sunday
267	6	19	20	12	5	16	17	16	36	13	19	29	20	25	21	21	16	21	22	16	19	20	9	14	432	Sep 24 Monday
268	6	8	9	17	3	24	21	24	24	37	24	31	23	31	26	11	0	0	0	0	0	0	0	0	319	Sep 25 Tuesday
269	0	0	0	0	0	6	10	17	23	23	26	14	18	24	14	19	33	41	21	2	7	13	15	11	337	Sep 26 Wednesday
270	14	7	8	6	9	39	24	12	25	15	39	27	23	33	34	26	29	12	22	17	12	27	22	9	491	Sep 27 Thursday
271	15	17	10	8	3	16	12	28	44	17	54	50	24	15	23	19	13	14	14	11	12	5	15	8	447	Sep 28 Friday
272	3	5	10	11	14	30	16	17	11	21	26	15	11	22	6	9	9	15	15	8	16	15	25	9	339	Sep 29 Saturday
273	3	5	10	11	6	14	13	8	14	7	6	5	10	23	21	10	12	20	29	26	24	34	11	11	333	Sep 30 Sunday
FRS	00	01	02	03	04	05	06	07	08	09	10	11	12	13	14	15	16	17	18	19	20	21	22	23		
Sum	2077		2558		3228		3949		4761		6097		4814		3440		3073		2728		3025		2171			
	1997		2096		2677		3639		4290		5348		5190		3959		3606		3431		2702		3347		84203	Total sum
183	11	11	11	14	15	18	20	22	23	26	29	33	28	26	22	19	20	17	19	15	15	17	18	12	460	Total average
123	11	11	11	12	13	18	21	24	26	28	30	36	32	28	24	21	20	17	19	15	14	18	18	12	481	Average workdays
60	10	12	12	17	17	18	18	15	19	21	27	27	20	22	16	15	20	16	19	14	15	13	18	12	413	Average weekends

Table 3.4.2. Daily and hourly distribution of ARCESS detections. For each day is shown number of detections within each hour of the day, and number of detections for that day. The end statistics give total number of detections distributed for each hour and the total sum of detections during the period. The averages show number of processed days, hourly distribution and average per processed day. (Page 4 of 4)

FIN .FKX Hourly distribution of detections

Day	00	01	02	03	04	05	06	07	08	09	10	11	12	13	14	15	16	17	18	19	20	21	22	23	Sum	Date
91	3	6	4	3	2	17	7	5	26	18	11	20	5	6	14	4	9	3	10	5	13	8	7	7	213	Apr 01 Sunday
92	2	6	1	7	2	2	11	11	14	21	23	11	10	20	8	7	11	2	8	9	9	8	5	8	216	Apr 02 Monday
93	6	9	6	7	3	5	3	11	25	7	11	34	9	9	23	67	4	33	3	8	0	2	10	11	306	Apr 03 Tuesday
94	8	8	7	14	5	4	6	15	18	20	16	31	16	15	13	9	8	11	10	10	6	2	5	6	263	Apr 04 Wednesday
95	9	11	8	10	10	14	7	17	21	22	26	42	15	16	16	8	7	7	9	4	5	35	27	29	375	Apr 05 Thursday
96	24	18	19	18	17	8	11	12	17	17	40	27	21	7	0	0	0	0	1	16	6	4	9	10	302	Apr 06 Friday
97	17	4	10	10	7	8	8	13	14	7	13	20	11	15	19	20	38	26	38	33	31	18	28	12	420	Apr 07 Saturday
98	13	21	19	27	38	25	14	19	14	11	21	32	34	13	17	16	10	14	19	14	10	12	12	11	436	Apr 08 Sunday
99	10	9	11	7	1	5	4	3	15	14	11	8	28	18	7	3	3	3	7	6	4	5	10	8	200	Apr 09 Monday
100	11	6	4	6	0	0	4	3	8	17	12	29	15	9	10	17	12	6	6	4	6	2	11	10	208	Apr 10 Tuesday
101	5	12	14	3	4	5	13	3	13	12	42	72	65	55	30	34	18	18	14	10	17	17	14	11	501	Apr 11 Wednesday
102	8	17	25	11	16	20	41	60	62	85	52	18	17	5	6	13	6	10	3	7	3	3	5	6	499	Apr 12 Thursday
103	3	7	7	4	9	5	16	13	18	15	42	63	17	7	5	3	6	4	8	5	2	9	2	6	276	Apr 13 Friday
104	3	4	2	3	13	4	4	6	9	17	15	57	28	27	29	25	3	6	5	0	6	3	3	4	276	Apr 14 Saturday
105	3	2	1	6	2	3	1	5	3	5	28	7	6	6	5	2	3	1	2	4	4	1	2	4	106	Apr 15 Sunday
106	2	14	4	4	9	2	4	3	6	11	16	20	23	3	6	8	4	7	4	9	7	3	7	7	183	Apr 16 Monday
107	10	3	8	1	5	7	4	10	16	6	11	16	14	9	11	3	15	13	3	5	8	17	8	5	7	5	7	541	Apr 17 Tuesday
108	5	8	8	5	3	7	3	13	21	9	15	21	8	20	0	18	9	15	9	12	12	12	17	15	5	12	4	15	967	Apr 18 Wednesday
109	9	14	7	0	0	0	2	9	16	14	23	20	26	13	14	15	11	5	8	6	4	4	7	7	234	Apr 19 Thursday
110	3	4	2	5	3	2	4	8	19	25	21	24	17	22	9	8	0	3	6	4	7	2	6	13	217	Apr 20 Friday
111	5	7	11	9	2	6	3	7	8	9	10	8	8	6	10	6	4	3	4	8	6	7	3	9	159	Apr 21 Saturday
112	9	8	5	3	7	3	4	6	3	8	7	5	1	4	11	5	10	13	10	11	7	8	7	12	167	Apr 22 Sunday
113	13	7	8	8	4	4	6	9	12	20	44	84	136	149	160	99	88	68	60	57	79	73	98	71	1357	Apr 23 Monday
114	55	33	41	29	6	33	41	69	91	119	136	171	169	199	208	179	***	0	0	0	0	0	0	0	2781	Apr 24 Tuesday
115	0	0	0	0	0	0	0	0	0	0	0	0	0	0	0	0	0	0	0	0	0	0	0	0	0	Apr 25 Wednesday
116	0	0	0	0	0	0	0	0	0	0	0	0	0	0	0	0	0	0	0	0	0	0	0	0	0	Apr 26 Thursday
117	0	0	0	0	0	0	0	0	0	0	0	0	0	0	0	0	0	0	0	0	0	0	0	0	0	Apr 27 Friday
118	0	0	0	0	0	0	0	0	0	0	0	0	0	0	0	0	0	0	0	0	0	0	0	0	0	Apr 28 Saturday
119	0	0	0	0	0	0	0	0	0	0	0	0	0	0	0	0	0	0	0	0	0	0	0	0	0	Apr 29 Sunday
120	7	8	7	6	12	5	5	10	7	0	12	22	34	22	36	23	8	9	7	8	3	5	5	7	268	Apr 30 Monday
121	4	4	3	0	8	12	8	12	16	34	8	16	7	12	7	8	13	8	9	6	9	5	14	6	229	May 01 Tuesday
122	13	13	16	11	5	2	6	18	6	27	43	20	17	20	28	9	11	10	4	10	6	9	14	13	331	May 02 Wednesday
123	6	9	13	5	4	9	8	0	0	0	0	0	0	5	25	15	13	6	4	8	12	12	9	10	173	May 03 Thursday
124	9	7	2	8	4	2	1	3	0	0	0	0	0	0	0	0	0	0	0	0	0	0	0	0	36	May 04 Friday
125	0	0	0	0	0	0	0	0	0	0	0	0	0	0	0	0	0	0	0	0	0	0	0	0	0	May 05 Saturday
126	0	0	0	0	0	0	0	0	0	0	0	0	0	0	0	0	0	0	0	0	0	0	0	0	0	May 06 Sunday
127	0	0	0	0	0	0	0	0	0	0	0	0	0	0	0	0	0	0	0	0	0	0	0	0	0	May 07 Monday
128	0	0	0	0	0	0	0	0	0	0	0	0	0	0	0	0	0	10	31	5	12	11	9	5	83	May 08 Tuesday
129	9	7	8	10	11	14	17	22	44	82	119	110	108	109	130	133	89	76	47	56	42	29	26	18	1316	May 09 Wednesday
130	19	22	16	7	15	9	14	17	34	50	80	88	97	119	68	0	0	0	0	0	0	0	0	0	655	May 10 Thursday
131	0	0	0	0	0	0	8	12	26	32	44	81	95	69	69	18	6	16	2	35	17	42	48	10	630	May 11 Friday
132	9	39	20	18	25	23	2	21	25	32	22	17	7	17	16	24	17	9	5	6	5	3	4	0	366	May 12 Saturday
133	1	3	5	2	14	4	6	6	11	14	17	7	7	9	14	4	14	7	9	14	10	6	5	6	195	May 13 Sunday
134	13	15	13	7	3	0	3	11	14	7	16	66	35	46	67	42	59	38	39	45	60	42	40	21	702	May 14 Monday
135	26	19	26	42	24	41	56	86	106	101	87	107	126	106	100	107	57	0	0	0	0	0	0	0	1217	May 15 Tuesday
136	0	0	0	0	0	0	0	0	0	0	0	108	110	99	80	55	49	54	43	34	35	36	26	26	755	May 16 Wednesday
137	31	45	12	17	32	11	15	15	21	22	53	31	43	43	13	11	39	31	17	13	13	14	17	14	573	May 17 Thursday
138	13	8	7	13	10	4	5	19	29	36	25	31	34	16	14	4	10	6	4	2	6	5	8	12	321	May 18 Friday
139	9	8	1	6	8	11	14	13	17	20	25	28	18	21	40	39	26	26	46	31	13	16	13	34	483	May 19 Saturday
140	8	10	7	16	37	17	28	28	52	37	41	42	26	40	45	42	37	39	21	11	15	16	25	21	661	May 20 Sunday
141	9	11	16	11	9	15	30	32	27	26	55	73	46	45	39	36	33	49	83	90	46	54	43	29	907	May 21 Monday
142	13	16	5	16	16	19	11	12	25	26	0	0	0	0	0	0	0	0	0	0	0	0	0	0	159	May 22 Tuesday
143	0	0	0	0	0	0	0	0	0	0	0	0	0	0	0	0	0	0	0	0	0	0	0	0	0	May 23 Wednesday
144	0	0	0	0	0	0	0	0	0	0	0	0	0	0	0	0	0	0	0	0	0	0	0	0	0	May 24 Thursday
145	0	0	0	0	0	0	0	0	0	0	0	0	0	0	0	0	0	0	0	0	0	0	0	0	0	May 25 Friday
146	0	0	0	0	0	0	0	0	0	0	0	0	0	0	0	0	0	0	0	0	0	0	0	0	0	May 26 Saturday

Table 3.4.3. (Page 1 of 4)

FIN .FKX Hourly distribution of detections

Day	00	01	02	03	04	05	06	07	08	09	10	11	12	13	14	15	16	17	18	19	20	21	22	23	Sum	Date
147	0	0	0	0	0	0	0	0	0	0	0	0	0	0	0	0	0	0	0	0	0	0	0	0	0	May 27 Sunday
148	0	0	0	0	0	0	0	0	0	0	0	0	0	0	0	0	0	0	0	0	0	0	0	0	0	May 28 Monday
149	0	0	0	0	0	0	0	0	0	0	0	0	0	0	0	0	0	0	0	0	0	0	0	0	0	May 29 Tuesday
150	0	0	0	0	0	0	0	0	0	0	0	0	0	0	0	0	0	0	0	0	0	0	0	0	0	May 30 Wednesday
151	0	0	0	0	0	0	0	0	0	0	0	0	0	0	0	0	0	0	0	0	0	0	0	0	0	May 31 Thursday
152	0	0	0	0	0	0	0	0	0	0	0	0	0	0	0	0	0	0	0	0	0	0	0	0	0	Jun 01 Friday
153	0	0	0	0	0	0	0	0	0	0	0	0	0	0	0	0	0	0	0	0	0	0	0	0	0	Jun 02 Saturday
154	0	0	0	0	0	0	0	0	0	0	0	0	0	0	0	0	0	0	0	0	0	0	0	0	0	Jun 03 Sunday
155	0	0	0	0	0	0	0	0	0	0	0	0	0	0	0	0	0	0	0	0	0	0	0	0	0	Jun 04 Monday
156	0	0	0	0	0	0	0	0	0	0	0	0	0	0	0	0	0	0	0	0	0	0	0	0	0	Jun 05 Tuesday
157	0	0	0	0	0	0	0	0	0	0	0	0	0	0	0	0	0	0	0	0	0	0	0	0	0	Jun 06 Wednesday
158	0	0	0	0	0	0	0	0	0	0	0	0	0	0	0	0	0	0	0	0	0	0	0	0	0	Jun 07 Thursday
159	0	0	0	0	0	0	0	0	0	0	0	0	0	0	0	0	0	0	0	0	0	0	0	0	0	Jun 08 Friday
160	0	0	0	0	0	0	0	0	0	0	0	0	0	0	0	0	0	0	0	0	0	0	0	0	0	Jun 09 Saturday
161	0	0	0	0	0	0	0	0	0	0	0	0	0	0	0	0	0	0	0	0	0	0	0	0	0	Jun 10 Sunday
162	0	0	0	0	0	0	0	0	0	0	0	0	0	0	0	0	0	0	0	0	0	0	0	0	0	Jun 11 Monday
163	0	0	0	0	0	0	0	0	0	0	0	0	0	0	0	0	0	0	0	0	0	0	0	0	0	Jun 12 Tuesday
164	0	0	0	0	0	0	0	0	0	0	0	0	0	0	0	0	0	0	0	0	0	0	0	0	0	Jun 13 Wednesday
165	0	0	0	0	0	0	0	0	0	0	0	0	0	0	0	0	0	0	0	0	0	0	0	0	0	Jun 14 Thursday
166	0	0	0	0	0	0	0	0	0	0	0	0	0	0	0	0	0	0	0	0	0	0	0	0	0	Jun 15 Friday
167	0	0	0	0	0	0	0	0	0	0	0	0	0	0	0	0	0	0	0	0	0	0	0	0	0	Jun 16 Saturday
168	0	0	0	0	0	0	0	0	0	0	0	0	0	0	0	0	0	0	0	0	0	0	0	0	0	Jun 17 Sunday
169	0	0	0	0	0	0	0	0	0	0	0	0	0	0	0	0	0	0	0	0	0	0	0	0	0	Jun 18 Monday
170	0	0	0	0	0	0	0	0	0	0	0	0	0	0	0	0	0	0	0	0	0	0	0	0	0	Jun 19 Tuesday
171	0	0	0	0	0	0	0	0	0	0	0	0	0	0	0	0	0	0	0	0	0	0	0	0	0	Jun 20 Wednesday
172	0	0	0	0	0	0	0	0	0	0	0	0	0	0	0	0	0	0	0	0	0	0	0	0	0	Jun 21 Thursday
173	0	0	0	0	0	0	0	0	0	0	0	0	0	0	0	0	0	0	0	0	0	0	0	0	0	Jun 22 Friday
174	0	0	0	0	0	0	0	0	0	0	0	0	0	0	0	0	0	0	0	0	0	0	0	0	0	Jun 23 Saturday
175	0	0	0	0	0	0	0	0	0	0	0	0	0	0	0	0	0	0	0	0	0	0	0	0	0	Jun 24 Sunday
176	0	0	0	0	0	0	0	0	0	0	0	0	0	0	0	0	0	0	0	0	0	0	0	0	0	Jun 25 Monday
177	0	0	0	0	0	0	0	0	0	0	0	0	0	0	0	0	0	0	0	0	0	0	0	0	0	Jun 26 Tuesday
178	0	0	0	0	0	0	0	0	0	0	0	0	0	0	0	0	0	0	0	0	0	0	0	0	0	Jun 27 Wednesday
179	0	0	0	0	0	0	0	0	0	0	0	0	0	0	0	0	0	0	0	0	0	0	0	0	0	Jun 28 Thursday
180	0	0	0	0	0	0	0	0	0	0	0	0	0	0	0	0	0	0	0	0	0	0	0	0	0	Jun 29 Friday
181	0	0	0	0	0	0	0	0	0	0	0	0	0	0	0	0	0	0	0	0	0	0	0	0	0	Jun 30 Saturday
182	0	0	0	0	0	0	0	0	0	0	0	0	0	0	0	0	0	0	0	0	0	0	0	0	0	Jul 01 Sunday
183	0	0	0	0	0	0	0	0	0	0	0	0	0	0	0	0	0	0	0	0	0	0	0	0	0	Jul 02 Monday
184	0	0	0	0	0	0	0	0	0	0	0	0	0	0	0	0	0	0	0	0	0	0	0	0	0	Jul 03 Tuesday
185	0	0	0	0	0	0	0	0	0	0	0	0	0	0	0	0	0	0	0	0	0	0	0	0	0	Jul 04 Wednesday
186	0	0	0	0	0	0	0	0	0	0	0	0	0	0	0	0	0	0	0	0	0	0	0	0	0	Jul 05 Thursday
187	0	0	0	0	0	0	0	0	0	0	0	0	0	0	0	0	0	0	0	0	0	0	0	0	0	Jul 06 Friday
188	0	0	0	0	0	0	0	0	0	0	0	0	0	0	0	0	0	0	0	0	0	0	0	0	0	Jul 07 Saturday
189	0	0	0	0	0	0	0	0	0	0	0	0	0	0	0	0	0	0	0	0	0	0	0	0	0	Jul 08 Sunday
190	0	0	0	0	0	0	0	0	0	0	0	0	0	0	0	0	0	0	0	0	0	0	0	0	0	Jul 09 Monday
191	0	0	0	0	0	0	0	0	0	0	0	0	0	0	0	0	0	0	0	0	0	0	0	0	0	Jul 10 Tuesday
192	0	0	0	0	0	0	0	0	0	0	0	0	0	0	0	0	0	0	0	0	0	0	0	0	0	Jul 11 Wednesday
193	0	0	0	0	0	0	0	0	0	0	0	0	0	0	0	0	0	0	0	0	0	0	0	0	0	Jul 12 Thursday
194	0	0	0	0	0	0	0	0	0	0	0	0	0	0	0	0	0	0	0	0	0	0	0	0	0	Jul 13 Friday
195	0	0	0	0	0	0	0	0	0	0	0	0	0	0	0	0	0	0	0	0	0	0	0	0	0	Jul 14 Saturday
196	0	0	0	0	0	0	0	0	0	0	0	0	0	0	0	0	0	0	0	0	0	0	0	0	0	Jul 15 Sunday
197	0	0	0	0	0	0	0	0	0	0	0	0	0	0	0	0	0	0	0	0	0	0	0	0	0	Jul 16 Monday
198	0	0	0	0	0	0	0	0	0	0	0	0	0	0	0	0	0	0	0	0	0	0	0	0	0	Jul 17 Tuesday
199	0	0	0	0	0	0	0	0	0	0	0	0	0	0	0	0	0	0	0	0	0	0	0	0	0	Jul 18 Wednesday
200	0	0	0	0	0	0	0	0	0	0	0	0	0	0	0	0	0	0	0	0	0	0	0	0	0	Jul 19 Thursday
201	0	0	0	0	0	0	0	0	0	0	0	0	0	0	0	0	0	0	0	0	0	0	0	0	0	Jul 20 Friday
202	0	0	0	0	0	0	0	0	0	0	0	0	0	0	0	0	0	0	0	0	0	0	0	0	0	Jul 21 Saturday

Table 3.4.3. (Page 2 of 4)

FIN .FKX Hourly distribution of detections

Day	00	01	02	03	04	05	06	07	08	09	10	11	12	13	14	15	16	17	18	19	20	21	22	23	Sum	Date
203	0	0	0	0	0	0	0	0	0	0	0	0	0	0	0	0	0	0	0	0	0	0	0	0	0	Jul 22 Sunday
204	0	0	0	0	0	0	0	0	0	0	0	0	0	0	0	0	0	0	0	0	0	0	0	0	0	Jul 23 Monday
205	0	0	0	0	0	0	0	0	0	0	0	0	0	0	0	0	0	0	0	0	0	0	0	0	0	Jul 24 Tuesday
206	0	0	0	0	0	0	0	0	0	0	0	0	0	0	0	0	0	0	0	0	0	0	0	0	0	Jul 25 Wednesday
207	0	0	0	0	0	0	0	0	0	0	0	0	0	0	0	0	0	0	0	0	0	0	0	0	0	Jul 26 Thursday
208	0	0	0	0	0	0	0	0	0	0	0	0	0	0	0	0	0	0	0	0	0	0	0	0	0	Jul 27 Friday
209	0	0	0	0	0	0	0	0	0	0	0	0	0	0	0	0	0	0	0	0	0	0	0	0	0	Jul 28 Saturday
210	0	0	0	0	0	0	0	0	0	0	0	0	0	0	0	0	0	0	0	0	0	0	0	0	0	Jul 29 Sunday
211	0	0	0	0	0	0	0	0	0	0	0	0	0	0	0	0	0	0	0	0	0	0	0	0	0	Jul 30 Monday
212	0	0	0	0	0	0	0	0	0	0	0	0	0	0	0	0	0	0	0	0	0	0	0	0	0	Jul 31 Tuesday
213	0	0	0	0	0	0	0	0	0	0	0	0	0	0	0	0	0	0	0	0	0	0	0	0	0	Aug 01 Wednesday
214	0	0	0	0	0	0	0	0	0	0	0	0	0	0	0	0	0	0	0	0	0	0	0	0	0	Aug 02 Thursday
215	0	0	0	0	0	0	0	0	0	0	0	0	0	0	0	0	0	0	0	0	0	0	0	0	0	Aug 03 Friday
216	0	0	0	0	0	0	0	0	0	0	0	0	0	0	0	0	0	0	0	0	0	0	0	0	0	Aug 04 Saturday
217	0	0	0	0	0	0	0	0	0	0	0	0	0	0	0	0	0	0	0	0	0	0	0	0	0	Aug 05 Sunday
218	0	0	0	0	0	0	0	0	0	0	0	0	0	0	0	0	0	0	0	0	0	0	0	0	0	Aug 06 Monday
219	0	0	0	0	0	0	0	0	0	0	0	0	0	0	0	0	0	0	0	0	0	0	0	0	0	Aug 07 Tuesday
220	0	0	0	0	0	0	0	0	0	0	0	0	0	0	0	0	0	0	0	0	0	0	0	0	0	Aug 08 Wednesday
221	0	0	0	0	0	0	0	0	0	0	0	0	0	0	0	0	0	0	0	0	0	0	0	0	0	Aug 09 Thursday
222	0	0	0	0	0	0	0	0	0	0	0	0	0	0	0	0	0	0	0	0	0	0	0	0	0	Aug 10 Friday
223	0	0	0	0	0	0	0	0	0	0	0	0	0	0	0	0	0	0	0	0	0	0	0	0	0	Aug 11 Saturday
224	0	0	0	0	0	0	0	0	0	0	0	0	0	0	0	0	0	0	0	0	0	0	0	0	0	Aug 12 Sunday
225	0	0	0	0	0	0	0	0	0	0	0	0	0	0	0	0	0	0	0	0	0	0	0	0	0	Aug 13 Monday
226	0	0	0	0	0	0	0	0	0	0	0	0	0	0	0	0	0	0	0	0	0	0	0	0	0	Aug 14 Tuesday
227	0	0	0	0	0	0	0	0	0	0	0	0	0	0	0	0	0	0	0	0	0	0	0	0	0	Aug 15 Wednesday
228	0	0	0	0	0	0	0	0	0	0	0	0	0	0	0	0	0	0	0	0	0	0	0	0	0	Aug 16 Thursday
229	0	0	0	0	0	0	0	0	0	0	0	0	0	0	0	0	0	0	0	0	0	0	0	0	0	Aug 17 Friday
230	0	0	0	0	0	0	0	0	0	0	0	0	0	0	0	0	0	0	0	0	0	0	0	0	0	Aug 18 Saturday
231	0	0	0	0	0	0	0	0	0	0	0	0	0	0	0	0	0	0	0	0	0	0	0	0	0	Aug 19 Sunday
232	0	0	0	0	0	0	0	0	0	0	0	0	0	0	0	0	0	0	0	0	0	0	0	0	0	Aug 20 Monday
233	0	0	0	0	0	0	0	0	0	0	0	0	0	0	0	0	0	0	0	0	0	0	0	0	0	Aug 21 Tuesday
234	0	0	0	0	0	0	0	0	0	0	0	0	0	0	0	0	0	0	0	0	0	0	0	0	0	Aug 22 Wednesday
235	0	0	0	0	0	0	0	0	0	0	0	0	0	0	0	0	0	0	0	0	0	0	0	0	0	Aug 23 Thursday
236	0	0	0	0	0	0	0	0	0	0	0	0	0	0	0	0	0	0	0	0	0	0	0	0	0	Aug 24 Friday
237	0	0	0	0	0	0	0	0	0	0	0	0	0	0	0	0	0	0	0	0	0	0	0	0	0	Aug 25 Saturday
238	0	0	0	0	0	0	0	0	0	0	0	0	0	0	0	0	0	0	0	0	0	0	0	0	0	Aug 26 Sunday
239	0	0	0	0	0	0	0	0	0	0	0	0	0	0	0	0	0	0	0	0	0	0	0	0	0	Aug 27 Monday
240	0	0	0	0	0	0	0	0	0	0	0	0	0	0	0	0	0	0	0	0	0	0	0	0	0	Aug 28 Tuesday
241	0	0	0	0	0	0	0	0	0	0	27	23	17	18	15	6	24	8	15	8	3	8	4	13	189	Aug 29 Wednesday
242	13	9	18	6	16	14	13	23	25	20	21	32	17	24	23	16	17	20	13	11	11	6	8	9	385	Aug 30 Thursday
243	20	29	9	5	12	15	14	18	26	24	20	29	0	0	0	0	0	0	0	0	7	3	3	12	246	Aug 31 Friday
244	4	6	7	2	3	1	1	5	2	0	8	3	6	8	4	8	5	5	7	7	8	5	5	0	110	Sep 01 Saturday
245	3	5	0	3	6	4	7	6	5	7	6	18	9	7	6	3	5	12	9	3	13	4	6	3	150	Sep 02 Sunday
246	7	7	8	3	3	3	0	6	10	5	18	23	9	16	7	3	3	1	10	3	12	8	8	12	185	Sep 03 Monday
247	8	10	5	8	2	2	2	4	16	12	15	26	15	11	7	12	2	5	4	4	4	10	4	5	193	Sep 04 Tuesday
248	5	6	7	8	1	5	8	11	15	23	15	21	17	13	14	3	1	10	2	4	1	5	5	9	209	Sep 05 Wednesday
249	2	7	9	4	5	6	4	10	18	13	0	0	0	0	0	0	0	0	0	0	0	0	0	0	78	Sep 06 Thursday
250	0	0	0	0	0	0	0	0	0	0	0	0	0	0	0	0	0	0	0	0	0	0	0	0	0	Sep 07 Friday
251	0	0	0	0	0	0	0	0	0	0	0	0	0	0	0	0	0	0	0	0	0	0	0	0	0	Sep 08 Saturday
252	0	0	0	0	0	0	0	0	0	0	0	0	0	0	0	0	0	0	0	0	0	0	0	0	0	Sep 09 Sunday
253	0	0	0	0	0	0	0	0	0	0	0	0	0	0	0	0	0	0	0	0	0	0	0	0	0	Sep 10 Monday
254	0	0	0	0	0	0	0	0	0	0	0	0	0	0	0	0	0	0	0	0	0	0	0	0	0	Sep 11 Tuesday
255	0	0	0	0	0	0	0	13	13	16	27	25	14	16	11	8	5	8	4	5	8	9	13	5	200	Sep 12 Wednesday
256	9	7	12	4	8	5	3	7	22	15	22	29	24	24	10	6	4	8	7	12	3	5	11	4	261	Sep 13 Thursday
257	11	8	8	13	10	10	14	20	27	26	28	25	4	9	6	3	6	13	4	2	7	3	2	4	263	Sep 14 Friday
258	4	4	7	10	9	11	13	5	13	27	26	21	5	26	28	2	6	5	2	0	5	4	3	8	244	Sep 15 Saturday

Table 3.4.3. (Page 3 of 4)

FIN .FKX Hourly distribution of detections

Day	00	01	02	03	04	05	06	07	08	09	10	11	12	13	14	15	16	17	18	19	20	21	22	23	Sum	Date
259	3	0	2	4	1	5	0	6	6	2	4	6	7	3	4	10	11	11	10	4	16	7	11	5	138	Sep 16 Sunday
260	7	13	6	7	1	9	3	17	35	37	26	40	28	19	24	6	3	7	7	7	4	5	9	7	327	Sep 17 Monday
261	10	11	10	9	5	21	20	26	24	24	16	37	31	19	19	6	6	11	8	5	6	1	8	9	342	Sep 18 Tuesday
262	5	9	5	7	5	9	14	20	13	17	20	11	14	5	4	5	6	4	6	1	6	4	5	5	200	Sep 19 Wednesday
263	6	12	8	6	10	11	15	24	26	40	21	26	26	8	8	3	3	1	5	11	10	11	4	11	306	Sep 20 Thursday
264	12	12	8	6	4	7	6	5	26	20	19	24	12	17	7	2	5	3	5	6	10	2	5	2	225	Sep 21 Friday
265	5	4	17	13	8	28	22	29	35	41	26	31	34	32	33	40	50	52	29	36	55	42	45	58	765	Sep 22 Saturday
266	53	57	36	23	21	36	62	56	51	57	37	28	18	19	7	9	6	4	17	13	8	15	21	14	668	Sep 23 Sunday
267	10	14	12	1	4	0	6	10	10	13	14	25	13	11	16	14	8	8	8	11	10	6	4	7	235	Sep 24 Monday
268	13	7	7	13	5	3	5	12	16	9	21	15	28	18	6	4	2	9	6	10	6	8	7	7	237	Sep 25 Tuesday
269	7	10	7	3	2	1	3	7	12	13	3	0	19	15	10	10	4	6	6	5	4	5	3	6	161	Sep 26 Wednesday
270	3	11	3	2	4	2	4	2	0	0	0	0	0	16	6	11	5	3	5	1	6	13	6	8	111	Sep 27 Thursday
271	6	14	10	6	7	4	5	10	17	17	23	22	16	3	4	7	5	6	5	4	12	2	4	1	210	Sep 28 Friday
272	4	2	2	3	2	11	19	12	8	10	18	16	8	13	4	13	7	4	3	1	1	7	3	1	172	Sep 29 Saturday
273	5	3	4	9	0	5	7	11	13	5	9	8	3	3	4	4	5	2	6	12	14	11	7	12	162	Sep 30 Sunday
FIN	00	01	02	03	04	05	06	07	08	09	10	11	12	13	14	15	16	17	18	19	20	21	22	23		
Sum	759	670	573	636	615	559	1042	728	1548	1413	2581	1888	1999	2194	1347	1870	883	2159	813	843	759	796	753	807	28235	Total sum
72	9	11	9	8	8	9	10	14	20	22	26	36	30	28	26	19	30	12	12	11	11	11	11	10	392	Total average
48	10	10	9	8	6	7	9	14	20	22	29	43	38	34	32	21	38	12	11	12	11	11	12	10	429	Average workdays
24	9	12	9	9	12	11	13	15	18	21	21	22	15	14	14	13	14	13	12	11	11	9	11	11	319	Average weekends

Table 3.4.3. Daily and hourly distribution of FINESA detections. For each day is shown number of detections within each hour of the day, and number of detections for that day. The end statistics give total number of detections distributed for each hour and the total sum of detections during the period. The averages show number of processed days, hourly distribution and average per processed day. (Page 4 of 4)

3.5 IMS operation

The Intelligent Monitoring System (IMS) was installed at NORSAR in December 1989 and has been operated experimentally since 1 January 1990 for automatic processing of multiple-array data. The current version of IMS processes data from the two-array network consisting of NORESS and ARCESS. Future upgrades of IMS will allow data from additional arrays and single stations to be incorporated.

In general, our routine operation of the IMS during the reporting period has progressed well, and the system has proved to be very powerful and flexible. The well-developed automatic processing combined with very versatile interactive tools has kept the analyst workload at a low level, and in fact only one analyst has been required to handle the regular processing at any time.

Since the IMS is still in an initial stage, there have naturally been some problems of a technical nature, but these have diminished considerably as the system has matured. At the end of the reporting period, the IMS system is running very smoothly.

Table 3.5.1 presents an overview of IMS event processor downtimes. Table 3.5.2 gives a summary of phase detections and processed regional events by IMS. From top to bottom, the table gives the total number of detections by the IMS, the detections that are associated with regional events declared by the IMS, the number of detections that are not associated with such events, the number of regional events declared by the IMS, the number of such events rejected by the analyst, the number of events accepted by the analyst, the number of events accepted by the analyst without any changes, and finally the number of events accepted after some sort of modification by the analyst. This last category is divided into three classes: Events where phases (not detected by the IMS) have been added by the analyst, events for which the phase assignments by the IMS have been changed or one or more phase detections have been removed, and events for which the changes by the analyst have amounted to retiming the phases only.

From initial review of the IMS bulletin, it is clear that the final output is of very high quality from a seismological point of view. More detailed evaluation will be conducted at a later stage.

B.Kr. Hokland
U. Baadshaug
S. Mykkeltveit

1990	May	29	14:47:01.000	-	1990	May	30	10:06:07.000
1990	May	30	13:13:30.000	-	1990	May	31	18:30:50.379
1990	Jun	8	14:20:32.713	-	1990	Jun	9	08:00:00.000
1990	Jun	9	12:55:30.000	-	1990	Jun	9	22:30:51.000
1990	Jun	10	11:22:22.752	-	1990	Jun	11	10:00:00.000
1990	Jun	15	13:23:21.700	-	1990	Jun	16	00:00:00.000
1990	Jun	16	13:24:57.500	-	1990	Jun	19	00:00:00.000
1990	Jun	22	20:13:36.000	-	1990	Jun	26	00:00:00.000
1990	Jun	26	03:34:17.000	-	1990	Jun	26	18:27:20.000
1990	Jun	30	10:20:53.800	-	1990	Jul	1	00:00:00.000
1990	Jul	6	07:45:52.000	-	1990	Jul	7	00:00:00.000
1990	Jul	9	17:56:50.500	-	1990	Jul	10	00:00:00.000
1990	Jul	10	23:29:23.700	-	1990	Jul	12	00:00:00.000
1990	Jul	13	13:26:07.600	-	1990	Jul	15	00:00:00.000
1990	Jul	16	16:15:52.800	-	1990	Jul	17	00:00:00.000
1990	Jul	17	09:17:33.300	-	1990	Jul	19	00:00:00.000
1990	Jul	19	21:39:56.200	-	1990	Jul	22	10:56:47.400
1990	Jul	22	20:27:00.000	-	1990	Jul	24	00:24:57.933
1990	Jul	24	09:55:22.500	-	1990	Jul	24	23:35:08.241
1990	Aug	5	05:26:02.840	-	1990	Aug	6	05:18:15.167
1990	Aug	13	20:15:28.400	-	1990	Aug	17	18:00:00.000
1990	Aug	18	20:38:30.200	-	1990	Aug	19	18:00:00.000
1990	Sep	1	05:14:22.800	-	1990	Sep	2	00:00:00.000
1990	Sep	10	04:43:55.100	-	1990	Sep	24	00:00:00.000
1990	Sep	28	09:40:09.800	-	1990	Sep	29	00:00:00.000
1990	Sep	30	10:29:13.300	-	1990	Sep	30	24:00:00.000

Table 3.5.1. IMS event processor (pipeline) downtimes. Logging of time intervals not processed by the event processor (pipeline) started the last week of May. The main reason for these downtimes was slow performance of the event processing, causing loss of waveform data from the disk before the events were processed.

	Apr 90	May 90	Jun 90	Jul 90	Aug 90	Sep 90	total
Phase detections	11843	13988	13178	10989	19267	15402	84667
- Associated phases	1685	2521	1863	1125	2361	1021	10576
- Unassociated phases	10158	11467	11315	9864	16906	14381	74091
Events declared	708	1002	834	493	943	278	4258
- Rejected events	183	196	237	131	218	43	1009
- Accepted events	525	806	597	361	725	235	3249
Unchanged events	85	186	293	172	290	78	1104
Modified events	440	620	304	189	435	157	2145
Phases added	46	63	23	9	30	16	187
Phases changed or removed	281	402	270	180	405	141	1679
Retiming only	113	155	11	0	0	0	279

Table 3.5.2. IMS phase detections and events summary. Statistics for "retiming only" have been compiled only up to June 4.

4 Improvements and Modifications

4.1 NORSAR

NORSAR data acquisition

No modification has been made to the NORSAR data acquisition system.

RD3 digitizers and acquisition equipment have been acquired from Nanometrics

to test recording at one subarray. There are two major tasks that need to be worked upon:

1. Solving the problem of getting enough DC current from the central vault to the digitizer at the seismometer.
2. Including SDLC communication in the Nanometrics system to get a continuous data stream from the subarray to the NORSAR data processing center. (This is currently not offered by the manufacturer.)

NORSAR detection processing

The NORSAR detection processor has been running satisfactorily on the IBM during this reporting period.

Detection statistics are given in section 2.

NORSAR event processing

There are no changes in the routine processing of NORSAR events, using the IBM system.

4.2 NORESS/ARCESS/FINESA/GERESS

Detection processing

The routine detection processing of the arrays is running satisfactorily on each of the arrays' SUN-3/280 acquisition systems. The same program is used for NORSAR/NORESS/ARCESS/ FINESA/GERESS, but with different recipes. The beam table for NORESS/ARCESS is found in NORSAR Sci. Rep. No. 1-89/90. A new beam table for FINESA is found in Table 4.2.1. This change of the beam table is related to changes in the FINESA array geometry in August. A new vertical sensor was installed at the array center (A0), and horizontal sensors were added at the existing A1 site. Test processing of GERESS data has been started, and the initial beam table is shown in Table 4.2.2.

Event processing. Phase estimation

This process does F-K and polarization analysis for each detection to determine phase velocity, azimuth and type of phase.

The processing using the EP program is now running on the IMS machines, and detections are put into the ORACLE detection data base for use by IMS.

Plot and epicenter determination

A description of single array event processing is found in NORSAR Sci. Rep. No. 2-88/89, and NORSAR Sci. Rep. No. 2-89/90.

J. Fyen

BEAM	Velocity	Azimuth	Filter band	Threshold		Configuration
C011	99999.9	0.0	0.5 - 1.5	4.4	7	C
C021	99999.9	0.0	1.0 - 3.0	4.4	7	C
C031	99999.9	0.0	1.5 - 3.5	4.4	7	C
C032	11.0	30.0	1.5 - 3.5	4.4	7	C
C033	11.0	90.0	1.5 - 3.5	4.4	7	C
C034	11.0	150.0	1.5 - 3.5	4.4	7	C
C035	11.0	210.0	1.5 - 3.5	4.4	7	C
C036	11.0	270.0	1.5 - 3.5	4.4	7	C
C037	11.0	330.0	1.5 - 3.5	4.4	7	C
C038	15.0	80.0	1.5 - 3.5	3.9	7	C
C039	10.0	20.0	1.5 - 3.5	3.9	7	C
C041	99999.9	0.0	2.0 - 4.0	4.4	7	C
C042	10.2	30.0	2.0 - 4.0	4.4	7	C
C043	10.2	90.0	2.0 - 4.0	4.4	7	C
C044	10.2	150.0	2.0 - 4.0	4.4	7	C
C045	10.2	210.0	2.0 - 4.0	4.4	7	C
C046	10.2	270.0	2.0 - 4.0	4.4	7	C
C047	10.20	330.0	2.0 - 4.0	4.4	7	C
C048	15.0	80.0	2.0 - 4.0	3.9	7	C
C049	10.0	20.0	2.0 - 4.0	3.9	7	C
C051	99999.9	0.0	2.5 - 4.5	4.4	13	BC
C052	8.9	30.0	2.5 - 4.5	4.4	13	BC
C053	8.9	90.0	2.5 - 4.5	4.4	13	BC
C054	8.9	150.0	2.5 - 4.5	4.4	13	BC
C055	8.9	210.0	2.5 - 4.5	4.4	13	BC
C056	8.9	270.0	2.5 - 4.5	4.4	13	BC
C057	8.9	330.0	2.5 - 4.5	4.4	13	BC
C058	15.0	80.0	2.5 - 4.5	3.9	13	BC
C061	99999.9	0.0	3.0 - 5.0	4.4	13	BC
C062	10.5	30.0	3.0 - 5.0	4.4	13	BC
C063	10.5	90.0	3.0 - 5.0	4.4	13	BC
C064	10.5	150.0	3.0 - 5.0	4.4	13	BC
C065	10.5	210.0	3.0 - 5.0	4.4	13	BC
C066	10.5	270.0	3.0 - 5.0	4.4	13	BC
C067	10.5	330.0	3.0 - 5.0	4.4	13	BC
C068	15.0	80.0	3.0 - 5.0	3.9	13	BC
C071	99999.9	0.0	3.5 - 5.5	4.4	16	ABC
C072	11.1	30.0	3.5 - 5.5	4.4	16	ABC
C073	11.1	90.0	3.5 - 5.5	4.4	16	ABC

C074	11.1	150.0	3.5 - 5.5	4.4	16	ABC
C075	11.1	210.0	3.5 - 5.5	4.4	16	ABC
C076	11.1	270.0	3.5 - 5.5	4.4	16	ABC
C077	11.1	330.0	3.5 - 5.5	4.4	16	ABC
C081	99999.9	0.0	4.0 - 8.0	4.4	16	ABC
C082	9.5	30.0	4.0 - 8.0	4.4	16	ABC
C083	9.5	90.0	4.0 - 8.0	4.4	16	ABC
C084	9.5	150.0	4.0 - 8.0	4.4	16	ABC
C085	9.5	210.0	4.0 - 8.0	4.4	16	ABC
C086	9.5	270.0	4.0 - 8.0	4.4	16	ABC
C087	9.5	330.0	4.0 - 8.0	4.4	16	ABC
C091	99999.9	0.0	5.0 - 10.0	4.9	16	ABC
C092	10.5	30.0	5.0 - 10.0	4.9	16	ABC
C093	10.5	90.0	5.0 - 10.0	4.9	16	ABC
C094	10.5	150.0	5.0 - 10.0	4.9	16	ABC
C095	10.5	210.0	5.0 - 10.0	4.9	16	ABC
C096	10.5	270.0	5.0 - 10.0	4.9	16	ABC
C097	10.5	330.0	5.0 - 10.0	4.9	16	ABC
C101	99999.9	0.0	8.0 - 16.0	4.9	10	AB
C102	9.9	30.0	8.0 - 16.0	4.9	10	AB
C103	9.9	90.0	8.0 - 16.0	4.9	10	AB
C104	9.9	150.0	8.0 - 16.0	4.9	10	AB
C105	9.9	210.0	8.0 - 16.0	4.9	10	AB
C106	9.9	270.0	8.0 - 16.0	4.9	10	AB
C107	9.9	330.0	8.0 - 16.0	4.9	10	AB
CI01	99999.9	0.0	0.5 - 1.5	2.9	7	C
CI02	99999.9	0.0	1.0 - 2.0	2.9	7	C
CI03	99999.9	0.0	1.5 - 2.5	2.9	7	C
CI04	99999.9	0.0	2.0 - 4.0	2.5	7	C
CI05	99999.9	0.0	3.5 - 5.5	2.5	7	C
CI06	99999.9	0.0	5.0 - 10.0	2.7	7	C

Table 4.2.1. FINESA beam table. Valid from 1990-237: (25 august 1990), when A0 was included. The table shows name of beam, velocity (km/sec), azimuth (degrees), filter band (Hz), STA/LTA threshold, and configuration. The configuration is described with number of sensors and A, B or C-rings. The sensor at A0 is included in all configurations. CI01 – CI06 are incoherent beams.

BEAM	Velocity	Azimuth	Filter band	Threshold	Configuration
G011	99999.9	0.0	0.5 - 1.5	4.5	10 D
G021	99999.9	0.0	1.0 - 3.0	4.5	17 CD
G031	99999.9	0.0	1.5 - 3.5	4.5	17 CD
G032	11.0	30.0	1.5 - 3.5	4.5	17 CD
G033	11.0	90.0	1.5 - 3.5	4.5	17 CD
G034	11.0	150.0	1.5 - 3.5	4.5	17 CD
G035	11.0	210.0	1.5 - 3.5	4.5	17 CD
G036	11.0	270.0	1.5 - 3.5	4.5	17 CD
G037	11.0	330.0	1.5 - 3.5	4.5	17 CD
G038	15.8	80.0	1.5 - 3.5	4.5	17 CD
G039	10.0	30.0	1.5 - 3.5	4.5	17 CD
G041	99999.9	0.0	2.0 - 4.0	4.5	17 CD
G042	10.2	30.0	2.0 - 4.0	4.5	17 CD
G043	10.2	90.0	2.0 - 4.0	4.5	17 CD
G044	10.2	150.0	2.0 - 4.0	4.5	17 CD
G045	10.2	210.0	2.0 - 4.0	4.5	17 CD
G046	10.2	270.0	2.0 - 4.0	4.5	17 CD
G047	10.2	330.0	2.0 - 4.0	4.5	17 CD
G048	15.8	80.0	2.0 - 4.0	4.5	17 CD
G049	10.0	30.0	2.0 - 4.0	4.5	17 CD
G051	99999.9	0.0	2.5 - 4.5	4.5	22 BCD
G052	8.9	30.0	2.5 - 4.5	4.5	22 BCD
G053	8.9	90.0	2.5 - 4.5	4.5	22 BCD
G054	8.9	150.0	2.5 - 4.5	4.5	22 BCD
G055	8.9	210.0	2.5 - 4.5	4.5	22 BCD
G056	8.9	270.0	2.5 - 4.5	4.5	22 BCD
G057	8.9	330.0	2.5 - 4.5	4.5	22 BCD
G058	15.8	80.0	2.5 - 4.5	4.5	22 BCD
G059	10.0	30.0	2.5 - 4.5	4.5	22 BCD
G061	99999.9	0.0	3.0 - 5.0	4.5	22 BCD
G062	10.5	30.0	3.0 - 5.0	4.5	22 BCD
G063	10.5	90.0	3.0 - 5.0	4.5	22 BCD
G064	10.5	150.0	3.0 - 5.0	4.5	22 BCD
G065	10.5	210.0	3.0 - 5.0	4.5	22 BCD
G066	10.5	270.0	3.0 - 5.0	4.5	22 BCD
G067	10.5	330.0	3.0 - 5.0	4.5	22 BCD
G068	15.8	80.0	3.0 - 5.0	4.5	22 BCD
G069	10.0	30.0	3.0 - 5.0	4.5	22 BCD
G071	99999.9	0.0	3.5 - 5.5	4.5	13 BC
G072	11.1	30.0	3.5 - 5.5	4.5	13 BC
G073	11.1	90.0	3.5 - 5.5	4.5	13 BC

G074	11.1	150.0	3.5 - 5.5	4.5	13	BC
G075	11.1	210.0	3.5 - 5.5	4.5	13	BC
G076	11.1	270.0	3.5 - 5.5	4.5	13	BC
G077	11.1	330.0	3.5 - 5.5	4.5	13	BC
G081	99999.9	0.0	4.0 - 8.0	4.5	13	BC
G082	9.5	30.0	4.0 - 8.0	4.5	13	BC
G083	9.5	90.0	4.0 - 8.0	4.5	13	BC
G084	9.5	150.0	4.0 - 8.0	4.5	13	BC
G085	9.5	210.0	4.0 - 8.0	4.5	13	BC
G086	9.5	270.0	4.0 - 8.0	4.5	13	BC
G087	9.5	330.0	4.0 - 8.0	4.5	13	BC
G091	99999.9	0.0	5.0 - 10.0	5.0	13	BC
G092	10.5	30.0	5.0 - 10.0	5.0	13	BC
G093	10.5	90.0	5.0 - 10.0	5.0	13	BC
G094	10.5	150.0	5.0 - 10.0	5.0	13	BC
G095	10.5	210.0	5.0 - 10.0	5.0	13	BC
G096	10.5	270.0	5.0 - 10.0	5.0	13	BC
G097	10.5	330.0	5.0 - 10.0	5.0	13	BC
G101	99999.9	0.0	8.0 - 16.0	5.0	9	AB
G102	9.9	30.0	8.0 - 16.0	5.0	9	AB
G103	9.9	90.0	8.0 - 16.0	5.0	9	AB
G104	9.9	150.0	8.0 - 16.0	5.0	9	AB
G105	9.9	210.0	8.0 - 16.0	5.0	9	AB
G106	9.9	270.0	8.0 - 16.0	5.0	9	AB
G107	9.9	330.0	8.0 - 16.0	5.0	9	AB
GH01	99999.9	0.0	2.0 - 4.0	3.0	8	AC_ne
GH02	99999.9	0.0	3.5 - 5.5	3.0	8	AC_ne
GH03	99999.9	0.0	5.0 - 10.0	3.0	8	AC_ne
GH04	99999.9	0.0	8.0 - 16.0	3.0	8	AC_ne
GV01	99999.9	0.0	0.5 - 1.5	3.0	10	D
GV02	99999.9	0.0	1.0 - 2.0	3.0	8	C
GV03	99999.9	0.0	1.5 - 2.5	3.0	8	C
GV04	99999.9	0.0	2.0 - 3.0	3.0	8	C
GV05	99999.9	0.0	2.0 - 4.0	3.0	8	C
GV06	99999.9	0.0	3.5 - 5.5	3.0	8	C

Table 4.2.2. GERESS beam table. Initial test beam set. The table shows name of beam, velocity (km/sec), azimuth (degrees), filter band (Hz), STA/LTA threshold, and configuration. The configuration is described with number of sensors and A, B, C or D-rings. Center A0 is always within the configuration. GH01 - GH04 are incoherent beams using horizontal components of the A2, D1, D4 and D7 three-component stations. GV01 - GV04 are incoherent beams using vertical components. This beam set has been in operation since 1990-294:03.

5 Maintenance Activities

5.1 Activities in the field and at the Maintenance Center

This section summarizes the activities in the field, at the Maintenance Center (NMC) Hamar and NDPC activities related to monitoring and control of the NORSAR, NORESS and ARCESS arrays.

Activities involve preventive and corrective maintenance, and in addition installation and modification of equipment in the field and at the Maintenance Center.

NORSAR

Visits were made to the arrays in connection with adjustment of channel gain and offset SP/LP. Adjustments of LP seismometer mass position (MP) and free period (FP) were made. Cables have been located/pointed out and also repaired/spliced. Subarrays have been visited in connection with loss of power. At the Well Head Vaults (WHVs) RA-5 amplifiers have been replaced. Communication lines have been tested and modems replaced.

NORESS

The NORESS array has been visited in connection with replacement of fiber optical transmitters on the Hub card (site C4). A water leakage was stopped in connection with C2 WHV. In June an AC power failure caused a visit to the central station (Hub). In September a new UPS (Uninterruptible Power Supply) system was installed.

ARCESS

Also here activities have been diverse. An air-conditioner in the central building at the array site has been replaced, and fiber optical transmitters have been replaced on fiber optical links. Fiber optical transmitters/receivers on the Hub 15 card were replaced (site C4). In addition, transmitters/receivers on a DHL 70 card were replaced (site D4). A GS- 13 seismometer was replaced (site D5).

Details are presented in Table 5.1.

Subarray/ area	Task	Date
NORSAR:	No visits	
NORESS:	Replaced fiber optical transmitters on Hub 15 card	5 April
NMC:	Tested/modified new equipment in connection with extension of the FINESA array	April
NDPC:	Daily check of NORSAR, NORESS, ARCESS and FINESA status Weekly calibration of NORSAR SP/LP instruments Continuous measurement of Mass Position and Free Period. Adjusted when outside tolerances	April
NORSAR:		
02C	Located faulty SLEM power supply	3 May
01B	Meausrements revealed faulty cable SP02,04	7 May
01B	Cable work SP02,04	14 May
06C	Channel gain and DC offset on all SP/LP channels adjusted	19 May
01B	Cable work SP02,04 terminated	22 May
04C	SP/LP checked	28 May
02C	Power failure stated; electricians from the local power plant had already arrived	30 May
NORESS:	Stopped water leakage to the C2 Well Head Vault	8,9,10 May
	Reinstalled equipment, including seismometers	10 May
	C4 repaired	18 May
NDPC:	Daily check of NORSAR, NORESS, ARCESS and FINESA status Weekly calibration of NORSAR SP/LP instruments Continuous measurement of Mass Position and Free Period	May

Table 5.1 Activities in the field and the NORSAR Maintenance Center, including NDPC activities related to the NORSAR, NORESS, ARCESS and FINESA arrays, 1 April — 30 September 1990.

Subarray/ area	Task	Date
NORSAR:		
02B	A modem was replaced	8 June
	AC failure	19 June
	Gain adjusted on all channels (LTA)	
	DC offset adjusted on all channels	
	"Old" modem reinstalled	22 June
04C	Lost AC power	1 June
06C	AC failure, 2 phases lost	28 June
NORESS:	AC failure	28 June
ARCESS:	Replaced air-conditioner	25,26
	Replaced optical transmitter at remote site D2	June
	Replaced all fiber optical links (to remote sites)	
	Replaced fiber optical transmitters at the Hub 15 card, site B1 and B3	
NDPC:	Daily check of NORSAR, NORESS, ARCESS and FINESA status	June
	Weekly calibration of NORSAR SP/LP instruments	
	Continuous measurement of Mass Position and Free Period	
	Adjustment of Mass Position and Free Period when outside tolerances	
NORSAR:		
02B	Visit in connection with loss of power	12 July
	SLEM reset	16 July
02C	Replaced FP/MP centering device EW seism.	4 July
	Cable splicing carried out SP05	10 July
04C	Comm. work in cooperation with NTA/Hamar	3,9 July
	SP02,03 repair	17 July
	Repair of LP EW seismometer	18,19 July
	Gain and offset adjustments all channels SP/LP	20 July
06C	Installed a new RA-5 amplifier SP02	12 July
	Cable work carried out at site D5	16 July
ARCESS:	Replaced fiber optical transm./receiver on Hub 15 card, site 4	24 July
	Reset "white box" communications unit	
	Replaced transm./receiver on DHL 68 card site A0	

Table 5.1 (cont.)

Subarray/ area	Task	Date
	Replaced DHL 70 card site D4 (vertical channel)	
	Replaced GS13 seismometer at site D5	
NDPC:	Daily check of NORSAR, NORESS, ARCESS and FINESA status	July
	Weekly calibration of NORSAR SP/LP instruments	
	Continuous measurement of Mass Position and Free Period	
	Adjustment of Mass Position and Free Period when outside tolerances	
NORSAR:	Visit in connection with power loss	27 Aug
02B	Cable work	27 Aug
04C	Repaired SP cal. generator	27 Aug
06C	Cable pointed out	31 Aug
FINESA:	NMC staff reinstalled data acquisition unit	20-26
	New channels A0Z, A0Z low channel, A1NS, A1EW installed	Aug
NDPC:	Daily check of NORSAR, NORESS, ARCESS and FINESA status	Aug
	Weekly calibration of NORSAR SP/LP instruments	
	Continuous measurement of Mass Position and Free Period	
	Adjustment of Mass Position and Free Period when outside tolerances	
NORSAR:		
01A	Replaced RA-5, SP02	27 Sep
	Channel gain all SP channels adjusted	
	MP/FP NS and EW LP seismometer adjusted	
04C	Replaced RCD (Remote Centering Device) NS LP seismometer	11 Sep
	Repaired improper connection in the EW data circuit	
06C	Cable SP05 pointed out	7 Sep
	Cable work SP04	10 Sep
	Splicing of cable SP04,05	24 Sep
NORESS:	Installed new UPS system	19-20 Sep
	Installation and initialization	26 Sep

Table 5.1 (cont.)

Subarray/ area	Task	Date
NDPC:	Daily check of NORSAR, NORESS, ARCESS and FINESA status Weekly calibration of NORSAR SP/LP instruments. Continuous measurement of Mass Position and Free Period Adjustment of Mass Position and Free Period when outside tolerances	Sep

Table 5.1 (cont.)

5.2 Array status

As of 30 September 1990 the following NORSAR channels deviated from tolerances.

01A 01 8 Hz filter
02 8 Hz filter
04 30 dB attenuator

O.A. Hansen

6 Documentation Developed

Alsaker, A., L.B. Kvamme, R.A. Hansen, A. Dahle and H. Bungum (1990): The M_L scale in Norway, *Bull. Seism. Soc. Am.*, in press.

Bungum, H. and A. Alsaker (1990): Source spectral inversion for two earthquake sequences offshore western Norway, *Bull. Seism. Soc. Am.*, in press.

Fyen, J. (1990): Diurnal and seasonal variations in the microseismic noise level observed at the NORESS array, *Phys. Earth Planet. Int.*, 63, 252–268.

Havskov, J., H. Bungum and L.B. Kvamme (1990): The Norwegian regional network and data center operation, *Phys. Earth Planet. Inter.*, submitted for publication.

Kværna, T. (1990): Sources of short-term fluctuations in the seismic noise level at NORESS, *Phys. Earth Planet. Int.*, 63, 269–276.

Mitchell, B.J., H. Bungum, W.W. Chan and P.B. Mitchell (1990): Seismicity and present-day tectonics of the Svalbard region, *Geophys. J. Int.*, 102, 139–149.

Mykkeltveit, S., J. Fyen, F. Ringdal and T. Kværna (1990): Spatial characteristics of the NORESS noise field and implications for array detection processing, *Phys. Earth Planet. Int.*, 63, 277–283.

Ringdal, F., S. Mykkeltveit, J. Fyen and T. Kværna (1990): Spectral analysis of seismic signals and noise recorded at the NORESS high-frequency element, *Phys. Earth Planet. Int.*, 63, 243–251.

Semiannual Tech. Summary, 1 Oct 1989 – 31 March 1990, NORSAR Sci. Rep. No. 1-89/90, Kjeller, Norway.

L.B. Loughran

7 Summary of Technical Reports / Papers Published

7.1 Detection and yield estimation studies

1. Yield estimation using Lg recordings

Over the past several years, extensive research has taken place at NORSAR to develop and evaluate the RMS Lg estimation technique for underground nuclear explosions. Some of the most recent results have been documented by Ringdal and Marshall (1989) and Hansen, Ringdal and Richards (1990).

These studies have so far concentrated on the Shagan River (Semipalatinsk) test site, using data from stations in Norway, Germany, USSR and China (Fig. 7.1.1). By using NORSAR as a reference system, and plotting observed RMS Lg for other stations against NORSAR values, it has been found that the standard deviations of the residuals are consistently as low as 0.03 magnitude units, as shown for selected stations in Fig. 7.1.2. Furthermore, comparing two of the stations with lowest Lg detection threshold (GAM and ARU in the Soviet Union), we have found that this consistency appears to span two full orders of event magnitude, down to approximately m_b = 4.0 (Hansen *et al*, 1990).

A possibility to compare the RMS Lg magnitudes to published yields for Semipalatinsk explosions has now emerged with the recent publication by Soviet scientists quoting yield estimates for a number of such explosions (Bocharov *et al*, 1989; see also Vergino, 1989a,b). We have made an effort to conduct detailed analysis of available NORSAR Lg data for the explosions in this data set. Since NORSAR is located at more than 4000 km distance from Semipalatinsk, only explosions of more than 10 kt yield will usually provide sufficient SNR for Lg measurements at this station, and even so, it must be noted that at these lower yields, the estimated RMS Lg is less precise than at yields exceeding 50 kt.

Table 7.1.1 gives the NORSAR Lg magnitudes obtained in these analyses. The table comprises altogether 8 explosions from both the Shagan River (Balapan), Degelen Mountains and Konystan (Murzhik) subareas. The NORSAR data for the four largest of these explosions have been previously presented in Ringdal (1989).

Fig. 7.1.3 (top part) shows a plot of NORSAR M(Lg) versus published yields for these 8 explosions. For comparison, the bottom part of Fig. 7.1.3 shows world-wide m_b (UK values as quoted by Vergino, 1989a) versus yield for the same 8 events. The slope in each plot has been restricted to 0.75, and the standard deviation in the vertical direction is 0.043 for M(Lg) and 0.081 for m_b versus log yield. We note that this data set is too small to allow any confident

estimate of the accuracy in estimating yield from M(Lg), especially in view of the aforementioned uncertainty in M(Lg) values for the smaller explosions. Nevertheless, the figure would appear to confirm the potential of RMS Lg as a stable estimator of yields for fully coupled explosions from this region, and indicates that even single station M(Lg) is better correlated to log(yield) than is world-wide m_b.

2. P-wave detectability studies

Ringdal (1990) has conducted a study of the NORESS array detection capability for Semipalatinsk explosions, both in terms of m_b and yield (Bocharov *et al*, 1989). In terms of NORESS m_b, the 50 per cent detection threshold is estimated at $m_b = 3.7 \pm 0.1$. A noteworthy feature, illustrated in Fig. 7.1.4, is the large difference in NORSAR m_b bias (S) for the subregions Shagan River ($S \approx 1.0$) and Degelen/Konystan ($S \approx 0.4$). In terms of world-wide m_b, the estimated NORESS detection threshold, at the 50 per cent level, thus becomes $m_b = 2.7$ and $m_b = 3.3$ for these subareas, respectively.

Fig. 7.1.5 shows NORESS m_b values (measured at the NORSAR seismometer 06C02 which is co-located with the present NORESS center site) versus log yield for 6 low-yield nuclear explosions (the only ones in Bocharov *et al* (1989) with available data that did not exceed NORSAR's dynamic range). As before, we have used a restricted slope of 0.75 in the magnitude-log yield relationship, and fitted a straight line with this slope to the observed data. The NORESS beam threshold range (plus/minus two standard deviations) is shown as dotted horizontal lines.

Fig. 7.1.5 indicates that, given similar coupling conditions and noise levels as in our data base of 6 explosions, Semipalatinsk explosions of yields at 0.1 kt would be expected to produce detectable signals at NORESS. We note that the 6 reference explosions are all from Degelen or Konystan. In view of the previous discussions, the detectability for Shagan River explosions would be expected to be even better.

In Fig. 7.1.6, we plot NORESS, ARCESS, FINESA and GERESS recordings of an $m_b = 5.7$ nuclear explosion at Novaya Zemlya. The figure shows an unfiltered, single sensor trace for each array, and the signal-to-noise rato on the best array beam (STA/LTA as computed by the online detector) is given in the figure caption. ARCESS has a strong S-phase detection, and there is some S-wave energy visible also for the three other arrays. The Lg phase is not visible on these unfiltered recordings, but in the best filter band, the energy in the Lg window still exceeds significantly the pre-P noise.

From Fig. 7.1.6 it is seen that the P-wave detection capability for Novaya Zemlya explosions is excellent for NORESS, FINESA and ARCESS, in particular the latter. Thus, ARCESS SNR for the event shown was 8383 on the array beam in the filter band 3–5 Hz. This is more than 3 orders of magni-

tude above the operational threshold, and we note that similar SNR has been observed for the other Novaya Zemlya explosions of similar size recorded at ARCESS (only 4 such events have been recorded since the array came into operation). While this is too limited a data base to give a reliable threshold estimate, a straight extrapolation would indicate that the ARCESS threshold at this site is well below $m_b = 3.0$. NORESS and FINESA also appear to have thresholds close to $m_b = 3.0$, whereas GERESS has a lower detectability for this test site.

3. Conclusions and Recommendations

Our studies confirm that Lg magnitude estimates of Semipalatinsk explosions are remarkably consistent between stations widely distributed in epicentral distance and azimuth. It thus appears that a single station with good signal-to-noise ratio can provide M(Lg) measurements with an accuracy (one standard deviation) of about 0.03 magnitude unit. It is noteworthy that this accuracy is consistently obtained for a variety of stations at very different azimuths and distances, even though the basic parameters remain exactly as originally proposed by Ringdal for NORSAR recordings (0.6–3.0 Hz bandpass filter, RMS window length of 2 minutes, centered at a time corresponding to a group velocity of 3.5 km/s). Moreover, the Lg phase shows considerable promise for use in yield determination, although more data will be needed before the accuracy of Lg-estimated yields can be firmly established.

The excellent detection capability of the regional arrays in northern Europe have been confirmed by case studies, comprising a detailed evaluation of the NORESS capability for Semipalatinsk explosions, and preliminary observations of ARCESS detection of Novaya Zemlya explosions.

Further work will be directed toward additional expansion of these studies, in particular analyzing new data as they become available, and pursuing our analysis of Novaya Zemlya recordings at regional arrays as well as other available stations.

F. Ringdal

References

Bocharov, V.S., S.A. Zelentsov and V.I. Mikhailov (1989). Characteristics of 96 underground nuclear explosions at the Semipalatinsk test facility, *Atomic Energy, 67* **3**, 210–214 (in Russian).

Hansen, R.A., F. Ringdal and P.G. Richards (1990). The stability of RMS Lg measurements, and their potential for accurate estimation of the yields of Soviet underground nuclear explosions, *Bull. Seism. Soc. Am.*, Special Issue (in press).

Ringdal, F. (1989): NORSAR P-wave detection and yield estimation of selected Semipalatinsk explosions, NORSAR Semiannual Tech. Summary, 1 April – 30 September 1989, NORSAR Sci. Rep. No. 1-89/90, Kjeller, Norway.

Ringdal, F. (1990): Teleseismic event detection using the NORESS array, with special reference to low-yield Semipalatinsk explosions, *Bull. Seism. Soc. Am.*, Special Issue, in press.

Ringdal, F., and P.D. Marshall (1989). Yield determination of Soviet underground nuclear explosions at the Shagan River Test Site, *NORSAR Semiannual Tech. Summary, 1 October 1988 – 31 March 1989*, NORSAR Sci. Rep. No. 2-88/89, Kjeller, Norway.

Vergino, E.S. (1989a). Soviet test yields, *EOS*, Trans. Am. Geophys. Union, 1511+, November 28.

Vergino, E.S. (1989b). Soviet test yields, Corrections and Additions, *EOS*, Trans. Am. Geophys. Union, 1569, December 26.

Date	Region	m_b	NORSAR M(Lg)	Yield (kt)
11/30/69	Shagan (TZ)	6.048	6.043	125
04/25/71	Degelen	6.076	5.862	90
06/06/71	Konystan	5.526	5.44	16
10/09/71	Konystan	5.371	5.25*)	12
10/21/71	Konystan	5.580	5.54	23
02/10/72	Shagan (NE)	5.370	5.37	16
11/02/72	Shagan (SW)	6.224	6.118	165
12/10/72	Shagan (NE)	5.996	6.095**)	140

*) Low precision due to low SNR

**) Adjusted for interfering explosion

Table 7.1.1. Parameters of eight explosions analyzed in this study. Yield estimates are from Bocharov *et al* (1989), and the m_b values are the "UK m_b" listed in Vergino (1989a).

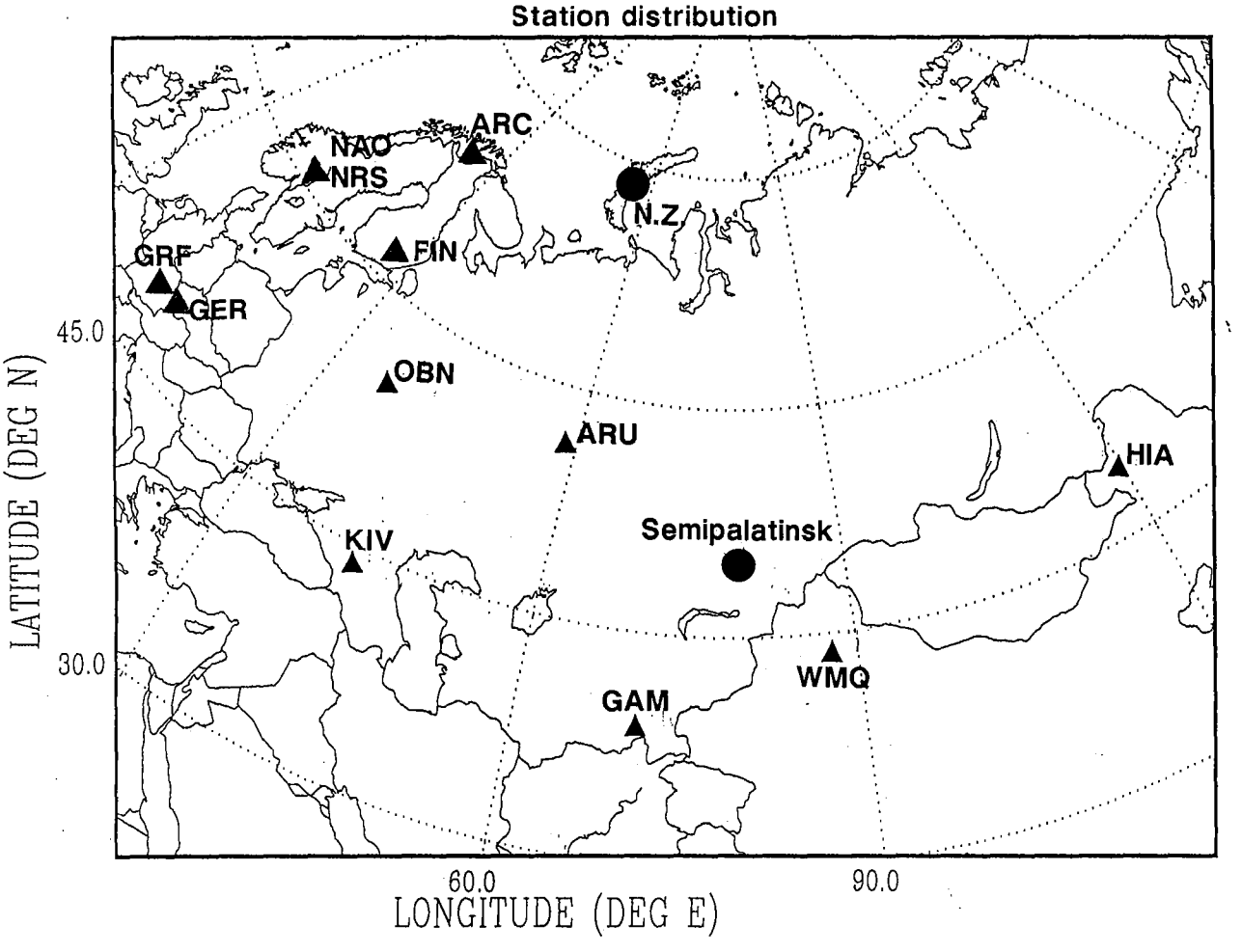

Fig. 7.1.1. Map showing the location of stations analyzed in this study (triangles). The two main USSR test sites (Novaya Zemlya and Semipalatinsk) are marked as filled circles.

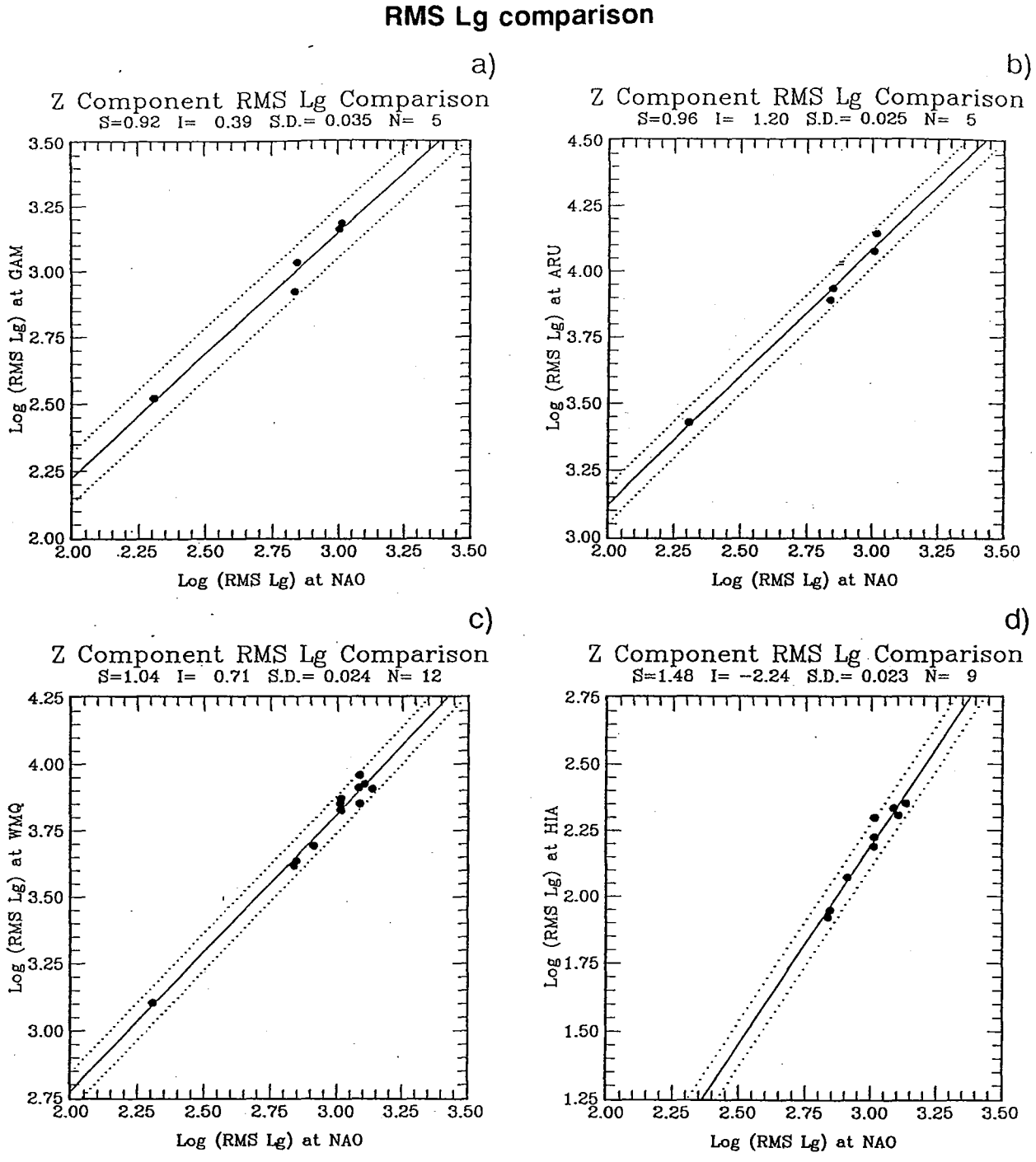

Fig. 7.1.2. Examples of observed correlations between RMS Lg at NORSAR and selected stations in the USSR and China. Note the excellent consistency in all of the plots.

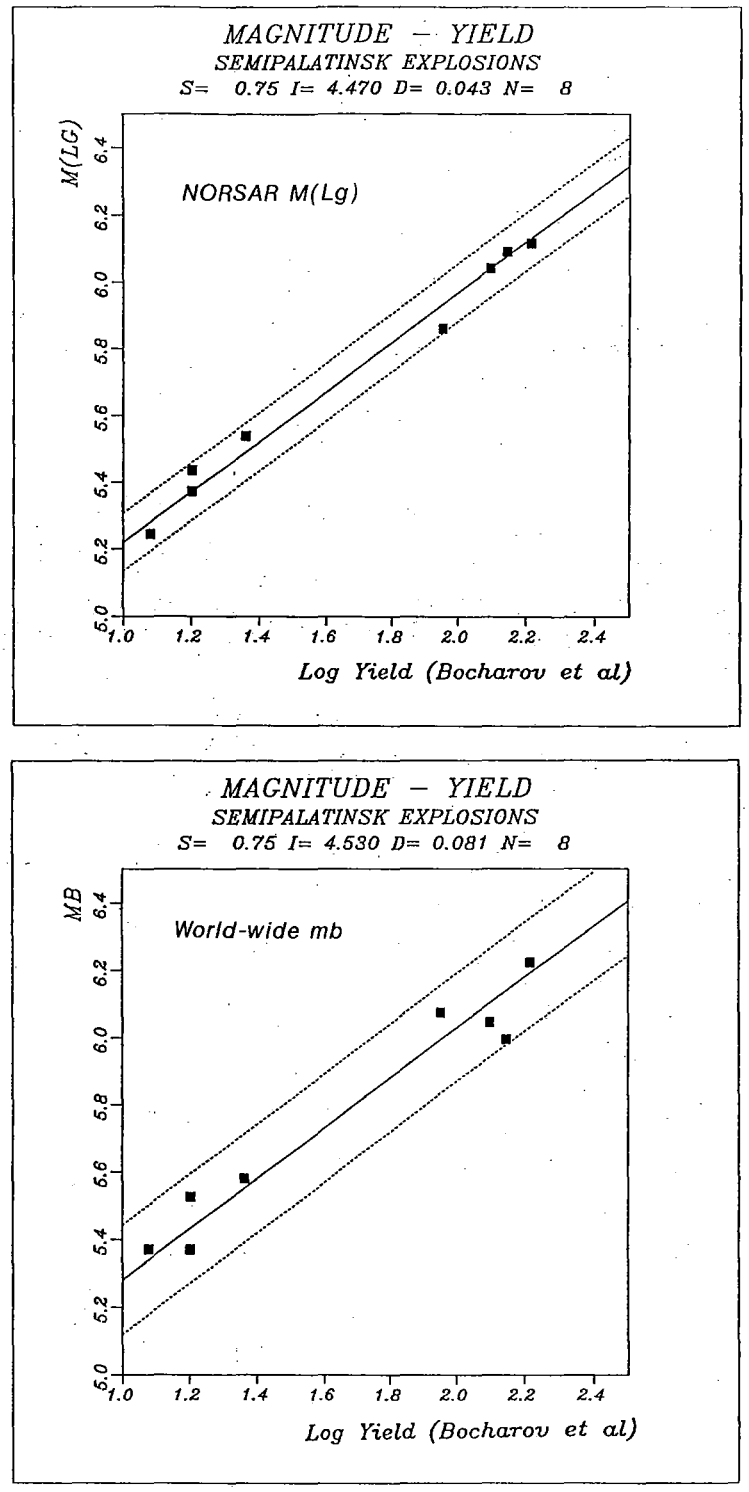

Fig. 7.1.3. Magnitude-yield relationships for 8 nuclear explosions at Semipalatinsk, with yields provided by Bocharov *et al* (1989): a) NORSAR M(Lg) versus log(yield) and b) world-wide m_b versus log(yield). The slopes of the straight lines have been restricted to 0.75. Note that the NORSAR values show significantly less scatter.

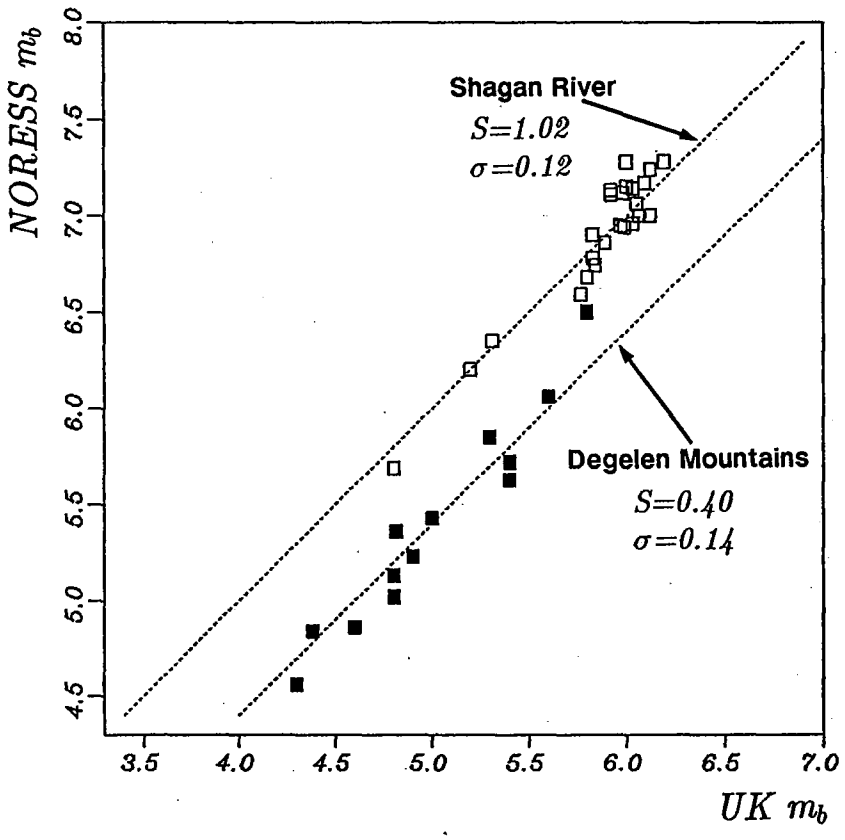

Fig. 7.1.4. Comparison of NORESS and world-wide m_b (as calculated at Blacknest, United Kingdom) for Semipalatinsk explosions. Note the difference in average m_b bias between events from Shagan River (1.0 m_b units) and Degelen Mountains (0.4 m_b units). The straight lines on the plot have a restricted slope of 1.00.

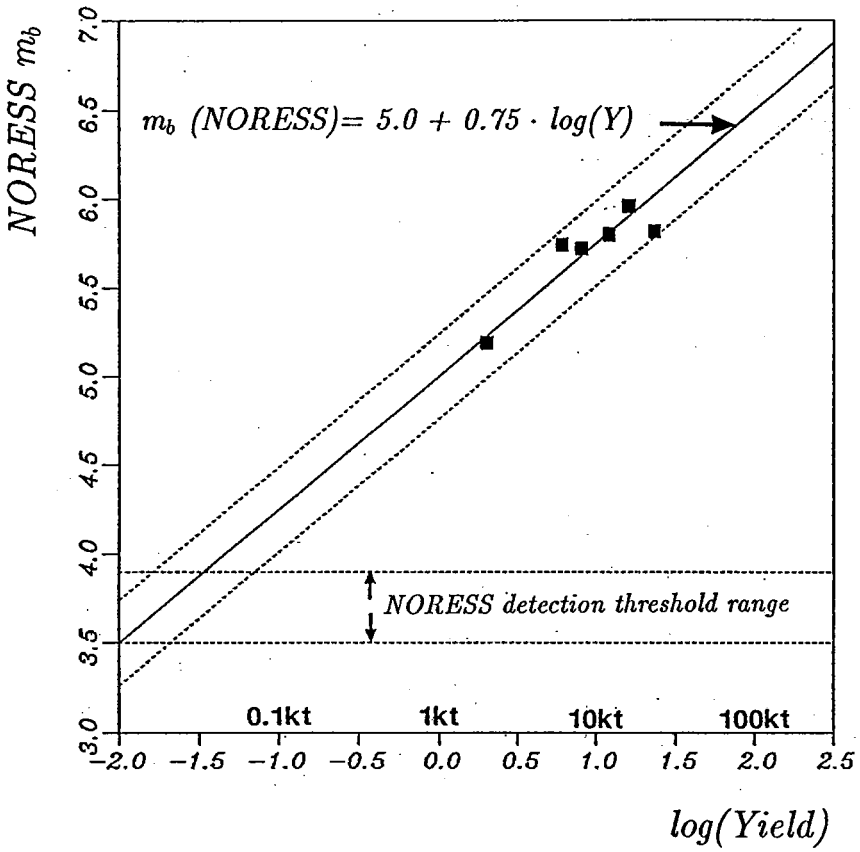

Fig. 7.1.5. Observed m_b versus yield (Bocharov *et al*, 1989) for six Semipalatinsk nuclear explosions listed in Table 7.1.1. The straight line has been fitted using a restricted slope of 0.75. The m_b values are based on NORSAR seismometer 06C02, located at the present NORESS center site. The estimated range of the NORESS m_b detection threshold is indicated (see text for details).

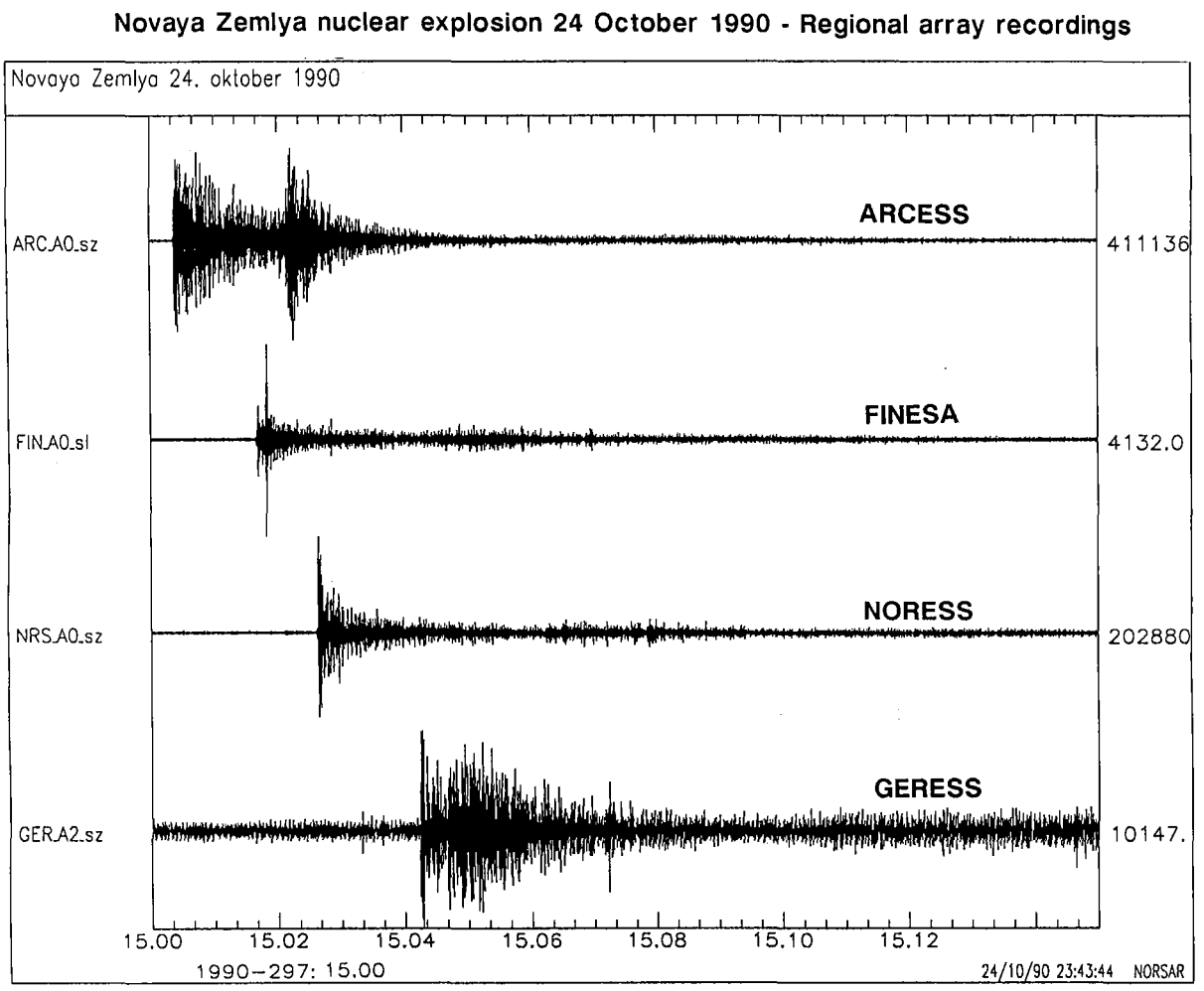

Fig. 7.1.6. Selected single seismometer SPZ recordings from the four regional arrays in northern Europe for the $m_b = 5.7$ nuclear explosion at Novaya Zemlya on 24 October 1990. Epicentral distances and maximum P-phase signal-to-noise ratios on the array beam are as follows:

ARCESS 1110 km, SNR = 8383; FINESA 1780 km, SNR = 2189
NORESS 2270 km, SNR = 2478; GERESS 3380 km, SNR = 105

7.2 Initial results from real-time processing of GERESS array data

Introduction

The GERESS array (Harjes, 1990) represents the most recent addition to the network of regional seismic arrays in Europe. GERESS, which is located in the Bavarian Forest area in southern Germany, has a geometry similar to that of NORESS in southern Norway and ARCESS in northern Norway, but with a slightly enlarged instrument spacing (Fig. 7.2.1). Thus the diameter of GERESS is 4 km, compared to 3 km for the two arrays in Norway.

Real-time data from GERESS are transmitted continuously both to Bochum, Germany (by land line), and to the NORSAR Data Processing Center (NDPC) at Kjeller (by satellite). At NDPC, the data are currently subjected to continuous real-time detection processing, using the RONAPP algorithm (Mykkeltveit and Bungum, 1984). In the near future, these data will also be incorporated into the Intelligent Monitoring System (IMS) (Bache *et al*, 1990).

GERESS real-time processing

The initial processing of GERESS data is conducted at NDPC using a beam set essentially identical to that being used for NORESS and ARCESS data (see Subsection 3.4). Although several modifications will undoubtedly be desirable after more experience is gained, it is still of interest to observe how a "generic" parameter set performs when applied to a regional array in a new geological environment. Below, we give some initial examples from this processing.

Table 7.2.1 shows excerpts from the automatic GERESS phase detection list for day 293 (23 October 1990). For each phase, the detection time, beam number, SNR, phase velocity and azimuth are listed, together with a number of attributes used in further characterization of the detected phase.

In Fig. 7.2.2 we show an automatically generated event plot (Fyen, 1989) for one of the located events during the time period covered by the detection list in Table 7.2.1. This event is located in the Lubin mining district in Poland, at a distance of 344 km from GERESS, and is probably one of a large number of rockbursts known to occur in that region (Gibowics, 1987). We note that this event was too small to be detected by either NORESS, ARCESS or FINESA.

Fig. 7.2.3 shows GERESS automatic output plot from the P-wave detection of the Novaya Zemlya explosion 24 October 1990 (Δ = 30.4 degrees). The phase velocity is indicative of a teleseismic signal, and the estimated azimuth is consistent with the actual epicenter. GERESS SNR is 105 on the array beam, which is naturally lower than for the three other arrays, all of which are within regional distances from Novaya Zemlya.

An interesting feature of the GERESS recordings of this event is a very sharp PcP detection at 2 min 59.5 seconds after P (Fig. 7.2.4). The time differential between P and PcP gives a very sharp constraint on the epicentral distance, in particular when the phase onset times can be read as precisely as in this case. Thus, given appropriate calibration, very useful location information could be derived.

Conclusions

Our initial experience shows that real-time processing of GERESS data will form a very valuable contribution to the regional array monitoring research network. So far, it appears that many new events in southern Europe within 500 km distance from GERESS will be added, and GERESS data will provide further constraints on the events detected and located by more than one array. The teleseismic potential of GERESS is also quite promising.

J. Fyen

References

Bache, T., S.R. Bratt, J. Wang, R.M. Fung, C. Kobryn and J. Given (1990): The Intelligent Monitoring System, *Bull. Seism. Soc. Am.*, Special Issue, in print.

Fyen, J. (1989): Event processor program package, . *Tech. Summary, 1 Oct 1988 - 31 Mar 1989*, NORSAR Sci. Rep. No. 2-88/89, Kjeller, Norway.

Gibowics, S. (1987): NORESS capability for detection and location of mining tremors in the Lubin area in Poland, **In:** *Semiannual Technical Summary, 1 September 1986 - 31 March 1987*, NORSAR Sci. Rep. No. 2-86/87, NORSAR, Kjeller, Norway.

Harjes, H.-P. (1990): Design and siting of a new regional array in central Europe, *Bull. Seism. Soc. Am.*, Special Issue, in print.

Mykkeltveit, S. and H. Bungum (1984): Processing of regional seismic events using data from small aperture arrays, *Bull. Seism. Soc. Am.*, 74, 2313–2333.

323	293:12.43.29.700	1.10	G053	4.8	2.6	nois	298.5	0.06	4	4.02	953.3	173.9	A3_sz	-1.00	-1.00	-1.00	-1.00
324	293:12.43.39.750	1.25	GV01	3.8	12.9	P	191.0	0.17	1	0.56	76.5	404.7	C1_sz	0.59	2.06	80.33	4.28
325	293:12.45.10.987	0.31	G084	7.7	2.5	nois	310.0	0.07	4	6.31	2650.3	505.5	D5_sz	-1.00	-1.00	-1.00	-1.00
326	293:12.45.19.300	1.20	GV01	7.2	4.3	S	201.9	0.11	3	0.72	289.1	658.7	D5_sz	-1.00	-1.00	-1.00	-1.00
327	293:12.47.07.050	0.75	G043	15.5	2.4	nois	124.5	0.05	4	3.16	1472.7	268.3	C5_sz	-1.00	-1.00	-1.00	-1.00
328	293:12.47.16.475	1.02	GV06	3.2	1.9	nois	310.0	0.09	3	4.79	1713.6	609.2	C5_sz	-1.00	-1.00	-1.00	-1.00
329	293:12.47.39.300	1.00	G011	7.2	14.7	P	202.8	0.29	1	1.31	74.5	340.9	C5_sz	0.42	1.34	8.20	4.21
330	293:12.56.39.725	0.98	GV01	6.0	35.9	P	346.7	0.54	1	1.04	118.7	498.4	A3_sz	0.54	3.06	89.38	3.18
331	293:12.58.45.675	0.22	GH03	3.9	2.9	nois	45.7	0.07	3	7.74	2095.2	299.4	C1_sz	-1.00	-1.00	-1.00	-1.00
332	293:12.58.50.300	0.50	G032	4.5	37.7	P	147.3	0.09	3	3.30	167.0	85.9	C1_sz	-1.00	-1.00	-1.00	-1.00
333	293:13.01.31.481	1.12	G103	6.8	2.8	nois	339.3	0.04	4	7.74	2619.1	659.5	A0_sz	0.34	1.85	86.29	33.93
334	293:13.04.21.800	1.30	G034	7.3	2.8	nois	145.4	0.07	3	2.13	477.6	126.0	A3_sz	-1.00	-1.00	-1.00	-1.00
335	293:13.04.27.650	0.65	G021	4.7	3.2	S	3.6	0.05	4	1.94	491.2	118.1	A3_sz	-1.00	-1.00	-1.00	-1.00
336	293:13.11.29.750	0.55	G036	7.3	2.8	nois	140.6	0.08	3	2.14	349.7	134.6	A3_sz	-1.00	-1.00	-1.00	-1.00
337	293:13.11.40.075	1.12	GV01	3.1	15.6	P	30.5	0.56	1	0.79	164.7	335.2	A3_sz	0.60	3.14	88.70	5.40
338	293:13.15.50.331	0.17	GH04	3.7	2.4	nois	31.0	0.05	4	8.29	689.6	256.7	A0_sz	0.19	2.25	64.50	5.08
339	293:13.22.49.575	0.52	G033	4.6	2.8	nois	150.1	0.10	4	2.51	398.6	77.3	D8_sz	-1.00	-1.00	-1.00	-1.00
340	293:13.27.39.625	1.07	GV01	5.6	11.6	P	124.1	0.47	1	0.93	45.0	464.5	A3_sz	-1.00	-1.00	-1.00	-1.00
341	293:13.27.59.675	1.32	GV01	3.7	4.0	S	343.5	0.48	1	0.64	195.2	334.5	B3_sz	-1.00	-1.00	-1.00	-1.00
342	293:13.28.19.875	1.12	GV01	3.6	7.8	Pgn	150.7	0.47	1	0.86	72.8	329.6	B3_sz	-1.00	-1.00	-1.00	-1.00
343	293:13.30.14.306	0.59	GH04	4.2	3.1	S	333.1	0.04	4	5.64	1212.3	388.4	A3_sz	0.30	0.96	31.26	47.69
344	293:13.33.19.525	1.27	G034	17.7	8.0	Pgn	130.7	0.39	1	2.60	315.6	260.1	A0_sz	0.75	0.50	45.92	75.59
345	293:13.33.29.425	1.17	G044	6.3	8.0	Pgn	150.7	0.40	1	2.95	646.6	300.4	A0_sz	-1.00	-1.00	-1.00	-1.00
346	293:13.36.05.362	0.44	G087	11.2	4.2	S	106.5	0.06	4	6.44	2133.4	697.2	A3_sz	-1.00	-1.00	-1.00	-1.00
347	293:13.36.15.700	1.10	G051	4.9	3.0	nois	149.1	0.06	4	3.88	971.7	137.3	A3_sz	0.16	0.80	65.16	87.88
348	293:14.18.12.350	0.95	G059	12.1	7.5	Pgn	352.9	0.19	1	2.82	643.5	190.8	A0_sz	0.73	0.90	47.35	54.70
349	293:14.18.34.725	1.38	G065	8.9	4.2	SN	354.6	0.14	3	3.25	1872.5	308.1	A0_sz	0.67	1.82	85.96	10.60
350	293:14.18.38.950	1.25	GV06	4.4	4.3	S	0.7	0.12	3	3.93	1300.8	691.4	A0_sz	-1.00	-1.00	-1.00	-1.00
351	293:14.25.06.875	0.92	G044	9.4	3.0	S	142.7	0.06	3	3.05	861.0	197.0	D2_sz	-1.00	-1.00	-1.00	-1.00
352	293:14.25.10.025	1.67	GV02	4.4	2.7	nois	149.5	0.06	3	1.86	406.4	279.0	D2_sz	-1.00	-1.00	-1.00	-1.00
353	293:14.25.36.925	1.38	G055	6.1	2.5	nois	267.7	0.06	4	4.18	645.3	128.0	D7_se	0.20	1.14	78.45	51.94
354	293:14.46.24.550	1.95	GV02	3.1	28.4	P	106.1	0.16	3	1.89	34.9	93.3	B3_sz	-1.00	-1.00	-1.00	-1.00
355	293:14.49.39.275	1.02	G058	5.6	3.2	S	167.3	0.06	3	3.47	472.1	95.7	A3_sz	-1.00	-1.00	-1.00	-1.00
356	293:14.50.26.100	1.20	G034	4.6	3.8	S	339.4	0.06	4	2.46	359.0	77.7	D2_sz	-1.00	-1.00	-1.00	-1.00
357	293:14.51.39.350	1.35	GV01	7.4	7.2	Pgn	164.6	0.30	1	0.45	96.4	572.0	C5_sz	-1.00	-1.00	-1.00	-1.00
358	293:14.53.21.975	0.82	G051	5.0	1.8	nois	226.2	0.07	4	3.96	466.9	92.2	C1_sz	0.17	1.21	72.27	33.76
359	293:14.54.31.281	0.82	G104	7.4	3.2	SN	160.4	0.04	4	8.96	3746.4	1052.4	A3_sz	0.27	2.95	89.00	4.00
360	293:14.55.49.975	0.62	G035	6.9	2.9	nois	274.0	0.05	4	2.69	537.3	110.2	D2_sz	-1.00	-1.00	-1.00	-1.00
361	293:14.57.11.050	1.05	G035	8.2	2.8	nois	140.7	0.07	3	1.98	713.8	133.3	C5_sz	-1.00	-1.00	-1.00	-1.00
362	293:14.57.19.325	1.48	G035	9.9	2.9	nois	153.5	0.05	3	2.15	881.3	225.2	C5_sz	-1.00	-1.00	-1.00	-1.00
363	293:14.57.24.750	0.95	GV02	3.6	2.9	nois	62.5	0.07	3	1.59	391.9	374.2	C5_sz	-1.00	-1.00	-1.00	-1.00
364	293:14.57.52.125	0.88	GV02	3.0	3.0	S	326.0	0.10	4	1.55	179.4	246.1	D5_sz	-1.00	-1.00	-1.00	-1.00
365	293:15.01.53.150	0.95	G034	5.3	3.0	S	153.8	0.08	3	2.18	383.9	79.6	A3_sz	-1.00	-1.00	-1.00	-1.00
366	293:15.07.29.725	0.88	G035	8.7	2.7	nois	284.7	0.05	4	2.47	846.6	144.6	D2_sz	0.35	1.61	82.97	53.64
367	293:15.09.02.475	1.12	G049	5.6	3.8	S	341.7	0.07	3	3.17	416.6	103.9	A3_sz	-1.00	-1.00	-1.00	-1.00
368	293:15.11.04.450	0.65	G042	5.1	3.1	S	254.3	0.05	4	2.82	1218.1	103.7	A3_sz	-1.00	-1.00	-1.00	-1.00
369	293:15.11.31.775	0.82	G056	6.6	35.3	P	223.5	0.06	4	3.84	118.4	170.2	A3_sz	0.30	1.61	87.77	22.09
370	293:15.18.34.575	0.52	G038	6.0	2.8	nois	147.0	0.09	3	2.08	762.8	86.8	C1_sz	0.20	0.77	83.64	79.27
371	293:15.18.39.225	1.07	G052	6.5	2.6	nois	105.5	0.09	3	4.59	647.0	147.5	D5_sz	0.17	1.60	87.76	4.35
372	293:15.45.33.575	0.52	G033	707.5	2.4	nois	295.2	0.03	4	2.26	26191.2	11225.5	A3_sz	0.26	1.46	83.60	34.12
373	293:16.08.43.925	2.17	G011	4.5	6.9	Pgn	348.1	0.19	3	1.08	320.3	183.4	D9_sz	0.39	2.50	89.11	21.66
374	293:16.12.06.075	1.23	G036	5.1	12.4	P	258.1	0.09	4	2.32	122.2	99.8	D8_sz	-1.00	-1.00	-1.00	-1.00
375	293:16.28.21.575	0.52	G049	4.8	2.9	nois	146.9	0.13	3	2.51	343.0	87.3	D5_sz	0.57	0.87	39.37	48.97
376	293:16.28.25.875	2.12	GV06	5.3	6.8	Pgn	33.3	0.19	3	4.82	880.2	566.5	D5_sz	0.59	0.94	41.68	50.28
377	293:16.28.35.800	0.50	G057	4.8	6.8	Pgn	32.3	0.21	2	3.71	417.6	147.1	D5_sz	-1.00	-1.00	-1.00	-1.00
378	293:16.29.10.675	0.52	GH01	6.2	4.6	S	40.1	0.20	3	2.88	2349.6	1100.9	B3_sz	0.22	1.45	71.53	14.51

Table 7.2.1. (Page 1 of 2)

379	293:16.29.14.425	1.57	GV02	4.0	3.3	LG	31.5	0.31	2	1.47	1019.1	508.0	B3_sz	0.55	1.41	79.68	77.38
380	293:16.29.18.375	1.62	GV02	3.1	4.4	S	24.5	0.32	1	1.59	1159.0	505.8	B3_sz	-1.00	-1.00	-1.00	-1.00
381	293:16.29.19.725	0.98	GV01	5.6	3.5	S	19.1	0.23	2	1.51	764.1	915.5	A0_sz	-1.00	-1.00	-1.00	-1.00
382	293:16.35.18.525	2.48	GV01	3.4	29.9	P	277.5	0.14	3	0.83	114.9	304.4	D4_sn	-1.00	-1.00	-1.00	-1.00
383	293:17.12.59.500	1.20	GV01	5.6	26.4	P	146.9	0.45	1	1.08	158.6	681.5	B3_sz	-1.00	-1.00	-1.00	-1.00
384	293:17.15.23.700	0.90	G093	7.1	6.3	Pgn	113.5	0.05	4	7.43	1175.0	453.0	A3_sz	-1.00	-1.00	-1.00	-1.00
385	293:17.36.39.750	0.95	GV01	7.6	5.0	S	206.3	0.14	4	1.03	286.6	902.8	B2_sz	-1.00	-1.00	-1.00	-1.00
386	293:17.48.42.350	0.95	G049	5.3	4.4	S	145.0	0.06	3	3.27	506.9	100.5	A3_sz	-1.00	-1.00	-1.00	-1.00
387	293:17.51.19.950	0.75	GV01	6.0	9.4	Pgn	315.4	0.24	1	0.57	94.2	460.0	A0_sz	-1.00	-1.00	-1.00	-1.00
388	293:18.38.37.850	3.15	GV01	3.4	8.2	Pgn	187.5	0.42	1	0.86	44.2	400.8	C1_sz	0.25	1.78	88.86	8.36
389	293:18.46.16.650	1.45	G042	4.9	2.9	nois	138.2	0.14	3	3.05	597.5	88.7	B5_sz	-1.00	-1.00	-1.00	-1.00
390	293:18.48.49.825	0.48	G071	5.0	3.3	S	121.9	0.05	4	4.77	435.7	166.8	A3_sz	-1.00	-1.00	-1.00	-1.00
391	293:18.49.08.950	1.55	GV04	3.1	2.7	nois	140.1	0.08	3	2.37	294.5	212.6	C5_sz	-1.00	-1.00	-1.00	-1.00
392	293:18.49.19.525	0.77	G054	5.2	13.0	P	290.4	0.06	4	4.01	86.6	103.2	D5_sz	-1.00	-1.00	-1.00	-1.00
393	293:18.51.32.550	1.55	G053	5.6	2.8	nois	321.8	0.07	4	3.68	521.0	101.3	A0_sz	0.54	2.47	85.13	18.21
394	293:18.56.19.125	1.57	GV01	4.0	4.8	S	294.2	0.16	3	1.02	369.7	423.5	D2_sz	-1.00	-1.00	-1.00	-1.00
395	293:19.08.01.150	1.55	GV02	3.1	2.2	nois	129.2	0.08	3	1.68	283.3	186.2	D2_sz	-1.00	-1.00	-1.00	-1.00
396	293:19.08.39.500	1.20	GV01	6.4	8.3	Pgn	162.1	0.42	1	0.63	130.4	774.7	D5_sz	-1.00	-1.00	-1.00	-1.00
397	293:19.10.00.175	0.82	GV01	3.8	5.8	S	23.0	0.32	1	0.64	251.0	385.7	B4_sz	-1.00	-1.00	-1.00	-1.00
398	293:19.19.29.750	0.55	G021	4.6	16.4	P	132.7	0.06	4	1.98	176.5	102.9	A3_sz	-1.00	-1.00	-1.00	-1.00
399	293:19.21.18.775	2.42	GV01	3.3	5.8	S	185.7	0.29	1	0.87	324.8	368.5	D8_sz	-1.00	-1.00	-1.00	-1.00
400	293:19.31.39.900	1.10	GV01	3.9	7.1	Pgn	167.2	0.26	1	0.85	64.1	377.5	D2_sz	-1.00	-1.00	-1.00	-1.00
401	293:19.40.59.925	1.07	GV01	3.3	22.8	P	14.2	0.44	1	0.93	65.9	314.0	A3_sz	1-1.00	-1.00	-1.00	-1.00
402	293:19.48.59.775	0.92	GV02	4.0	2.2	nois	29.2	0.08	3	1.97	211.5	213.5	C1_sz	-1.00	-1.00	-1.00	-1.00
403	293:20.07.57.375	2.92	G011	5.1	34.3	P	310.0	0.17	3	1.06	241.5	234.1	D2_sz	-1.00	-1.00	-1.00	-1.00
404	293:20.10.40.450	0.55	GV05	3.3	2.9	nois	146.0	0.13	3	2.16	285.6	256.6	C1_sz	-1.00	-1.00	-1.00	-1.00
405	293:20.18.48.525	0.77	G065	5.0	2.1	nois	218.7	0.06	4	4.11	363.7	89.4	D7_sn	-1.00	-1.00	-1.00	-1.00
406	293:20.20.40.025	0.98	GV02	3.0	6.1	Pgn	359.9	0.08	4	1.79	55.2	173.2	D9_sz	0.27	1.47	85.01	40.82
407	293:20.51.39.850	0.75	G053	4.8	3.2	SN	266.1	0.06	3	3.93	252.0	57.4	D2_sz	0.28	1.81	86.86	14.22
408	293:21.08.19.750	1.25	GV01	3.6	16.4	P	179.1	0.53	1	0.57	135.1	387.1	D8_sz	-1.00	-1.00	-1.00	-1.00
409	293:21.15.19.675	1.32	GV01	3.4	13.8	P	228.6	0.15	3	0.48	63.1	325.8	D5_sz	-1.00	-1.00	-1.00	-1.00
410	293:21.27.39.925	1.07	GV01	4.2	12.1	P	278.5	0.32	3	0.88	170.9	317.6	A3_sz	0.28	2.03	84.67	15.54
411	293:22.09.09.175	2.62	G021	5.1	48.6	P	329.0	0.32	2	1.33	179.7	110.9	A0_sz	-1.00	-1.00	-1.00	-1.00
412	293:22.40.00.225	0.77	GV01	4.0	4.8	S	317.6	0.33	1	0.96	229.5	341.6	B3_sz	-1.00	-1.00	-1.00	-1.00
413	293:23.17.59.375	1.62	GV01	3.1	8.8	Pgn	227.4	0.37	1	0.96	82.7	237.1	D5_sz	-1.00	-1.00	-1.00	-1.00
414	293:23.21.19.750	1.25	GV01	3.2	4.6	S	315.9	0.49	1	0.75	203.8	242.9	A3_sz	-1.00	-1.00	-1.00	-1.00
415	293:23.49.17.775	3.23	GV01	3.2	10.4	P	85.5	0.10	3	0.86	65.2	326.6	D9_sz	-1.00	-1.00	-1.00	-1.00

Table 7.2.1. Automatic event processor detection log for the GERESS array. From left to right the columns give arrival identification number, estimated onset time, difference in seconds between STA/LTA trigger time and onset time, beam name, SNR, velocity in km/sec, phase name, azimuth, broadband FK relative coherence measure and quality of FK (1=good), frequency in Hz of estimated maximum amplitude of the phase, phase maximum amplitude in uncorrected digital counts, STA. The next column with channel names gives, in case of many data gaps, the name of one channel that due to gaps/spikes, etc., may have contributed to a false detection. The four last numbers are result of three-component polarization analysis, and give rectilinearity, horizontal/vertical ratio, angle of incidence 1 and 3. (Page 2 of 2)

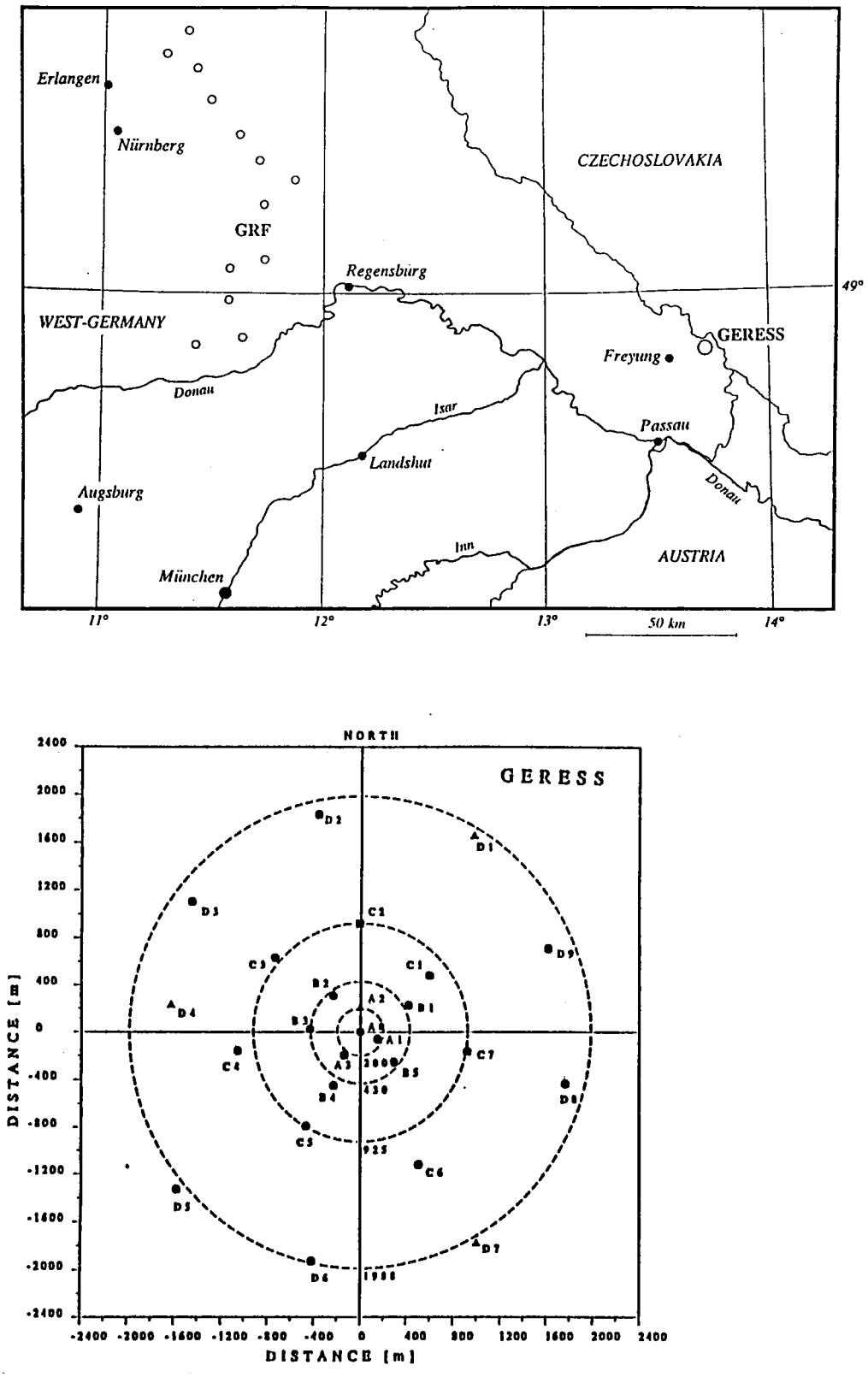

Fig. 7.2.1. Geographical location and geometry of the GERESS array in Germany (after Harjes, 1990).

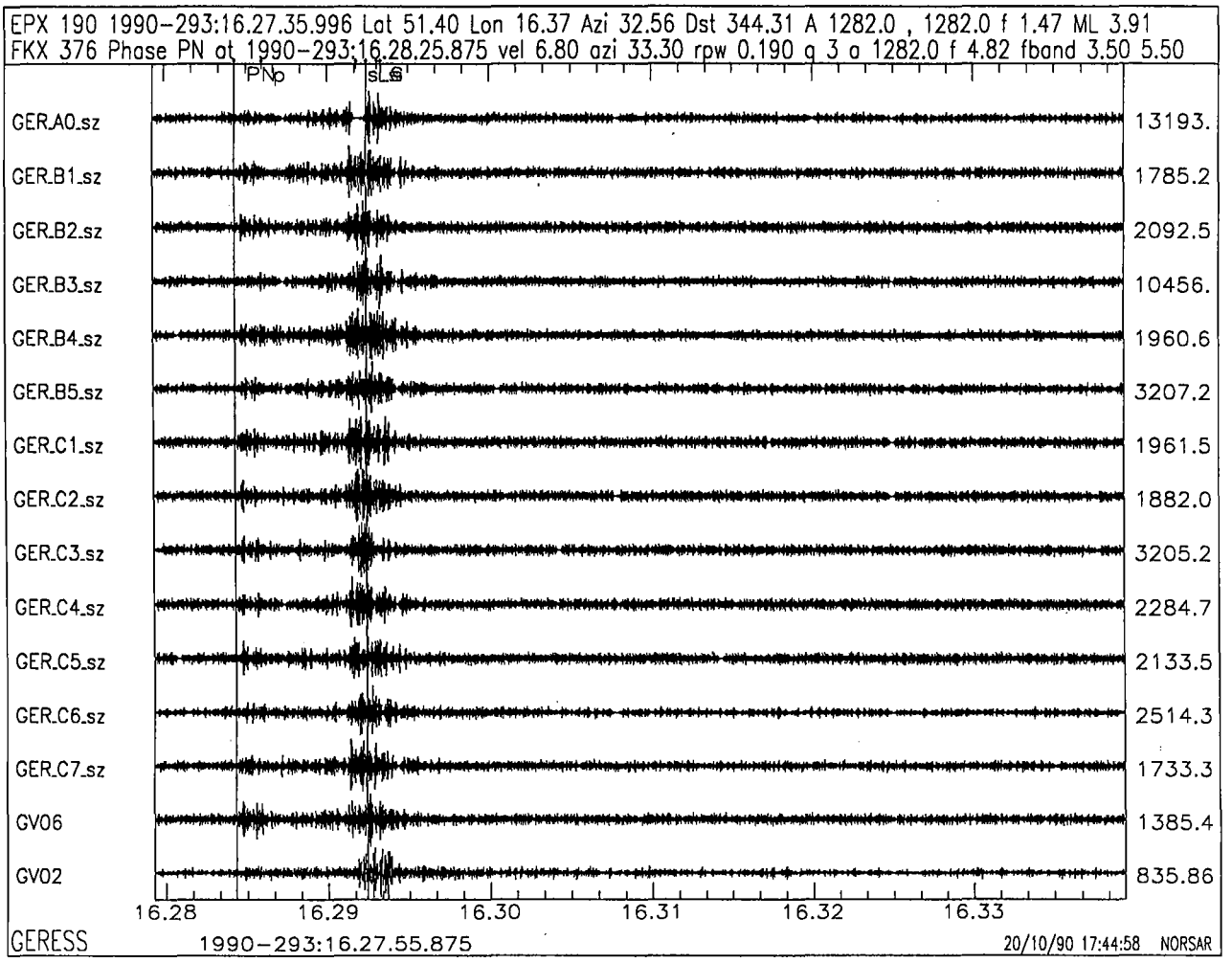

Fig. 7.2.2. Automatically generated event plot for GERESS. The traces shown are a selection of single instruments filtered in the band 3.5–5.5 Hz. The bottom two traces are the P- and S-beams using the velocities and azimuths determined by broadband F-K analysis. (The S-beam, which is the lowermost trace, is filtered in the band 1.0–2.0 Hz). The time window is 6 minutes.

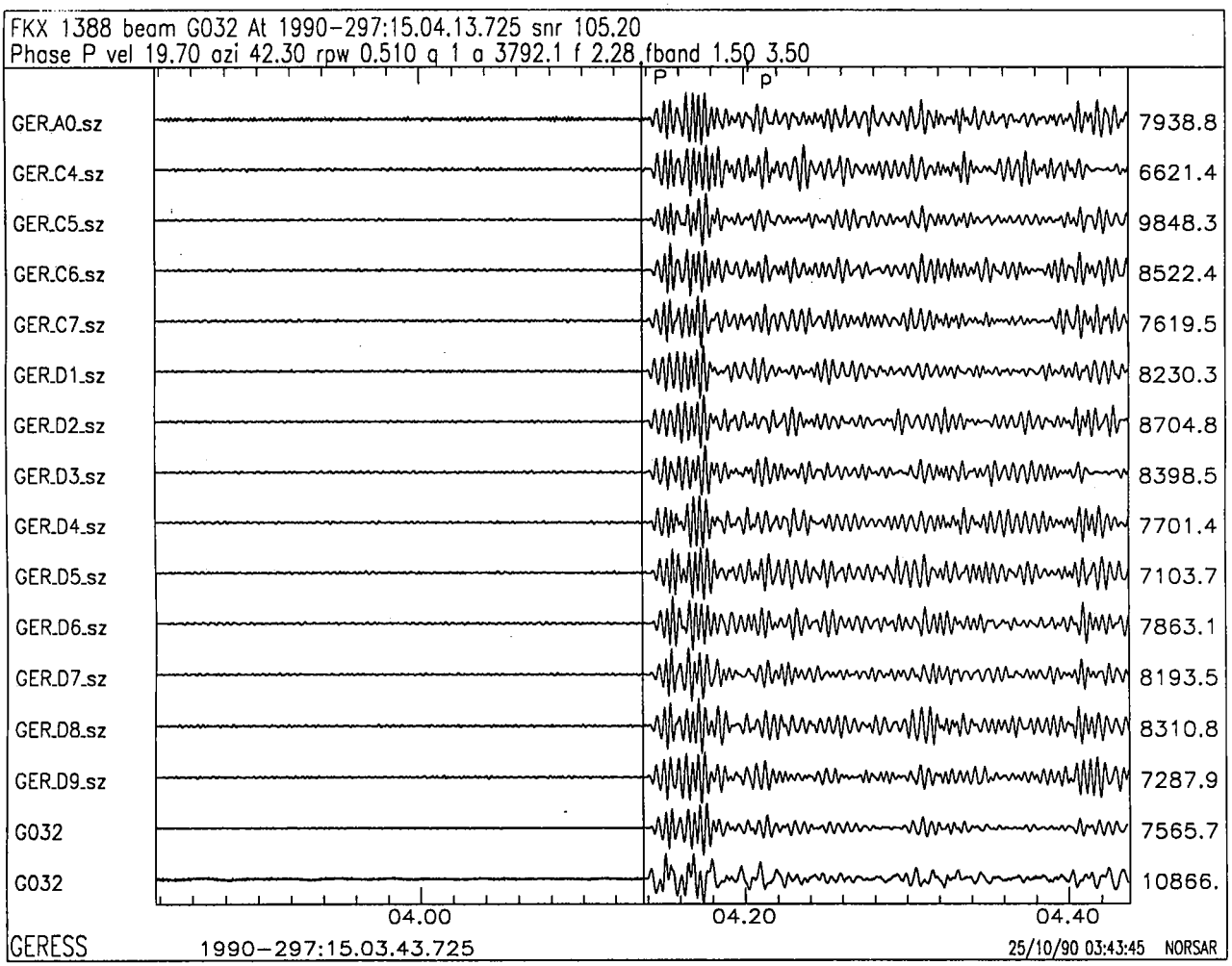

Fig. 7.2.3. Automatically generated teleseismic phase plot for GERESS, corresponding to the P-wave detection of the Novaya Zemlya explosion on 24 October 1990. The traces shown are a selection of single instruments filtered in the band 1.5–3.5 Hz. The bottom two traces are the P-beam filtered and unfiltered, using the velocity and azimuth determined by broadband FK analysis. The time window is 60 seconds.

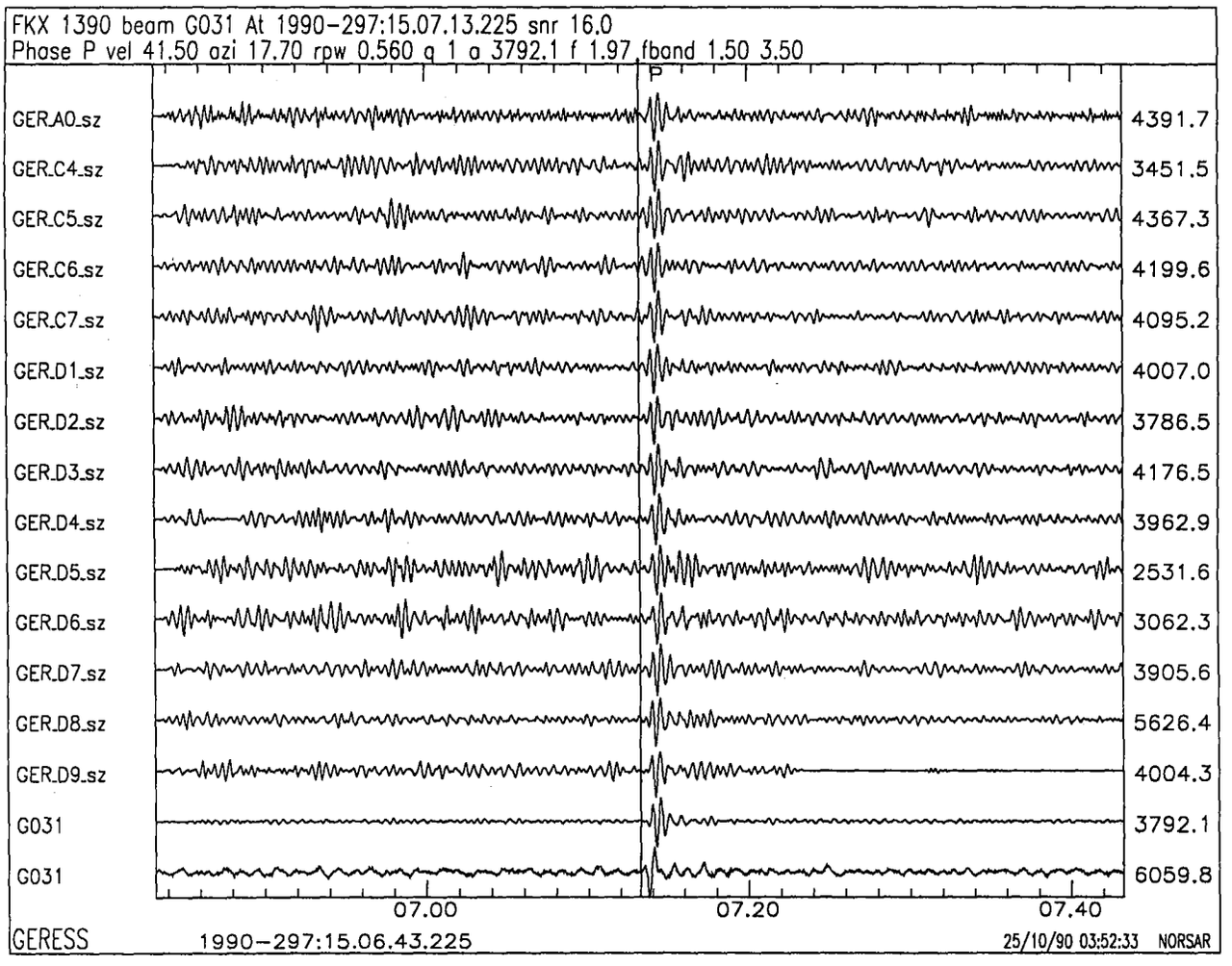

Fig. 7.2.4. Similar to Fig. 7.2.3, but showing the automatic plot for the PcP phase of the Novaya Zemlya explosion. Note the clear onset and the significant noise suppression on the filtered beam (second trace from bottom). Also note that the high estimated phase velocity (41.50 km/s) is a clear indication that this is indeed a core phase.

7.3 Generalized beamforming using a network of four regional arrays

The generalized beamforming method (GBF) for automatic phase association and event location (Ringdal and Kværna, 1989) has now been implemented for processing of data from the four regional arrays, ARCESS, FINESA, GERESS and NORESS. This method works from a list of phase detections for each array. For a large set of hypothetical event locations, GBF searches for a pattern of detections that fit the theoretically expected phase arrivals from the hypothetical locations. When a group of matching detections is found, the event location having the best fit to the data is chosen as the most likely epicenter.

In the following we present a brief report on our initial experience from applying GFB experimentally to the four-array network during a continuous five-day period.

Data analysis

A total of 600 beam grid points with an average separation of 150 km is used to span the geographical area of interest (see Fig. 7.3.1). This grid represents the initial (coarse) set of test locations, and whenever a match is found, a beampacking algorithm with a much denser grid is applied to refine the locations.

The GBF output from a typical 12-hour period is given in Table 7.3.1. For each associated event, the table lists the individual phase detections that either have defined the event or been associated as coda phases (p or s). Phase attributes (SNR, apparent velocity, dominant frequency, etc.) are also listed for each entry.

From Table 7.3.1 we find that the majority of the events are observed by one array only, whereas larger events have phase observations at two or more arrays. This is consistent with earlier studies of two-array and three-array networks.

It is interesting to notice that the incorporation of data from GERESS enables us to obtain more reliable event locations for events in northern Europe, as seen for the event in Poland with origin time 292:21.57.40 and epicenter location 51.70°N, 15.68°E. This event is presumed to be a rockburst in the Lubin mining area, and the location estimate is very close to that site.

In order to evaluate the performance of the method, we have analyzed GBF results from five consecutive working days (10/22/90 – 10/26/90). The results can be summarized as follows:

1. Several hundred regional events were associated, where the large majority were detected by one array only.

2. A total of 37 events had four or more associated phase detections, and the corresponding locations are shown in Fig. 7.3.2. After inspection we found that all but one of these events were properly associated and located. From Fig. 7.3.2 we see that the large majority of these events are located in the active mining areas of western USSR. We also notice a precise location of a nuclear explosion at Novaya Zemlya.

3. The occurrence of incorrect phase associations increases when we allow fewer than four phases to define an event.

Future work

From inspecting phase attributes, the analyst can in many cases identify erroneous phase associations based on inconsistencies among parameters like epicentral distance, apparent velocity and dominant frequency. Our next step will be to compile statistics on such attributes and make this kind of information available to the GBF program for use in the automatic computations.

We have also found that there is a need to refine the travel time models and also to improve the estimation of onset time for the different phase detections. Thereby, the automatic event locations will become even more precise.

Dynamic consistency checks using thresholds computed by the threshold monitoring method are also expected to help in identifying and removing unlikely phase associations. This will be particularly important at the time when detection data from the two three-component systems in Poland will be incorporated into GBF.

T. Kværna

References

Ringdal, F. and T. Kværna (1989): A multichannel processing approach to real time network detection, phase association and threshold monitoring, *Bull. Seism. Soc. Am.*, 79, 1927–1940.

Origin time	Lat	Lon	Azres	Timres	Wres	Nphase
1990-292:12.00.03.0	59.80	27.26	3.65	2.71	3.63	3

Sta	Dist	Az	Ph	Time	Tres	Azim	Ares	Vel	Snr	Amp	Freq	Fkq	Pol	Arid
FIN	194.4	160.1	Pn	12.00.33.3	-0.6	155.1	-5.0	6.4	18.4	752.9	6.07	3		115935
FIN	194.4	160.1	Sn	12.01.07.3	7.1	162.3	2.2	4.4	19.6	1474.2	3.45	3	-2	115936
NRS	874.8	90.0	Pn	12.01.57.9	0.3	86.2	-3.8	10.7	5.3	237.0	3.59	3		115940

Origin time	Lat	Lon	Azres	Timres	Wres	Nphase
1990-292:12.04.36.0	50.50	12.11	0.58	0.43	0.58	2

Sta	Dist	Az	Ph	Time	Tres	Azim	Ares	Vel	Snr	Amp	Freq	Fkq	Pol	Arid
GER	217.0	328.6	Pn	12.05.09.5	-0.6	327.6	-1.0	7.4	13.2	4020.5	9.03	3		181
GER	217.0	328.6	p	12.05.17.1		335.9	7.3	7.9	4.5	831.1	2.69	2		182
GER	217.0	328.6	s	12.05.30.5		330.1	1.5	3.3	12.3	2018.7	1.25	1	-2	183
GER	217.0	328.6	Lg	12.05.37.0	0.2	328.5	-0.1	3.9	3.8	1857.8	2.28	2		184

Origin time	Lat	Lon	Azres	Timres	Wres	Nphase
1990-292:12.06.12.0	59.50	24.04	3.52	0.32	1.20	3

Sta	Dist	Az	Ph	Time	Tres	Azim	Ares	Vel	Snr	Amp	Freq	Fkq	Pol	Arid
FIN	244.1	208.2	Pn	12.06.48.9	-0.6	203.1	-5.1	7.1	28.7	754.8	5.48	3	-1	115939
FIN	244.1	208.2	Lg	12.07.20.2	-0.1	206.2	-2.0	4.1	17.0	1227.7	3.23	3	-2	115941
NRS	708.0	95.7	Lg	12.09.29.8	-0.2	99.1	3.4	4.3	3.6	1032.6	1.50	1	-3	115946
NRS	708.0	95.7	s	12.09.32.7		96.0	0.3	3.7	2.7	834.6	2.12	2		115947

Origin time	Lat	Lon	Azres	Timres	Wres	Nphase
1990-292:12.08.49.0	59.20	27.52	2.89	0.35	1.07	2

Sta	Dist	Az	Ph	Time	Tres	Azim	Ares	Vel	Snr	Amp	Freq	Fkq	Pol	Arid
FIN	262.6	161.7	Pn	12.09.28.8	0.0	157.8	-3.9	7.3	6.1	306.5	9.90	3		115948
FIN	262.6	161.7	Lg	12.10.03.1	0.7	159.8	-1.9	3.8	4.7	708.1	7.40	3		115949

Origin time	Lat	Lon	Azres	Timres	Wres	Nphase
1990-292:12.28.03.0	67.60	32.68	2.05	1.11	1.63	3

Sta	Dist	Az	Ph	Time	Tres	Azim	Ares	Vel	Snr	Amp	Freq	Fkq	Pol	Arid
ARC	363.9	123.0	Pn	12.28.56.4	1.1	121.8	-1.2	8.0	90.0	3292.0	4.73	2		115970
ARC	363.9	123.0	p	12.29.04.5		125.5	2.5	7.1	9.6	1945.9	6.38	3		115971
ARC	363.9	123.0	Sn	12.29.35.2	-1.8	118.3	-4.7	3.7	2.5	1338.2	4.72	3		115973
ARC	363.9	123.0	Lg	12.29.44.3	-0.4	122.8	-0.2	3.2	3.8	2015.0	3.25	2	-2	115974
ARC	363.9	123.0	s	12.29.47.5		125.3	2.3	4.3	3.6	3113.7	4.44	2		115975

Origin time	Lat	Lon	Azres	Timres	Wres	Nphase
1990-292:12.28.38.0	50.20	14.30	1.97	3.22	3.72	3

Sta	Dist	Az	Ph	Time	Tres	Azim	Ares	Vel	Snr	Amp	Freq	Fkq	Pol	Arid
GER	156.8	15.7	Pg	12.29.04.3	1.0	16.6	0.9	7.5	4.6	2374.7	9.98	4		187
GER	156.8	15.7	Rg	12.29.22.5	-8.7	12.3	-3.4	3.1	22.7	650.6	1.01	1	3	188
NRS	1186.2	170.4	Sn	12.33.08.1	0.1	172.0	1.6	4.3	2.5	409.1	4.49	3		115982
NRS	1186.2	170.4	s	12.33.12.3		173.7	3.3	3.9	11.9	1522.1	3.95	2	-1	115985

Origin time	Lat	Lon	Azres	Timres	Wres	Nphase
1990-292:12.30.18.0	50.80	12.59	8.90	4.50	6.72	3

Sta	Dist	Az	Ph	Time	Tres	Azim	Ares	Vel	Snr	Amp	Freq	Fkq	Pol	Arid
GER	231.8	340.2	Pn	12.30.55.6	1.6	325.8	-14.4	6.3	7.7	3574.5	8.32	3		190
GER	231.8	340.2	Lg	12.31.11.1	-11.8	330.2	-10.0	3.0	8.6	1874.4	1.60	1	-3	192
NRS	1108.7	176.2	Pn	12.32.40.9	-0.1	173.8	-2.4	6.7	5.3	280.3	4.13	3		115978

Table 7.3.1. GBF output from a typical 12-hour period. For each associated event, the table lists the individual phase detections that either have defined the event (Pn, Sn, Lg, Rg) or been associated as coda phases (p or s). Phase attributes (SNR, apparent velocity, dominant frequency, etc.) are also listed for each entry. (Page 1 of 3)

Origin time	Lat	Lon	Azres	Timres	Wres	Nphase
1990-292:12.31.08.0	56.20	26.39	11.07	3.89	6.66	4

Sta	Dist	Az	Ph	Time	Tres	Azim	Ares	Vel	Snr	Amp	Freq	Fkq	Pol	Arid
FIN	584.9	178.1	Pn	12.32.28.5	1.2	155.4	-22.7	9.4	4.5	77.3	4.56	3		115980
FIN	584.9	178.1	p	12.32.56.1		185.0	6.9	7.1	32.1	1286.9	3.91	1		115984
FIN	584.9	178.1	Sn	12.33.24.0	-6.4	180.3	2.2	4.5	8.7	767.9	2.38	1	-2	115986
NRS	1000.7	113.8	Lg	12.35.55.0	7.1	99.4	-14.4	3.4	2.7	660.2	2.35	2		115991
GER	1185.3	41.6	Pn	12.33.39.4	-0.9	46.6	5.0	6.2	9.1	143.9	4.49	4		193

Origin time	Lat	Lon	Azres	Timres	Wres	Nphase
1990-292:12.31.45.0	67.60	33.47	2.34	1.17	1.75	4

Sta	Dist	Az	Ph	Time	Tres	Azim	Ares	Vel	Snr	Amp	Freq	Fkq	Pol	Arid
ARC	390.1	119.8	Pn	12.32.40.0	-0.5	122.5	2.7	7.6	202.2	18647.9	6.78	1		115977
ARC	390.1	119.8	p	12.32.46.3		121.6	1.8	8.5	4.2	1185.3	3.09	3		115979
ARC	390.1	119.8	p	12.32.50.5		117.8	-2.0	7.4	2.8	1568.1	8.43	4		115983
ARC	390.1	119.8	Sn	12.33.21.4	-3.2	124.8	5.0	4.5	6.9	5042.9	2.92	2	-1	115987
ARC	390.1	119.8	Lg	12.33.34.6	0.4	118.2	-1.6	3.2	7.8	11233.4	2.86	2		115990
ARC	390.1	119.8	s	12.33.39.0		120.4	0.6	4.8	5.4	10591.9	3.67	2		115994
NRS	1302.7	44.8	Pn	12.34.32.1	0.5	44.7	-0.1	8.4	4.0	265.2	3.35	3		115988

Origin time	Lat	Lon	Azres	Timres	Wres	Nphase
1990-292:12.35.44.0	61.00	29.03	4.27	2.23	3.29	8

Sta	Dist	Az	Ph	Time	Tres	Azim	Ares	Vel	Snr	Amp	Freq	Fkq	Pol	Arid
FIN	166.4	106.0	Pn	12.36.09.8	-1.1	117.9	11.9	6.6	29.3	3083.2	6.99	3	-1	115989
FIN	166.4	106.0	Lg	12.36.29.2	-1.3	102.0	-4.0	4.0	25.2	1883.8	1.85	1	-2	115992
FIN	166.4	106.0	Rg	12.36.37.7	-2.7	111.3	5.3	3.4	10.9	4734.5	1.24	1		115993
NRS	948.8	80.6	Pn	12.37.46.5	-1.0	83.3	2.7	11.4	8.9	730.2	6.35	2		115995
NRS	948.8	80.6	Lg	12.40.07.4	-2.0	80.5	-0.1	4.6	2.6	835.6	1.36	2		115997
NRS	948.8	80.6	s	12.40.12.6		77.5	-3.1	4.1	3.9	1353.3	1.90	1		116001
ARC	966.4	168.6	Pn	12.37.51.7	2.0	169.2	0.6	9.1	9.9	466.4	5.42	2		115998
ARC	966.4	168.6	Sn	12.39.27.9	1.2	162.5	-6.1	4.7	3.0	402.9	4.30	2		116000
ARC	966.4	168.6	Lg	12.40.07.8	-6.5	172.0	3.4	3.5	2.8	695.1	2.41	2	-3	116002

Origin time	Lat	Lon	Azres	Timres	Wres	Nphase
1990-292:13.18.05.0	59.50	27.85	0.83	0.19	0.39	2

Sta	Dist	Az	Ph	Time	Tres	Azim	Ares	Vel	Snr	Amp	Freq	Fkq	Pol	Arid
FIN	237.7	155.0	Pn	13.18.41.7	0.0	154.4	-0.6	6.8	7.1	204.3	8.91	3		116032
FIN	237.7	155.0	Sn	13.19.12.4	0.3	153.9	-1.1	3.8	5.0	563.3	7.06	3	-2	116033

Origin time	Lat	Lon	Azres	Timres	Wres	Nphase
1990-292:13.36.54.0	59.50	24.83	7.98	0.66	2.66	3

Sta	Dist	Az	Ph	Time	Tres	Azim	Ares	Vel	Snr	Amp	Freq	Fkq	Pol	Arid
FIN	227.4	198.1	Pn	13.37.30.0	0.6	191.0	-7.1	7.8	16.5	392.4	3.37	1		116045
FIN	227.4	198.1	Lg	13.37.56.3	-1.4	193.0	-5.1	4.0	23.2	1195.6	2.83	1	-2	116046
NRS	750.8	94.7	Lg	13.40.24.1	0.0	83.1	-11.6	4.1	2.5	533.1	2.58	2		116050

Origin time	Lat	Lon	Azres	Timres	Wres	Nphase
1990-292:13.49.09.0	60.40	29.68	1.23	0.47	0.77	2

Sta	Dist	Az	Ph	Time	Tres	Azim	Ares	Vel	Snr	Amp	Freq	Fkq	Pol	Arid
FIN	227.6	119.2	Pn	13.49.44.1	-0.4	118.6	-0.6	7.1	6.6	460.8	9.05	3	1	116071
FIN	227.6	119.2	s	13.50.06.4		121.2	2.0	4.1	5.8	769.0	5.57	3	-3	116073
FIN	227.6	119.2	Lg	13.50.12.1	-0.6	117.3	-1.9	3.1	3.9	444.4	1.14	1	-3	116074

Origin time	Lat	Lon	Azres	Timres	Wres	Nphase
1990-292:14.24.30.0	57.40	6.13	10.65	1.13	3.79	3

Sta	Dist	Az	Ph	Time	Tres	Azim	Ares	Vel	Snr	Amp	Freq	Fkq	Pol	Arid
NRS	484.2	222.2	Pn	14.25.36.3	-0.8	211.3	-10.9	9.0	10.8	635.0	8.20	1	1	116090
NRS	484.2	222.2	Lg	14.26.44.9	-0.5	224.7	2.5	4.0	3.6	909.2	2.13	1		116092
NRS	484.2	222.2	s	14.26.47.9		221.6	-0.6	4.1	3.2	954.8	2.56	1		116093
GER	1077.6	334.9	Sn	14.28.39.2	2.1	353.5	18.6	4.0	3.6	175.5	1.54	4	1	218

Origin time	Lat	Lon	Azres	Timres	Wres	Nphase
1990-292:14.33.35.0	48.40	30.42	5.87	0.22	1.69	2

Sta	Dist	Az	Ph	Time	Tres	Azim	Ares	Vel	Snr	Amp	Freq	Fkq	Pol	Arid
FIN	1478.5	167.3	Pn	14.36.43.0	0.0	155.6	-11.7	8.4	6.5	94.6	4.32	3		116095
NRS	1825.2	130.3	Pn	14.37.24.7	-0.4	130.3	0.0	10.1	5.8	197.2	4.71	3		116096

Table 7.3.1. (Page 2 of 3)

Origin time	Lat	Lon	Azres	Timres	Wres	Nphase
1990-292:14.44.52.0	64.60	37.82	4.45	0.29	1.41	2

Sta	Dist	Az	Ph	Time	Tres	Azim	Ares	Vel	Snr	Amp	Freq	Fkq	Pol	Arid
ARC	766.1	130.0	Pn	14.46.32.8	-0.5	131.8	1.8	8.3	5.5	131.2	8.81	3		116109
ARC	766.1	130.0	Sn	14.47.52.6	0.1	122.9	-7.1	4.2	2.8	285.2	8.16	3	1	116111

Origin time	Lat	Lon	Azres	Timres	Wres	Nphase
1990-292:14.56.29.0	49.90	12.11	4.25	0.48	1.54	2

Sta	Dist	Az	Ph	Time	Tres	Azim	Ares	Vel	Snr	Amp	Freq	Fkq	Pol	Arid
GER	164.9	316.0	Pn	14.56.55.2	-0.4	310.5	-5.5	6.9	3.0	1375.0	7.64	3		221
GER	164.9	316.0	Lg	14.57.15.7	0.6	319.0	3.0	4.2	7.2	1416.7	4.18	3	-2	222

Origin time	Lat	Lon	Azres	Timres	Wres	Nphase
1990-292:15.59.44.0	59.20	11.31	2.60	0.52	1.17	2

Sta	Dist	Az	Ph	Time	Tres	Azim	Ares	Vel	Snr	Amp	Freq	Fkq	Pol	Arid
NRS	171.7	184.5	Pn	16.00.11.8	0.2	185.3	0.8	7.0	13.6	462.6	4.38	1		116126
NRS	171.7	184.5	Sn	16.00.34.5	-0.8	180.1	-4.4	3.9	4.7	864.1	9.00	3	-3	116127

Origin time	Lat	Lon	Azres	Timres	Wres	Nphase
1990-292:16.09.58.0	49.60	11.64	5.55	0.29	1.68	2

Sta	Dist	Az	Ph	Time	Tres	Azim	Ares	Vel	Snr	Amp	Freq	Fkq	Pol	Arid
GER	171.9	300.0	Pn	16.10.25.2	-0.5	289.5	-10.5	6.5	4.0	800.7	9.71	4		228
GER	171.9	300.0	Lg	16.10.46.0	-0.1	300.6	0.6	4.0	3.3	758.0	4.95	3		229

Origin time	Lat	Lon	Azres	Timres	Wres	Nphase
1990-292:20.46.18.0	60.70	21.82	5.40	0.43	1.78	2

Sta	Dist	Az	Ph	Time	Tres	Azim	Ares	Vel	Snr	Amp	Freq	Fkq	Pol	Arid
FIN	244.7	252.1	Pn	20.46.55.3	-0.3	261.7	9.6	8.7	5.7	115.6	4.22	2		116244
FIN	244.7	252.1	Sn	20.47.27.1	0.5	253.2	1.1	4.6	3.8	241.1	4.66	3	-3	116245

Origin time	Lat	Lon	Azres	Timres	Wres	Nphase
1990-292:21.57.40.0	51.70	15.68	4.23	1.70	2.75	6

Sta	Dist	Az	Ph	Time	Tres	Azim	Ares	Vel	Snr	Amp	Freq	Fkq	Pol	Arid
GER	347.5	23.2	Pn	21.58.30.3	0.0	29.3	6.1	8.9	64.9	2858.7	2.75	1	1	253
GER	347.5	23.2	p	21.58.38.2		25.0	1.8	6.4	17.3	3017.5	2.64	1	1	254
GER	347.5	23.2	p	21.58.43.8		25.6	2.4	6.3	8.7	4004.7	2.49	3		255
GER	347.5	23.2	Lg	21.59.25.2	8.0	26.2	3.0	4.2	3.4	8589.2	2.27	1		257
GER	347.5	23.2	s	21.59.38.5		29.8	6.6	5.3	3.2	4114.4	1.00	1	3	258
NRS	1038.4	163.9	Pn	21.59.54.8	0.4	166.3	2.4	8.3	17.1	383.9	3.42	1		116282
NRS	1038.4	163.9	p	22.00.04.8		162.3	-1.6	9.7	4.5	245.6	4.02	1		116283
NRS	1038.4	163.9	Sn	22.01.38.5	-0.4	167.9	4.0	4.8	3.7	417.7	2.27	1		116284
FIN	1256.7	215.0	Pn	22.00.21.3	0.3	217.4	2.4	9.8	23.8	195.6	3.78	2	1	116281
FIN	1256.7	215.0	Sn	22.02.26.0	1.1	207.5	-7.5	4.9	2.6	202.5	2.84	1		116286

Origin time	Lat	Lon	Azres	Timres	Wres	Nphase
1990-292:23.36.38.0	67.90	19.99	7.23	2.29	4.09	5

Sta	Dist	Az	Ph	Time	Tres	Azim	Ares	Vel	Snr	Amp	Freq	Fkq	Pol	Arid
ARC	288.7	233.4	Pn	23.37.20.6	-0.4	225.4	-8.0	7.4	55.2	1175.6	6.11	2	-1	116311
ARC	288.7	233.4	p	23.37.25.5		221.6	-11.8	6.7	7.3	695.8	4.11	2		116312
ARC	288.7	233.4	p	23.37.46.9		221.7	-11.7	7.1	2.4	762.6	3.67	1		116313
ARC	288.7	233.4	Sn	23.37.53.4	-2.5	227.8	-5.6	5.0	15.2	2346.3	3.61	2		116314
ARC	288.7	233.4	Lg	23.38.03.4	4.7	225.3	-8.1	4.0	3.0	2834.8	1.42	1		116315
FIN	776.3	340.7	Lg	23.40.11.7	-3.4	346.2	5.5	4.1	3.0	198.6	1.79	1		116310
NRS	896.3	23.3	Pn	23.38.34.8	-0.4	32.3	9.0	8.3	5.4	114.1	3.45	3		116309

Origin time	Lat	Lon	Azres	Timres	Wres	Nphase
1990-292:23.42.32.0	67.30	20.04	1.54	2.52	2.90	3

Sta	Dist	Az	Ph	Time	Tres	Azim	Ares	Vel	Snr	Amp	Freq	Fkq	Pol	Arid
ARC	335.7	224.6	Pn	23.43.21.2	0.4	225.2	0.6	7.5	24.7	979.0	6.33	1	-1	116316
ARC	335.7	224.6	p	23.43.23.5		220.3	-4.3	7.3	6.1	470.3	5.04	2		116317
ARC	335.7	224.6	p	23.43.32.7		226.8	2.2	7.4	4.8	443.2	3.99	3		116318
ARC	335.7	224.6	Sn	23.43.53.8	-6.2	225.5	0.9	4.8	6.3	944.5	4.68	2		116319
ARC	335.7	224.6	Lg	23.44.06.9	1.0	221.5	-3.1	4.3	4.8	1896.3	2.90	1		116320

Table 7.3.1. (Page 3 of 3)

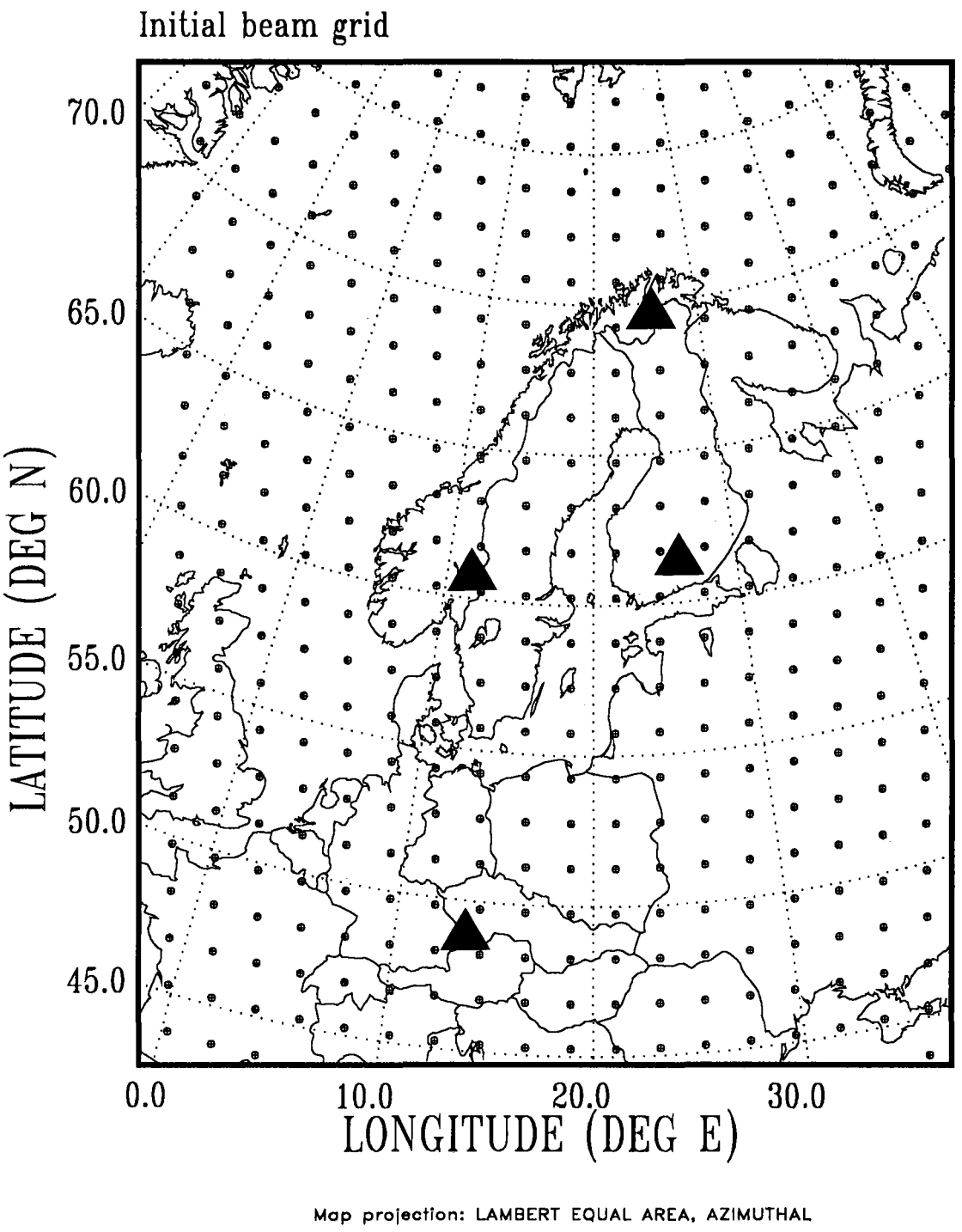

Fig. 7.3.1. Initial beam grid used by the generalized beamforming method when processing data from four regional arrays. ARCESS, FINESA, NORESS and GERESS are marked with solid triangles.

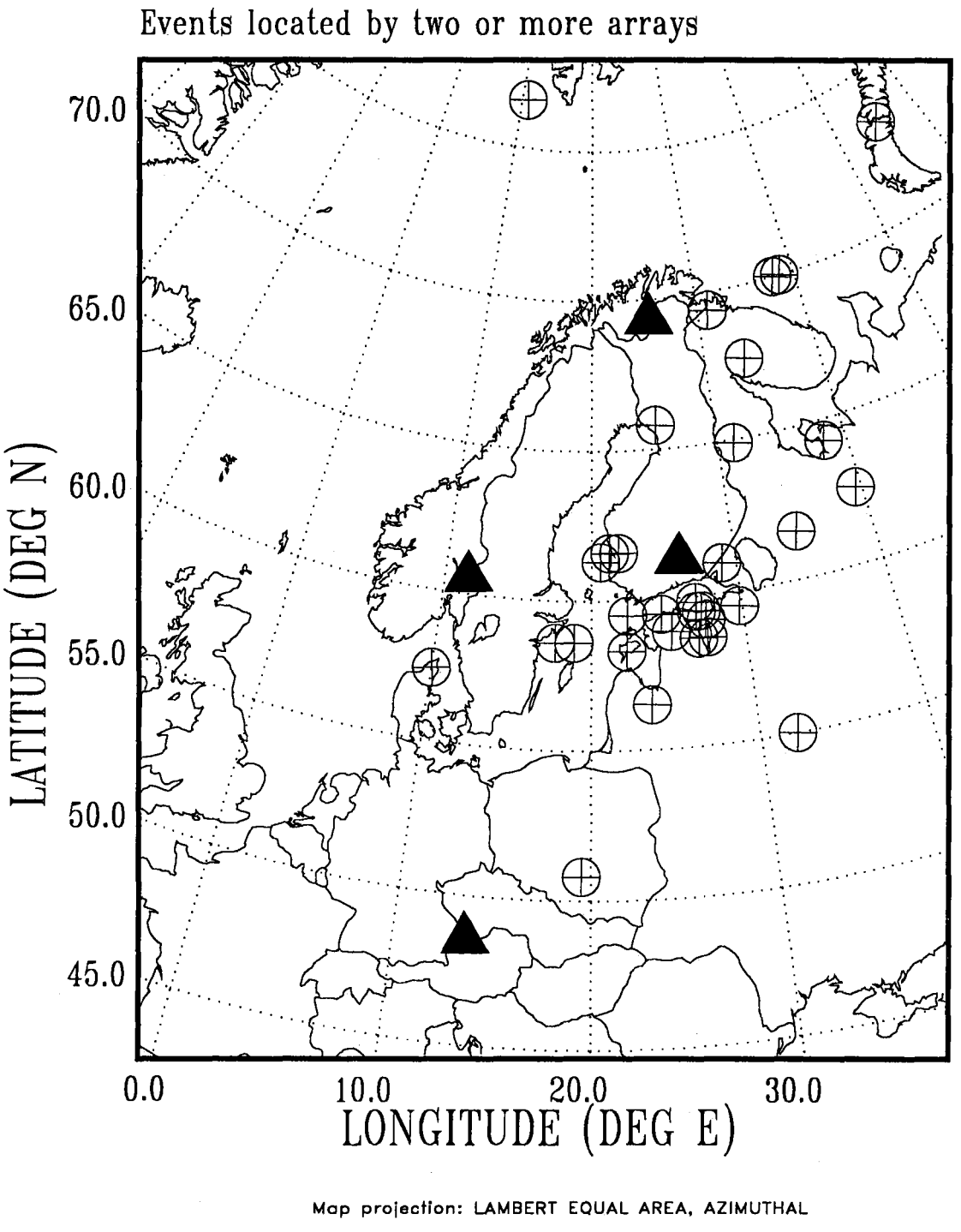

Fig. 7.3.2. Events located by GBF having four or more associated phase detections. The data cover the five-day period 22–26 October 1990. Out of a total of 37 events, 12 were located by two arrays, 22 by three arrays and 3 by four arrays. The four regional arrays, ARCESS, FINESA, NORESS and GERESS, are marked with solid triangles.

7.4 Continuous threshold monitoring of the Novaya Zemlya test site

Introduction

The continuous threshold monitoring technique (Ringdal and Kværna, 1989) represents a new approach toward achieving reliable seismic monitoring for the purpose of verifying nuclear test ban treaties.

Traditionally, seismic monitoring has relied upon applying signal detectors to individual stations within a monitoring network, associating detected phases and locating possible events in the region of interest. This procedure has been accompanied by assessments of network capabilities for the target region, usually by applying statistical models for the noise level distribution, introducing station corrections for signal attenuation and devising a combinational procedure to determine the detection threshold as a function of the number of phase detections required for reliable location.

The statistical noise models used in these capability assessments are not able to accommodate the effect of interfering signals, such as the coda of large earthquakes, which may cause the estimated thresholds to be quite unrealistic at times. Furthermore, only a statistical capability assessment is achieved, and no indication is given as to particular time intervals when the possibility of undetected clandestine explosions is particularly high.

The continuous threshold monitoring technique alleviates all of these problems. It makes it possible to ascertain, at any point in time, for a given target region, the maximum magnitude of a possible clandestine explosion at a predefined level of confidence. This makes it possible to focus attention upon those specific time intervals when realistic evasion opportunities exist, while retaining confidence that no treaty violation has occurred at other times.

Application to the Novaya Zemlya test site

In order to demonstrate how such monitoring could be performed in a practical operational situation, we have conducted an experiment during which we have applied continuous threshold monitoring to the Novaya Zemlya test site for a full one-week period. Our data base has been the Fennoscandian regional array network (NORESS, ARCESS, FINESA). As illustrated in Fig. 7.4.1, these three arrays are all within regional distances from the test site, with excellent P-phase detection capabilities (Fig. 7.4.2). The ARCESS array also detects S phases from Novaya Zemlya explosions quite well, whereas NORESS and FINESA have a lower S-phase detection capability.

The parameters used in the threshold monitoring experiment are given in Table 7.4.1. For each array, we steer "optimum" P and S beams towards the test site, and calibrate these beams using actually observed signal attenuation

from Novaya Zemlya explosions. By focusing in this way on the target region, we can at any point in time measure the "noise magnitude" for a given phase at a given array, and combine these data to obtain a network threshold as explained in detail by Ringdal and Kværna (1989).

Results

Figs. 7.4.3–7.4.9 show the result of the monitoring experiment. Each of these figures covers one data day, starting 24 October 1990. The upper three traces of each figure represent the thresholds (i.e., 90 % upper magnitude limits) obtained from the three individual arrays, whereas the bottom trace illustrates the network threshold. Typically, the individual array traces have a number of significant peaks for each 24-hour period, due to interfering events (local or teleseismic). On the network trace, the number and sizes of these peaks are greatly reduced, because an interfering event will usually not provide matching signals at all the stations. From probabilistic considerations, it can in such cases be inferred that the actual network threshold is lower than these individual peaks might indicate.

On each of the one-day figures, we have included comments explaining the presence of the most significant peaks on the network trace. Here, we will just note that the first day, 24 October 1990, was the day of an actual nuclear explosion (m_b = 5.7) on Novaya Zemlya, and this event naturally stands out on the plot. While the peak value of the network threshold plot does not represent the actual magnitude of the event, it is in fact quite close (5.64).

As a general comment to Figs. 7.4.3–7.4.9, we note that such plots, which are easily generated by the Intelligent Monitoring System (IMS) (Bache *et al*, 1990), will enable the analyst to obtain an instant assessment of the actual threshold level of the monitoring network. The peaks on the network traces may be quickly correlated with the IMS detection bulletin, in order to decide whether they originate from interfering events or from events in the target region.

Discussion

In a monitoring situation, it will be important to isolate and analyze more extensively those time intervals which offer significant evasion opportunities. Table 7.4.2 gives a statistic of the number of occasions during which the upper magnitude limit exceeded a given level. In theory, if this limit is, e.g., at 3.0, it might be possible that a clandestine m_b = 3.0 explosion had occurred without being detected. There are many options available to investigate such a hypothesis in more detail, although we have not attempted to do so in this study. The most immediate approach would be to analyze high-frequency signals for the time interval being considered. For example, on ARCESS records Novaya Zemlya explosions will contain significant energy at 10 Hz and above, even at magnitudes well below 3.0. Teleseismic events, even of large m_b, will

not contain much energy at these frequencies and thus it might be possible to obtain additional indications from these data.

To assess interfering phases from events at regional distances is more difficult, since the high-frequency energy might not discriminate such events from Novaya Zemlya explosions. In such cases, additional procedures, such as maximum likelihood beamforming, might become useful to suppress signals from the interfering event and thereby obtain a more realistic estimate of the signal energy arriving from the target region.

It is significant that the 3-array network studied in this paper can monitor the Novaya Zemlya test site down to m_b 2.5 or below more than 99 % of the time (Fig. 7.4.10). Further improvements would clearly be possible by adding more stations to the monitoring network, especially highly sensitive stations at other azimuths than those covered by the Fennoscandian network. This would in particular contribute to lowering the peaks due to interfering events, whereas any event truly originating in the target region would of course still stand out clearly on the combined network traces.

In conclusion, the continuous threshold monitoring has been demonstrated to provide a simple and very effective tool in day-to-day monitoring of a site of particular interest. Further research will focus upon developing methods to analyze time intervals during which significant evasion possiblities might exist. Data from the regional arrays, the large-aperture NORSAR arrray, as well as other available stations, will be used in these analyses.

T. Kværna
F. Ringdal

References

Bache, T.C., S.R. Bratt, J. Wang, R.M. Fung, C. Kobryn and J. Given (1990): The Intelligent Monitoring System, *Bull. Seism. Soc. Am.*, Special Issue, in print.

Ringdal, F. and T. Kværna (1989): A multichannel processing approach to real time network detection, phase association and threshold monitoring, *Bull. Seism. Soc. Am.*, 79, 1927–1940.

Station	Phase	Tr. Time	App. Vel.	Azim.	Filter	Config.	STA_len.	Tim. Tol.	Sta_Calib
ARC	Pn	148.0	9.9	60.5	3.0–5.0	A0,B,C,D	2.0	2.0	0.754
ARC	Sn	257.0	4.9	53.2	3.0–5.0	A0,B,C,D	5.0	3.0	1.176
FIN	P	228.0	9.6	32.9	2.0–4.0	A0,B,C,	2.0	2.0	1.520
NRS	P	284.0	10.4	28.1	1.5–3.5	A0,B,C,D	2.0	2.0	0.677

Tr. time — Travel time of phase
App. vel. — Apparent velocity from broadband F-K measurement
Azim. — Azimuth from broadband F-K measurement
Filter — Cutoffs of bandpass filter (3rd order Butterworth)
Config. — Array configuration used in beamforming. A0,B,C means A0Z, B-ring and C-ring
STA_len. — STA length in seconds
Tim. tol. — Time tolerance when searching for maximum STA
STA_calib. — Calibration factor used when converting STA values (in quantum units) to magnitude.
Magnitude = log10(STA) + STA_calib.

Table 7.4.1.

	Day-of-Year							Total
	297	298	299	300	301	302	303	(one week)
$m_b \geq 4.0$	1	0	0	0	0	0	0	1
$m_b \geq 3.5$	1	1	0	0	0	0	0	2
$m_b \geq 3.0$	3	2	2	0	0	0	0	7
$m_b \geq 2.5$	5	12	5	0	3	6	3	34

Table 7.4.2. Statistics of peaks in the network threshold traces. See also comments on Figs. 7.4.3–7.4.9.

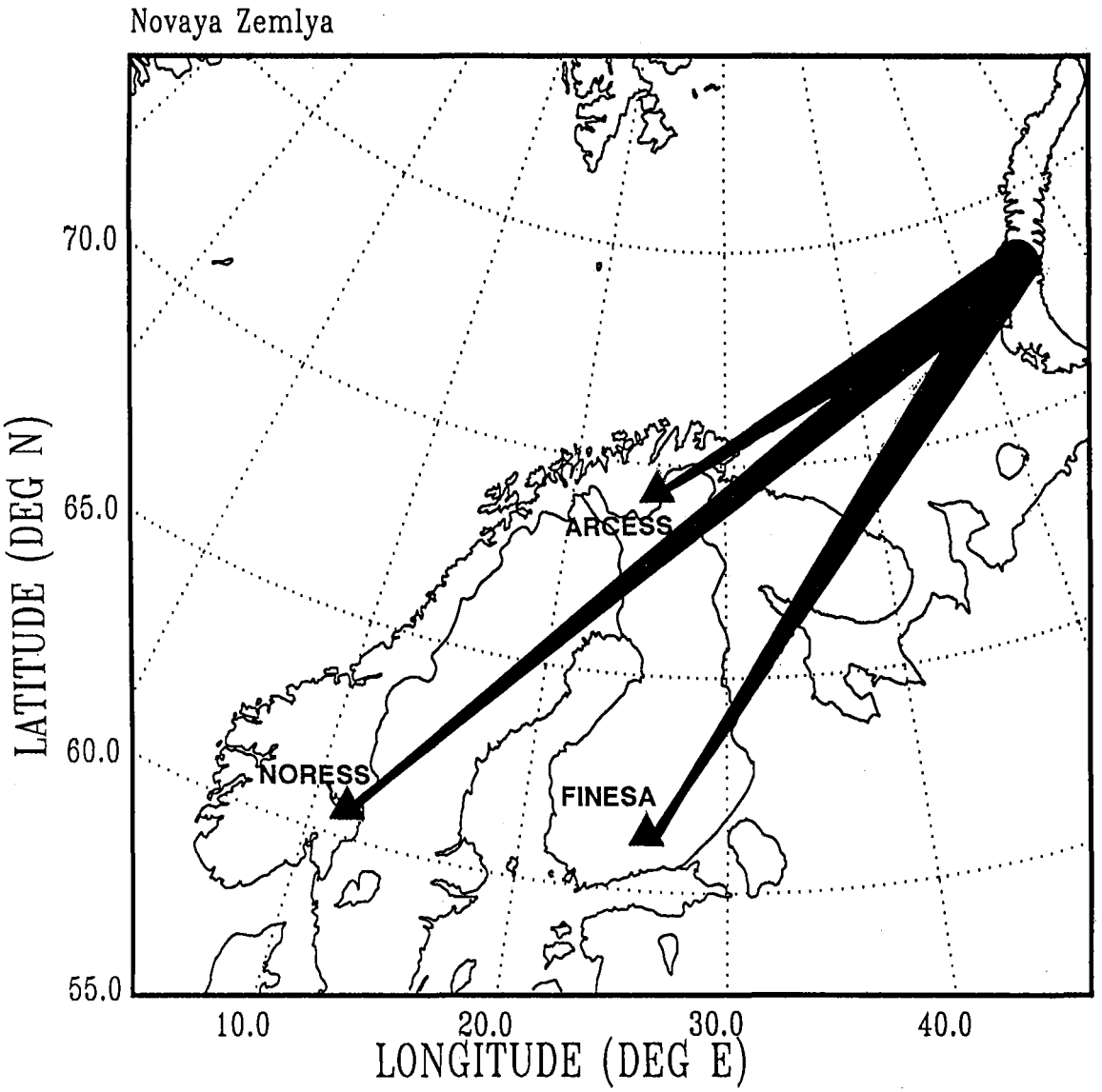

Fig. 7.4.1. Location of the target area (Novaya Zemlya) for the threshold monitoring experiment. The locations of the three arrays NORESS (Δ = 2280 km), ARCESS (Δ = 1110 km) and FINESA (Δ = 1780 km) are indicated.

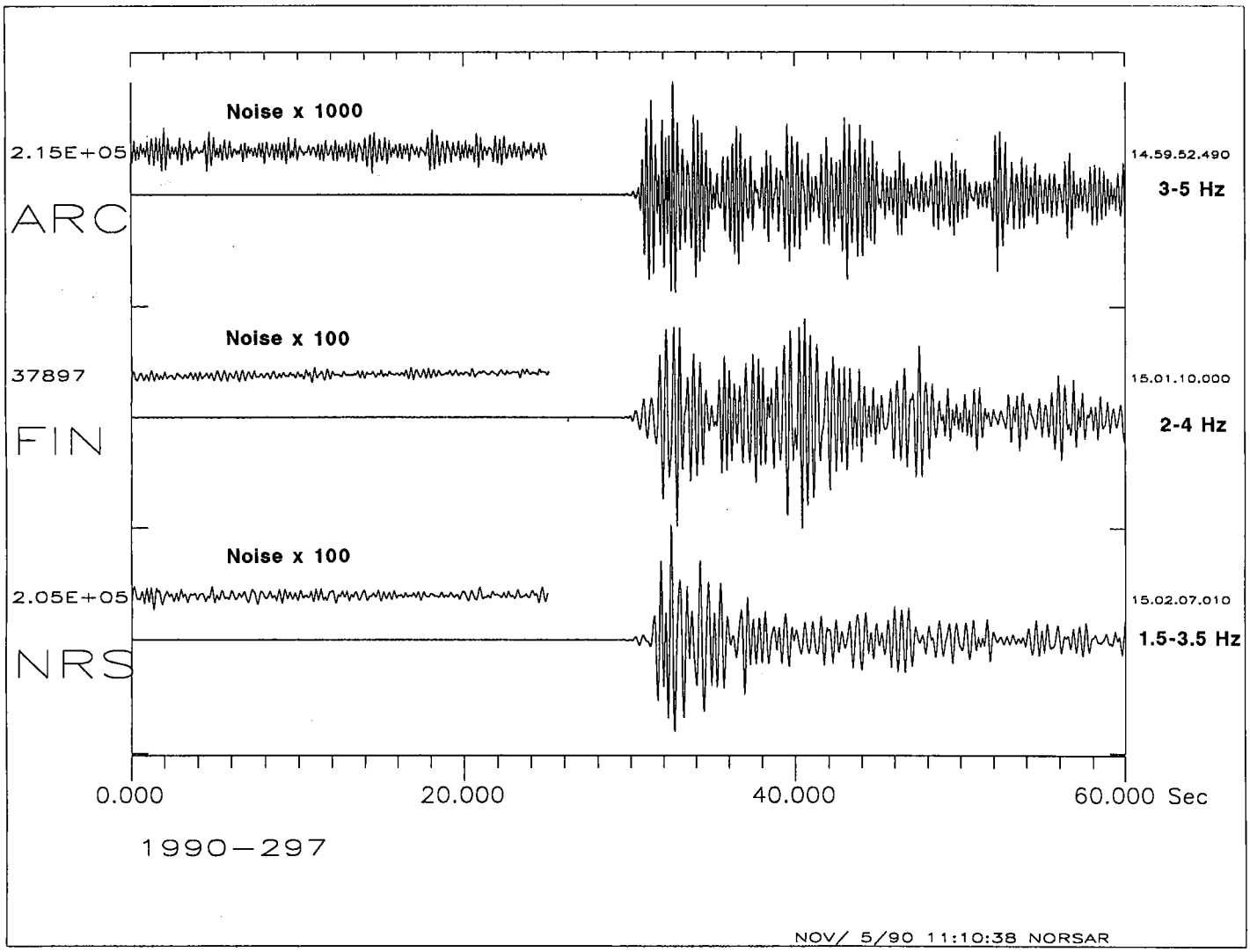

Fig. 7.4.2. P-wave recordings (filtered array beams) at ARCESS, FINESA and NORESS for the Novaya Zemlya nuclear explosion 24 October 1990. To illustrate the high signal-to-noise ratios, noise traces scaled by factors of 1000 (ARCESS) and 100 (FINESA and NORESS) are displayed for each array.

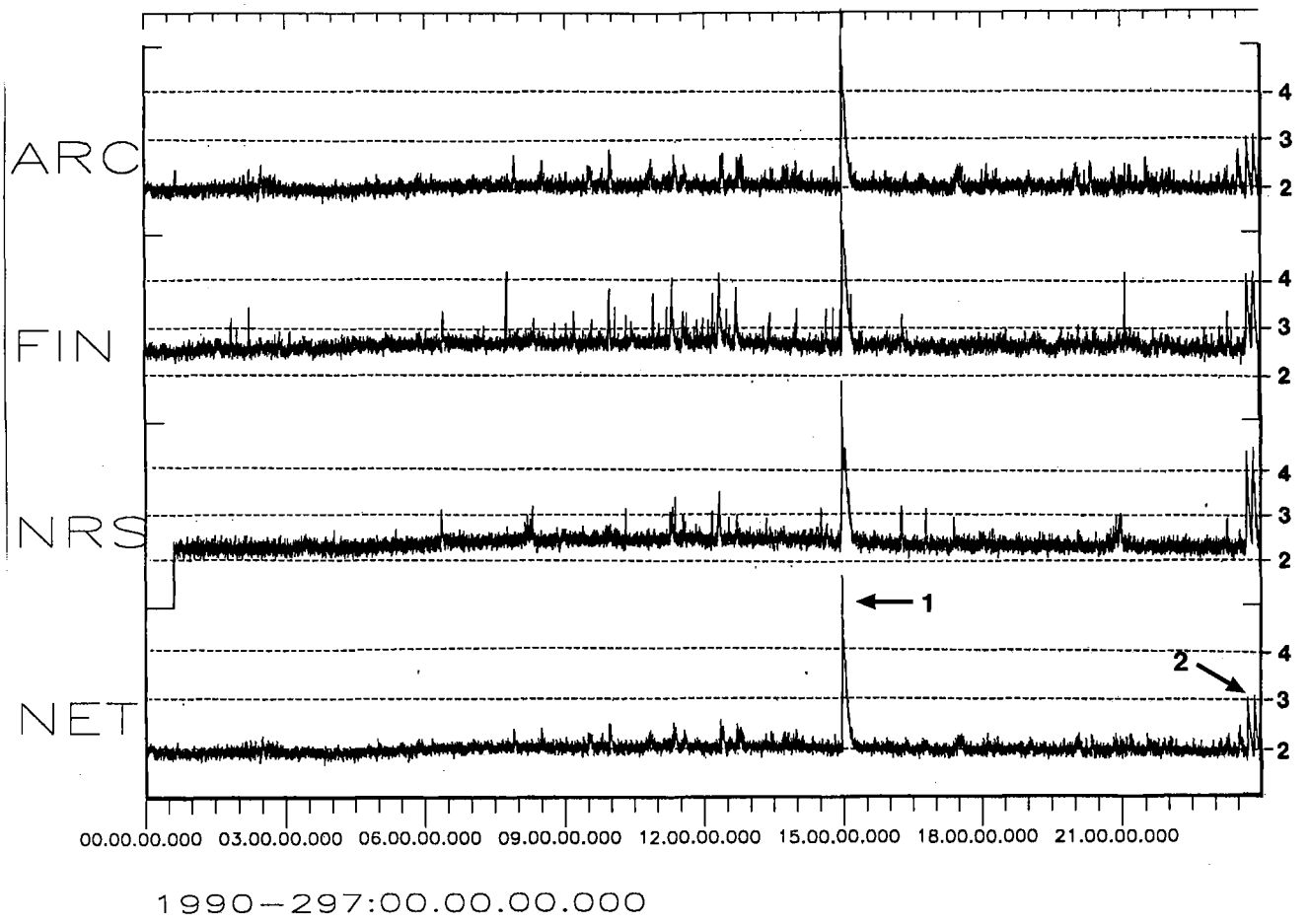

Fig. 7.4.3. Threshold monitoring of the Novaya Zemlya test site for day 297 (24 October 1990). The top three traces represent thresholds (upper 90 per cent magnitude limits) obtained from each of the three arrays (ARCESS, FINESA, NORESS), whereas the bottom trace shows the combined network thresholds.

Notes:

1. An underground nuclear explosion (m_b = 5.7) at Novaya Zemlya at 14.58.00 GMT. The peak of the network trace is 5.64.
2. Two teleseismic earthquakes from N. Xinjang province, China (m_b = 5.2 and 5.4). The P-wave train from each of these earthquakes causes the network threshold to increase to about m_b = 3.0 for the target region.

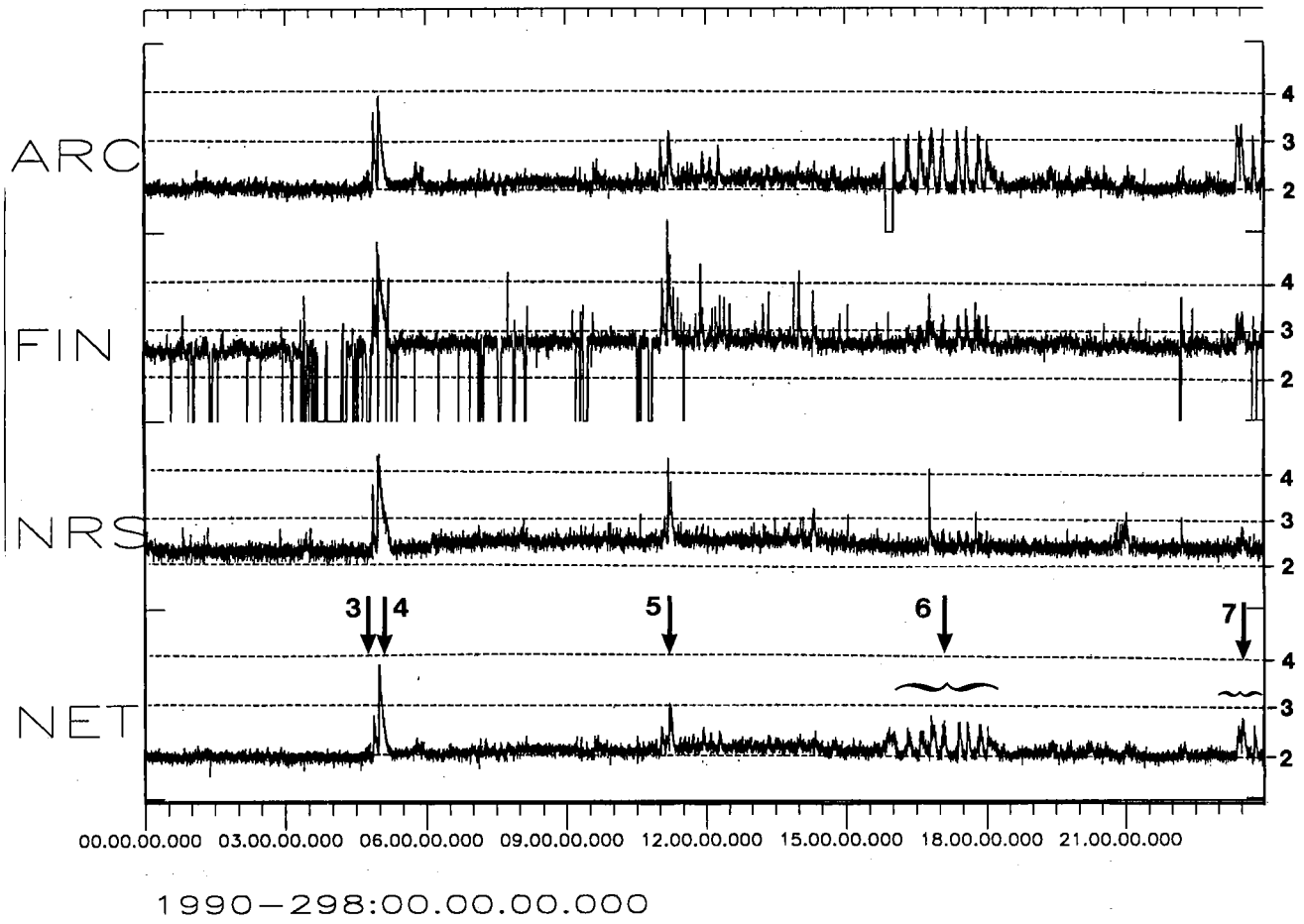

Fig. 7.4.4. Same as Fig. 7.4.3, but for day 298 (25 October 1990). The FINESA array had several short outages this day, but this caused no particular problems in terms of network threshold capacity.

Notes:

3. An earthquake (m_b = 4.5) near Jan Mayen. The corresponding network threshold peak for Novaya Zemlya is m_b=2.8.
4. A teleseismic earthquake (m_b = 6.0) at Hindu Kush. The relatively strong P-wave train caused a peak threshold of m_b = 3.8 for monitoring Novaya Zemlya.
5. A teleseismic earthquake (m_b = 5.9) at Mindanao, Philippine Islands. Corresponding threshold is m_b = 3.0.
6-7. A sequence of seismic events (presumably underwater explosions) near Murmansk, Kola Peninsula. The network threshold for monitoring Novaya Zemlya is about m_b = 2.5 to 2.8 at the times of these events.

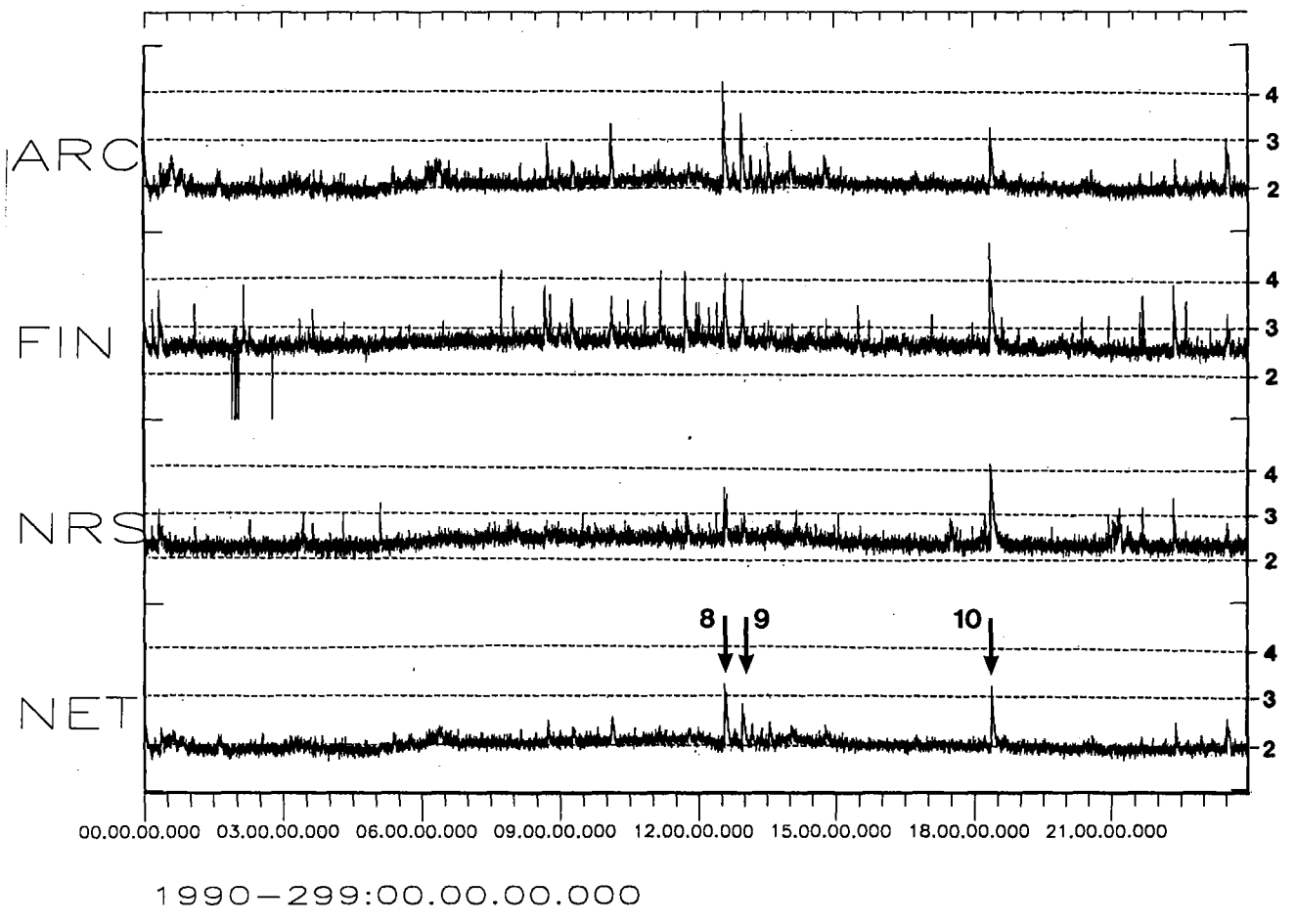

Fig. 7.4.5. Same as Fig. 7.4.3, but for day 299 (26 October 1990).

Notes:

8. A large mining explosion (M_L = 3.0) near the Norway–USSR border. The Novaya Zemlya threshold peak is m_b = 3.2. Note that this threshold exceeds the event magnitude; this is because of the proximity of the event to the network stations.
9. A large mining explosion (M_L = 2.5) at the Kola Peninsula. The Novaya Zemlya threshold peak is m_b = 2.8.
10. A teleseismic earthquake (m_b = 5.1) near Lake Baikal. The network threshold peak is m_b = 3.2.

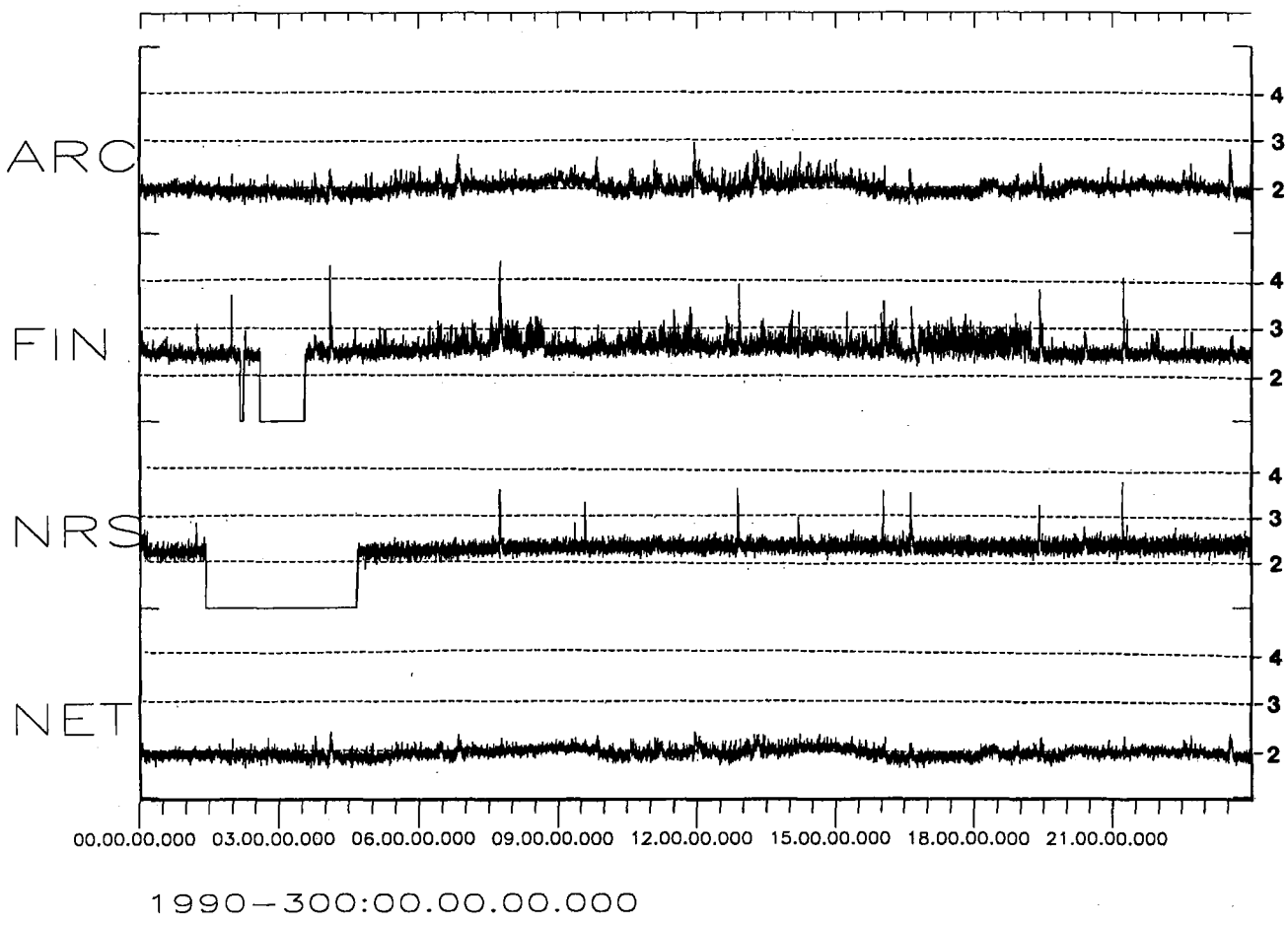

Fig. 7.4.6. Same as Fig. 7.4.3, but for day 300 (27 October 1990).

Notes:
No significant peak during this day. The simultaneous outages at FINESA and NORESS did not cause significant problems for the network threshold monitoring.

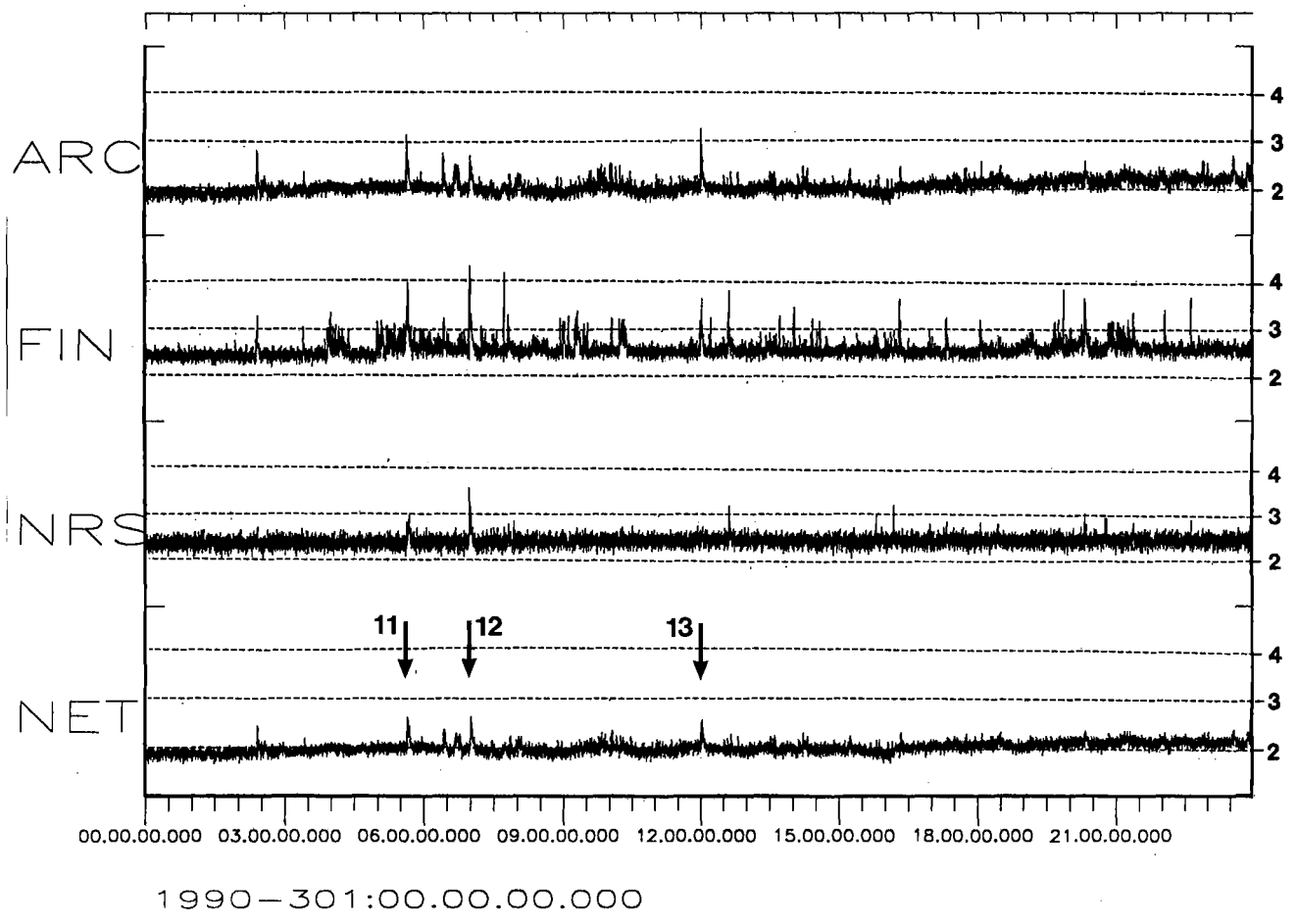

Fig. 7.4.7. Same as Fig. 7.4.3, but for day 301 (28 October 1990).

Notes:

11 and 13.	Two large mining explosions (M_L = 2.5) on the Kola Peninsula. Network threshold is about m_b = 2.6.
12.	A teleseismic earthquake (m_b = 5.3) at the Kurile Islands. Network threshold is m_b = 2.7.

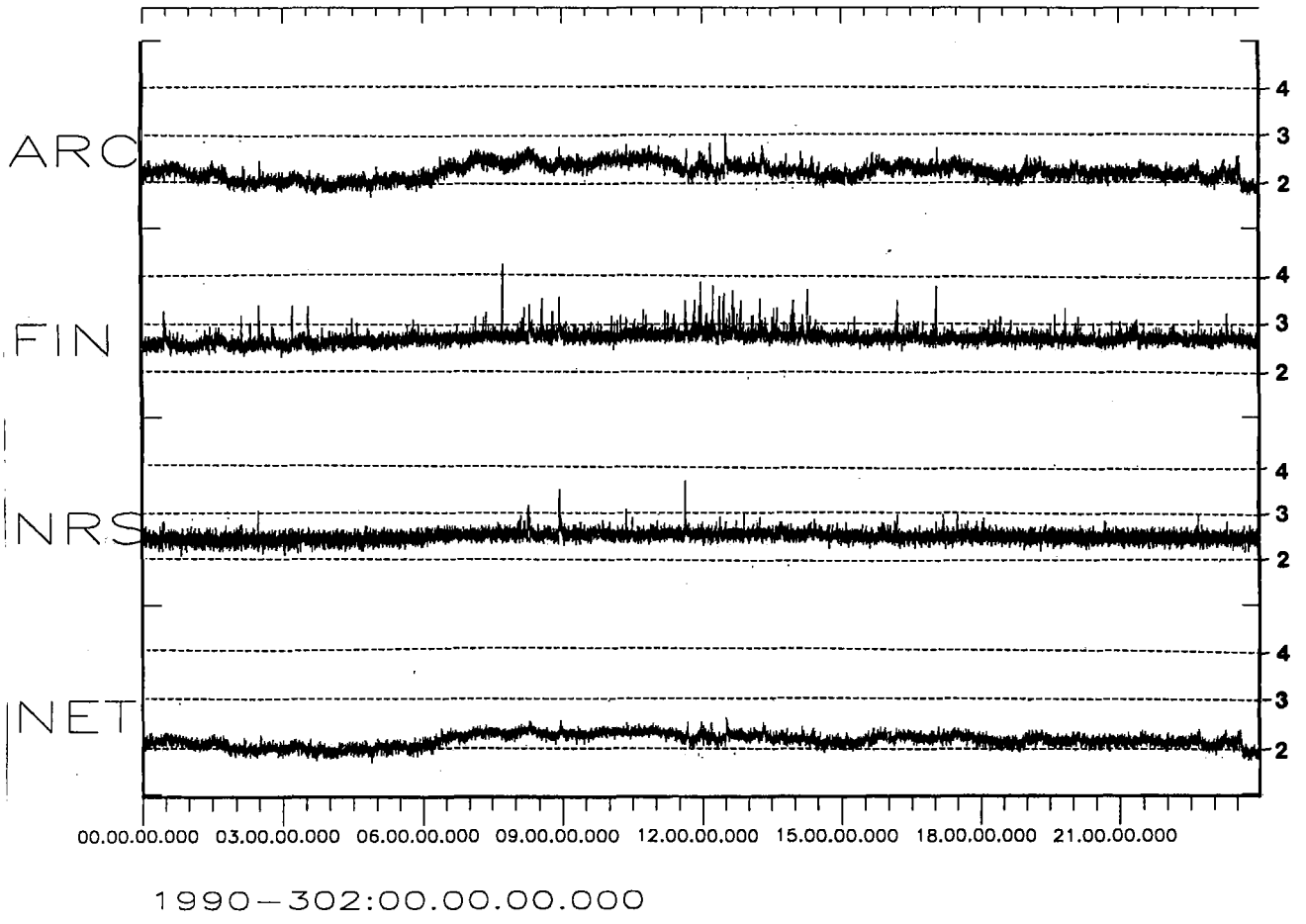

Fig. 7.4.8. Same as Fig. 7.4.3, but for day 302 (29 October 1990).

Notes:
No significant peaks in the network threshold plot this day.

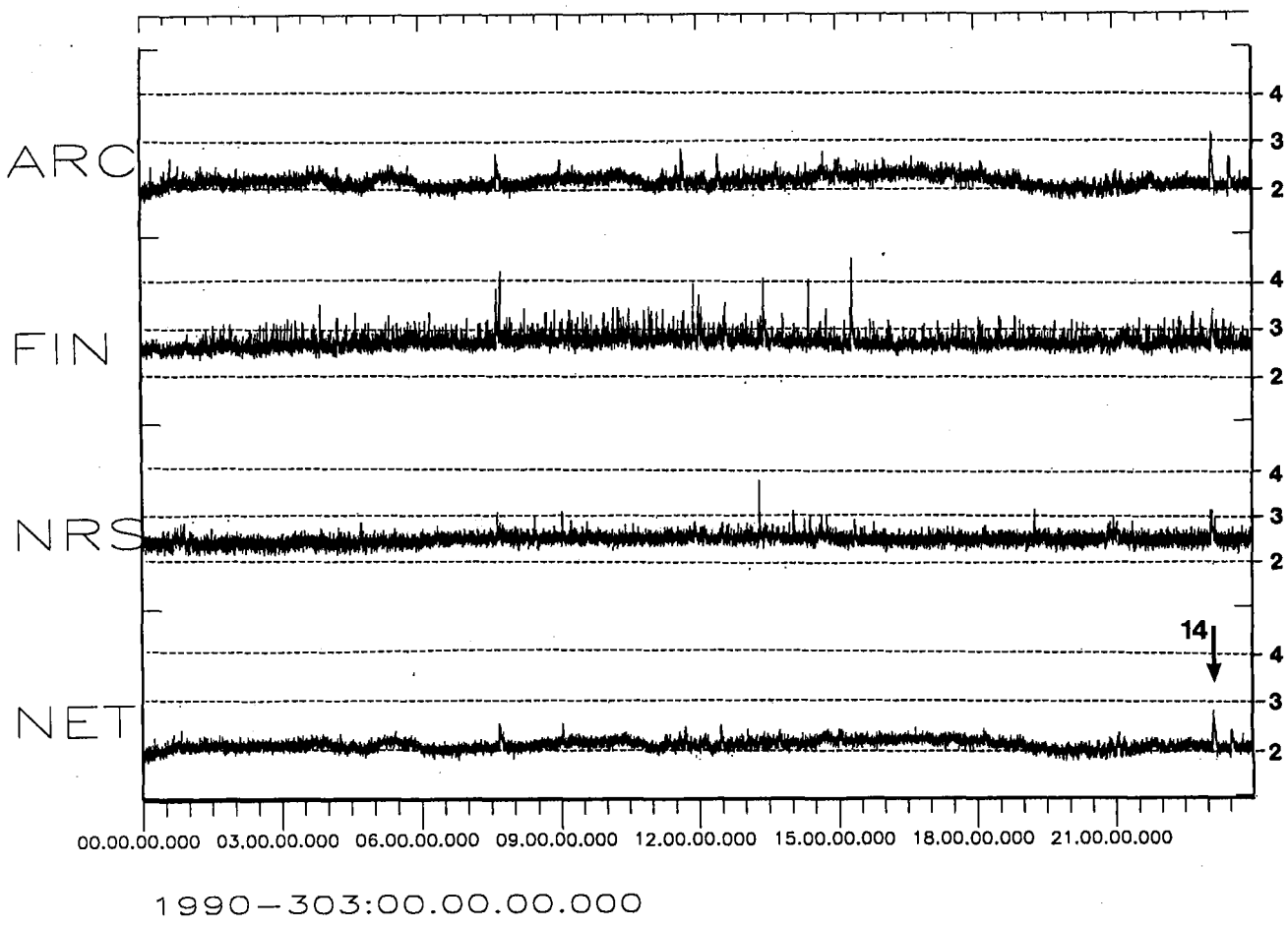

Fig. 7.4.9. Same as Fig. 7.4.3, but for day 303 (30 October 1990).

Notes:

14. A small earthquake (M_L = 2.8) in Nordland, N. Norway, caused an increase in the network threshold for Novaya Zemlya to m_b = 2.8.

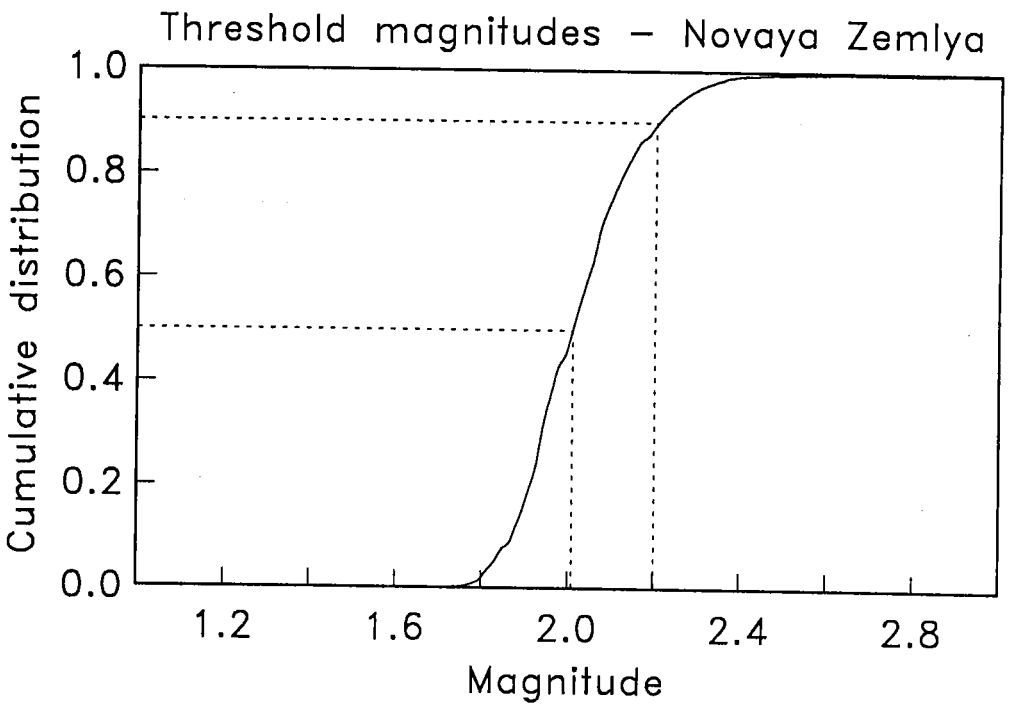

Fig. 7.4.10. Cumulative statistics of the network threshold magnitudes from Figs. 7.4.3–7.4.9, covering one full week of data.

7.5 Real-time processing using a hybrid 3-component / small array station

Introduction

In recent years, much effort has been devoted to developing and assessing various methods for 3-component seismic data processing. It has been demonstrated that polarization analysis can provide P azimuth estimates with good accuracy from a single 3-component station. Using SH or SV particle motion models, some success has also been reported in determining azimuth from S and Lg phases, although there is often a 90 or 180 degree ambiguity in the resulting estimates.

These efforts notwithstanding, a fundamental problem in automatic 3-component processing still remains. This is the problem of phase identification, which of course is essential in deciding which particle motion model to apply. From our experience at NORESS, a high degree of rectilinearity, which in theory would indicate the presence of a P phase, is quite often seen also for S and Lg phases, and even for noise bursts, when applying polarization analysis. As a result, an automatic P-type solution found by 3-component processing is often of limited usefulness, since it may either be a P phase (with correct azimuth) or some other phase (in which case the azimuth estimate is useless).

Small-aperture arrays of the NORESS-type have proved to be very effective in processing regional as well as teleseismic phases. Their primary features are:

- Significant SNR gains at high frequencies
- Reliable phase identification (P-type versus S-type phases)
- Precise azimuth estimates of all phase types.

While the accuracy of NORESS azimuth estimates can be as good as $\pm$ 1 degrees for well-calibrated regions, the uncertainty of uncalibrated azimuth estimates is often of the order of 10 degrees or more, due to lateral inhomogeneities near the receivers. In practical schemes for automatic phase association (e.g., Mykkeltveit and Bungum, 1984), a tolerance of 30 degrees in azimuth deviation from the true value is often assumed. Given that the acceptable limits in azimuth estimation for phase association purposes are much less restrictive than the optimum array capability, a natural question is whether a smaller regional array can achieve reliable phase identification as well as an acceptable uncertainty in azimuth estimation.

We have attempted to address this question, and have chosen to evaluate the smallest such array available to us: the NORESS A-ring subarray (Fig. 7.5.1). This subarray comprises a center 3-component seismometer A0, surrounded by a triangular SPZ array A1–3. The diameter of this subarray is

only 0.3 km, i.e., a factor of 10 less than NORESS, and it thus spans an area only 1 per cent of that of the full NORESS array. In this paper, we present an initial evaluation of automatic detection processing using this very small array.

Automatic processing

We conducted automatic detection processing of the A-ring subarray for a period of 5 days (22–26 October 1990), using a standard multi-filter power detector with parameters as specified in Table 7.5.1. For each detected signal, broadband F-K analysis was conducted using the 4 SPZ sensors, and compared to the NORESS F-K results. We also carried out polarization analysis (using a P-wave particle motion model) for each detected phase, applying the method of Kværna and Doornbos (1986) to the 3-component A0 system.

To obtain a data base for the evaluation, we extracted all seismic phases detected by NORESS and associated to verified regional events for the 5-day period. The generalized beamforming procedure (Ringdal and Kværna, 1989) and the results from IMS processing (Bache *et al*, 1990) were used in order to ensure correct location of these reference events. P-coda detections and multiple S-phases were ignored, so that each event provided a maximum of 3 phases (P, S and Lg). These phases were then matched to the detection lists produced from the A-ring SPZ subarray and the 3-component analysis, and the phase velocity and azimuth estimates were compared.

Phase identification

Fig. 7.5.2 shows the A-ring phase velocity F-K estimates for P phases (circles) and S phases (crosses) for the reference data set. The separation is better than 95 per cent, which implies that even this small array is able to provide correct phase identification automatically and with high confidence. The corresponding picture for the full NORESS array is shown in Fig. 7.5.3, and naturally shows a better separation. It should be noted here that all the reference phases were by definition correctly identified by NORESS, so it is not surprising that the separation is 100 per cent. But it is still interesting to compare the scatter in the two data sets.

P-wave azimuths

Fig. 7.5.4 compares P-wave azimuths estimated by the full NORESS SPZ array and the small A-ring SPZ subarray using broadband F-K analysis in both cases. The estimates are very consistent, and the large majority are well within a tolerance limit of 30 degrees.

A corresponding plot for P waves analyzed from 3-component records is given in Fig. 7.5.5, and shows a similar amount of scatter. In fact, the scatter is slightly less than in Fig. 7.5.4. Thus, the polarization analysis can give very useful contributions to regional azimuth estimates, assuming that the

phase first has been identified as a P phase. An interesting approach would be to combine the two azimuth estimates (A-ring SPZ and 3-comp) in order to obtain increased stability.

S-wave azimuths

Fig. 7.5.6 compares azimuths of S-type phases estimated by the A-ring SPZ subarray and the full NORESS array. Again, the correspondence is quite good, and thus shows that automatic regional phase association using RONAPP-type processing can be achieved even when using an array as small as 0.3 km in diameter. We note that our 3-component processing provides no useful azimuth information for S phases, but it is of course possible that such information could be obtained in certain cases, given that the phase first has been identified as S or Lg.

Detectability

Figs. 7.5.7 and 7.5.8 illustrate the P and S wave detectability of the A-ring array as a function of NORESS SNR. From Fig. 7.5.7, it is seen that all P phases with SNR > 20 dB (i.e., STA/LTA > 10 at NORESS) have been detected. At distances below 500 km, several events of relatively low SNR at NORESS have also A-ring detections; this is due to the high signal frequencies which cause the full array SNR gains of these phases to be less than the theoretical $\sqrt{N}$. At distances above 500 km, the superiority of the full NORESS array becomes apparent.

In Fig. 7.5.8 it is seen that the A-ring subarray is close to matching NORESS S-phase detectability at all distances. This is because the horizontal components of the A0 3-component system provide quite efficient detection of S and Lg phases, in particular when added incoherently to the vertical component. The full array does not have the same SNR gain for secondary phases as for P-phases, because of less signal coherency and (in particular) coherent noise caused by P coda. Thus, as expected, there is not a significant difference in secondary phase detection.

False alarm consideration

In practical operation of any seismic system, the problem of false detections is very important. This is especially the case if the online detector is operated at a low detection threshold, and it is essential to be able to identify false alarms at as early a stage as possible.

To address this problem, we have analyzed in detail all the A-ring detections for one full data day (24 October 1990). The results are presented in Table 7.5.2, again with NORESS results as a reference. From the table, it is seen that out of 117 total phase detections, 105, or 90 per cent, were correctly classified using the broadband F-K analysis applied to A-ring SPZ data. Of these 105 phases, 37 were P, 36 S (or Lg) and 32 noise (i.e., low-velocity de-

tections). Note that P coda detections were counted as P and S coda were counted as S in these statistics. None of the 37 phases which (according to NORESS) were of the P type were misclassified by the A-ring. Of the 40 S phases, 4 were misclassified (2 P and 2 noise). Out of 40 noise detections, 3 were given P-phase velocities and 5 were given S-phase velocities when using the A-ring.

These statistics must be considered quite satisfactory. In fact, it appears that the SNR threshold for the A-ring detector could be lowered significantly, and still produce a reasonable false alarm rate.

Conclusions

The problems encountered when using a 3-component system in a real-time automatic processing environment appear to be effectively alleviated by supplementing the 3-C system with a very small (aperture 0.3 km) 3-element array. Based on the studies in this paper of the NORESS A-ring subarray, we conclude that:

- Phase identification (P or S) can be reliably achieved (better than 95 % success rate) using F-K analysis of the A-ring array data.
- Azimuth estimates, with accuracy generally to within 30 degrees can be obtained for both P and S phases using A-ring array processing, and (at least) for P-phases using 3-component polarization analysis of the A0 3-component station..
- Good regional P-phase detectability can be obtained from the A-ring array out to 500 km epicentral distance. At greater distances, P-wave detectability relative to that of NORESS deteriorates sharply.
- Detectability of S-phases using the A-ring array is excellent at all distances, and comes close to matching that of the full NORESS array.
- The A-ring array analysis makes it possible to isolate the majority of noise detections, thus giving an acceptable false alarm rate for online operation.

It would be an interesting experiment to supplement some existing 3-component stations with a triangular small array as described here, and conduct network detection and location experiments. Before doing so, it is of course important to verify that these results can be obtained in other geological and geographical environments, e.g., by analyzing similar data for other existing arrays (ARCESS, GERESS, FINESA).

A very small array of the A-ring type is especially suited for processing high signal frequencies. In fact, one might consider a dense sensor deployment within the A-ring aperture, as an experiment aimed at conducting array processing at frequencies of 20–40 Hz. This would of course require a higher sampling rate than the 40 Hz currently used at NORESS. Array processing at these frequencies would be of particular interest in the context of developing methods for monitoring cavity decoupled explosions, which might have significant signal energy in this frequency band.

T. Kværna
F. Ringdal

References

Bache, T.C., S.R. Bratt, J. Wang, R.M. Fung, C. Kobryn and J. Given (1990): The Intelligent Monitoring System, *Bull. Seism. Soc. Am.*, Special Issue, in print.

Kværna, T. and D.J. Doornbos (1986): An integrated approach to slowness analysis with arrays and three-component stations, *NORSAR Semiannual Technical Summary, 1 Oct 1985 - 31 Mar 1986*, NORSAR Sci. Rep. No. 2-85/86, Kjeller, Norway.

Mykkeltveit, S. and H. Bungum (1984): Processing of regional seismic events using data from small aperture arrays, *Bull. Seism. Soc. Am.*, 74, 2313–2333.

Ringdal, F. and T. Kværna (1989): A multichannel processing approach to real time network detection, phase association and threshold monitoring, *Bull. Seism. Soc. Am.*, 79, 1927–1940.

Coherent beams:

Beam	Apparent vel.	Azimut	Filter band	Configuration	Threshold
NZ01	9999.9	0.0	0.5- 1.5	A0z,A1z,A2z,A3z	4.0
NZ02	9999.9	0.0	1.0- 2.0	A0z,A1z,A2z,A3z	3.7
NZ03	9999.9	0.0	1.0- 3.0	A0z,A1z,A2z,A3z	3.7
NZ04	9999.9	0.0	1.5- 2.5	A0z,A1z,A2z,A3z	3.5
NZ05	9999.9	0.0	1.5- 3.5	A0z,A1z,A2z,A3z	3.5
NZ06	9999.9	0.0	2.0- 3.0	A0z,A1z,A2z,A3z	3.5
NZ07	9999.9	0.0	2.0- 4.0	A0z,A1z,A2z,A3z	3.5
NZ08	9999.9	0.0	2.5- 4.5	A0z,A1z,A2z,A3z	3.5
NZ09	9999.9	0.0	3.0- 5.0	A0z,A1z,A2z,A3z	3.5
NZ10	9999.9	0.0	3.5- 5.5	A0z,A1z,A2z,A3z	3.7
NZ11	9999.9	0.0	4.0- 8.0	A0z,A1z,A2z,A3z	3.7
NZ12	9999.9	0.0	5.0-10.0	A0z,A1z,A2z,A3z	3.7
NZ13	9999.9	0.0	8.0-16.0	A0z,A1z,A2z,A3z	4.0

Incoherent beams:

Beam	Apparent vel.	Azimut	Filter band	Configuration	Threshold
NA01	9999.9	0.0	0.5- 1.5	A0z,A0n,A0e	2.7
NA02	9999.9	0.0	1.0- 2.0	A0z,A0n,A0e	2.6
NA03	9999.9	0.0	1.0- 3.0	A0z,A0n,A0e	2.5
NA04	9999.9	0.0	1.5- 2.5	A0z,A0n,A0e	2.5
NA05	9999.9	0.0	1.5- 3.5	A0z,A0n,A0e	2.5
NA06	9999.9	0.0	2.0- 3.0	A0z,A0n,A0e	2.6
NA07	9999.9	0.0	2.0- 4.0	A0z,A0n,A0e	2.8
NA08	9999.9	0.0	2.5- 4.5	A0z,A0n,A0e	3.4
NA09	9999.9	0.0	3.0- 5.0	A0z,A0n,A0e	3.5
NA10	9999.9	0.0	3.5- 5.5	A0z,A0n,A0e	2.8
NA11	9999.9	0.0	4.0- 8.0	A0z,A0n,A0e	2.5
NA12	9999.9	0.0	5.0-10.0	A0z,A0n,A0e	2.5
NA13	9999.9	0.0	8.0-16.0	A0z,A0n,A0e	2.8

Table 7.5.1. Parameters used for the A-ring detector experiment.

	Classified as:		
Correct Phase id	P (v>6 km/s)	S or Lg (3.4<v≤6 km/s)	Noise (v≤3.4 km/s)
P	37	0	0
S or Lg	2	36	2
Noise	3	5	32

Total phases detected by the A-ring detector : 117
Total phases correctly classified : 105 (90 %)

Table 7.5.2. Statistics of detected phases for the A-ring array for a 24-hour period. The phases are classified based on estimated phase velocities using A-ring SPZ broadband F-K, and the "correct" phase id is based on F-K results from the full NORESS array.

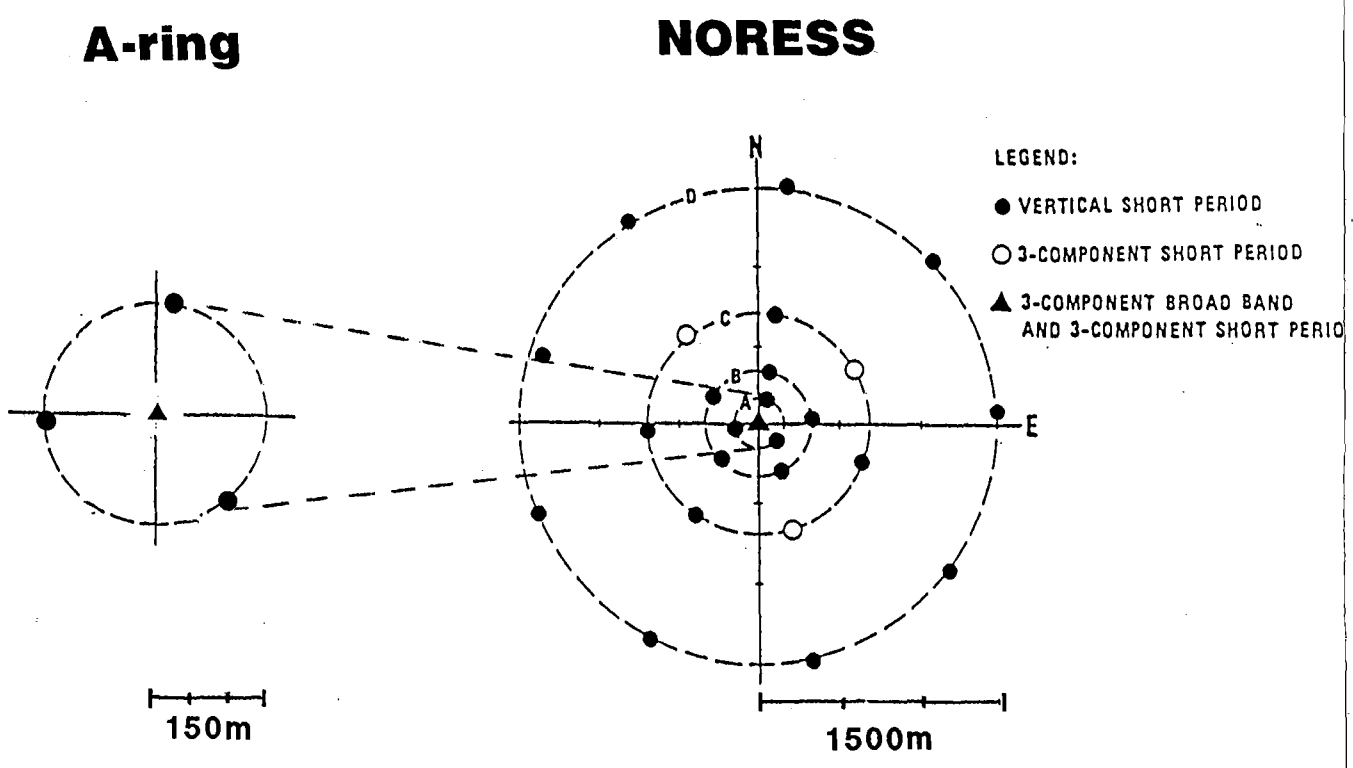

Fig. 7.5.1. Geometry of the full NORESS array and of the A-ring subarray used in this study.

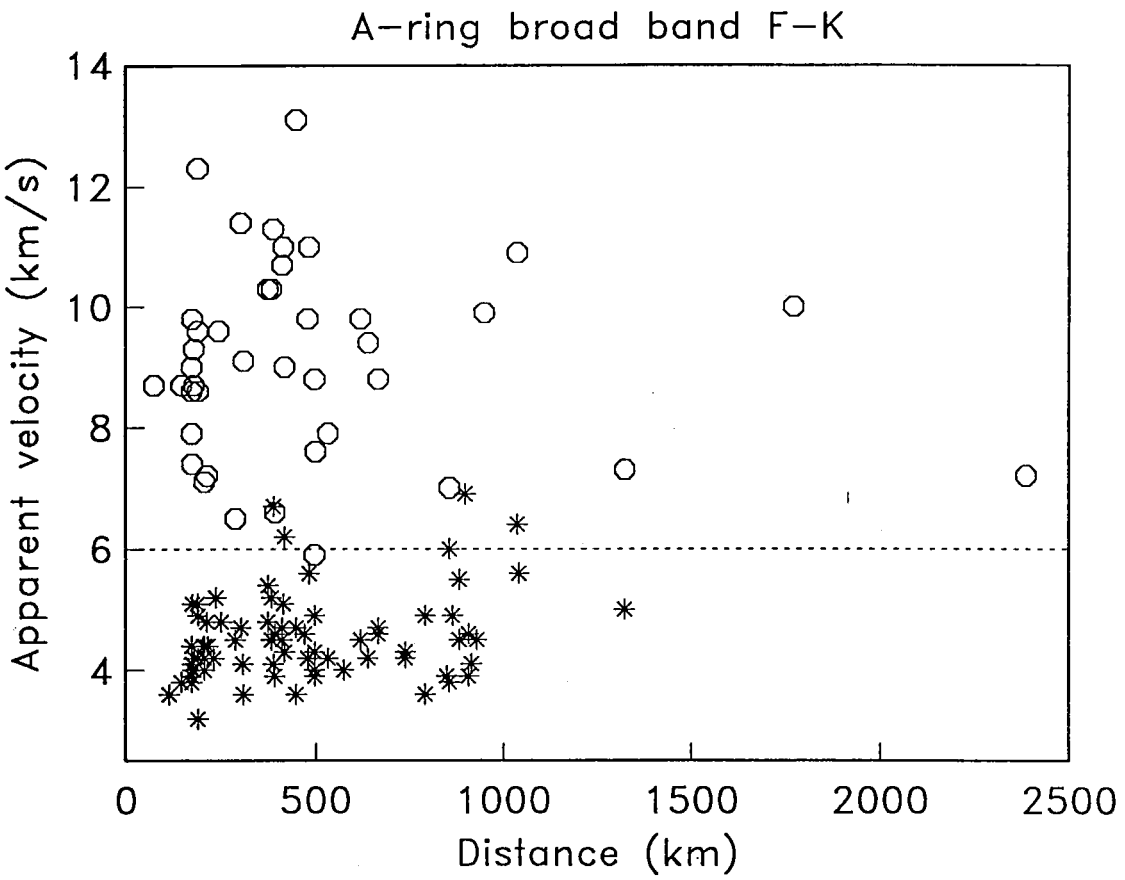

Fig. 7.5.2. Estimated phase velocities using the A-ring SPZ array (broadband F-K) for detected P phases (circles) and S phases (asterisks). Note that the phases can be identified from phase velocity with more than 95 % accuracy.

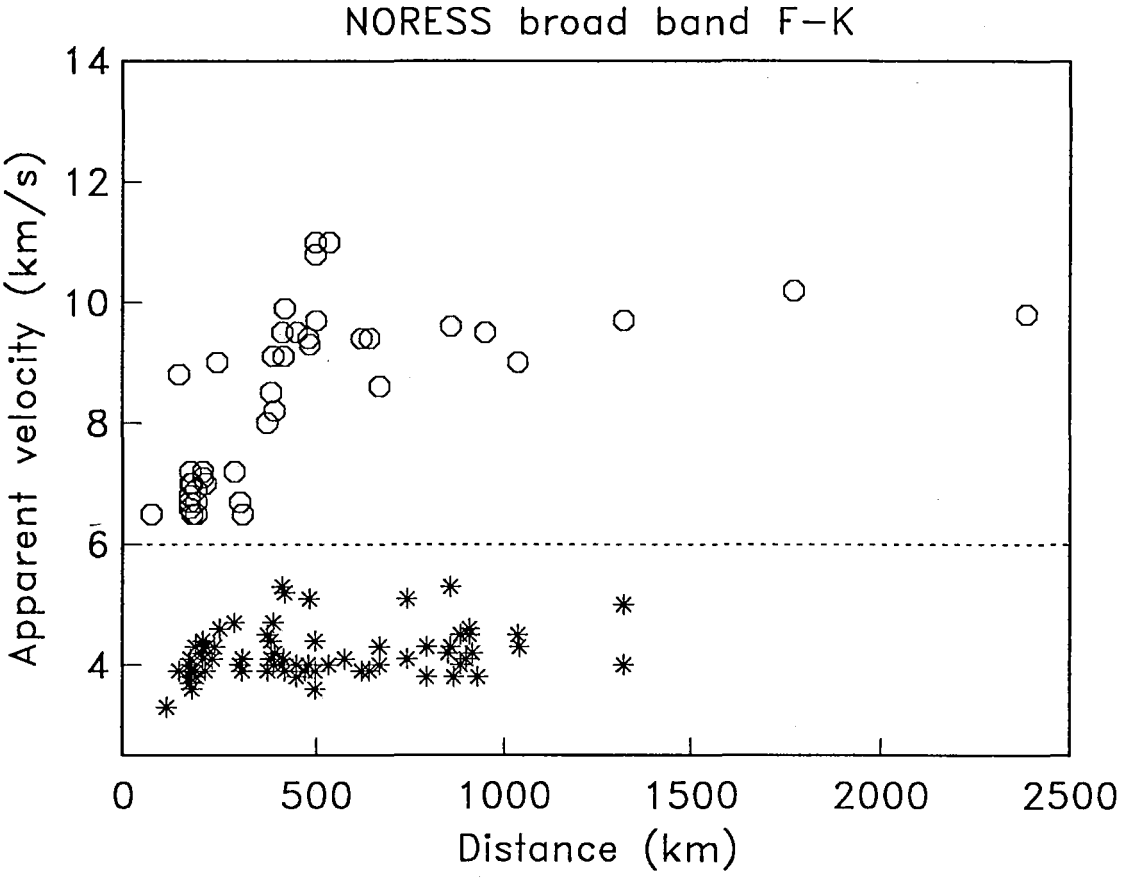

Fig. 7.5.3. Similar to Fig. 7.5.2, but with phase velocities estimated using the full NORESS array.

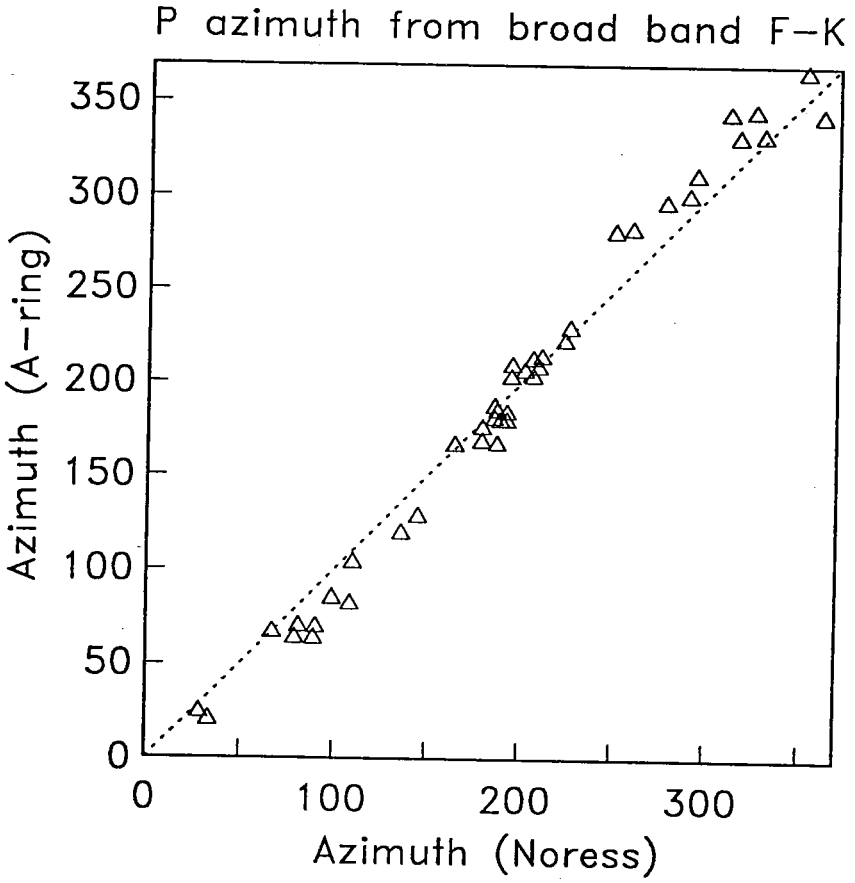

Fig. 7.5.4. Comparison of estimated azimuths of P phases using the full NORESS array and the A-ring SPZ array (broadband F-K). Note the excellent consistency.

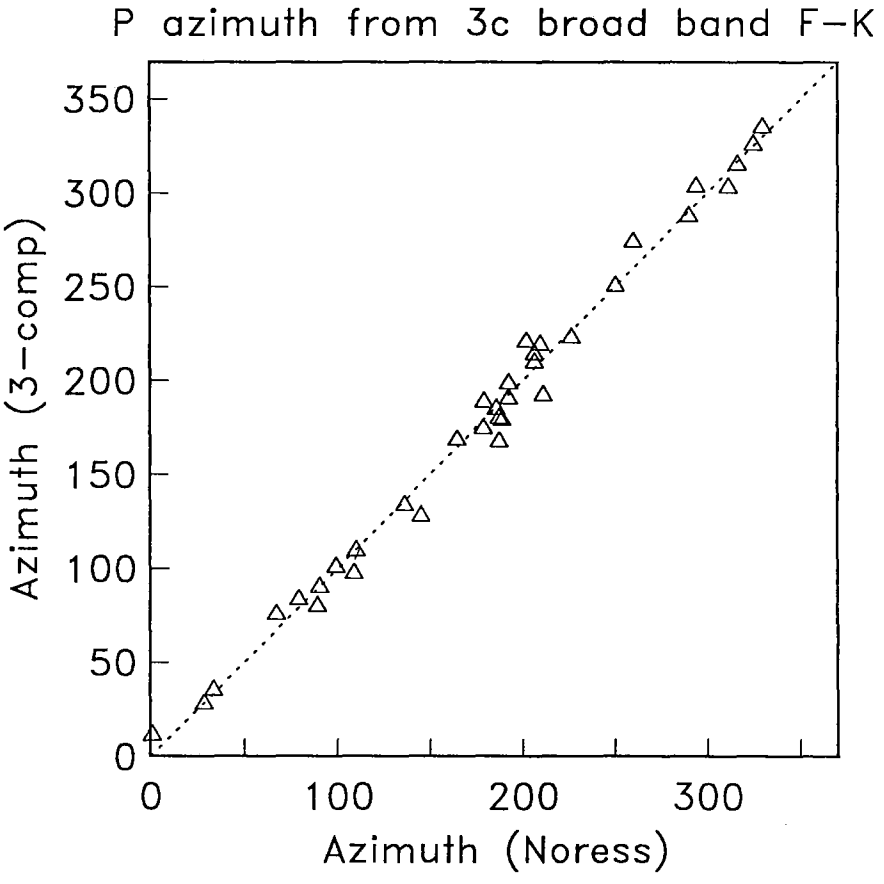

Fig. 7.5.5. Comparison of estimated azimuths of P phases using the full NORESS array (broadband F-K) and the A0 3-component system (polarization analysis). Note that the consistency is similar to that of Fig. 7.5.4.

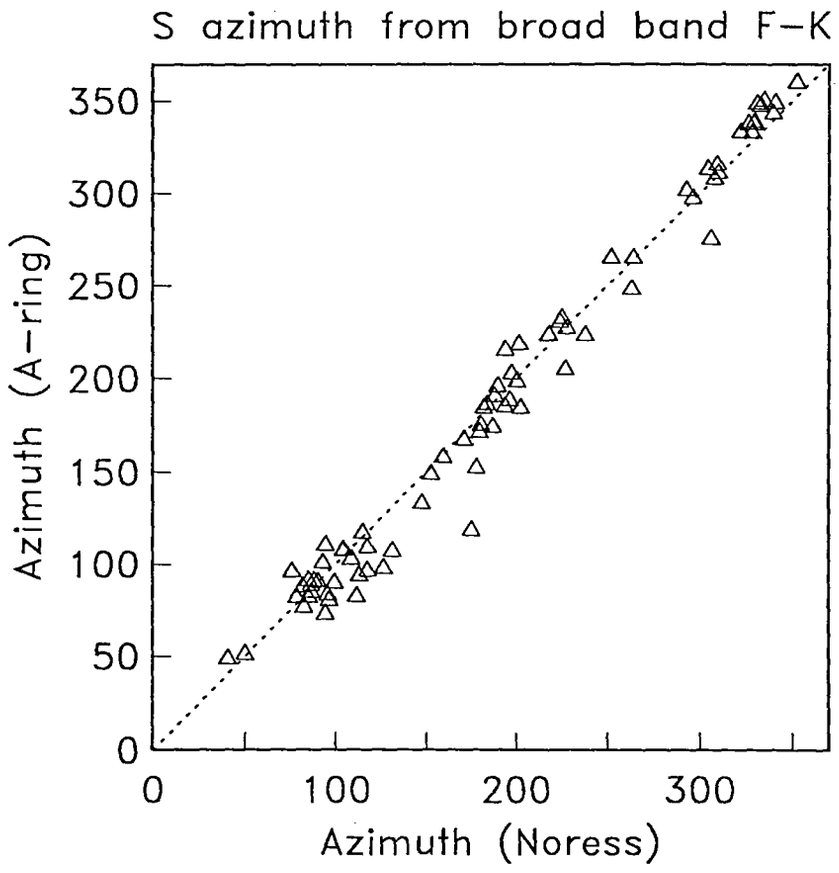

Fig. 7.5.6. NORESS and A-ring azimuth comparison for S phases. Note that the consistency is as good as for P phases (in Fig. 7.5.4).

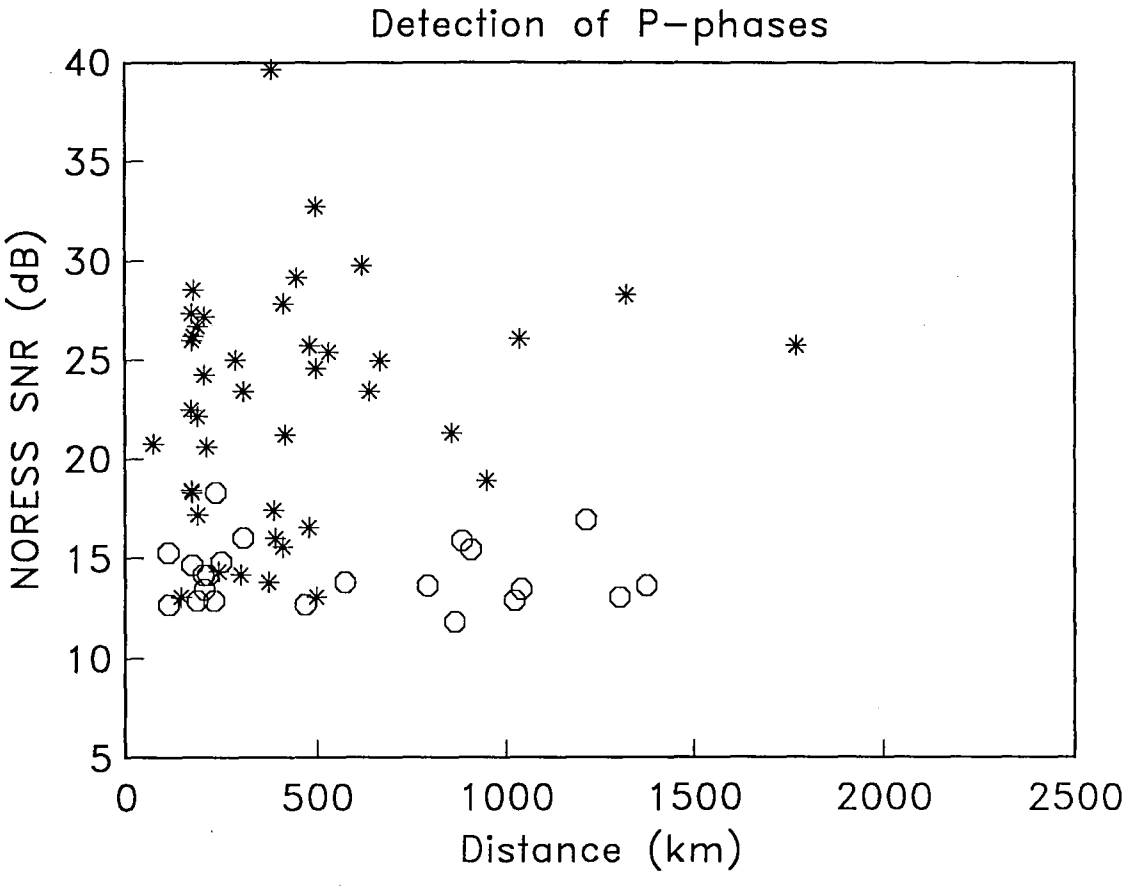

Fig. 7.5.7. Illustration of P-phase detectability of the A-ring SPZ array combined with the 3-component A0 system. P-phases detected by the A-ring SPZ/3-component system are marked as asterisks, whereas nondetected phases are marked as circles. Note that the reference array (NORESS) is clearly superior at distances > 500 km.

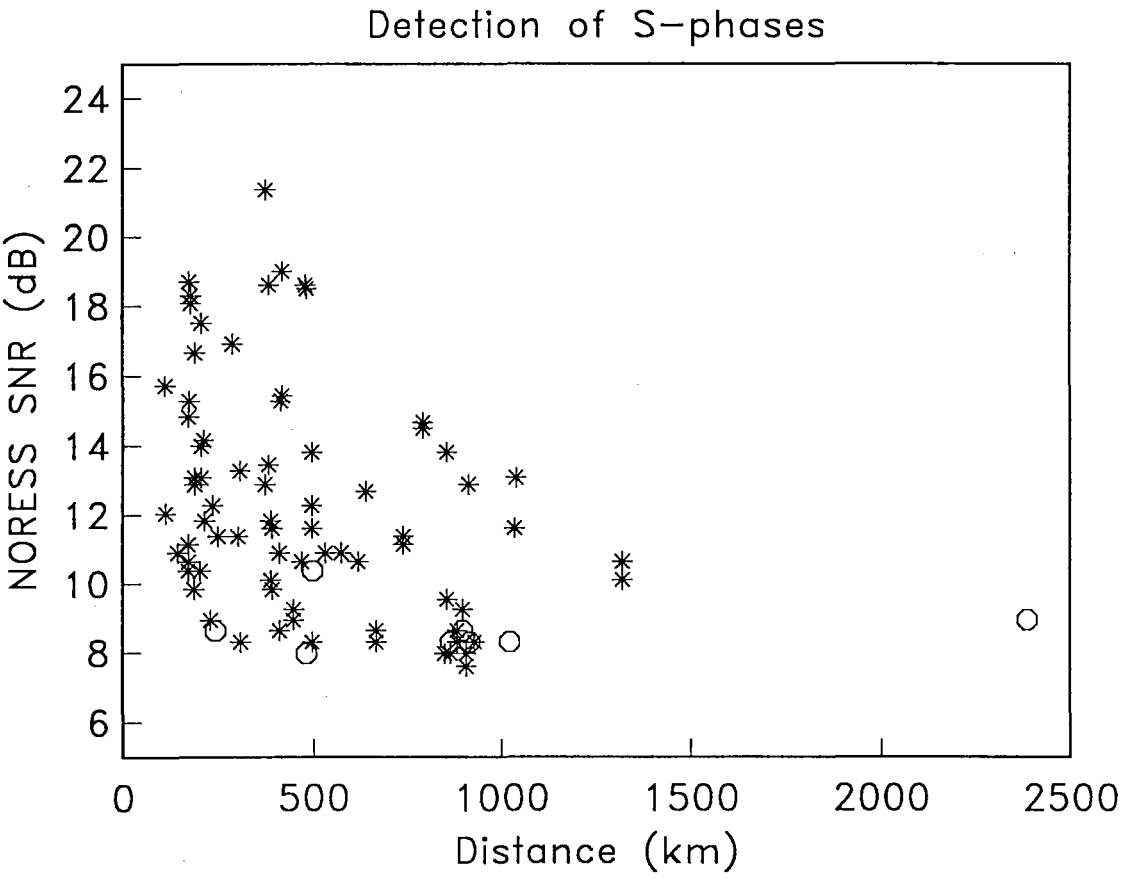

Fig. 7.5.8. Same as Fig. 7.5.7, but for S phases. Note that in this case the small array/3-component system comes close to matching the full array performance.

7.6 Development of two three-component stations in Poland

Background

A network of four regional arrays currently contributes data to the NORSAR Data Processing Center in Norway. These arrays are the NORESS and ARCESS arrays in Norway, the FINESA array in Finland and the GERESS array in the Federal Republic of Germany (see Fig. 7.6.1). Data from ARCESS and NORESS are processed jointly in the Intelligent Monitoring System (IMS) that has been installed at NORSAR this year. A forthcoming upgrade of IMS will allow joint processing of data from N arrays and M single stations.

As a cooperative effort between Poland and the United States, two modern seismic stations, including workstations for on-site data recording and analysis, are now being installed in Poland. Each installation comprises a three-component broad band station and a three-component short period station. These stations represent a valuable extension of the existing network of regional arrays in northeastern Europe. In order for IMS, however, to take full advantage of these new stations, the data from Poland must be transmitted continuously and in real time to Norway. This contribution gives descriptions of the field systems installed in Poland, the communications arrangements between Poland and Norway, and the system configured at NORSAR for the purpose of acquiring the data from the two stations in Poland.

Installations in Poland

The two stations in Poland are located at Ksiaz, in the vicinity of the town of Walbrzych in southwestern Poland, and at Stary Folwark, near the town of Augustow in northeastern Poland (see Fig. 7.6.1).

Teledyne Geotech installed in June this year a seismic system at Ksiaz, comprising a short period three-component station (GS-13 sensors), a broad band three-component station (BB-13 sensors), an RDAS-200 data acquisition unit, and a SUN-2 based NOMAD workstation for local data analysis and archiving. Ksiaz is an existing seismological observatory affiliated with the Department of Seismology of the Institute of Geophysics (in Warsaw) of the Polish Academy of Sciences. The local staff at the observatory at Ksiaz will operate the new station and use the workstation in their daily data analysis.

The new station in Stary Folwark will be installed by Teledyne in November. It will be identical to the station at Ksiaz, except there will be no workstation, since there will be no local seismological staff.

Communications links

Reliable communications links between the NORSAR Data Processing Center in Norway and the two sites in Poland can only be accomplished via satellite. Discussions were conducted with the telecommunication authorities

in both Poland and Norway in order to determine how such links could be established, and the Polish PTT responded that they would allow the Norwegian Telecommunication Administration (NTA) to deliver and put into operation the ground station equipment needed in Poland.

NTA decided to use the EUTELSAT SMS system for the satellite links between Poland and Norway, and communications were installed in October/November as depicted in Fig. 7.6.2. The data transmission links each have a capacity of 64 kbits/s. The link between Stary Folwark and NORSAR is simplex, while the Ksiaz-NORSAR link is full duplex. The backlink from NORSAR to Ksiaz provides the staff at the Ksiaz observatory with access to data bases at NORSAR, including Stary Folwark data. The Ksiaz to NORSAR link uses a set of multiplexers to enable division of the capacity into several channels, as shown in Fig. 7.6.2. The seismic data from Ksiaz use a 19.2 kbits/s channel, the other 19.2 kbits/s channel will be running the SLIP protocol and used for general purposes, one of the 9.6 kbits/s channels will be used for general terminal access, and two remaining channels (9.6 and 2.4 kbits/s, not shown in Fig. 7.6.2) are spare ones.

Data acquisition and analysis at NORSAR

A data acquisition system to handle the data from the two stations in Poland has been configured at NORSAR, that is essentially identical to the data acquisition systems currently handling the data streams from the regional arrays. As seen in Fig. 7.6.2, the communications interface is NORSAR's BUSC system (see Paulsen *et al*, 1989). Otherwise, the data acquisition system comprises a SUN 3/260 computer with a Floating Point Accelerator, a 1.2 Gb disk drive with controller, an Exabyte tape drive with SCSI controller, and Ethernet. This system will make it possible to present the data from Poland to the IMS in the same way data from the arrays are made available.

The 24 October 1990 nuclear test at Novaya Zemlya was recorded by the new seismic station at Ksiaz, and the recordings for both the short period and the broad band stations are shown in Fig. 7.6.3.

S. Mykkeltveit
R. Paulsen

References

Paulsen, R., J. Fyen, P.W. Larsen and S. Mykkeltveit (1989): A new data acquisition system for FINESA. **In:** *Semiannual Technical Summary, 1 April – 30 September 1989*, NORSAR Sci. Rep. No. 1-89/90, Kjeller, Norway.

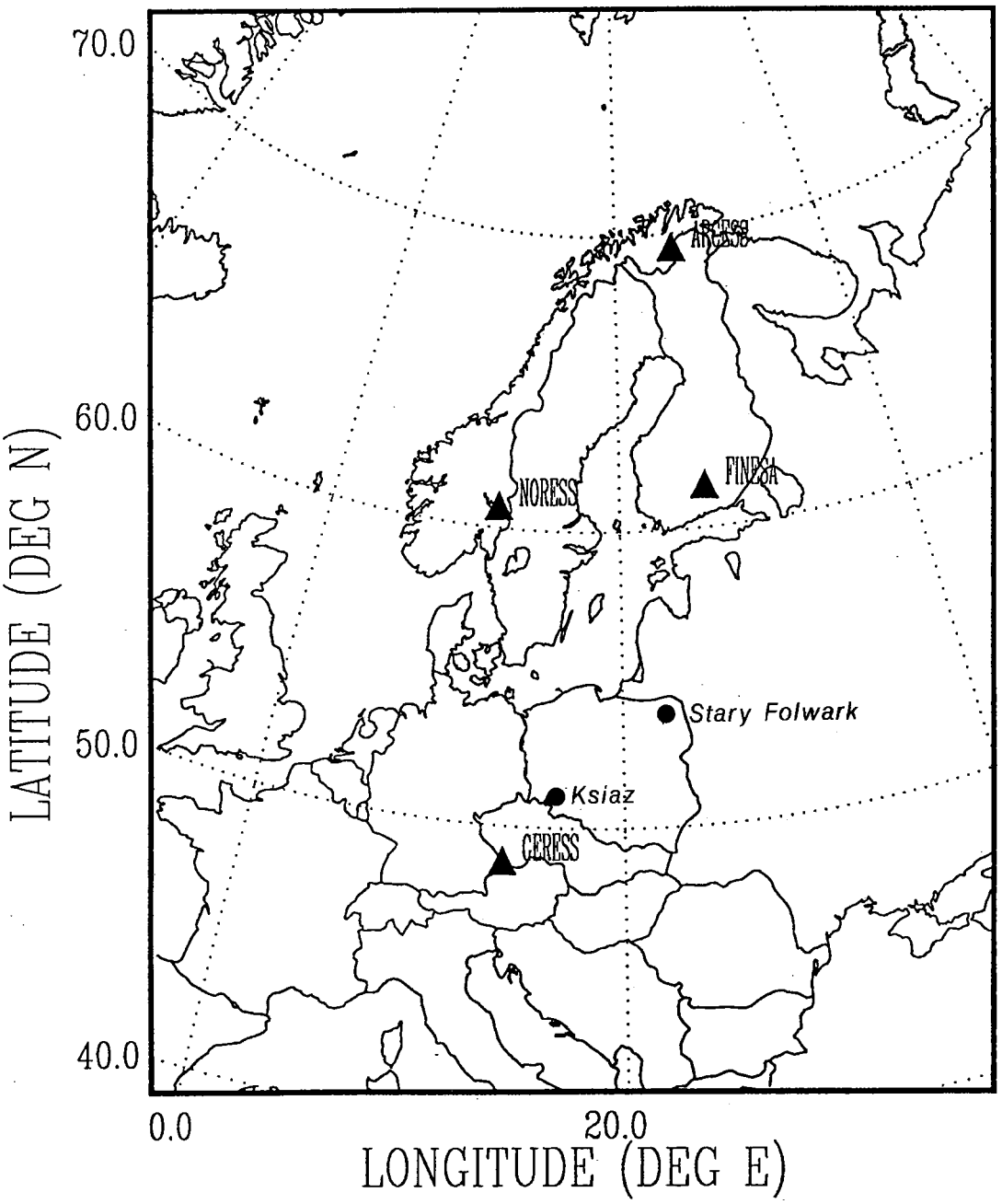

Fig. 7.6.1. The map shows the location of the regional arrays NORESS, ARCESS, FINESA and GERESS, as well as the two new stations in Poland.

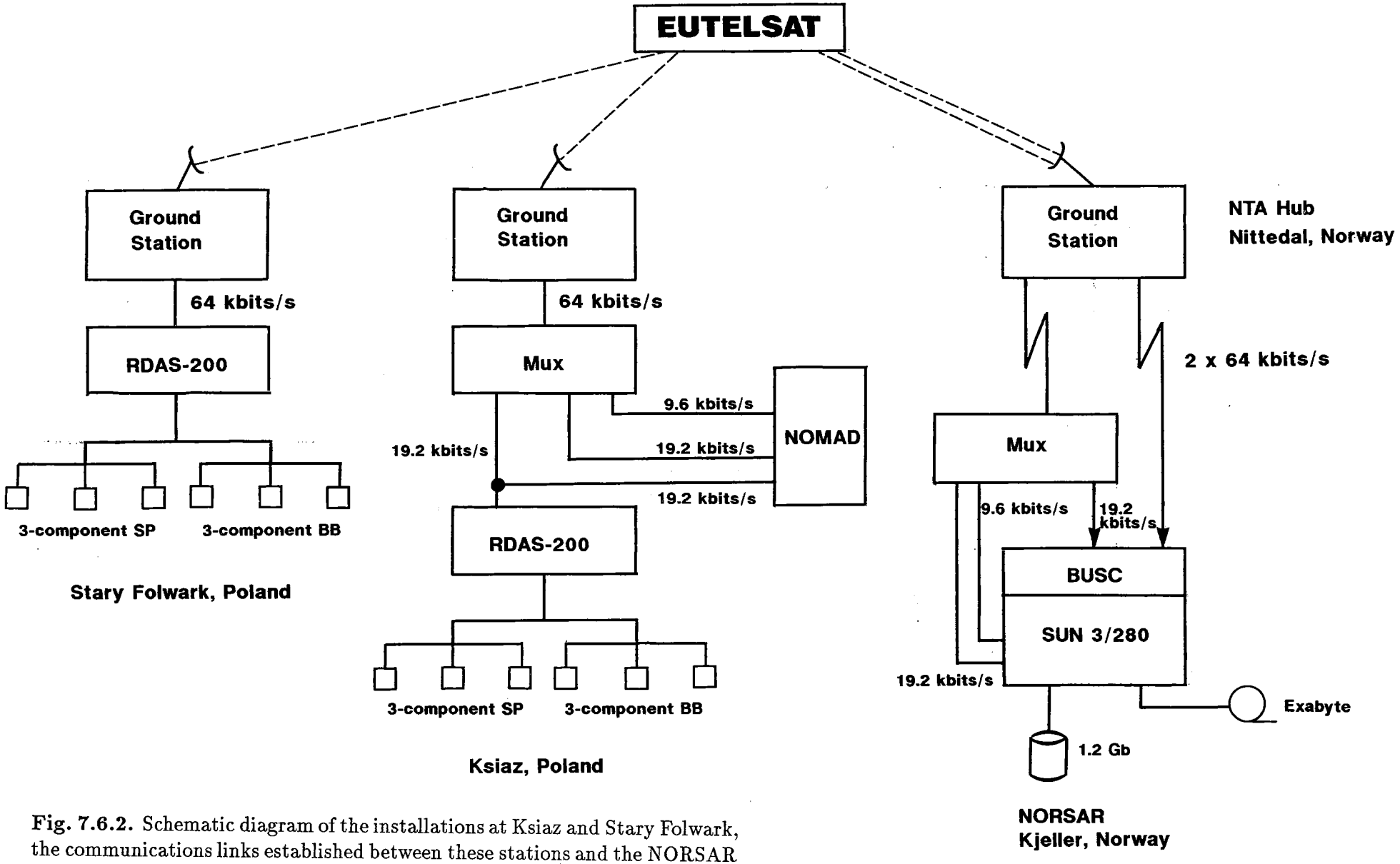

Fig. 7.6.2. Schematic diagram of the installations at Ksiaz and Stary Folwark, the communications links established between these stations and the NORSAR Data Processing Center in Norway, and the NORSAR data acquisition system for the two data streams from Poland.

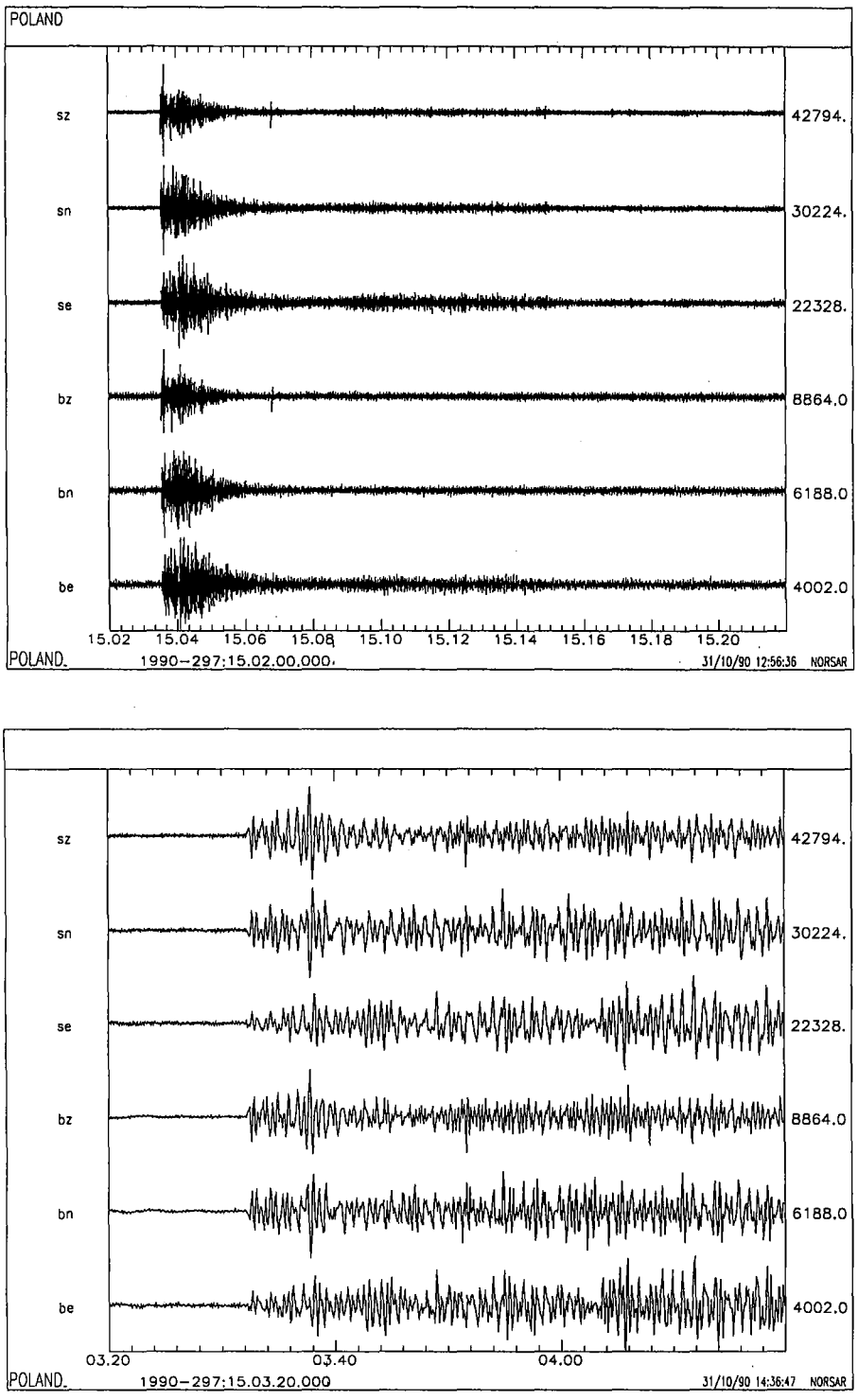

Fig. 7.6.3. Short period (sz, sn, se) and broad band (bz, bn, be) 3-component recording at Ksiaz of the 24 October 1990 nuclear explosion at Novaya Zemlya. The upper frame shows 20 minutes of data, whereas the lower frame covers a one-minute interval around the P onset.

7.7 Optimal group filtering and noise attenuation for the NORESS and ARCESS arrays

A generalization of Capon's (1970) maximum likelihood technique for detection and estimation of seismic signals has recently been introduced by Kushnir *et al* (1990). By using a multidimensional autoregressive approximation of seismic array noise, a technique to use Capon's multichannel filter for online processing has been developed. Such autoregressive adaptation to the current noise matrix power spectrum has been shown to yield good suppression of coherent noise processes. This paper presents further results of our studies of of adaptive optimal group filtering (AOGF) which now has been applied to more than 80 earthquake and underground nuclear explosion recordings at the small aperture arrays NORESS and ARCESS in Norway (Fig. 7.7.1).

Compared to conventional beamforming, AOGF is demonstrated to provide high signal-to-noise ratio (SNR) gains (12–18 dB) over a wide frequency band (0.2–5.0 Hz), while retaining an undistorted signal waveform. This gain is mainly due to suppression of noise at low frequencies, where both noise power and noise coherency is greatest.

AOGF has also been tested in combination with statistically optimal algorithms for detection and onset time estimation using the maximum likelihood principle. Here, narrow-band filtering has been applied, selecting the frequency band most appropriate for detecting weak arrivals by conventional beamforming. Even in this case, AOGF provides significant gain in SNR (typically 6–8 dB in the 2–4 Hz band) compared to the array beam.

Description of software used

The conventional technique for array signal processing is based on beamforming, band pass filtering and STA/LTA detection. Beamforming is the statistically optimal procedure under the assumption of independent noise among the M different receivers of the array and in this case it improves power signal-to-noise ratio by a factor of M. For correlated noise this procedure is not optimal in the statistical sense. Bandpass filtering gives additional improvement of SNR, but this procedure, evidently, may reduce available information about the signals. The STA/LTA detector is a simple procedure, but it is sensitive only to variations of recorded power due to signal arrival, and it does not make use of spectral differences between signal and noise. So there is room left for improvement of this technique, and a possibility is to use statistically optimal procedures accounting for noise and signal features.

Now, at NORSAR a technique based on statistically optimal procedures has been tested. This technique is illustrated in Fig. 7.7.2 and consists of adapative optimal group filtering (AOGF) followed by optimal detection (OD) and optimal signal onset time estimation (OE) (see Pisarenko *et al*, 1987).

AOGF is based on a Wiener optimal filter with frequency response

$$\vec{H}(\lambda) = \vec{G}^*(\lambda)F^{-1}(\lambda)/\vec{G}^*(\lambda)F^{-1}(\lambda)\vec{G}(\lambda)$$

using the multichannel array record $\vec{X}_t = \vec{S}_t + \vec{\xi}_t$, $\vec{S}_t = \vec{\tilde{G}}_t^* u_t$ for input. The output of this filter Y_t is a scalar. AOGF reduces the noise power to a minimum, using the estimated inverse matrix power spectrum $F^{-1}(\lambda)$ of the array noise $\vec{\xi}_t$. The vector function $\vec{G}(\lambda)$ represents the medium frequency response along the paths from the seismic source to the array sensors, u_t is the scalar signal of the seismic source (waveform). For a homogeneous medium, $\vec{\tilde{G}}_t$ is determined by signal arrival delays at different stations. If AOGF is tuned properly ($\vec{G} = \vec{\tilde{G}}$) and $\vec{\xi} = 0$, then the AOGF output Y_t coincides with the signal waveform u_t. The procedure thus avoids introducing any distortion of the signal. If the noise is uncorrelated ($F(\lambda) = I$) (I - identity matrix) and $\vec{G}(\lambda)$ depends on delays only, then AOGF coincides with beamforming.

The inverse power spectrum matrix $F^{-1}(f)$ is estimated from pure noise preceding the signal by a procedure of adaptation using multichannel autoregressive (AR) modelling. AR estimation of this large size matrix function considerably reduces computations and has experimentally proved to be an excellent procedure for estimating the coherent noise matrix power spectrum.

The optimal detector (OD) (Fig. 7.7.2) is based on autoregressive modelling and moving window detection. In a series of experiments OD proved to exceed STA/LTA results due to optimal accounting of spectral variations in the moving window. The optimal estimator (OE) (Fig. 7.7.2) is a maximum likelihood procedure applied to the time interval around the detection time. It is likewise based on an autoregressive modelling procedure and is sensitive to small variations of spectra in a chosen time interval.

Coherency of noise and optimal group filtering

In Kushnir and Lapshin (1984) it is shown that the SNR at the output of OGF tends to infinity with increasing noise coherency. Coherent noise may be represented as a superposition of noise contributions from several spatially distributed sources. ARCESS and NORESS noise seems to have a strong coherent component, which made it possible to achieve power SNR gain factors of AOGF relative to beamforming of about 70–80 at ARCESS and 20–30 at NORESS (Kushnir *et al*, 1990; Kushnir *et al*; 1989). Coherent noise may be recognized from spatial spectral FK-analysis, where noise and signals coming from different sources correspond to different peaks in the slowness vector plane. Strong coherent noise may be represented in the frequency domain as

$$\vec{\xi}(\lambda) = \sum_{k=1}^{N} \xi_k(\lambda)\vec{\phi}_k + \epsilon\vec{\eta}(\lambda), \qquad \lambda \in (0, 2\pi]$$

where $\xi_k(\lambda)$ are scalar noise source signals, $\vec{\phi}(\lambda)$ is the vector frequency response from the k-th noise source to the array receivers, and $\vec{\eta}(\lambda), k = 1, \ldots, N$

are independent power spectrum matrices.

$$F(\lambda) = \sum_{k=1}^{N} f_k(\lambda)\vec{\phi}_k(\lambda)\vec{\phi}_k^*(\lambda) + \epsilon^2\Phi(\lambda) \qquad (1)$$

where $f_k(\lambda)$ is the spectral density of $\xi_k(\lambda)$ and $\Phi(\lambda)$ is the matrix power spectrum of diffuse noise, and $\vec{\phi}_k^*$ is the transposed conjugated vector. It can be seen that if $\epsilon \to 0$, the matrix $F(\lambda)$ projects each vector signal $\vec{Q}(\lambda)$ recorded by the array to the "noise" subspace, i.e., linear subspace

$$\left\{\vec{\phi}_k(\lambda),\ k = 1, \ldots, N\right\}:$$

$$f(\lambda)\vec{Q}(\lambda) \underset{\epsilon \to 0}{\longrightarrow} \sum_{k=1}^{N} C_k\vec{\phi}_k(\lambda)$$

and $F^{-1}(\lambda)$ projects $\vec{Q}(\lambda)$ to the orthogonal subspace $\{\phi_k(\lambda)\}^{\perp}_{k=1,\ldots,N}$. Hence, the power of each signal, coming from the "noise" subspace, will be greatly reduced by OGF. We would like to note that compensation of noise by OGF does not require stationarity of the noise source signals $\xi_k(\lambda)$, but stationarity of $\vec{\phi}(\lambda)$ is important.

Description of experiments

Checking of noise attenuation stability. This paper is the second report concerning our attempts to use AOGF at NORSAR. In the first one (Kushnir *et al*, 1989), we described theoretical capabilities of AOGF and its successful application for broad band extraction of one of the smallest nuclear explosion signals recorded at ARCESS. But in the case described in Kushnir *et al* (1989), adaptation was done just before the onset time. Therefore some doubts remained as to whether AOGF would work continuously without losing its good features during long periods of filtering time. To check the AOGF performance stability, we applied AOGF to some long-term records of pure ARCESS and NORESS noise.

In Fig. 7.7.3 we show the results of filtering by AOGF the 25 channels of a 40- minute long NORESS noise record. Only the first 2 minutes of the time interval were used for adaptation. AOGF output noise power is gradually increasing, but SNR power gain relative to the beam does not become less than 20. It means that if a signal arrives during this time interval, its SNR will be enhanced by AOGF at least 20 times better than by the beam. Looking at Fig. 7.7.3, one may predict that OGF can work much better than the beam during one hour or even more.

We applied AOGF to 5 ARCESS and 5 NORESS records each consisting of 25 minutes of pure noise, computing the SNR power for each 5 minutes. The results are presented in Fig. 7.7.4. From Fig. 7.7.4b we see that the gain of AOGF relative to beamforming for NORESS is between 15 and 25, for

ARCESS from 30 to 75. Again, adaptation is done during the first 2 minutes, and that is why we have the largest gain for the first 5 minutes, including the interval of adaptation. AOGF includes two stages: adaptation and filtering. The first is time consuming, the second is not. If readaptation is only needed once an hour or so, one may attempt to use several AOGFs, tuned to different azimuths and apparent velocities in the same manner as done by beamforming at NORSAR, and this may be more effective for noise suppression in online processing. An illustration of such an application of AOGF is shown in Fig. 7.7.5, where the gain of AOGF is presented versus azimuth. The velocity is constant and equal to 13 km/sec. The peak of the gain corresponds to the southern direction.

Extraction of missed phases. The capability of AOGF to work for a long time without readaptation also makes it possible, using pure noise before P arrivals for adaptation, to enhance the SNR of seismic phases located in time far from the P arrival. Two examples, described below, illustrate the application of all three optimal algorithms: adaptive optimal group filtering, optimal detection, and onset time estimation for extraction of missed seismic phases. It sometimes happens that regional phases like Pn or Lg are missed by the detector applied at NORSAR in the regular processing of NORESS and ARCESS data. We tried to use AOGF, OD and OE to remedy this situation for some of these cases, and they seemed to work well. Two cases were considered.

a) For case 1 (Fig. 7.7.6a), the Lg phase was detected on NORESS, but the Pn and Sn phases were missed. Fig. 7.7.6b shows data for the same event, as recorded on the FINESA array in Finland. In Fig. 7.7.6c the result of AOGF, OD and OE and beamforming are shown for a window containing the presumed Pn onset. The onset time of the Pn wave is clearly seen, and the maximum of the OE curve is close to the theoretical Pn arrival. (The theoretical Pn arrival time is computed from the event location derived from the FINESA array data.) The theoretical and experimental P arrivals are shown on Fig. 7.7.6a. The first detection shown in Fig. 7.7.6d is questionable (is it caused by the Sn phase from the event considered or not) because the theoretical Sn arrival time differs from the experimental one. The second detection in Fig. 7.7.6d is more likely related to the Sn phase from the event considered.

b) For case 2 (Fig. 7.7.7a) the regular NORESS processing detected the Pn and Sn phases, but no Lg was detected. This interpretation is confirmed by inspecting the ARCESS records. We have done an adaptation for AOGF just before the Pn arrival. The results are shown in Fig. 7.7.7b, where all three phases Pn, Sn and Lg are evidently detected. Their arrival times are shown on Fig. 7.7.7a as well.

These results suggest possible applications of AOGF in combination with

OD and OE for improvement of the detection lists generated by NORSAR's regular processing of array data.

Adaptive group filtering of seismic signals

AOGF was applied to the processing of 35 teleseismic earthquakes and 44 nuclear explosion signals recorded at NORESS. Earthquake locations are shown in Fig. 7.7.8. Most of the explosions are located at the Shagan River site. This selection of events was made with a view to future work on the discrimination problem. In all the cases, the SNR was much improved by AOGF, but the events may be divided into two classes. One class is where SNR was small in the first place and the other where it was large. In the first class (example in Fig. 7.7.9) improvement of SNR by AOGF is evident, and in the other example (Fig. 7.7.10a) the improvement is not evident in a broad frequency band (0.2–5.0 Hz). But if we consider only the low frequency band (for example, 0.2–0.5 Hz) the advantage of the group filter is seen clearly (Fig. 7.7.10b). This is due to two factors: The first is that at this latter frequency band the SNR is worse for the short-period records used, and the second is that the gain of AOGF seems to be largest due to the high noise coherency in this band.

Conclusion

By application of advanced techniques (apative optimal group filtering, optimal detector, optimal estimator), based on statistical algorithms, processing of NORESS and ARCESS array data may be improved. This improvement could be achieved by taking optimal advantage of array noise coherency and signal frequency contents. Compared to conventional beamforming, AOGF is demonstrated at NORESS and ARCESS to provide SNR gains from 12 to 18 dB over a wide frequency band from 0.2 to 5 Hz, while retaining an undistorted signal waveform. This gain is mainly due to suppression of noise at low frequencies, where both noise power and noise coherency is greatest. But even for the frequency band from 2 to 4 Hz, AOGF provides a typical gain in SNR of the order 6 to 8 dB compared to the array beam. The performance of AOGF appeared to be stable in time without need for readaptation, for time intervals at least one hour long. This may result in possible application of AOGF to supplement conventional beamforming for online signal detection and extraction. The proposed technique may be utilized also in post-processing for detecting and onset time estimating of seismic phases missed by conventional methods. As a result, it may reduce the detection threshold and improve the reliability of event detection and location using array signals.

A.F. Kushnir, V.I. Pinsky, S. Tsvang, Int. Inst. of Earthquake Prediction Theory, Moscow, USSR
J. Fyen, S. Mykkeltveit, F. Ringdal, NORSAR

References

Capon, J. (1970): Application of signal detection and estimation theory to the large array seismology. *Proc. IEEE*, Vol. 58, 170–186.

Kushnir, A.F. and V.M. Lapshin (1984): Optimal processing of the signals received by a group of spatially distributed sensors. *Computational Seismology*, Vol. 17, Allerton Press, Inc., 163–174.

Kushnir, A.F., V.I. Pinsky and J. Fyen (1989): Statistically optimal event detection using small array data. *Semiannual Technical Summary, 1 April - 30 September 1989*, NORSAR Sci. Rep. 1-89/90, Kjeller, December 1989.

Kushnir, A.F., V.M. Lapshin, V.I. Pinsky and J. Fyen (1990): Statistically optimal event detection using small array data. *Bull. Seism. Soc. Am.*, 80, in print.

Pisarenko, V.F., A.F. Kushnir and I.V. Savin (1987): Statistical adapative algorithms for estimation of onset moments of seismic phases. *Phys. Earth Planet. Inter.*, 47, 4–10.

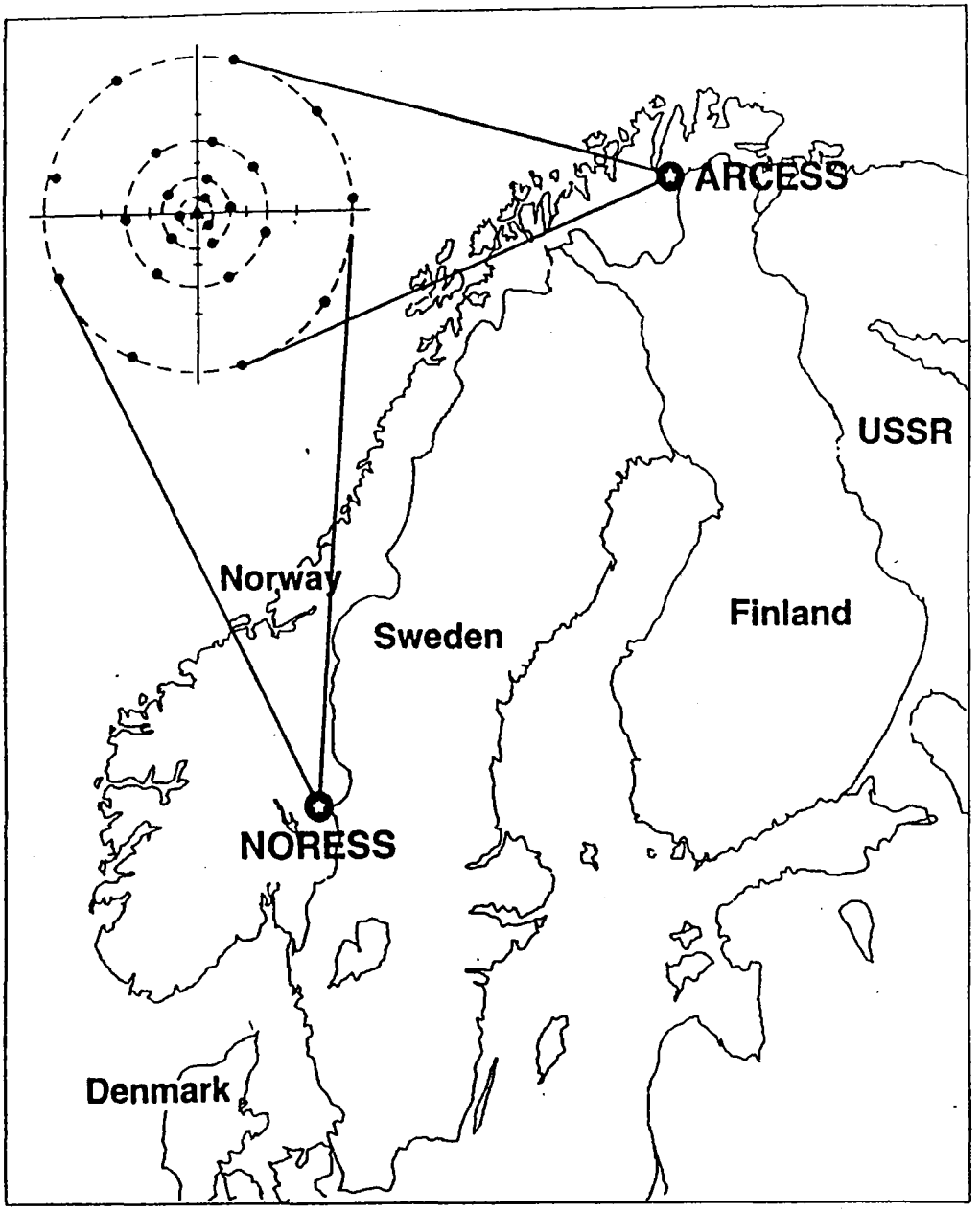

Fig. 7.7.1. The locations and array geometry for the NORESS and ARCESS arrays. The two arrays are essentially identical, each having 24 elements in four concentric rings (A, B, C, D) plus a center element (A0). The diameter of the outer (D) ring is 3.0 km. There are 3-component seismometers at A0 and three of the seven sites in the C-ring.

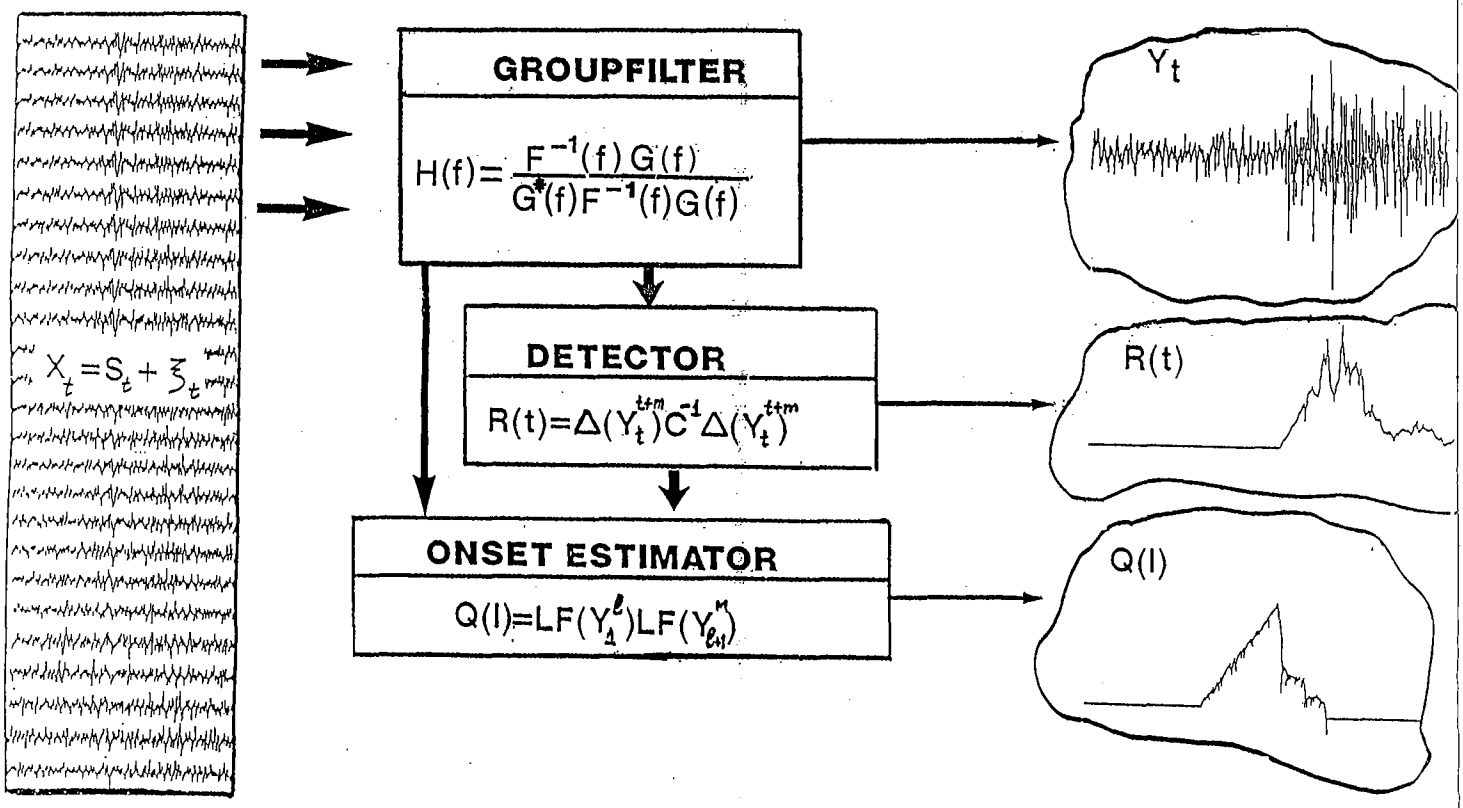

Fig. 7.7.2. Statistically optimal algorithms for preliminary array signal processing. X_t — multichannel seismic record; S_t — signal; ξ_t — noise; $H = H(\lambda)$ — frequency response of OGF; $F^{-1} = F^{-1}(\lambda)$ — inverse matrix power spectrum; $G = G(\lambda)$ — vector medium frequency response; Y_t — scalar output of AOGF, $R(t)$ — detector statistic; Y_t^{t+m} — observations in moving window (width = m samples); Δ — asymptotically sufficient statistics; C^{-1} — inverse covariance matrix of Δ computed at adaptation step; $Q(\ell)$ — likelihood function of onset time t_e; LF — likelihood functions of observations $Y_1^\ell = (Y_1, \ldots, Y_\ell), Y_{\ell+1}^M = (Y_{\ell+1}, \ldots, Y_M)$.

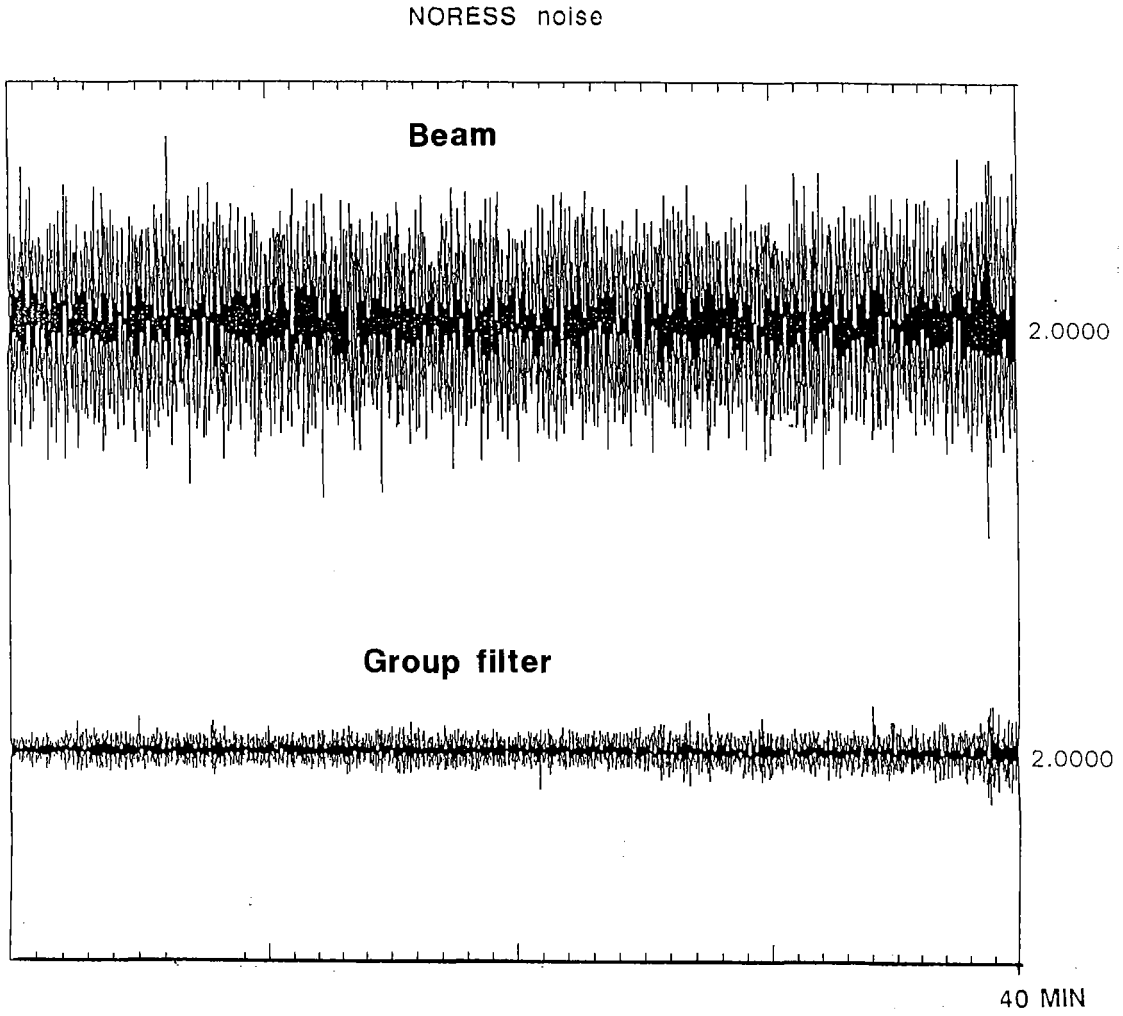

Fig. 7.7.3. 40 minutes of pure NORESS noise filtered by beam and optimal group filter in the same scale.

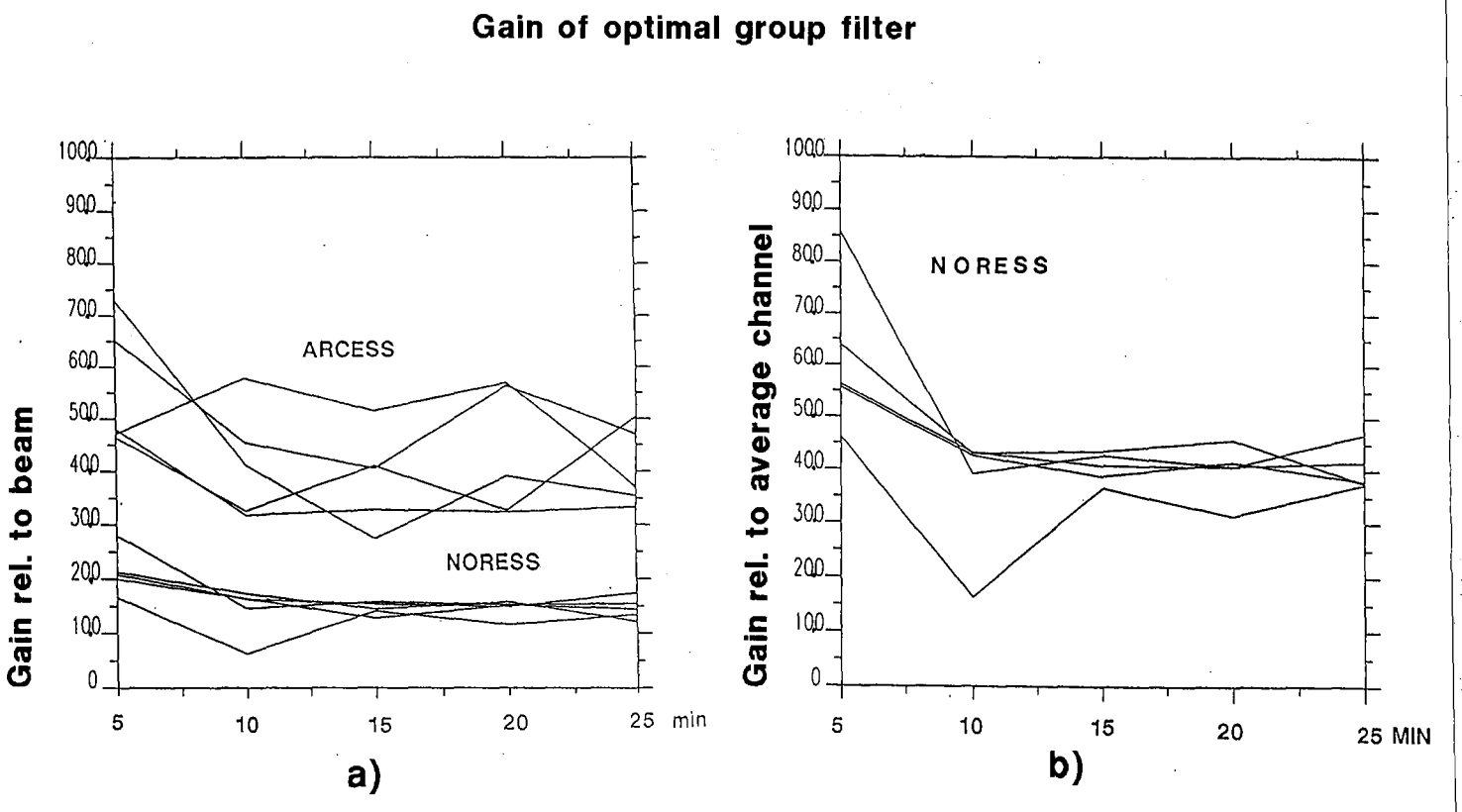

Fig. 7.7.4. Power SNR gain of optimal group filter computed each five minutes: a) relative to beamforming; and b) relative to average NORESS channel.

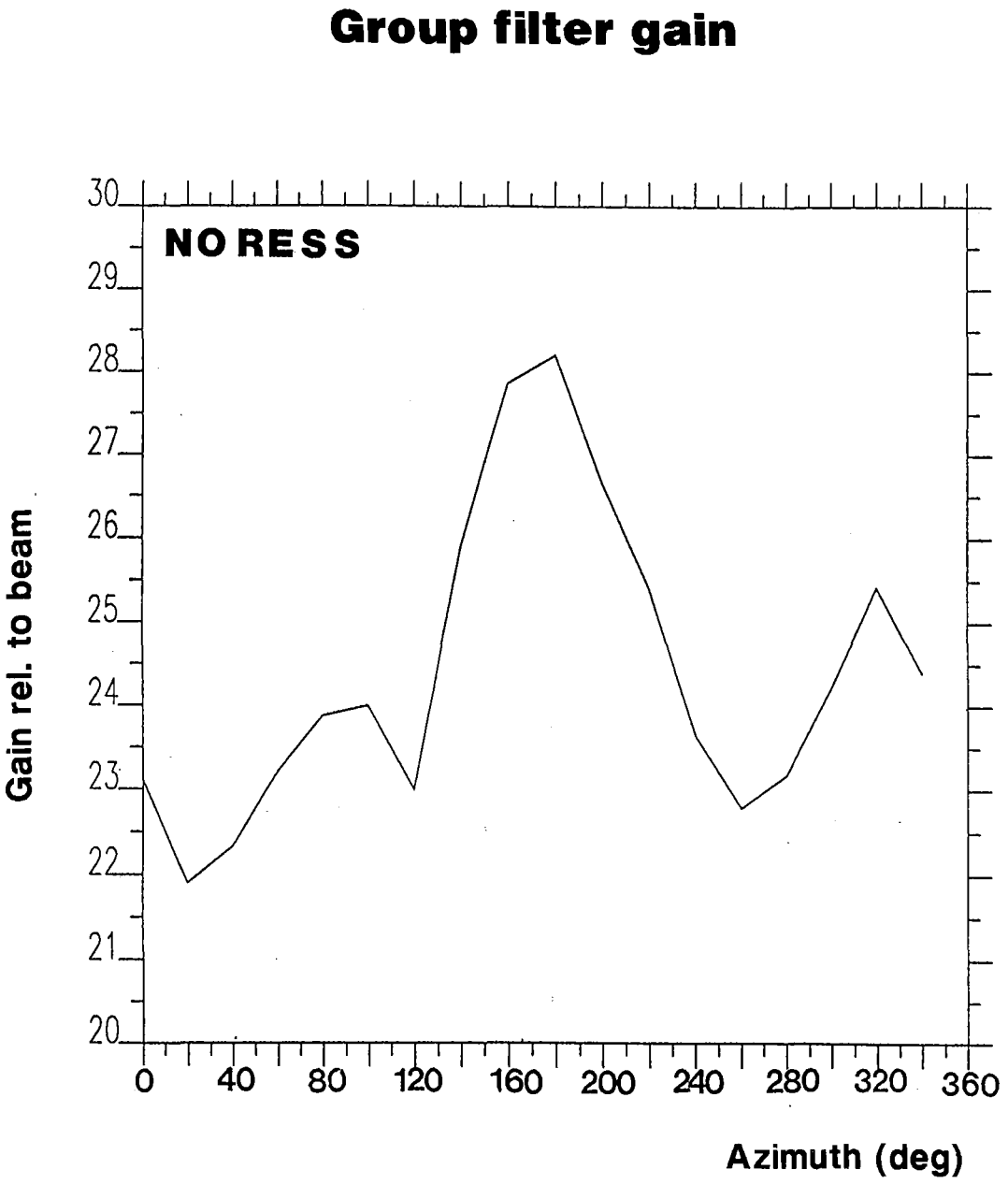

Fig. 7.7.5. Group filter gain for pure noise versus azimuth. The apparent velocity is equal to 13 km/sec. The maximum corresponds to the southern direction.

NORESS data. No Pn detection on NORESS. Only Lg detected.

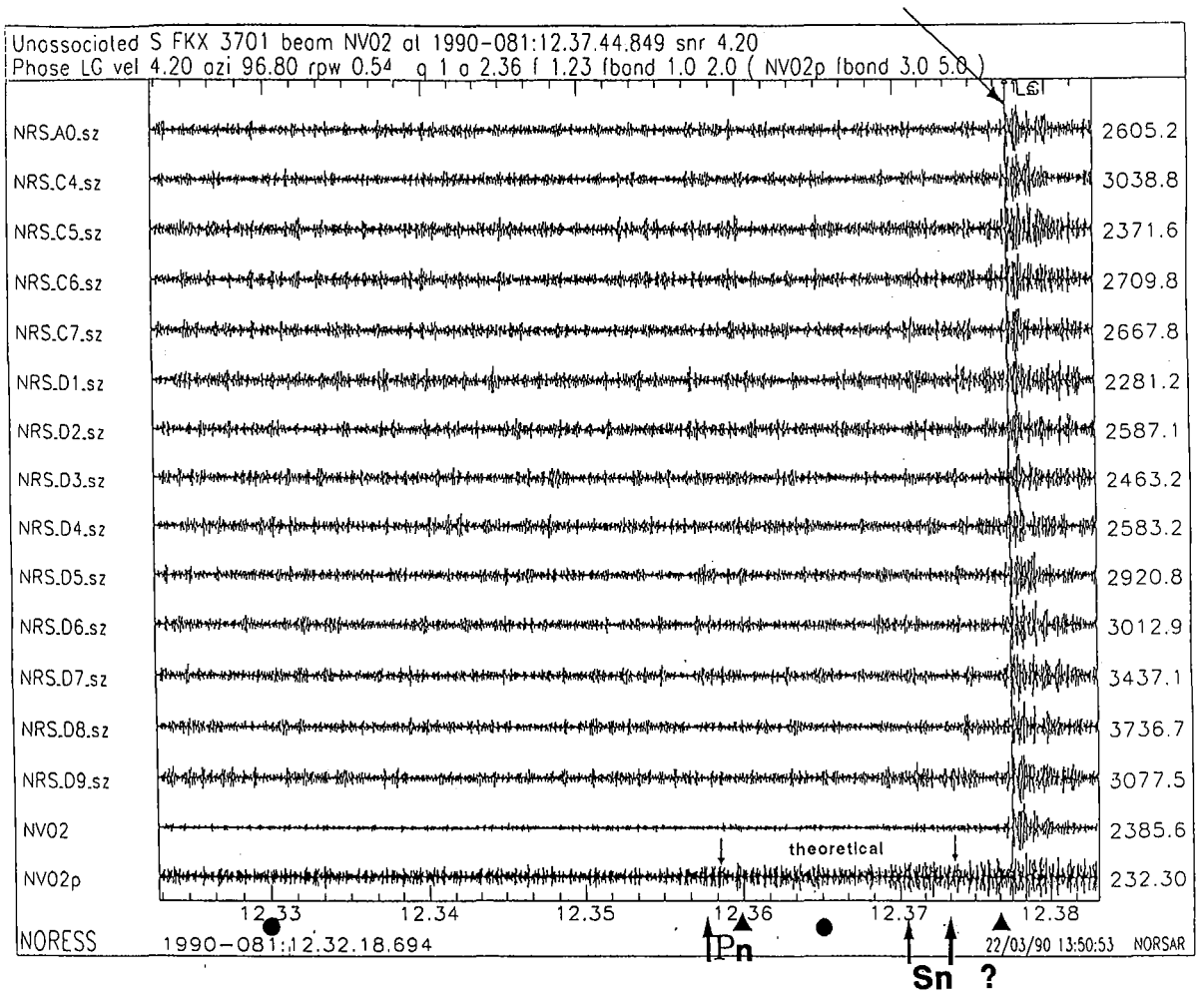

Fig. 7.7.6a. Illustration of the AOGF, OD and OE procedures as applied to NORESS data for a small event in Estonia, from which only the Lg phase was detected by the regular processing at NORSAR of NORESS data. The arrows show theoretical and computed (by the OE procedure) arrival times for Pn and Sn phases. Circles mark the time interval, in which there was a search for a Pn phase (see Fig. 7.7.6c), triangles mark the interval for searching for the Sn phase (see Fig. 7.7.6d).

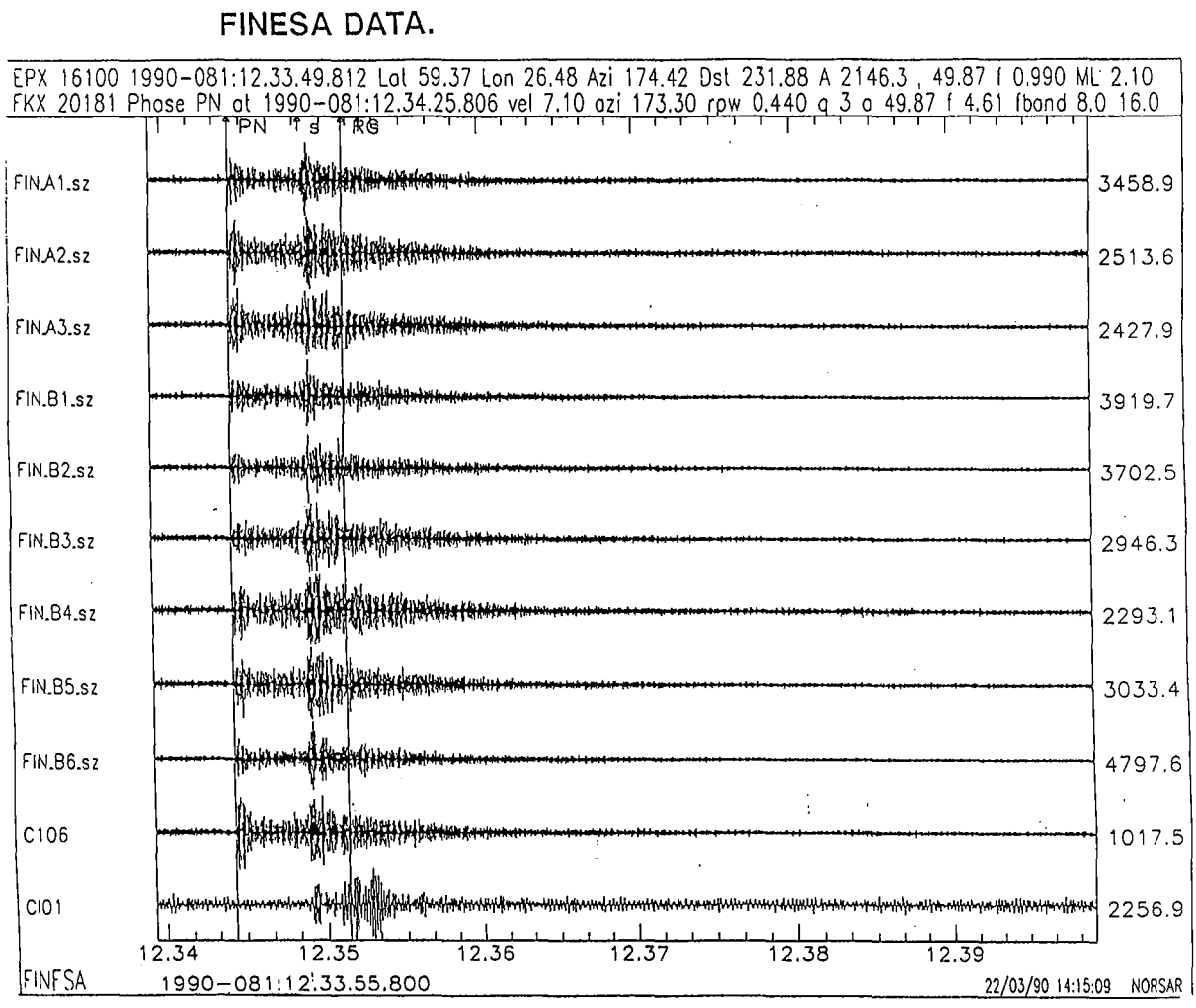

Fig. 7.7.6b. FINESA recording of the event for which Lg at NORESS is seen in Fig. 7.7.6a.

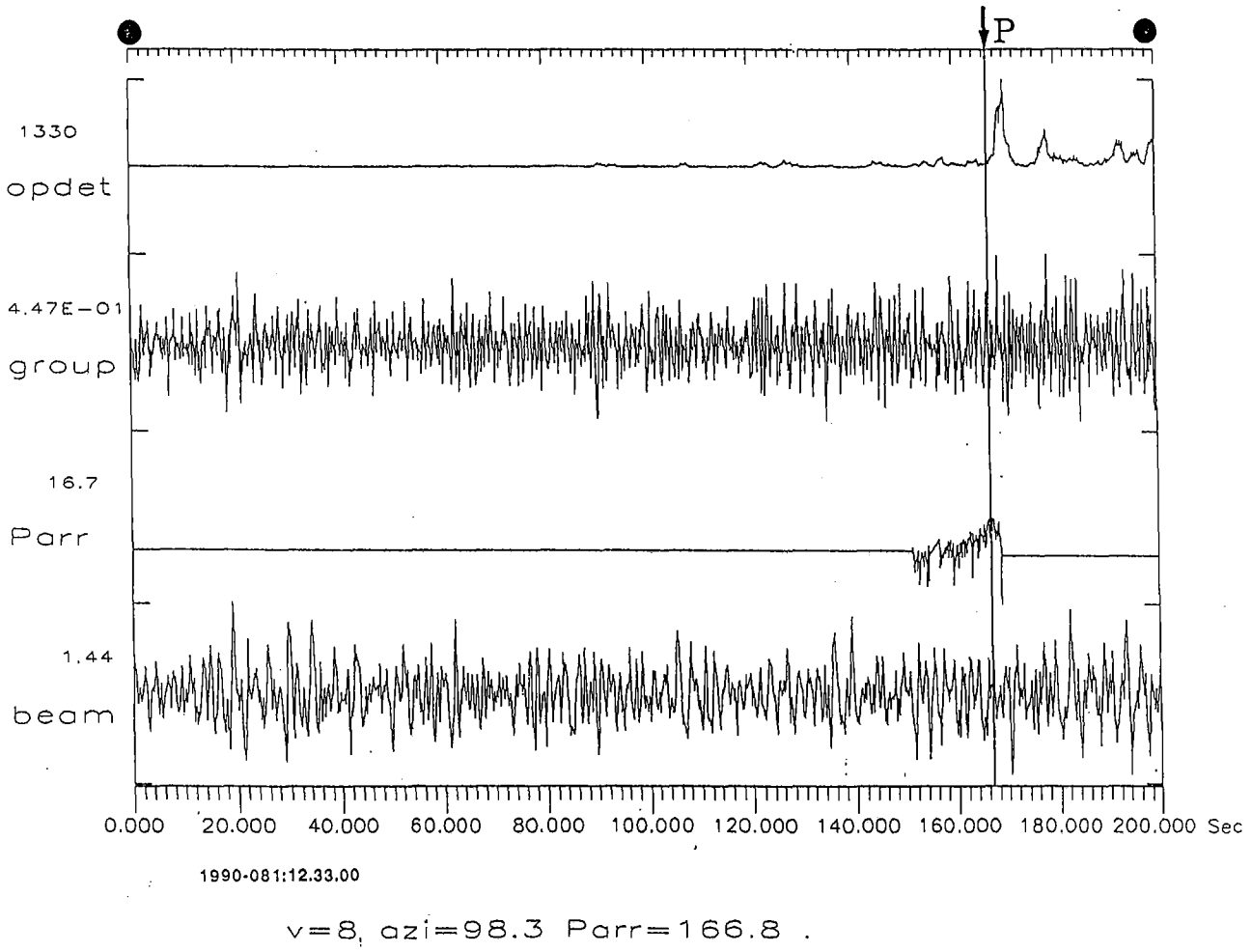

Fig. 7.7.6c. NORESS Pn-wave detection and onset estimation performed on AOGF output data. "V" and "AZI" correspond to apparent velocity and azimuth used in AOGF, "Parr" is computed by OE relative to the beginning of the interval for the search for the Pn phase.

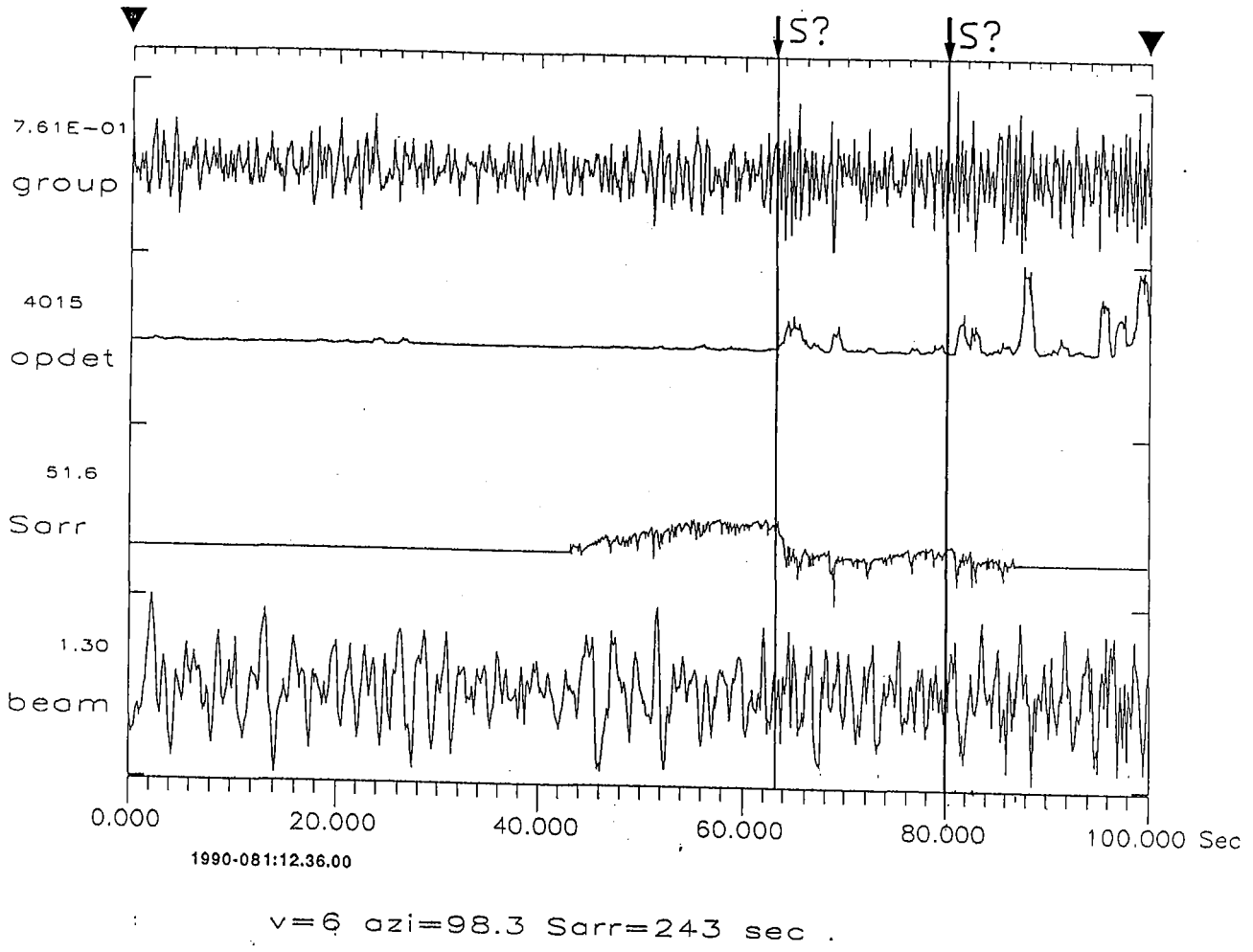

Fig. 7.7.6d. NORESS Sn-wave detection and onset estimation performed on AOGF output data. "V" and "AZI" correspond to apparent velocity and azimuth used in AOGF, "Sarr" is computed by OE relative to the beginning of the interval for the search for the Pn-phase.

NORESS data. No Lg detected on NORESS.

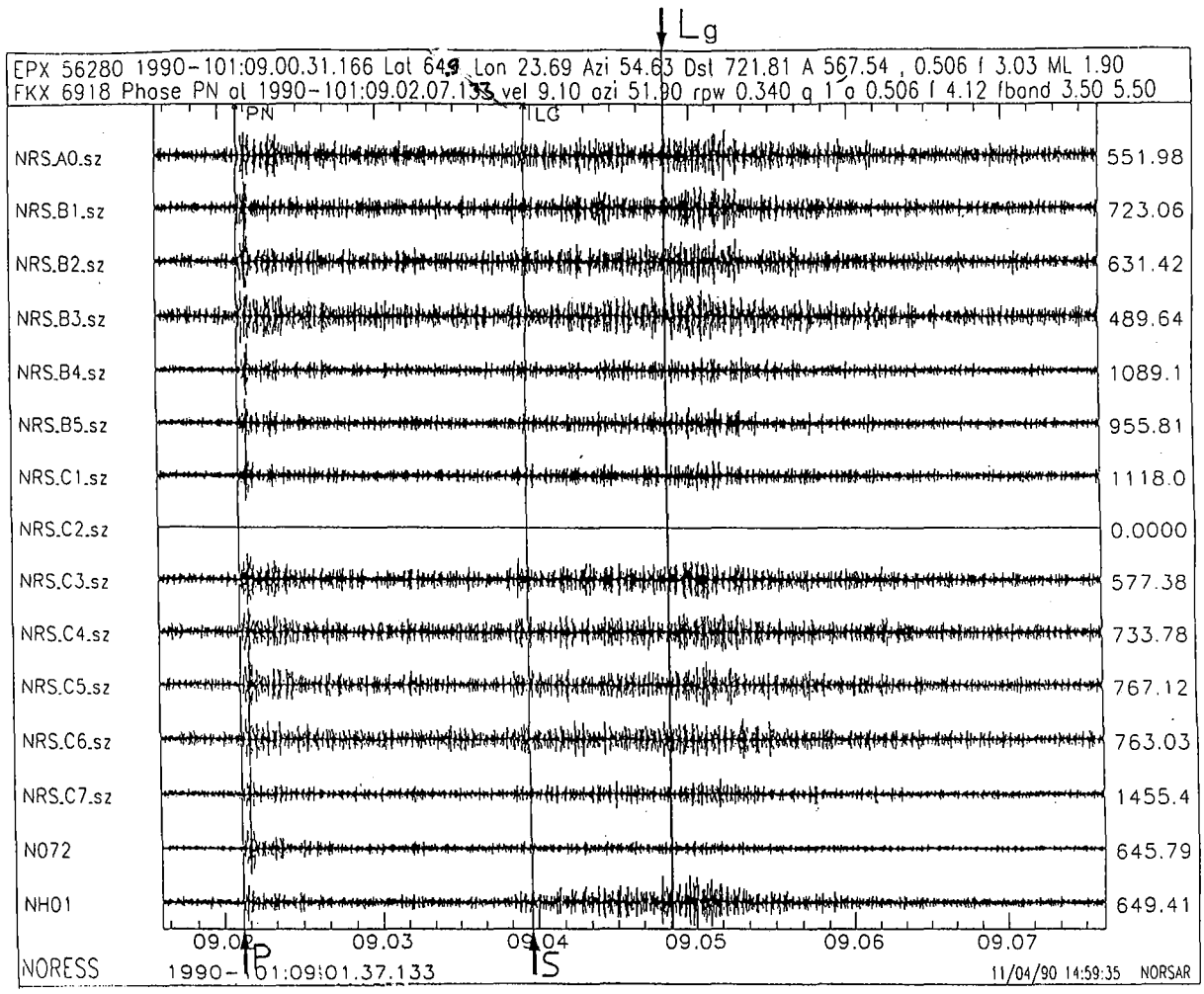

Fig. 7.7.7a. Illustration of the AOGF, OD and OE procedures as applied to an event from the USSR/Finland border region, for which the Lg phase was not detected by the NORESS regular processing. (The Sn phase at approximately 09.04 was detected, but incorrectly assigned as Lg.) Arrows show estimates of arrival times, using the OE procedure.

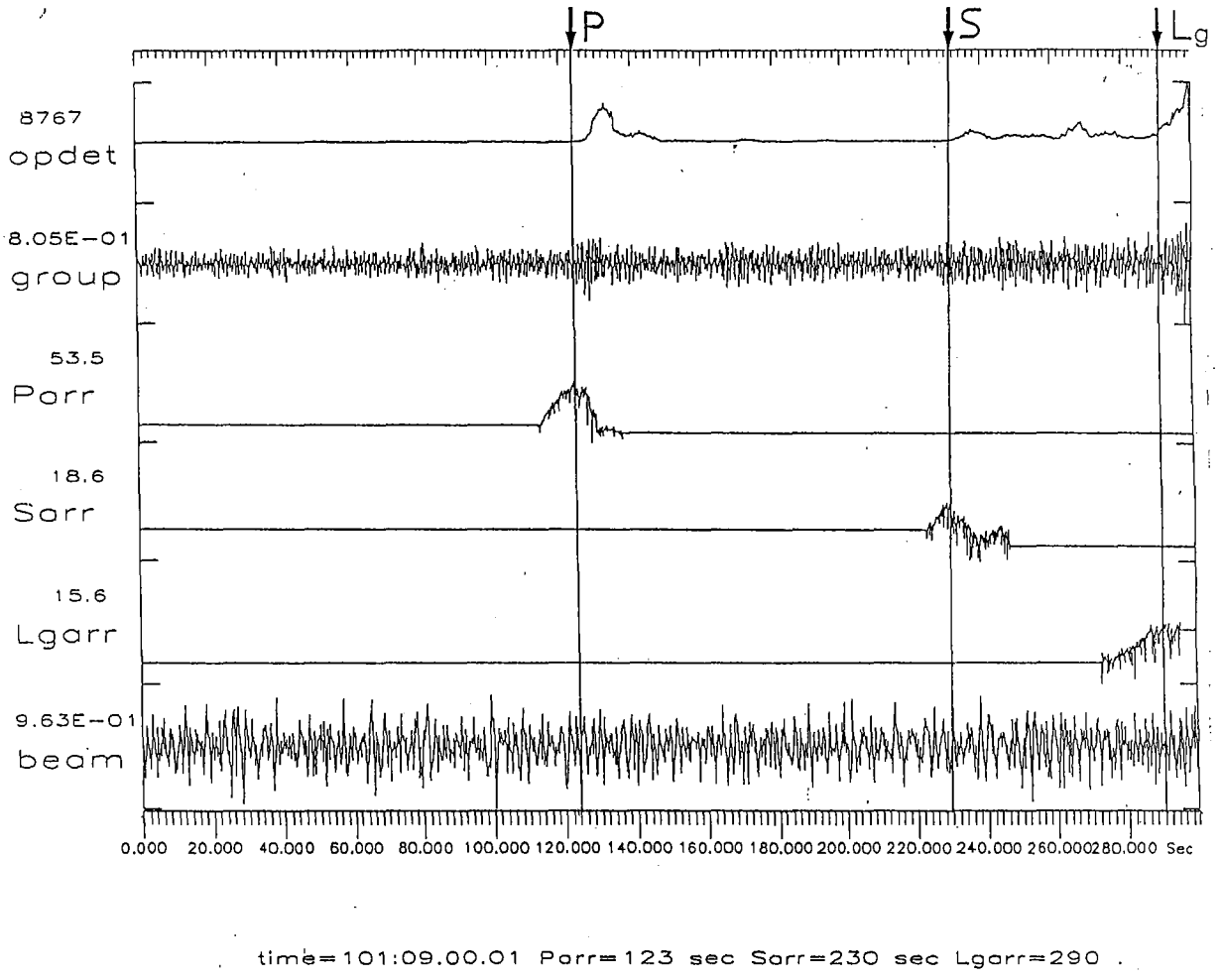

Fig. 7.7.7b. Pn, Sn and Lg detection and estimation performed on AOGF output data. "Time" gives the time of the beginning of the adaptation. "Parr", "Sarr" and "Lgarr" are computed by OE relative to the beginning of the interval.

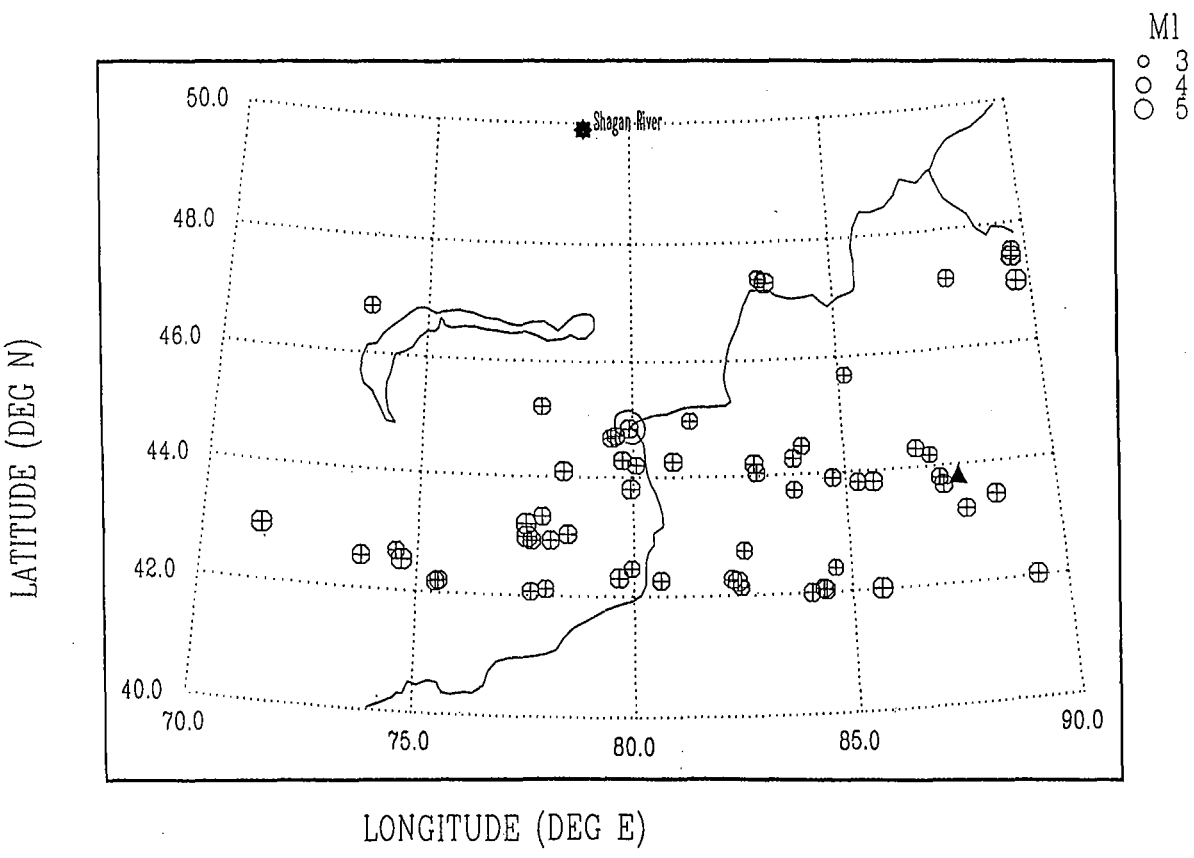

Fig. 7.7.8. Map showing the location of 35 earthquakes used in this study. Most explosions used are located at the Shagan River site.

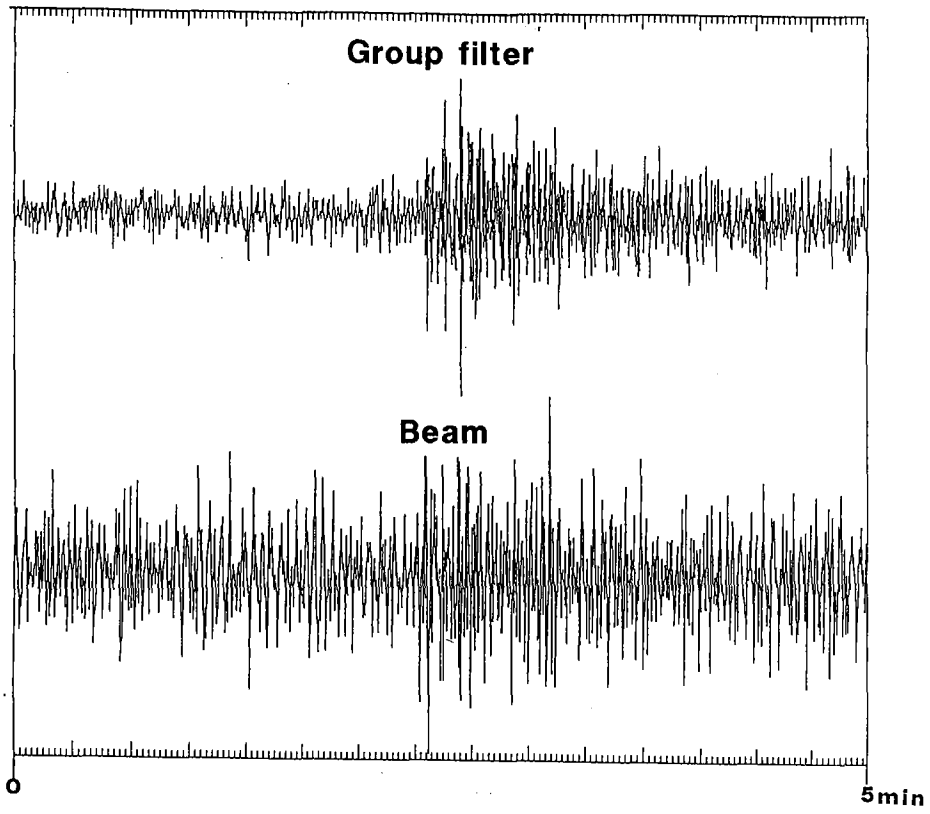

Fig. 7.7.9. Example of earthquake record filtered by beam and AOGF.

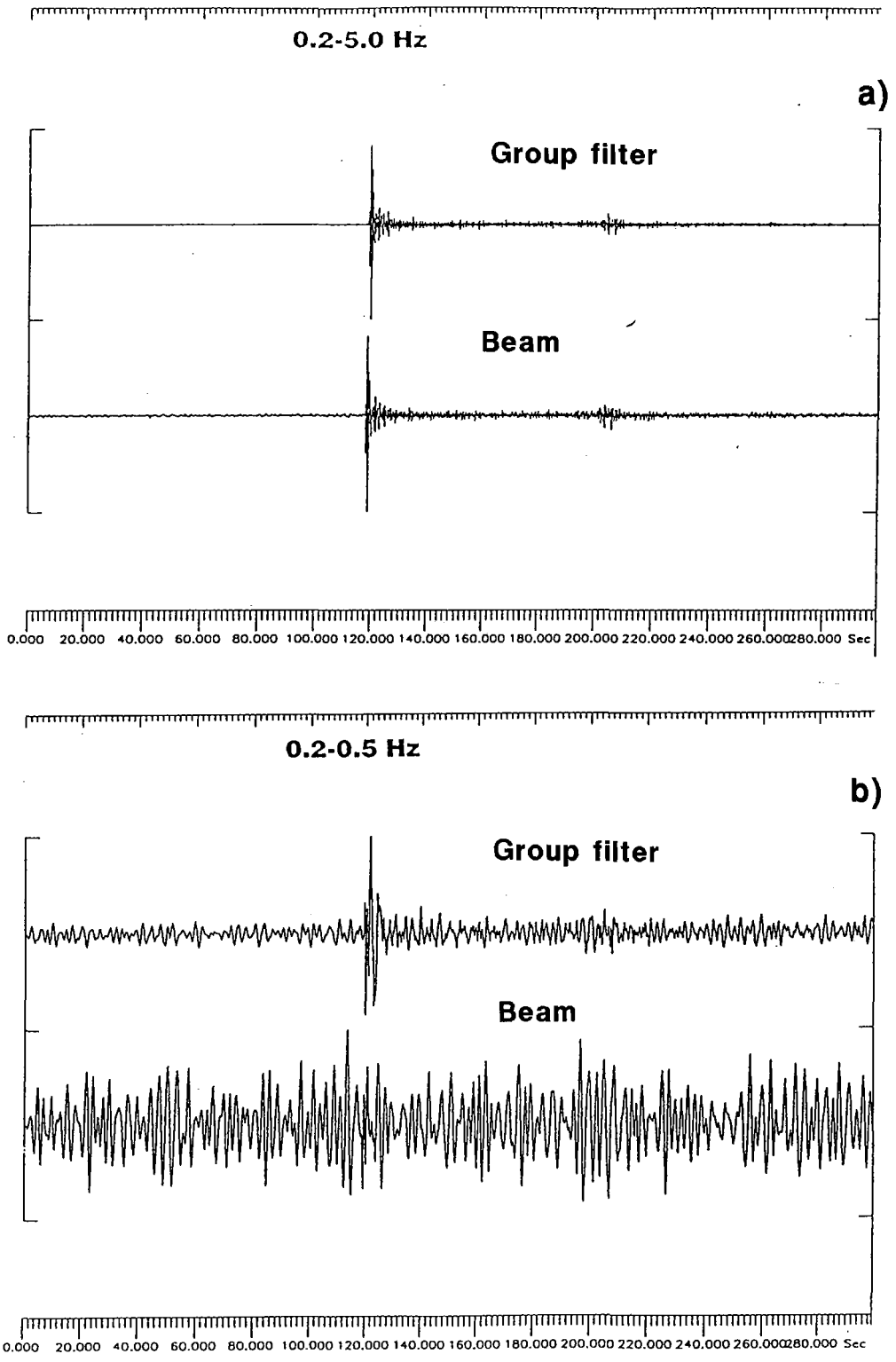

Fig. 7.7.10. Example of nuclear explosion record filtered by beam and AOGF in: a) broad frequency band and b) low frequency band.